Photoperiod-dependent proteolytic processing of neuropeptide precursors

DISSERTATION

zur

Erlangung des Doktorgrades
der Naturwissenschaften
(Dr. rer. nat.)

dem Fachbereich Biologie der Philipps-Universität Marburg
vorgelegt von

Michael Helwig
aus Kassel

Marburg / Lahn 2008

Vom Fachbereich Biologie der Philipps-Universität Marburg als Dissertation am

_____ angenommen.

Erstgutachter:

_____

Zweitgutachter:

_____

Tag der mündlichen Prüfung am:

_____

CONTENTS

GLOSSARY OF TERMS

SUMMARY

INTRODUCTION 1

AIMS & SCOPE 8

METHODS 9

RESULTS & DISCUSSION 10

CONCLUSION 21

REFERENCES 23

PUBLICATIONS & MANUSCRIPTS

CHAPTER I ---- 27

"PC1/3 and PC2 gene expression and post-translational endoproteolytic POMC processing is regulated by photoperiod in the seasonal Siberian hamster (*Phodopus sungorus*)"
M. Helwig, M.H. Khorooshi, A. Tups, P. Barrett, C. Exner, J. Rozman, L.J. Braulke, J.G. Mercer and M. Klingenspor. J Neuroendocrinol. 2006 Jun;18(6):413-25.

CHAPTER II ---- 40

"Photoperiod-dependent regulation of carboxypeptidases D and E and exoproteolytic processing of pro-opiomelanocortin in the seasonal Siberian hamster (*Phodopus sungorus*)"
M. Helwig, P. Ludewig, G. Heldmaier, J.G. Mercer, and M. Klingenspor. (in preparation)

CHAPTER III ---- 68

"CART neuronal system in the rostral arcuate nucleus mediates seasonal regulation of energy balance in the Djungarian hamster (*Phodopus sungorus*)"
R.M. Khorooshi, **M. Helwig**, A. Werckenthin. N. Steinberg, M. Klingenspor. Gen Comp Endocrinol. 2008 Jun;157(2):142-7.

CHAPTER IV ---- 74

"Photoperiodic regulation of satiety mediating neuropeptides in the brainstem of the seasonal Siberian hamster (*Phodopus sungorus*)"
M. Helwig, Z.A. Archer, G. Heldmaier, A. Tups, J.G. Mercer and M. Klingenspor. (in preparation)

CHAPTER V ---- 104

"Photoperiodic regulation of insulin receptor mRNA and intracellular insulin signalling in the arcuate nucleus of the Siberian hamster, *Phodopus sungorus*"
A. Tups, **M. Helwig**, S. Stöhr, P. Barrett, JG Mercer and M. Klingenspor. Am J Physiol Regul Integr Comp Physiol. 2006 Sep;291(3):R643-50.

CHAPTER VI ---- 112
"Circulating ghrelin levels and central ghrelin receptor expression is elevated in response to food deprivation in the seasonal hamster (*Phodopus sungorus*)".
A. Tups, **M. Helwig**, M.H. Khorooshi, Z.A. Archer, M. Klingenspor, J.G. Mercer. J Neuroendocrinol. 2004 Nov;16(11):922-8.

FURTHER SCIENTIFIC CONTRIBUTIONS

CHAPTER VII ---- 119
"Functional characterisation of UCP1 in the common carp: uncoupling activity in liver mitochondria and cold-induced expression in the brain."
M. Jastroch, J.A. Buckingham, **M. Helwig**, M. Klingenspor and M. Brand. J Comp Physiol [B]. 2007 Oct;177(7):743-52. Epub 2007 Jun 19.

CHAPTER VIII ---- 129
"Marsupial uncoupling protein 1 sheds light on the evolution of mammalian nonshivering thermogenesis"
M. Jastroch, K.W. Withers, S. Taudien, P. B. Frappell, **M. Helwig**, T. Fromme, V. Hirschberg, G. Heldmaier, B. M. McAlan, B.T. Firth, T. Burmester, M. Platzer, and M. Klingenspor, Physiol Genomics. 2008 Jan 17;32(2):161-9. Epub 2007 Oct 30.

CHAPTER IX ---- 138
"Conferences & Book Abstracts"

ZUSAMMENFASSUNG 147

CURRICULUM VITAE 148

ACKNOWLEDGEMENTS 151

ERKLÄRUNG 152

GLOSSARY OF TERMS

3V, 4V	third and fourth ventricle
α-MSH	α-melanocyte-stimulating hormone
ACTH	adrenocorticotropic hormone
AP	area postrema
AGRP	agouti-related peptide
ARC	arcuate nucleus
β-END	beta-endorphin
CART	cocaine- and amphetamine-regulated transcript
Cb	cerebellum
CBS	caudal brainstem
CC	central canal
CCK	cholecystokinin
CLIP	corticotropin-like intermediate lobe peptide
CNS	central nervous system
CPD/E	carboxypeptidase D/E
GAL	galanin
GHSR	growth hormone secretagogue receptor
GIT	gastro intestinal tract
GLP-1	glucagon-like peptide 1
ICV	intra-cerebroventricular
IHC	immunohistochemistry
IP	intraperitoneal
-ir	immunoreactivity
ISH	*in situ* hybridization
JP	joint peptide
LD	long day-length
LHA	lateral hypothalamic area
MALDI-TOF	matrix assisted laser desorption/ionisation–time of flight
MC4-R	melanocortin receptor 4
mRNA	messenger ribonucleic acid
MS	mass spectrometry
NAT	N-acetyltransferase
ND	natural day-length

NPY	neuropeptide Y
NT	neurotensin
NTS	nucleus of the solitary tract
PAM	peptidyl α-amidating monooxygenase
PBN	parabrachial nucleus
PC	pro-hormone convertase
POMC	pro-opiomelanocortin
PPG	prepro-glucagon
PVN	paraventricular nucleus
Py	pyramidal tract
PYY	peptide YY
RSP	regulated secretory pathway
SCN	suprachiasmatic nucleus
SD	short day-length
TNG	trans-Golgi network
UCP	uncoupling protein

INTRODUCTION

Central regulation of energy balance

Energy balance and body weight are regulated by the central nervous system (CNS) through an intriguing interplay of numerous peripheral and central signals (*Fig.1*). Among the key sites of the CNS where a constant influx of peripheral information gets integrated into central processing circuitries are the hypothalamus and the caudal brainstem (1). Relayed by either direct neuronal pathways or transmitted by a set of humoral signals, information on the status of energy balance gets encoded into a system of interacting peptidergic neurons. Organized into specific subnuclei, this neuropeptidergic network is responsible for the generation of an appropriate feeding behaviour in response to changes in energy balance. The precise processing of incoming energy balance related signals within distinct regions of the CNS is hence a prerequisite for the maintenance of energy homeostasis.

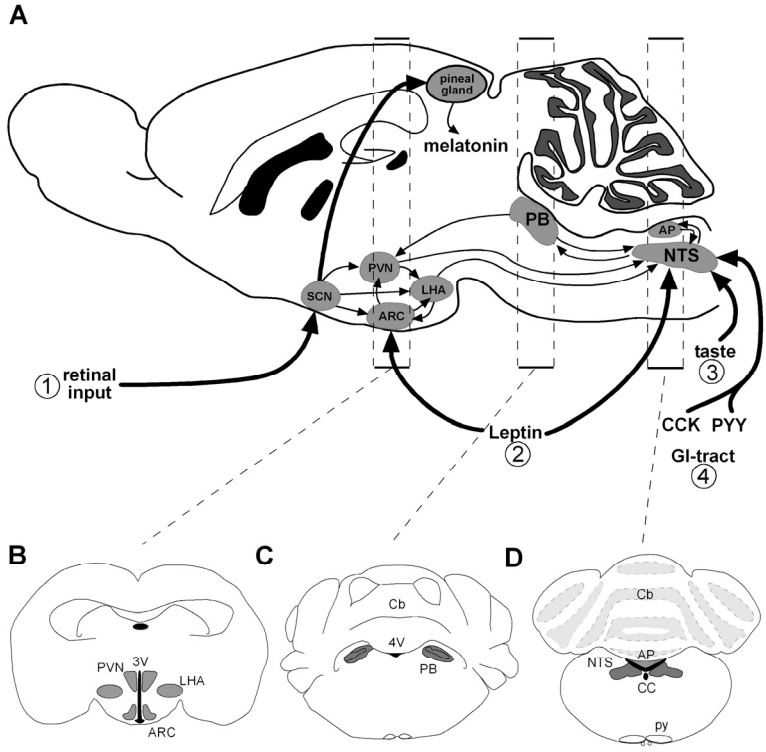

Fig.1: Central signalling pathways involved in the regulation of energy balance. (A) Sagittal brain section of the rodent brain. 1) In seasonal mammals retinal input provides the CNS with information on photoperiod. This information gets processed in the hypothalamic SCN and is transduced into pineal melatonin. 2) Information about stored fat reserves is delivered via leptin to the ARC and NTS. 3) Input on the quality of food (taste) enters the brain at the NTS. 4) Visceral input arising from the gastro-intestinal tract reaches the NTS by neuronal innervation from the vagus nerve and by postprandially released CCK/PYY. B-D) Representative coronal brain sections showing key sites at level of the B) hypothalamus, C) parabrachial nucleus (PBN), D) nucleus of the solitary tract (NTS).

Hypothalamic circuitries and long-term regulation of energy balance

Our current understanding of the basic neuroendocrine mechanism underlying body weight regulation has dramatically increased since systematic genetical modification became a tool in standard laboratory rodents. Naturally occurring mutations in the mouse, such as leptin-deficient ob/ob and carboxypeptidase E (CPE)-deficient fat/fat, provided a comprehensive resource for identifying genes and characterizing proteins involved in energy homeostasis. The subsequent analysis of genetically engineered mouse knockout (KO) models such as melanocortin receptor 4 KO (2) and pro-opiomelanocortin KO (3) has greatly expanded the number of genes known to influence energy balance by affecting metabolic rate, physical activity, and/or appetite (4). Certainly the adipocyte-secreted hormone leptin and insulin released from the pancreas are among the best characterized peripheral adiposity signals. Leptin is released from adipocytes in proportion to body fat mass and provides the CNS with information about the availability of stored energy in terms of fat (5). Insulin on the other hand is secreted in proportion to blood glucose levels and encodes information on the availability of circulating metabolites (6). Together, both humoral signals are principally secreted in times of a long-term positive energy flux and act centrally by activation of catabolic and anorexigenic effector neurons (*Fig.2*). The primary brain target of leptin and insulin appears to be the hypothalamic arcuate nucleus (ARC) since receptors for both molecules are highly concentrated in this specific region (7,8). Two functionally and anatomically distinct populations of arcuate neurons have been identified which express a complementary set of anorexigenic and orexigenic

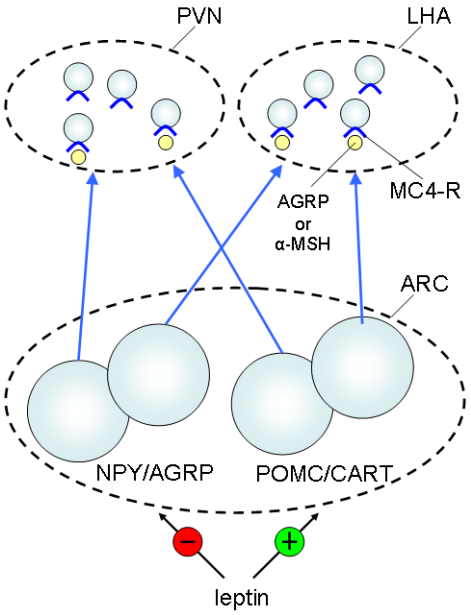

Fig.2: NPY/AGRP and POMC/CART neurons of the ARC are regulated by leptin. POMC-derived α-MSH binds to the MC4-R and stimulates CRH neurons of the PVN and inhibits Orexin neurons in the LHA leading to decreased food intake. NPY and AGRP have the opposing effect.

neuropeptides (9,10). Identification of this neuropeptidergic system was a significant step in order to understand the basic principles of leptins anorexigenic action within the CNS. Downstream to its receptor leptin inhibits orexigenic neuropeptide Y (NPY)/ agouti-related peptide (AGRP) co-expressing neurons and stimulates anorexigenic pro-opiomelanocortin (POMC)/ cocaine- and amphetamine-regulated transcript (CART) expressing neurons. From the ARC, NPY/AGRP and POMC/CART neurons project to second-order orexin-expressing (orexigenic) neurons of the lateral hypothalamic area (LHA) and anorexigenic corticotrophin releasing hormone (CRH) expressing neurons of the paraventricular nucleus (PVN). In particular neuropeptides of the melanocortin system have become focus of intense research activity since POMC-derived alpha melanocyte stimulating hormone (α-MSH) has been identified to potently inhibit food intake (11). The anorexigenic effect of POMC-derived neuropeptides is mediated through specific G protein-coupled seven-transmembrane receptors. Among the five identified melanocortin receptors (MC-R's) three are present in the brain (MC3-R, MC4-R, MC5-R). Here, MC3-R and MC4-R have been identified to function in the regulation of energy balance. Suppression of food intake by the melanocortin system is primarily facilitated by activation of MC-4R through binding of α-MSH. Agouti-related peptide reduces MC4-R activity and therefore promotes food intake (12).

Caudal brainstem and short-term control of meal size

While hypothalamic peptidergic circuitries have been target of extensive studies it is still not fully understood if and/or how long-term energy balance regulation is influenced by the short-term satiety-mediating caudal brainstem (CBS) network. However, from hypothalamic neurons of the PVN and LHA projections have been identified that relay to the CBS (13). Here, incoming information about the acute digestive status arising from the gastrointestinal tract (GIT) is integrated into incoming information from hypothalamic circuitries. The primary projection site for GIT-arising visceral-signals is the nucleus of the solitary tract

(NTS). Together with the adjacent area postrema (AP), the NTS receives direct neural innervations from the gut-ascending vagus nerve and the glossopharyngeal nerve originating from the oral cavity. Furthermore, postprandially released gastro-intestinal hormones such as cholecystokinin (CCK) and peptide YY (PYY) are transported to the NTS and AP via the bloodstream where they bind to their respective receptors and transmit information on the acute feeding state (14,15). In combination these signals provide the NTS with short-term satiety information on a meal-to-meal basis. Most regulatory neuropeptidergic components of the hypothalamus are also present within the NTS, including the leptin receptor (ObRb)(16) and the members of the melanocortin system (POMC, MC3-R and MC-4R)(17). Interestingly experiments in decerebrated rats have impressively demonstrated that these neuropeptidergic circuitries are sufficient to generate a meal related satiety response despite denervation and thus lacking input from the hypothalamus (18). It has been proposed, however, that hypothalamic long-term adiposity input alters the acute satiety response of NTS neurons (19). In turn extensive projections from the NTS to the hypothalamic peptidergic network either directly, or indirectly via a mandatory inter-neuron pathway involving the parabrachial nucleus (PBN, *Fig.1*), suggest a contribution of processed satiety information to the long-term regulation of energy balance (20).

Post-translational processing of neuropeptides

Most neuropeptides and hormones involved in the central regulatory circuitries are initially synthesized into large, inactive polypeptide precursors and have to undergo extensive post-translational processing before their neuropeptide products achieve biological activity (21). Followed by limited and tissue specific post-translational proteolysis these precursors are origin for different bioactive molecules. The initial processing event in the synthesis pathway of POMC is endoproteolytic cleavage at the C-terminal side of specific single/double and tetra basic amino acid residues by prohormone convertases (PCs, *Fig. 3)*, which ultimately results

in the release of smaller neuropeptides such as α-MSH and β-END. Pro-hormone convertases belong to a family of seven calcium dependent substilisin-like serine proteases including furin, PC1 (also known as PC3), PC2, PC4, PACE4, PC5-A (also known as PC6-A), its isoform PC5-B (also known as PC6-B), PC7 (also known as LPC), and PC8 (also known as SPC7). While most of these enzymes are found in endocrine tissue (e.g. pancreas or thyroid gland), PC1/3 and PC2 are specifically expressed in the CNS suggesting that PC1/3 and PC2 possess an important role in neuropeptide processing (22). And indeed it was demonstrated that both PCs process neuropeptides such as pro-thyroid-releasing-hormone (TRH), prosomatostatin, pre-proglucagon (PPG), proNPY, proCART and POMC to various intermediate-sized molecules and end products.

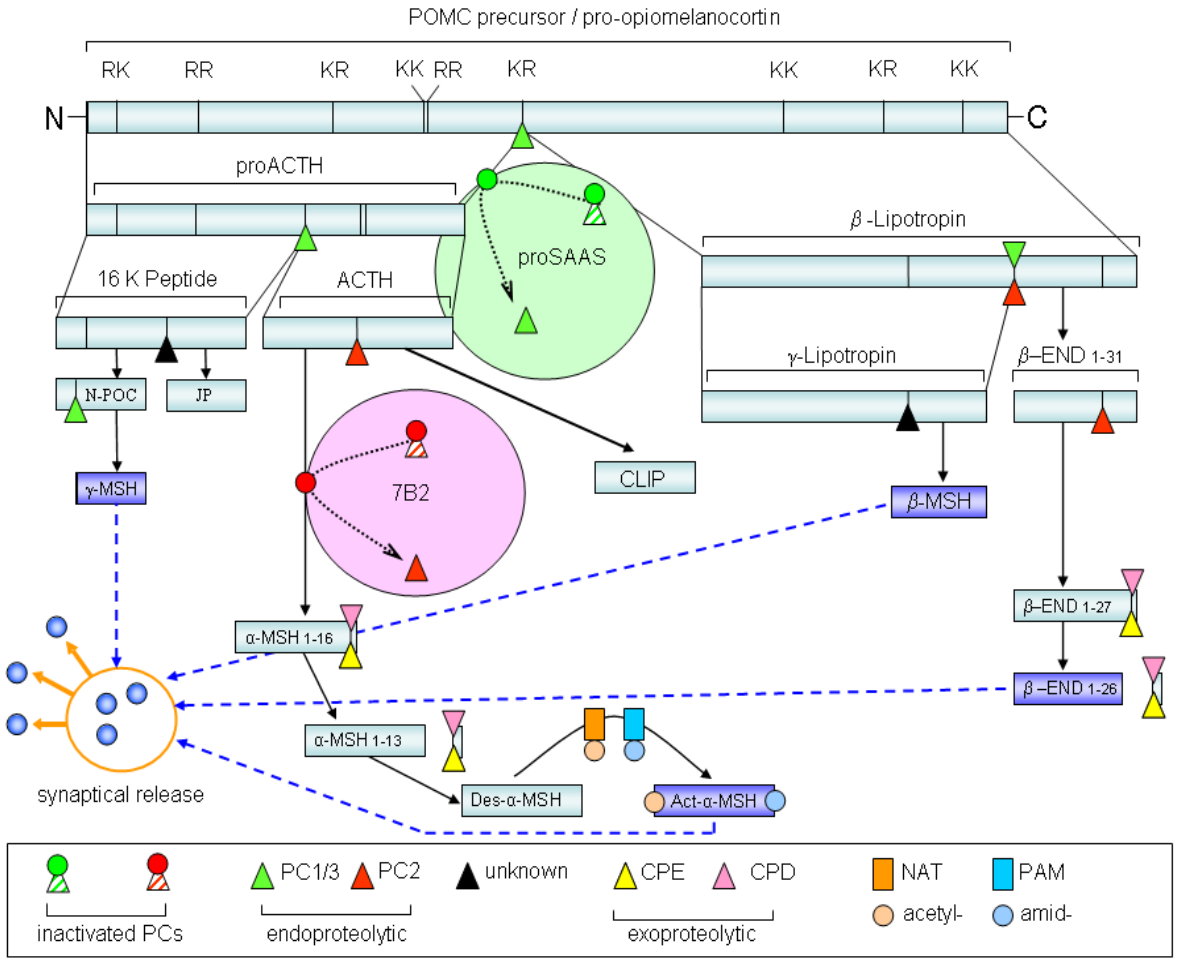

Fig.3: Post-translational processing pathway of pro-opiomelanocortin (POMC) in the hypothalamus. POMC gets initially cleaved by endoproteolytic pro-hormone convertases (PCs) next to specific dibasic amino acid residues motifs (R, arginine; K, lysine) followed by the removal of remaining C-terminal basic residues by exoproteolytic carboxypeptidases (CPs). Activity of PCs is regulated by inhibitory peptides proSAAS and 7B2. Processing end product α-MSH gets further acetylated by an N-acetyltransferase (NAT) and amidated by α-amidating monooxygenase (PAM) prior to synaptic release.

PC1/3 is endogenously inhibited by the binding protein proSAAS. The acute enzymatic activity of PC1/3 within the regulated secretory pathway (RSP) is therefore dependent on the presence of this inhibitory peptide (23). Interestingly proSAAS itself is processed into a number of smaller peptides designated as big SAAS, little SAAS, PEN, and LEN (24). However, the biochemical and physiological functions of these smaller peptides remain unclear. In case of PC2, enzymatic activity is regulated by the neuroendocrine peptide 7B2. Within the RSP an inactive PC2/7B2 complex arrives at the trans-Golgi network (TNG) where auto-cleavage of 7B2 initiates folding and a conformational rearrangement of the enzyme (25). This event activates the catalytically active domain and enables PC2 to enter the maturing secretory granules.

Following endoproteolytic cleavage of neuropeptides by PCs, carboxypeptidases D and E (CPD, CPE) cleave the remaining C-terminal basic residues of the intermediate neuropeptides to generate bioactive peptides (26,27). In certain cases, additional modifications, such as C-terminal amidation by peptidyl α-amidating monooxygenase (PAM), N-terminal acetylation by an N-acetyltransferase (NAT), and/or sulfation, enhance the activity, or are required for the peptides to become biological active (28). The severe obese phenotype revealed in mice lacking these enzymes by genetical knockout corroborates the importance of these enzymes in the maturation of energy balance regulating neuropeptides (29).

Seasonal body weight regulation in the Siberian hamster

A fascinating animal model with pronounced physiological metabolic adaptation is the Siberian hamster (or Djungarian hamster, *Phodopus sungorus*). The main focus of the current work is the characterization of neuroendocrine mediators of energy balance regulation in this valuable species that exhibits natural variations in energy homeostasis (30-32). In the wild, Siberian hamsters have adapted to the annual climatic cycle that influences the availability of food. The annual change in photoperiod is the major trigger that induces reversible

physiological adaptations such as a decrease in food intake, loss of body weight, a fur colour and insulation change and altered reproductive status (33,34). Under laboratory conditions a simple square-wave switch in photoperiod induces a voluntary body weight loss by an average of 30-40 % during a period of 12-18 weeks following transition from a summer-like day length (long-day, 16h light: 8h dark) to a winter-like day length (short day, 8h light: 16h dark) (*Fig4.*) (35). This natural and direct regulation of body weight is a feature which makes the hamster a powerful animal model to elucidate the mechanisms of the underling regulatory pathways. Most studies investigated the gene expression profiles of key neuropeptides and receptors within the ARC of the Siberian hamster following photoperiod manipulation.

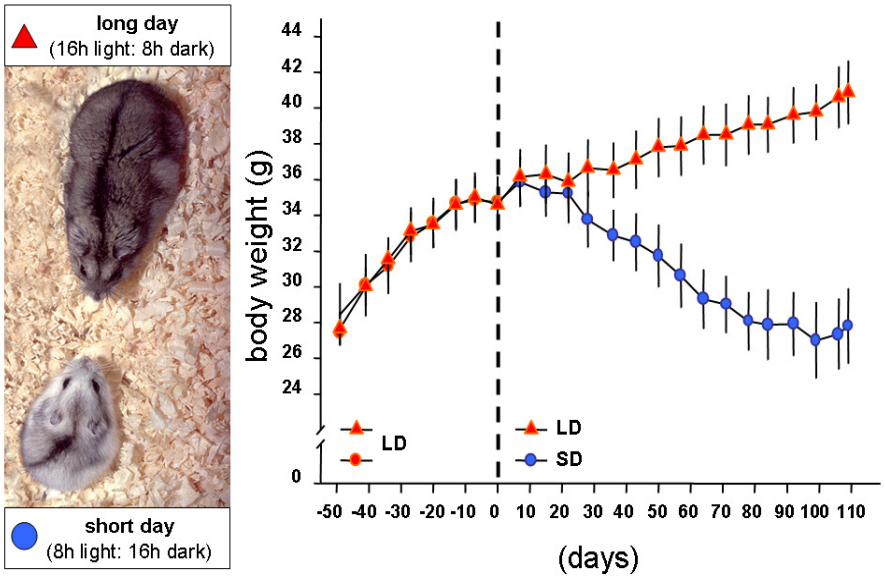

Fig.4: Siberian hamsters fed ad lib, either acclimated to long-day (LD) or short-day (SD) for 14 weeks. Body weight of hamsters kept in SD decreases following transition to SD whereas body weight of hamsters in LD steadily increases. (Graph: Anne Figge, Photo: The Rowett Research Institute).

While gene expression of orexigenic NPY seems not to be affected by changes of photoperiod it could be demonstrated that levels of CART and AGRP mRNA are increased following transition to SD (36-38). On the other hand, gene expression of POMC was demonstrated to be down-regulated after exposure to SD (38). In the case of CART, observed changes in SD were in the direction that would be anticipated for an anorexigenic neuropeptide. The increase in gene expression of orexigenic AGRP and the decrease of POMC in SD, if translated into protein, are counterintuitive since this expression ratio would lead to an increased antagonist availability at the MC4-R and thus further reduce the anorexigenic drive that would normally be expected in SD.

AIMS & SCOPE

A number of previous studies have consistently demonstrated that gene expression of POMC is unaltered or even down-regulated in the hypothalamus of Siberian hamsters following transition to short-day photoperiod (38). This observation contradicts to the anorexigenic properties of POMC since hamsters in SD are characterized by a profound anorexigenic (or catabolic) drive. POMC, however, undergoes extensive post-translational processing resulting in neuropeptides with individual anorexigenic function. Thus investigation of POMC as a whole is not sufficient to characterise this important system. The main focus of this PhD project was therefore to identify a possible photoperiod influence on major enzymatic components of the neuropeptide processing cascade in order to unravel this "POMC-paradox". Furthermore, it was addressed whether neuroanatomical and peptidergic components of the brainstem are influenced by photoperiod. This might be the clue to better understand the complex circuitries regulating seasonal energy balance.

The following specific aims and research objectives were addressed during my PhD study period:

1.) Is the seasonal change in body weight associated with a regulatory change in post-translational processing of hypothalamic anorexigenic neuropeptide precursors?
2.) If so, a) what are the enzymatic key mediators of the proposed differential proteolytic processing and b) what is the result of this differential processing regarding the generated products?
3.) To establish a peptidomic approach by mass spectrometry that enables us to determine specific post-translational modifications of neuropeptides products.
4.) To investigate whether modulation of photoperiod alters neuropeptidergic components of the ascending gut-brain axis located in the brainstem of the seasonal Siberian hamster.

METHODS

Several molecular biological and proteomic approaches were employed to address the specific questions raised in this study. These methods are hereby briefly summarized:

Messenger RNA levels of selected neuropeptide- and receptor candidates were quantified utilizing ***in situ*** **hybridization** (ISH) in coronal sections of the hamster brain. Therefore riboprobes complementary to partial fragments of PC1/3, PC2, POMC and PPG were cloned from hamster cDNA. Riboprobes specific to CART, galanin, GHS-R, MC3-R and MC4-R were kindly provided by the laboratory of Prof. Dr. Julian Mercer (The Rowett Research Institute, UK).

Localization and quantification of neuronal protein (antigen) content was assessed by **immunohistochemistry** (IHC) using antibodies raised against selected peptide candidates. For this purpose two major procedures were employed: a) single immunostaining using a two-step nickel-intensified avidin/biotinylated enzyme complex-horseradish peroxidase (ABC-HRP) staining procedure, b) dual immunostaining using red/green fluorescent dyes to confirm a physiological relation between POMC-substrates and their corresponding enzymes by assessment of co-localization at the intra-cellular level.

Due to methodological limitations of IHC in distinguishing between different states of peptide modifications, POMC-products and other components of the POMC-processing cascade were identified by ***in situ*****-MALDI-TOF MS**. Besides providing information on potential post-translational modifications represented by a change in peptide masses this method also involves a neuroanatomical localization component. This pioneering and innovative technique was modified according to our specific needs in the Siberian hamster with kind assistance of Dr. Christian Wegener.

RESULTS & DISCUSSION

Post-translational processing of POMC

The results of this PhD thesis demonstrate that maturation and biosynthesis of hypothalamic POMC-derived neuropeptides are regulated by photoperiod in the seasonal Siberian hamster. As part of my diploma thesis we initially scrutinized the gene expression profiles of PC1/3 and PC2 in the ARC of Siberian hamsters either kept under natural day light conditions (ND) from October – April or under artificially maintained summer-like LD photoperiod. Strikingly the temporal gene expression pattern of PC2 followed a seasonal trajectory and paralleled the changing ambient ND photoperiod with maximal mRNA levels in January when photoperiod was shortest. Based on this observation I continued to elucidate the post-translational processing cascade and developed several approaches to unravel the detailed mechanism by which maturation of POMC-derived neuropeptides is regulated.

Firstly, I aimed to verify our initial observation by a so called “switch back” experiment. For this purpose, Siberian hamsters were kept in SD for 14 weeks; following transition back to LD and brain tissue sampling at weekly intervals (animals were kindly provided by Dr. P. Barrett). We then assessed the temporal responsiveness of PC1/3 and PC2 gene expression following this switch in photoperiod. Secondly, we scrutinized the protein distribution of PC1/3, PC2 and POMC and its derived peptides ACTH, α-MSH and β-END in SD and LD acclimated hamsters by means of immunohistochemistry. After 14 weeks in SD, we discovered that levels of PC1/3 and PC2 mRNA were significantly increased compared to those observed in LD. Following transition of SD hamsters back to LD we observed an acute regulatory change in gene expression of both prohormone convertases substantiating the correlation with photoperiod. The increase of PC expression in SD on the transcriptional level was also reflected on protein level as revealed by IHC. Furthermore, within the same neurons of the ARC we found up-regulation of PCs in SD accompanied by higher levels of the smaller POMC-derived peptides α-MSH and β-END. One can conclude that, despite unchanged gene

expression of POMC following alterations in photoperiod, post-translational processing by endoproteolytic cleavage is the decisive factor leading to a seasonally dependent maturation of melanocortin peptides. The results of our experiments are comprehensively discussed in *Chapter I*: "PC1/3 and PC2 gene expression and post-translational endoproteolytic POMC processing is regulated by photoperiod in the seasonal Siberian hamster (*Phodopus sungorus*)" (39). However, the mere presence of PCs in the regulated secretory pathway is not the only parameter that regulates prohormone processing. Inhibitory peptides proSAAS and 7B2 have been reported to regulate the enzymatic activity of PC1/3 and PC2 by direct binding (23),(25). Hence, we performed IHC on proSAAS and its derived peptides and 7B2 to evaluate a possible regulatory effect of these inhibitory proteins in the ARC of either SD and LD acclimated hamsters. Preliminary results obtained from a small number of SD and LD acclimated hamsters (n=3 per group, data not shown) suggested that this is not the case. We found no differential expression of either of these peptides. However, further detailed investigations are now subject to a diploma thesis performed by P. Ludewig.

We systematically continued the analysis along the post-translational POMC processing pathway and focused on the exoproteolytic cleavage of POMC-derived peptides by CPD and CPE. Both carboxypeptidases are supposed to be the terminal activation event in neuropeptide synthesis. Thus, it seems intuitive that activation of POMC-derived neuropeptides in the seasonal Siberian hamster may be critically regulated by either one or a combination of both of these enzymes. To test this hypothesis we performed a quantitative IHC study on brain slides of hamsters kept in the photoperiod paradigm. In addition, in this experiment we treated hamsters with leptin in order to scrutinize the effect of long-term adiposity signals on post-translational processing of POMC. While expression of CPD remained largely unaffected by changes in photoperiod, we observed an increase of hypothalamic CPE-ir in SD. Leptin administration only in SD induced an up-regulation of CPD and CPE. The increase of CPE-ir in SD was accompanied by an increase in total-α-MSH-ir and β-END-ir. Moreover,

expression of CPE was mainly confined to melanocortinergic neurons of the ARC as revealed by dual-fluorescence IHC. Together these observations strongly suggest a functional relation between CPE and POMC that most likely results in a higher abundance of biological active melanocortinergic peptides in SD. The results of this study are presented in *Chapter II*: "Photoperiod-dependent regulation of carboxypeptidases D and E and exoproteolytic processing of pro-opiomelanocortin in the seasonal Siberian hamster (*Phodopus sungorus*)".

We were able to demonstrate that major enzymatic components of the POMC processing pathway are regulated in a photoperiod dependent and temporal coordinated fashion. However, antibodies raised against POMC-derived neuropeptides cannot distinguish between the two fractions of non-truncated/inactive (β-END_{1-31} and α-MSH_{1-16}) and truncated/active peptides (β-END_{1-26} and α-MSH_{1-13}). To evaluate the yield of c-terminally cleaved and bioactive α-MSH_{1-13} by CPE we utilised direct analysis of hypothalamic neuropeptides with neuroanatomical precision by *in situ* MALDI-TOF mass-spectrometry. POMC-containing neurons in the hypothalamus, however, are especially sensitive to post-mortem changes and are subject to rapid degradation (40). We therefore combined MALDI-TOF MS with a brain tissue fixation procedure by microwave irradiation. We initially tested this novel neuropeptidomic approach using brain slices of mice and were able to detect many peptide products resulting from the posttranslational POMC processing pathway including POMC, PC2 and proSAAS (*Fig.5*). Subsequent sequencing of the Siberian hamster POMC gene enabled us to calculate and predict masses of POMC derived neuropeptides in *P. sungorus* (*Fig.6*).

Based on these preliminary results this project is currently continued as a part of the diploma thesis performed by P. Ludewig. The ultimate identification and quantification of bioactive anorexigenic POMC-derived neuropeptide products in the Siberian hamster remains a key future target. The peptidomic approach established in my PhD thesis has clearly the potential to reveal some major insights into this exciting new field.

Precursor	peptide name	predicted mass	observed mass
Chromogranin B	Phosphorylated357- 374	2179,1	2178, 5
Proopiomelanocortin	Glycosylated J- Peptide	2305,1	2305,6
Provasopressin	154-end	1634,8	1634
Preprotachykinin A	Substance P	1346,7	1348,9
Proenkephalin	Octapeptide	929,5	929,9
Prohormone convertase 2	Fragment from pro-region	1278,6	1279,9
ProSAAS	Big LEN	1754,9	1756,2
ProSAAS	Little SAAS I	1812,01	1813,3
Calmodulin-1	C- terminal Fragment	1773,8	1774
NADH dehydrogenase	C- terminal Fragment	1522,7	1522,5
Proenkephalin	219-229	1465,6	1466,1
Prooxytocin	Oxytocin 200-211	1348,6	1348,9
ProSAAS	198-214	1707,9	1707,1
ProSAAS	Little SAAS II	1968,1	1968,4
Secretogranin II	205-218	1554,8	1554,4

Fig.5: Selected peptides identified by *in situ* MALD-TOF MS in the hypothalamus of mouse (observed mass). Peptides involved in the POMC-processing pathway are highlighted in blue. Data on predicted masses adopted from Che *et al.* 2005 (41).

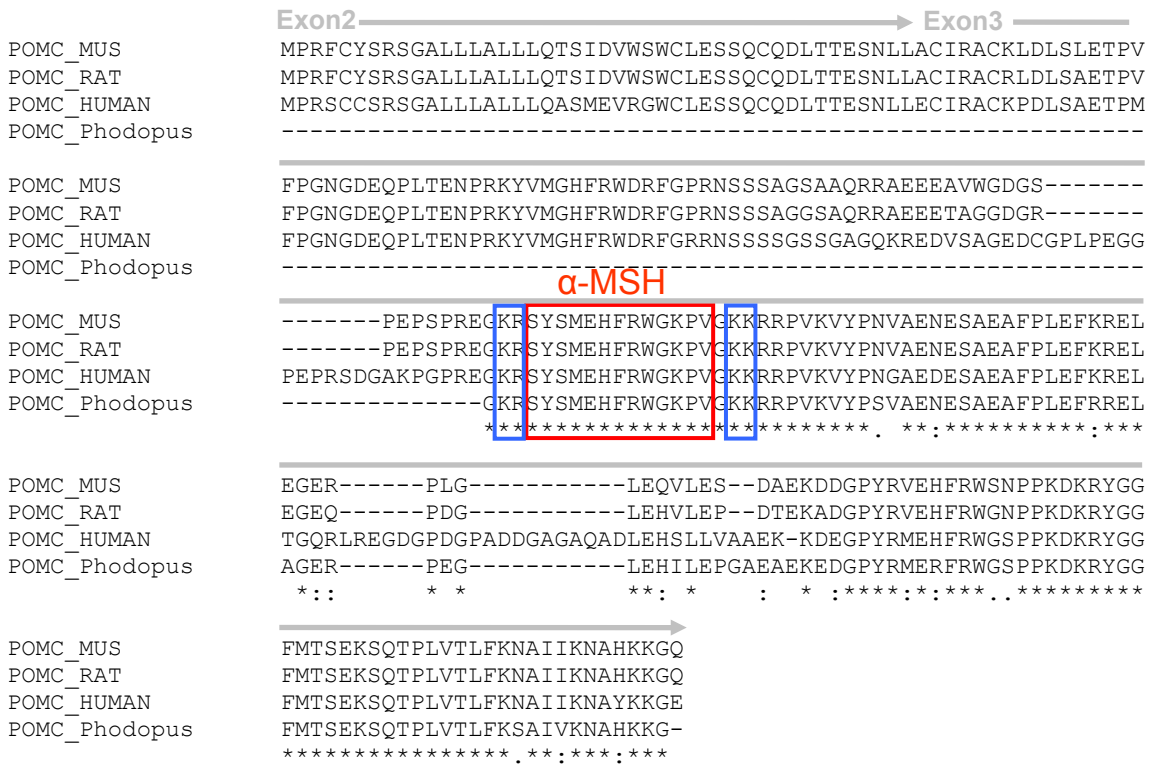

Fig.6: Amino acid sequence comparison of POMC from mouse, rat, human and Siberian hamster. Sequence encoding for α-MSH is boxed in red, flanked by di-basic amino acid residues (KR and KK) where cleavage is initiated (boxed in blue). Amino acid sequence of POMC is highly conserved throughout the different species; partial sequence encoding for α-MSH is identical therefore peptide masses are identical. Analyses in Siberian hamster brain are now possible in respect to the predicted peptide masses for α-MSH_{1-16} and α-MSH_{1-13} (Sequence of P. sungorus kindly provided by Dr. A. Ross, Aberdeen, UK)

The arcuate nucleus CART neuronal system

The arcuate nucleus neuropeptidergic circuitry exerts its regulatory action on energy balance through competing orexigenic NPY/AGRP and anorexigenic POMC/CART coexpressing neurons, forming a regulatory network that is responsive to leptin via leptin receptors (Ob-R) expressed on their surface (42). In the Siberian hamster, this neural network is also involved in the seasonal regulation of energy metabolism induced by changes in photoperiod. So far, we concentrated on the melanocortinergic component of the anorexigenic part of the arcuate neuronal network. In *Chapter III*: "CART neuronal system in the rostral arcuate nucleus mediates seasonal regulation of energy balance in the Djungarian hamster (Phodopus sungorus)" (43) we aimed to investigate the impact of photoperiod on the expression of CART within this regulatory system. On the transcriptional level it has been previously demonstrated that gene expression of CART in the Siberian hamster is tightly regulated by changes in photoperiod with increased CART mRNA in SD (37). Contrary to this observation, however, is a study that showed decreased gene expression of anorexigenic CART in SD acclimated hamsters (44). We therefore performed an immunohistochemical study on CART peptide content in the ARC of either LD- or SD-acclimated Siberian hamsters. Our study on the protein level generally reflected those previous results that showed CART expression increased in SD and thus substantiated the hypothesis that CART is a major peptidergic mediator of seasonal body weight regulation. Furthermore, we were able to demonstrate that food restriction and associated loss of body weight leads to a substantial decrease of CART-ir in SD but not in LD. This observation corroborates CARTs supposed anorexigenic function but raises the possibility of a differential responsiveness of CART to changes in photoperiod. I significantly contributed to this study and was involved in performing the IHC experiments, quantification of CART-ir and subsequent statistical analysis. Moreover, in the course of the peer-reviewing process I was able to contribute to the preparation and development of the manuscript.

Caudal brainstem and integration of photoperiod

In another project I extended the focus on hypothalamic neuroendocrine circuitries to neuroanatomical structures of the brainstem. We scrutinized the impact of photoperiod on peptidergic components of distinct areas of the caudal brainstem. Therefore, we focused on two major nuclei known to be involved in mediating a short-term related satiety response following food intake, the nucleus of the solitary tract (NTS) and the parabrachial nucleus (PBN)(45). The NTS is the primary CNS integration site for ascending visceral gut-derived satiety signals. Both, receptors for postprandial gut-released satiety hormones, and afferent vagal nerves are located or terminate in the NTS, providing the CNS with information on digestive status. Following this combined neuronal and neuroendocrine stimulation, NTS neuropeptidergic circuitries are responsible for generating an appropriate feeding behaviour by termination of food intake. Subsequently, processed satiety information is also transduced from the NTS to the PBN, a neuroanatomical relay centre, that transmits ascending signals to the paraventricular nucleus (PVN) of the hypothalamus (46). Within the hypothalamus, satiety-related information is integrated into neuroendocrine circuits of long-term energy balance regulation. We hypothesized that photoperiod modulates the expression of satiety mediating neuropeptides in the caudal brainstem, which in turn could contribute to the pronounced differential body weight trajectory observed in LD and SD acclimated Siberian hamsters. The results of this project are comprehensively summarized in *Chapter IV*: "Photoperiodic regulation of satiety mediating neuropeptides in the brainstem of the seasonal Siberian hamster (*Phodopus sungorus*)". We found a significant photoperiod-dependent effect on the expression of a number of neuropeptides and receptors, with higher levels of pre-proglucagon- (PPG) and melanocortin 4 receptor- (MC4-R) mRNA and increased cholecystokinin-ir (CCK) in the NTS of LD-acclimated hamsters. All of these are components of anorexigenic systems that have been demonstrated to potently suppress food intake. We concluded that increased expression of PPG, MC4-R and CCK in LD is a primary response to

increased feeding activity in LD. In the PBN, however, CCK-ir was diminished in LD and an up-regulation of anorexigenic corticotrophin realising hormone-ir (CRH) and neurotensin-ir (NT) occurred in SD. This photoperiod-related switch in anorexigenic gut-brain signalling may provide the long-term energy balance regulating circuitries of the hypothalamus with satiety-related information in SD and may therefore partially explain the decrease in body weight following transition to SD. In summary, for the first time we demonstrated that expression of major satiety mediating peptides is influenced by photoperiod in the brain stem. Conclusively, short-term hunger/satiety-mediating peptidergic components of the caudal gut-brain axis may act as an important mechanism contributing to the seasonal long-term adipostatic regulation of energy balance in the Siberian hamster.

Peripheral signals and central regulation of energy balance

Peripherally secreted hormones such as leptin, insulin and ghrelin provide the CNS with vital information on the availability of energy stores and acute feeding status. Thus, they are essential in the central orchestration and regulation of energy balance. The following two chapters of my PhD thesis are dedicated to these blood borne hormones and their integration to the central regulatory network. Under the leading initiative of Dr. A. Tups, we performed a number of studies aimed to elucidate the impact of these peripheral hormones and their intracellular signalling cascades on the seasonal regulation of body weight in *P. sungorus*.

It is well established that photoperiod-induced changes in body weight displayed by the Siberian hamster are associated by a reversible switch in leptin sensitivity. The apparent insensitivity to anorexigenic effects of leptin in LD acclimated hamsters, which are marked by a pronounced weight gain despite substantial body fat stores, initiated extensive research in order to identify the responsible molecular mediators. However, leptin is not the only "adipostatic" hormone that exerts an anorexigenic drive on central regulatory circuitries in

times of a positive energy balance. Insulin is acutely secreted from the pancreas in response to increased blood glucose but its basal levels are also directly correlated with the amount of body fat stores (47). Insulin is then transported to the brain and binds to its receptor (IR), in particular those expressed on neurons in the hypothalamic ARC, leading to the activation of downstream anorexigenic signalling pathways. Interestingly, leptin and insulin share molecular components of the intracellular signal transduction cascade. The question addressed in the first study was therefore, if body weight regulation in the seasonal Siberian hamster is associated in a modification of insulin signal transduction, similar to those observed for leptin. We therefore scrutinized the gene expression of IR and major components of the intracellular insulin signalling cascade, including phosphatidylinositol 3-kinase (PI3-kinase) and insulin signaling inhibiting peptide PTP1B. Furthermore, we investigated phosphorylation of AKT (also known as protein kinase B) by immunohistochemistry in the photoperiod paradigm. The outcome of this study resulted in a publication presented in *Chapter V*: "Photoperiodic regulation of insulin receptor mRNA and intracellular insulin signalling in the arcuate nucleus of the Siberian hamster, Phodopus sungorus" (48). Surprisingly, we found reduced insulin signalling in SD represented by a down-regulation of IR gene expression. Associated, we observed decreased phospho-AKT-ir in neurons of the ARC and a decrease of PTB1B mRNA. The decrease in insulin signalling in SD was rather counterintuitive with respect of the strong anorexigenic potential of insulin. I contributed to this study by verifying the results on PTB1B gene expression by performing *in situ* hybridization on brain slices of hamsters kept in a photoperiod paradigm experiment. The results obtained by quantification of PTB1B gene expression in this experiment reassemble those observed in the photoperiod experiment presented in the present study.

In contrast to leptin and insulin, ghrelin is the only peripheral orexigenic hormone identified so far. Ghrelin is a gastric polypeptide produced by the stomach in times of gastric idleness (49). Circulating ghrelin enters the brain via the bloodstream and exerts its orexigenic

action by binding to the hypothalamic growth hormone secretagogue receptor (GHS-R) (50). Acute food restriction has been reported to induce a substantial increase in either blood ghrelin and GHS-R mRNA levels in rat. In *Chapter VI*: "Circulating ghrelin levels and central ghrelin receptor expression is elevated in response to food deprivation in the seasonal hamster (Phodopus sungorus)" we investigated the effect of long-term metabolic changes induced by photoperiod and chronic food restriction on the expression of central GHS-R mRNA and circulating ghrelin levels. Our study revealed that seasonal adaptations induced by photoperiod in the Siberian hamster are not accompanied by changes in ghrelin signalling. However, we found significantly higher GHS-R mRNA and serum ghrelin levels following food deprivation for 48h in LD and SD hamsters. Our results suggest that ghrelin is an acute regulator of energy balance with rather minor impact on seasonal long-term body weight regulation. I performed IHC on the two isoforms of GHS-R (1a and 1b) and western blot analysis on hypothalamic tissue from LD- and SD-acclimated Siberian hamsters. These data, however, were excluded from the manuscript in the following review process.

Further scientific contributions

Beyond my core PhD project, I applied my acquired neuroanatomical and methodogical skills in other projects. This work resulted in a significant contribution of the peer-reviewed publications in *Chapter VII*: "Functional characterisation of UCP1 in the common carp: uncoupling activity in liver mitochondria and cold-induced expression in the brain."(51) and *Chapter VIII*: "Marsupial uncoupling protein 1 sheds light on the evolution of mammalian nonshivering thermogenesis" (52).

In both studies, we aimed to characterise the phylogenetic origin and functional role of the thermogenic mammalian uncoupling proteins (UCPs) in vertebrates. UCPs are located in the inner membrane of mitochondria, and in particular UCP1 can only be found in brown adipose tissue (BAT) of small eutherian mammals. In BAT, this protein is responsible for adaptive

nonshivering thermogenesis by uncoupling of oxidative phosphorylation from ATP synthesis which dissipates proton motive force as heat (for review see (53). So far, almost all eutherian species under investigation express UCP-1, giving them a crucial advantage in coping with hostile environmental challenges like cold temperatures. However, it was recently demonstrated that UCP-1 orthologues can also be found in ectothermic members of the animal kingdom (54). Data on the function and distribution of UCPs obtained from other species than eutherian mammals can thus provide valuable information on the phylogenetic evolution of thermogenesis. In this context the first study was designed to scrutinize the anatomical localization and biochemical function of UCP-1 in an ectothermic vertebrate, the common carp (*Cyprinus carpio*). The major outcome of this study was that UCP-1 of ectothermic vertebrates excretes similar biochemical functions than those observed in placental mammals. Contrary to its expression in BAT of eutherian mammals, UCP-1 is not expressed in fat tissue of fish. However, higher levels of UCP-1 mRNA were found in whole brains of cold-adapted carps, suggesting an involvement of UCP-1 in maintaining an appropriate temperature guaranteeing the functionality of the central nervous system under cold conditions. Most interestingly, a brain heater organ in the swordfish has been previously described but the molecular mechanisms of heat production could not be pinpointed in these studies (55). Dr. M. Jastroch and I performed *in-situ* hybridization to localize UCP-1 transcripts with neuroanatomical precision within the brain of *C. carpio*. Therefore cryo-sectioning on carp brains was employed, following hybridization of sagittal and coronal brain sections with a radioactive-labelled riboprobe complementary to partial fragments of UCP-1. The result is presented in *Chapter VIII*, Fig. 4 b-c. We found strong expression of UCP-1 in the periventricular grey zone of the optic tectum and the descending trigeminal and solitary tract of the brainstem. While the optic tectum is related to sensory functions such as the visual system, descending trigeminal tract and the solitary tract function in the regulation of motor activity and energy homeostasis. With respect of the pivotal role of all of these three

regulating systems it seems intuitive, that expression of UCP-1 may therefore be part of a thermocompensatory mechanism that helps maintaining a functional neural activity in times of cold-stress.

In the second paper, we identified the expression of UCP-1 in marsupials and examined its physiological role. Comparative studies on the role of marsupials were performed in three different members of the two major marsupial subgroups: *Sminthopsis crassicaudata*, and *Antechinus flavipes*, belonging to Australian marsupials, as well as *Monodelphis domestica*, a Southamerican species. While UCP1 mRNA was expressed in high amounts in *S. crassicaudata*, resembling tissue-specificity and gene regulation observed in eutherian mammals, low expression levels (only detectable using PCR techniques) were only found in 70 days old juvenile *M. domestica.* Therefore, it was of major importance to develop a whole-mount *in situ* hybridization protocol to detect UCP-1 and UCP-2 transcripts in embryos of *M. domestica* in order to assign gene expression to different tissue-types. The results are presented in *Chapter IX*, Fig. 3B. We found no signal for UCP-1 in sagittal sections of 22-25 days old *M. domestica,* however, we were able to detect UCP-2 mRNA in heart, liver and spleen. Together, these results imply that UCP-1 is expressed in certain marsupials, but, as it is the case in *M. domestica,* its expression is restricted to early stages of their development. Furthermore, the above described histological procedure on whole rodent bodies became integral part of following studies in our group.

Along with my PhD project I tried to expand my theoretical knowledge by attending to different symposia. In return I took the advantage to share achieved results with the scientific community and to establish fruitful collaborations with other colleagues. This engagement is documented by a list of abstracts that were part of active participations to national and international meetings and conferences. Selected abstracts are presented in *Chapter IX*: “Conferences & Book Abstracts”.

CONCLUSION

The neuroendocrine control of seasonal energy balance comprises different levels of regulation ranging from integration and processing of photoperiod to peripheral and central neuronal circuitries, to the interaction and modulation of numerous neuropeptides and intracellular signalling cascades at the molecular level. The present PhD thesis therefore aimed to address different aspects of seasonal energy balance regulation.

Certainly POMC/CART expressing neurons of the arcuate nucleus are part of an anorexigenic hypothalamic network that potently inhibits food intake and induces a body weight decrease upon stimulation. In the seasonal Siberian hamster, however, it remained unclear if this peptidergic network is involved in the regulation of short day photoperiod-induced body weight decrease. Gene expression of POMC has been reported to be unaffected by changes in photoperiod. Pro-opiomelanocortin, however, is a polypeptide precursor and has to undergo extensive post-translational processing before its neuropeptide products achieve biological activity. Despite unchanged gene expression we discovered a higher abundance of anorexigenic POMC-derived neuropeptides α-MSH and β-endorphin in SD-acclimated hamster. Subsequently, we were able to identify the molecular proteolytic mechanism that regulates maturation of POMC-derived peptides at the post-translational level leading to the increased production of anorexigenic peptides. We comprehensively investigated the initial cleavage events by endoproteolytic acting pro-hormone convertases and observed that a higher abundance of PC2 in SD is associated with increased levels of α-MSH and β-endorphin within the melanocortinergic neurons of the ARC. We substantiated this finding and identified carboxypeptidase E, an enzyme responsible for the terminal activation of neuropeptides, to be photoperiod-dependently regulated. Hence, observed body weight loss in SD is most likely in parts attributable to a higher turn over of inactive to active anorexigenic α-MSH. In summary this PhD thesis establishes post-translational processing

events as a key regulatory mechanism that is necessary for the coordinated biosynthesis of energy homeostasis regulating neuropeptides.

In addition, in a second approach, we identified several peptidergic candidates expressed in structures of the caudal brainstem that were influenced by photoperiod. To our knowledge this is the first study addressing the question if caudal brainstem circuitries related to short-term control of food intake are modulated in response to changing photoperiod. In this study we found increased satiety signalling in the parabrachial nucleus that relays gut-related information to hypothalamic circuitries of long-term energy balance regulation in SD. Thus, we concluded that satiety information is photoperiod-dependent modulated in the Siberian hamster most likely contributing to establish the seasonal body weight differential. The precise mechanism, however, by which photoperiod effects the observed changes in the caudal brainstem remains unclear.

Taken together certain questions remain to be answered. Are there any further post-translational events such as amidation or acetylation influenced by photoperiod? Are the observed changes in enzyme expression converted to modification of neuropeptides? If so, we need to establish a peptidomic approach to quantify the resulting peptide modifications. Future studies will be necessary to further elucidate the post-translational fate of other neuropeptides involved in the regulation of energy balance in the seasonal Siberian hamster.

REFERENCES

1. Schwartz MW, Woods SC, Porte D, Jr., Seeley RJ, Baskin DG. Central nervous system control of food intake Nature 2000; 404**:** 661-671.

2. Huszar D, Lynch CA, Fairchild-Huntress V, Dunmore JH, Fang Q, Berkemeier LR, Gu W, Kesterson RA, Boston BA, Cone RD, Smith FJ, Campfield LA, Burn P, Lee F. Targeted disruption of the melanocortin-4 receptor results in obesity in mice Cell 1997; 88**:** 131-141.

3. Yaswen L, Diehl N, Brennan MB, Hochgeschwender U. Obesity in the mouse model of pro-opiomelanocortin deficiency responds to peripheral melanocortin Nat Med 1999; 5**:** 1066-1070.

4. Butler AA, Cone RD. Knockout models resulting in the development of obesity Trends Genet 2001; 17**:** S50-S54.

5. KENNEDY GC. The role of depot fat in the hypothalamic control of food intake in the rat Proc R Soc Lond B Biol Sci 1953; 140**:** 578-596.

6. Bruning JC, Gautam D, Burks DJ, Gillette J, Schubert M, Orban PC, Klein R, Krone W, Muller-Wieland D, Kahn CR. Role of brain insulin receptor in control of body weight and reproduction Science 2000; 289**:** 2122-2125.

7. Mercer JG, Hoggard N, Williams LM, Lawrence CB, Hannah LT, Trayhurn P. Localization of leptin receptor mRNA and the long form splice variant (Ob-Rb) in mouse hypothalamus and adjacent brain regions by in situ hybridization FEBS Lett 1996; 387**:** 113-116.

8. Marks JL, Porte D, Jr., Stahl WL, Baskin DG. Localization of insulin receptor mRNA in rat brain by in situ hybridization Endocrinology 1990; 127**:** 3234-3236.

9. Cheung CC, Clifton DK, Steiner RA. Proopiomelanocortin neurons are direct targets for leptin in the hypothalamus Endocrinology 1997; 138**:** 4489-4492.

10. Baskin DG, Breininger JF, Schwartz MW. Leptin receptor mRNA identifies a subpopulation of neuropeptide Y neurons activated by fasting in rat hypothalamus Diabetes 1999; 48**:** 828-833.

11. McMinn JE, Wilkinson CW, Havel PJ, Woods SC, Schwartz MW. Effect of intracerebroventricular alpha-MSH on food intake, adiposity, c-Fos induction, and neuropeptide expression Am J Physiol Regul Integr Comp Physiol 2000; 279**:** R695-R703.

12. Cone RD, Lu D, Koppula S, Vage DI, Klungland H, Boston B, Chen W, Orth DN, Pouton C, Kesterson RA. The melanocortin receptors: agonists, antagonists, and the hormonal control of pigmentation Recent Prog Horm Res 1996; 51**:** 287-317.

13. Berthoud HR, Sutton GM, Townsend RL, Patterson LM, Zheng H. Brainstem mechanisms integrating gut-derived satiety signals and descending forebrain information in the control of meal size Physiol Behav 2006; 89**:** 517-524.

14. Dhillo WS, Bloom SR. Gastrointestinal hormones and regulation of food intake Horm Metab Res 2004; 36**:** 846-851.

15. Murphy KG, Bloom SR. Gut hormones and the regulation of energy homeostasis Nature 2006; 444**:** 854-859.

16. Mercer JG, Moar KM, Hoggard N. Localization of leptin receptor (Ob-R) messenger ribonucleic acid in the rodent hindbrain Endocrinology 1998; 139**:** 29-34.

17. Joseph SA, Pilcher WH, nett-Clarke C. Immunocytochemical localization of ACTH perikarya in nucleus tractus solitarius: evidence for a second opiocortin neuronal system Neurosci Lett 1983; 38**:** 221-225.

18. Grill HJ, Kaplan JM. Sham feeding in intact and chronic decerebrate rats Am J Physiol 1992; 262**:** R1070-R1074.

19. Morton GJ, Blevins JE, Williams DL, Niswender KD, Gelling RW, Rhodes CJ, Baskin DG, Schwartz MW. Leptin action in the forebrain regulates the hindbrain response to satiety signals J Clin Invest 2005; 115**:** 703-710.

20. Norgren R. Projections from the nucleus of the solitary tract in the rat Neuroscience 1978; 3**:** 207-218.

21. Nillni EA. Regulation of prohormone convertases in hypothalamic neurons: implications for prothyrotropin-releasing hormone and proopiomelanocortin Endocrinology 2007; 148**:** 4191-4200.

22. Steiner DF. The proprotein convertases Curr Opin Chem Biol 1998; 2**:** 31-39.

23. Fricker LD, McKinzie AA, Sun J, Curran E, Qian Y, Yan L, Patterson SD, Courchesne PL, Richards B, Levin N, Mzhavia N, Devi LA, Douglass J. Identification and characterization of proSAAS, a granin-like neuroendocrine peptide precursor that inhibits prohormone processing J Neurosci 2000; 20**:** 639-648.

24. Mzhavia N, Berman Y, Che FY, Fricker LD, Devi LA. ProSAAS processing in mouse brain and pituitary J Biol Chem 2001; 276**:** 6207-6213.

25. Muller L, Zhu X, Lindberg I. Mechanism of the facilitation of PC2 maturation by 7B2: involvement in ProPC2 transport and activation but not folding J Cell Biol 1997; 139**:** 625-638.

26. Song L, Fricker LD. Tissue distribution and characterization of soluble and membrane-bound forms of metallocarboxypeptidase D J Biol Chem 1996; 271**:** 28884-28889.

27. Fricker LD. Carboxypeptidase E Annu Rev Physiol 1988; 50**:** 309-321.

28. Pritchard LE, White A. Neuropeptide processing and its impact on melanocortin pathways Endocrinology 2007; 148**:** 4201-4207.

29. Cawley NX, Zhou J, Hill JM, Abebe D, Romboz S, Yanik T, Rodriguiz RM, Wetsel WC, Loh YP. The carboxypeptidase E knockout mouse exhibits endocrinological and behavioral deficits Endocrinology 2004; 145**:** 5807-5819.

30. Klingenspor M, Niggemann H, Heldmaier G. Modulation of leptin sensitivity by short photoperiod acclimation in the Djungarian hamster, Phodopus sungorus J Comp Physiol [B] 2000; 170**:** 37-43.

31. Tups A, Ellis C, Moar KM, Logie TJ, Adam CL, Mercer JG, Klingenspor M. Photoperiodic regulation of leptin sensitivity in the Siberian hamster, Phodopus sungorus, is reflected in arcuate nucleus SOCS-3 (suppressor of cytokine signaling) gene expression Endocrinology 2004; 145**:** 1185-1193.

32. Mercer JG, Tups A. Neuropeptides and anticipatory changes in behaviour and physiology: seasonal body weight regulation in the Siberian hamster Eur J Pharmacol 2003; 480**:** 43-50.

33. Heldmaier G, Steinlechner S, Rafael J, Latteier B. Photoperiod and ambient temperature as environmental cues for seasonal thermogenic adaptation in the Djungarian hamster, Phodopus sungorus Int J Biometeorol 1982; 26**:** 339-345.

34. Steinlechner S, Heldmaier G. Role of photoperiod and melatonin in seasonal acclimatization of the Djungarian hamster, Phodopus sungorus Int J Biometeorol 1982; 26**:** 329-337.

35. Steinlechner S, Heldmaier G, Becker H. The seasonal cycle of body weight in the Djungarian hamster: photoperiodic control and the influence of starvation and melatonin. In: Oecologica; Vol. 60, No. 3: 1983: 401-405.

36. Mercer JG, Lawrence CB, Beck B, Burlet A, Atkinson T, Barrett P. Hypothalamic NPY and prepro-NPY mRNA in Djungarian hamsters: effects of food deprivation and photoperiod Am J Physiol 1995; 269**:** R1099-R1106.

37. Mercer JG, Ellis C, Moar KM, Logie TJ, Morgan PJ, Adam CL. Early regulation of hypothalamic arcuate nucleus CART gene expression by short photoperiod in the Siberian hamster Regul Pept 2003; 111**:** 129-136.

38. Mercer JG, Moar KM, Ross AW, Hoggard N, Morgan PJ. Photoperiod regulates arcuate nucleus POMC, AGRP, and leptin receptor mRNA in Siberian hamster hypothalamus Am J Physiol Regul Integr Comp Physiol 2000; 278**:** R271-R281.

39. Helwig M, Khorooshi RM, Tups A, Barrett P, Archer ZA, Exner C, Rozman J, Braulke LJ, Mercer JG, Klingenspor M. PC1/3 and PC2 gene expression and post-translational endoproteolytic pro-opiomelanocortin processing is regulated by photoperiod in the seasonal Siberian hamster (Phodopus sungorus) J Neuroendocrinol 2006; 18**:** 413-425.

40. Che FY, Lim J, Pan H, Biswas R, Fricker LD. Quantitative neuropeptidomics of microwave-irradiated mouse brain and pituitary Mol Cell Proteomics 2005; 4**:** 1391-1405.

41. Che FY, Biswas R, Fricker LD. Relative quantitation of peptides in wild-type and Cpe(fat/fat) mouse pituitary using stable isotopic tags and mass spectrometry J Mass Spectrom 2005; 40**:** 227-237.

42. Ellacott KL, Cone RD. The central melanocortin system and the integration of short- and long-term regulators of energy homeostasis Recent Prog Horm Res 2004; 59**:** 395-408.

43. Khorooshi R, Helwig M, Werckenthin A, Steinberg N, Klingenspor M. Seasonal regulation of cocaine- and amphetamine-regulated transcript in the arcuate nucleus of Djungarian hamster (Phodopus sungorus) Gen Comp Endocrinol 2008; 157**:** 142-147.

44. Robson AJ, Rousseau K, Loudon AS, Ebling FJ. Cocaine and amphetamine-regulated transcript mRNA regulation in the hypothalamus in lean and obese rodents J Neuroendocrinol 2002; 14**:** 697-709.

45. Edwards GL, Ritter RC. Lateral parabrachial lesions attenuate ingestive effects of area postrema lesions Am J Physiol 1989; 256**:** R306-R312.

46. Guo L, Munzberg H, Stuart RC, Nillni EA, Bjorbaek C. N-acetylation of hypothalamic alpha-melanocyte-stimulating hormone and regulation by leptin Proc Natl Acad Sci U S A 2004; 101**:** 11797-11802.

47. Woods SC, Seeley RJ. Insulin as an adiposity signal Int J Obes Relat Metab Disord 2001; 25 Suppl 5**:** S35-S38.

48. Tups A, Helwig M, Stohr S, Barrett P, Mercer JG, Klingenspor M. Photoperiodic regulation of insulin receptor mRNA and intracellular insulin signaling in the arcuate nucleus of the Siberian hamster, Phodopus sungorus Am J Physiol Regul Integr Comp Physiol 2006; 291**:** R643-R650.

49. Kojima M, Kangawa K. Ghrelin, an orexigenic signaling molecule from the gastrointestinal tract Curr Opin Pharmacol 2002; 2**:** 665-668.

50. Kamegai J, Tamura H, Shimizu T, Ishii S, Sugihara H, Wakabayashi I. Central effect of ghrelin, an endogenous growth hormone secretagogue, on hypothalamic peptide gene expression Endocrinology 2000; 141**:** 4797-4800.

51. Jastroch M, Buckingham JA, Helwig M, Klingenspor M, Brand MD. Functional characterisation of UCP1 in the common carp: uncoupling activity in liver mitochondria and cold-induced expression in the brain J Comp Physiol [B] 2007; 177**:** 743-752.

52. Jastroch M, Withers KW, Taudien S, Frappell PB, Helwig M, Fromme T, Hirschberg V, Heldmaier G, McAllan BM, Firth BT, Burmester T, Platzer M, Klingenspor M. Marsupial uncoupling protein 1 sheds light on the evolution of mammalian nonshivering thermogenesis Physiol Genomics 2008; 32**:** 161-169.

53. Klingenspor M, Fromme T, Hughes DA, Jr., Manzke L, Polymeropoulos E, Riemann T, Trzcionka M, Hirschberg V, Jastroch M. An ancient look at UCP1 Biochim Biophys Acta 2008.

54. Jastroch M, Wuertz S, Kloas W, Klingenspor M. Uncoupling protein 1 in fish uncovers an ancient evolutionary history of mammalian nonshivering thermogenesis Physiol Genomics 2005; 22**:** 150-156.

55. Carey FG. A brain heater in the swordfish Science 1982; 216**:** 1327-1329.

Journal of Neuroendocrinology, 2006, Vol. 18, 413–425 doi:10.1111/j.1365-2826.2006.01431.x

PC1/3 and PC2 Gene Expression and Post-Translational Endoproteolytic Pro-Opiomelanocortin Processing is Regulated by Photoperiod in the Seasonal Siberian Hamster (*Phodopus sungorus*)

M. Helwig,*† R. M. H. Khorooshi,‡ A. Tups,† P. Barrett,* Z. A. Archer,* C. Exner,† J. Rozman,† L. J. Braulke,† J. G. Mercer* and M. Klingenspor†

*Molecular Endocrinology Group, Division of Obesity and Metabolic Health, Rowett Research Institute, Aberdeen Centre for Energy Regulation and Obesity (ACERO), Aberdeen, UK.

†Department of Animal Physiology, Biology Faculty, Philipps University Marburg, Marburg, Germany.

‡Medical Biotechnology Centre, University of Southern Denmark, Odense, Denmark.

Key words: seasonal body weight regulation, proteolytic processing, photoperiod, prohormone convertases, POMC.

Abstract

A remarkable feature of the seasonal adaptation displayed by the Siberian hamster (*Phodopus sungorus*) is the ability to decrease food intake and body weight (by up to 40%) in response to shortening photoperiod. The regulating neuroendocrine systems involved in this adaptation and their neuroanatomical and molecular bases are poorly understood. We investigated the effect of photoperiod on the expression of prohormone convertases 1 (PC1/3) and 2 (PC2) and the endoproteolytic processing of the neuropeptide precursor pro-opiomelanocortin (POMC) within key energy balance regulating centres of the hypothalamus. We compared mRNA levels and protein distribution of PC1/3, PC2, POMC, adrenocorticotrophic hormone (ACTH), α-melanocyte-stimulating hormone (MSH), β-endorphin and orexin-A in selected hypothalamic areas of long day (LD, 16 : 8 h light : dark), short day (SD, 8 : 16 h light : dark) and natural-day (ND, photoperiod depending on time of the year) acclimated Siberian hamsters. The gene expression of PC2 was significantly higher within the arcuate nucleus (ARC, $P < 0.01$) in SD and in ND (versus LD), and is reflected in the day length profile between October and April in the latter. PC1/3 gene expression in the ARC and lateral hypothalamus was higher in ND but not in SD compared to the respective LD controls. The immunoreactivity of PC1/3 cleaved neuropeptide ACTH in the ARC and PC1/3-colocalised orexin-A in the latyeral hypothalamus were not affected by photoperiod changes. However, increased levels of PC2 mRNA and protein were associated with higher abundance of the mature neuropeptides α-MSH and β-endorphin ($P < 0.01$) in SD. This study provides a possible explanation for previous paradoxical findings showing lower food intake in SD associated with decreased POMC mRNA levels. Our results suggest that a major part of neuroendocrine body weight control in seasonal adaptation may be effected by post-translational processing mediated by the prohormone convertases PC1/3 and PC2, in addition to regulation of gene expression of neuropeptide precursors.

Seasonal animals such as the Siberian hamster (*Phodopus sungorus*) exhibit remarkable physiological and metabolic adaptations in response to the seasonally changing environment. These adaptations include changes in coat insulation and colour, reproductive activity, food intake and body weight (1). The drive to reduce food intake in shortening winter photoperiod persists even if food is provided *ad lib* demonstrating the importance of this regulatory energy balance mechanism. A key neuronal centre that regulates these physiological responses is the hypothalamus, an area of the central nervous system (CNS) that integrates photoperiodic and peripheral inputs in a complex network of interacting orexigenic and anorexigenic neuropeptides (2, 3). The Siberian hamster processes information on changing photoperiod through the pineal hormone, melatonin, and about internal energy stores via peripherally released hormones such

Correspondence to: Michael Helwig, Animal Physiology, Department of Biology, Philipps-University, Karl-von-Frisch-Str. 8, 35032 Marburg, Germany (e-mail: helwigmi@staff.uni-marburg.de).

as leptin and ghrelin, to generate appropriate responses in terms of energy balance regulation (4–6). The voluntary decrease in food intake and body weight in short day (SD) presumably reflects the increased activity of anorexigenic components of this neuroendocrine system. One of the neuropeptides that would meet this criterion is alpha-melanocyte-stimulating hormone (α-MSH) (7, 8), a product of the 30–32 kDa molecule pro-opiomelanocortin (POMC), which exerts an inhibitory control on food intake and energy storage through its action in the CNS at the melanocortin 3 and 4 receptors (9). Unexpectedly, previous studies demonstrated decreased gene expression of the precursor POMC in SD which could in principal result in lower concentrations of α-MSH during winter (10–12). However, most neuropeptide precursors such as POMC have to undergo post-translational processing by proteolytic cleavage before their products acquire biological activity. The post-translational process is accomplished by highly specific cleavage enzymes (prohormone convertases) and is therefore an essential step not only as a part of the protein biosynthetic process, but also as a regulatory step in neuropeptide synthesis. In mammals, prohormone convertases 1/3 (PC1/3) and 2 (PC2), which are members of the subtilisin-like proprotein convertases, have been identified to be responsible for the proteolytic processing of neuropeptides and peptide hormones in neuronal endocrine tissue (13).

Both PC1/3 and PC2 are expressed in neuroendocrine tissues such as hypothalamic neurones and cleave prohormones at paired basic residues. The biosynthesis of several major orexigenic and anorexigenic peptides derived from precursors within this neuroendocrine network is reliant on the post-translational activity of these enzymes. Neuropeptides such as neuropeptide-Y (NPY) (14), and cocaine- and amphetamine-regulated transcript (CART) (15), which are involved in the regulation of energy homeostasis and feeding, are subject to enzymatic processing by PC1/3 and PC2. Consequently, this system must be considered an extensive control mechanism in neuropeptide maturation. Interestingly, PC2 has been shown to be mainly involved in the production of the anorexigenic peptides, α-MSH and CART, whereas PC1/3 is responsible for the generation of potent orexigenic NPY in the hypothalamus (16–18).

The cleavage-specificity of PC1/3 and PC2 in POMC processing was reported by cell transfection experiments. It has been demonstrated that PC1/3 cleaves POMC into large intermediate molecules, such as adrenocorticotrophic hormone (ACTH) and β-lipotrophin, whereas PC2 subsequently cleaves ACTH and β-lipotrophin into α-MSH and β-endorphin, respectively (Fig. 1) (19, 20). Thus, coordinated cleavage activity of both prohormone convertases is necessary to process neuropeptide precursors such as POMC into specific neuropeptides. Because PC1/3 and PC2 are essential for the post-translational processing of various neuropeptide precursors, it is likely that changes in gene expression and biosynthesis have fundamental effects on the maturation of neuropeptides and hence energy homeostasis.

We hypothesised that POMC processing is photoperiodically regulated by differential expression of PC1/3 and PC2. It is likely that decreasing body weight in SD acclimated hamsters is associated with higher levels of anorexigenic neuropeptides

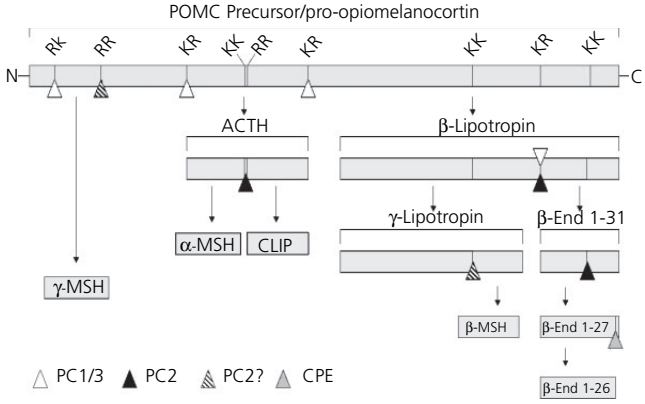

Fig. 1. Diagrammatic representation of post-translational endoproteolytic pro-opiomelanocortin (POMC) processing by prohormone convertases 1/3 (PC1/3) and 2 (PC2) and carboxypeptidase E (CPE). Cleavage sites are marked by paired basic amino acids R (Lysine) and K (Arginine). Sites believed but not confirmed as being processed by PC2 are indicated by hatched triangles. ACTH, Adrenocorticotrophic hormone; CLIP, corticotrophin-like intermediate peptide.

such as α-MSH despite down-regulated gene expression of POMC. We suggest that differential endoproteolytic activity of prohormone convertases in SD and long day (LD) is responsible for photoperiod-regulated biosynthesis of smaller POMC-derived neuropeptides. To test this, gene expression of PC1/3 and PC2 was investigated in hamsters exposed to ambient photoperiod in winter (October to April) to profile long-term effects. In addition, we measured mRNA expression levels of PC1/3 and PC2 following transfer of Siberian hamsters back into LD, after 14 weeks in artificial SD photoperiod. This experimental setup provided a better assessment of the temporal responsiveness of photoperiod-induced regulation of gene expression. Neuroanatomical protein distribution and differential expression of PC1/3, PC2, POMC, ACTH, α-MSH, and β-endorphin in SD and LD acclimated hamsters were investigated by immunohistochemistry. In a second approach, we used dual-fluorescence immunohistochemistry to colocalise the prohormone convertases with POMC and the derived neuropeptides to evaluate the ratio of proteolytic activity of PC1/3 and PC2 in SD and LD, respectively.

Previous reports have indicated neuroanatomical localisation of PC1/3 mRNA in the lateral hypothalamus (LH) (21), an important region of energy balance regulation (22) containing various potential targets for PC1/3 cleavage. As a consequence, we also focused on a neuropeptide precursor candidate for post-translational modification within this region. Although POMC is not expressed in this region, several pro-forms of different neuropeptides have been localised in the LH including pro-dynorphin (23), pro-melanin-concentrating hormone (24) and pro-orexin (25). All of these molecules are precursors of anabolic neuropeptides that exert opposing effects to those derived from POMC in the arcuate nucleus (ARC) (26). Pro-orexin was selected for investigation because we previously observed PC1/3 mRNA localised in prepro-orexin mRNA expressing neurones in the LH, which suggested a functional relationship of these neuroendocrine components. These recent observations at the mRNA level were extended to the protein level using immunohistochemical methods.

Materials and methods

Animals and experimental procedures

All described procedures were performed in accordance with German animal welfare regulation, or were licensed under the UK Home Office Animals (Scientific Procedures) Act, 1986, and had local ethical approval.

Siberian hamsters (*P. sungorus*) were drawn from breeding colonies established in the Biology Faculty in Marburg (Germany) and at the Rowett Research Institute in Aberdeen (Scotland). All animals were housed individually and had *ad lib* access to food (Marburg: Standard breeding chow diet, 7014, Altromin, Lage, Germany; Aberdeen: Labsure pelleted diet, Special Diet Services, Witham, UK) and water. Body weights were assessed weekly. Photoperiods referred to in this article are defined as LD (long day, 16 : 8 h light : dark), SD (short day, 8 : 16 h light : dark) and ND (natural day, with day length depending on time of the year).

Experiment 1

Siberian hamsters (n = 72, Marburg colony) were born and reared in ND at 23 °C. At the age of 4–6 months, they were divided into two groups. One group (n = 36, matched for sexes) was transferred to LD whereas the other (n = 36, matched for sexes) was maintained in ND and exposed to the progressive change in natural day length from October until April. At intervals of 40 days (October, November, January, February, March, April), hamsters from the LD and ND group (three males, three females per group) were killed with CO_2 and decapitated. Brains were immediately dissected, frozen on dry ice and stored at − 80 °C until required. The day length in ND photoperiod was calculated using the Sunrise/Sunset Calculator software (National Oceanic and Atmospheric Administration, Washington, DC, USA) based on the geographical location of the breeding facility in Marburg (8°46′17, 7′/50°48′17, 5′).

Experiment 2

Male Siberian hamsters (n = 32, Aberdeen colony) were housed individually at 22 °C. Hamsters used in this experiment were born and reared in LD. When they were 4–6 months old, half the animals (n = 16) were transferred to SD. After 14 weeks (week 0), a group of LD and SD hamsters (n = 4/group) were killed by cervical dislocation. All the remaining SD hamsters were transferred back to LD photoperiod. LD controls and hamsters transferred back from SD to LD (n = 4 per group) were then killed at intervals of 2 weeks (week 2, 4 and 6; 27). Brains were immediately dissected, frozen on dry ice and stored at −80 °C until required.

In situ *hybridisation*

Messenger RNA levels for PC1/3 and PC2 were quantified by *in situ* hybridisation in 15-μm coronal sections. Sections were collected throughout the extent of the hypothalamus onto two sets of 12 slides with six or seven sections mounted on each slide. Accordingly, slides spanned the lateral hypothalamic region approximating from −1.5 mm to −3.2 mm and the arcuate nucleus from −1.8 mm to −3.7 mm relative to Bregma, according to the atlas of the golden hamster brain (27). Two slides (one per set) from each animal were hybridised with a Siberian hamster specific PC1/3 or PC2 riboprobe cloned from cDNA, using techniques described in detail elsewhere (28). A control was performed by hybridising sections with equal length sense riboprobes of PC1/3 and PC2 resulting in no signal. Riboprobes complementary to partial fragments of PC1/3 and PC2 gene were generated from cloned Siberian hamster brain cDNA. The amplification of the PC1/3 (248 bp, GenBank AY625692) and PC2 (232 bp GenBank AY625693) fragments was performed by PCR using the primers: 5′-ATGGGGGTCGTCAAGGAG-ATAACT-3′ and 5′-GATGCCAGCAGCAGCCAGAGGTG-3′ (rat PC1/3, GenBank M76705) and 5′-GCGGCCGGGCTTCTCTTCT-3′ and 5′-GCT-GCCGCTTGTGATGTAGG-3′ (rat PC2, GenBank M76706), respectively. Both DNA fragments were ligated into pGEM-T-easy (Promega, Madison, WI, USA), transformed into *Escherichia coli* DH5α and sequenced. Sequence alignment of the species-specific fragments cloned from *P. sungorus* revealed a 96.4% (PC1/3) and 97% (PC2) identity to rat prohormone convertases at the nucleotide level. Sections were fixed, acetylated, and hybridised overnight at 58 °C using ^{35}S-labelled antisense riboprobes ($1–1.5 \times 10^7$ d.p.m./ml). Slides were treated with RNase A to remove unhybridised probe and then desalted with a final high stringency wash in 0.1 × saline-sodium citrate (SSC) at 60 °C for 30 min. Hybridised slides were apposed with Kodak BioMax MR film (Kodak, Rochester, NY, USA) and, where appropriate, were coated with LM-1 film emulsion (Amersham, Bucks, UK). The levels of hypothalamic mRNAs were analysed and quantified by computerised densitometry (Image Pro-Plus software, Version 5.5.1; Media Cybernetics, Wokingham, Berkshire, UK) of *in situ* hybridisation autoradiograms. This determined the intensity and area of the hybridisation signal on the basis of set parameters; the integrated intensity was then computed using standard curves generated from ^{14}C autoradiographic microscales (Amersham). Image analysis was performed on representative sections, by an observer blind to the respective treatment groups, on four or five comparable sections spanning the ARC and three sections spanning the lateral hypothalamus. Micropictures of emulsion autoradiography sections were taken by bright field microscopy using an Olympus BX-50 microscope (Olympus Microscopes Ltd, Middlesex, UK) with attached digital camera system (Hitachi HV-C20, Hitachi Europe Ltd, Maidenhead, UK).

Dual immunostaining

Male Siberian Hamsters (n = 24, Aberdeen colony) were kept under conditions described above (Experiment 2). Half of them (n = 12) were transferred to SD. After 14 weeks in LD or SD, hamsters were anaesthetised with sodium pentobarbital and perfused with 4% paraformaldehyde (PFA) in 0.1 M phosphate-buffered saline (PBS, pH 7.4). Brains were dissected and transferred into a 4% PFA-PBS solution (8 h, 4 °C), followed by cryoprotection in 30% sucrose–0.1 M PBS (48 h, 4 °C), and were deep frozen in isopentane over dry ice (1 min). Coronal sections (35 μm) of the brain, corresponding to −1.5 to −3.7 mm relative to Bregma (27), were processed on a cryostat. Free-floating sections were treated with blocking solution (BS) containing 3% bovine serum albumin (BSA) in 0.5% Triton X-100–0.1 M PBS (0.5% PBS-T) for 1 h to block nonspecific reactions. Then, sections of LD (n = 3) and SD (n = 3) hamster brains were incubated with polyclonal rabbit anti-orexin-A (dilution 1 : 200, H-003–30, Phoenix Pharmaceuticals Inc., Belmont, CA, USA), anti-POMC (dilution 1 : 100, H-029–30, Phoenix), or anti-β-endorphin (dilution 1 : 100, H-022–33, Phoenix) in BS overnight (4 °C). Following washes in 0.25% PBS-T, sections were incubated for 2 h with unconjugated goat anti-rabbit Fab-fragment antibody (111-007-003, Jackson ImmunoResearch, West Grove, PA, USA) diluted 1 : 60 in BS at room temperature (RT). Sections were rinsed briefly in 0.25% PBS-T and incubated with Cy3 (Ex_{max} 554 nm, Em_{max} 566 nm) conjugated donkey anti-goat secondary antibody in BS (dilution 1 : 250, 705-165-147, Jackson) for 2 h at RT, rinsed again in 0.25% PBS-T and incubated with the second polyclonal rabbit anti-PC1/3 primary antibody (dilution 1 : 400, AB1260, Chemicon Inc., Temecula, CA, USA) or anti-PC2 (dilution 1 : 400, AB1262, Chemicon), in BS overnight at 4 °C. Sections were incubated with Alexa 488 dye (Ex_{max} 492 nm, Em_{max} 520 nm) conjugated goat anti-rabbit secondary antibody (dilution 1 : 250, Molecular Probes, Eugene, OR, USA) in BS for 2 h at RT. Colocalisation for α-MSH was performed with polyclonal sheep anti-α-MSH antibody (dilution 1 : 15.000, Chemicon) in BS overnight at 4 °C. In this case, different host species in which the applied primary antibodies were raised made an intermediate step of Fab-fragment incubation obsolete. α-MSH was visualised by incubation with Fluorescein (Ex_{max} 494 nm, Em_{max} 520 nm) conjugated donkey anti-sheep secondary antibody (dilution 1 : 100, AP184F, Chemicon) in BS for 2 h at RT. Incubation with the second primary antibodies and secondary antibody matched the steps described above. Sections were then rinsed in PBS, mounted on gelatin-coated slides, air-dried, dehydrated in graded alcohol, cleared in xylene and coverslipped with Enthelan (Merck Biosciences, Darmstadt, Germany). Sections were examined under a conventional Leica DMR epifluorescent microscope (Leica Microsystems, Wetzlar, Germany). Cell bodies were counted in two distinct hypothalamic regions, the lateral hypothalamus and the arcuate nucleus approximating from −1.5 mm to −3.2 mm (LH) and −1.8 mm to −3.7 mm (ARC) relative to Bregma, according to the atlas of the golden hamster brain (27). Immunoreactive (ir) cells in three (ARC) or four (LH) comparable sections of each individual animal were counted without knowledge of the experimental treatment. Total ir-cell number for each individual animal from the respective regions was calculated followed by the assessment of mean values for each experimental group. Images were taken by a digital camera system mounted on the microscope. Merging of images was performed by colour channel overlay using image processing software (Adobe Photoshop version 7.0; Adobe Systems Inc., San Jose, CA, USA). The anatomical localisation of neuropeptides within the brain of Siberian

hamsters was annotated according to the atlas of the golden hamster brain (27).

Controls

For controls, each of the primary antibodies was preincubated with its complementary peptide (α-MSH, 043-01, Phoenix; β-endorphin, 022-33, Phoenix; orexin-A, 003-30, Phoenix; POMC, 029-30, Phoenix; PC 1/3, AB5011, Abcam; PC2, AB5012, Abcam), prior to application. Incubation with preadsorbed primary antibodies resulted in no staining. Additional negative controls were performed by incubation of sections lacking primary antisera. Labelling of the primary antibodies by incubation with interchanged secondary antibodies showed an identical staining pattern.

Single immunostaining

Female Siberian hamsters (n = 20, Marburg colony) at 7 months of age were divided into two groups of 10. One group was kept in LD, whereas the other was transferred to SD. After 14 weeks, hamsters were killed in a CO_2 atmosphere and decapitated. Brains were excised, fixed in 4% PFA (48 h, 4 °C), and cryoprotected in 20% sucrose in 0.1 M PBS for 24 h at 4 °C. Brains were deep frozen in isopentane over dry ice (1 min) and stored in −80 °C until required. Coronal sections were cut on a cryostat at 30 μm. Endogenous peroxidase activity was inhibited in sections using 80% PBS, 10% methanol and 10% H_2O_2 for 15 min at RT. Free-floating sections were rinsed in PBS and 0.5% PBS-T. Following preincubation in a blocking solution containing 0.5% PBS-T and 3% BSA, sections were incubated with primary polyclonal rabbit anti-ACTH (Phoenix; H-001-21) antibody diluted 1 : 350 in BS overnight at 4 °C. Following washing in 0.5% PBS-T, sections were then incubated with peroxidase-conjugated goat anti-rabbit antibody (Jackson Immunoresearch, 111-035-144) diluted 1 : 500 in BS for 1 h at RT. Using Vector SG substrate kit for peroxidase (SK-4700, Vector Laboratories, Burlingame, CA, USA), the colour reaction resulted in dark-grey/blue immunostaining. Sections were then rinsed in PBS, mounted on gelatin-coated slides, air-dried, dehydrated in graded alcohol, cleared in xylene and coverslipped with Enthelan (Merck). Immunoreactive cell bodies were counted as for the dual-immunostaining protocol, using a Zeiss Axioskop (Carl Zeiss, Jena, Germany) microscope (objective, ×20). Images were taken by a mounted digital camera. Quantification and illustration of PC1/3, PC2, POMC, α-MSH, β-endorphin and orexin-A immunohistochemistry was performed on sections obtained from the dual-staining experiment described above. Micrographs showing the neuroanatomical distribution were colour inverted to greyscale mode using image editing software for enhanced visibility.

Controls

The specificity of primary antibody was tested by adding an excess of ACTH-(Phoenix; 001-21) peptide to the primary antibody for 3 h at RT before application to sections, or by omission of the primary antibody. Brain sections incubated either with preadsorbed primary antiserum or in the absence of primary antibodies did not exhibit any ACTH-ir (data not shown).

Statistical analysis

Data were analysed by two-way analysis of variance (ANOVA) followed by the Student–Newman–Keuls multiple comparison test, where appropriate (for *in situ* experiments), and one-way ANOVA (for immunohistochemistry data) using a statistical software package (SigmaStat, Jandel Corp, Richmond, VA, USA). Data from *in situ* hybridisation experiments are presented as means ± SEM; Data for immunohistochemistry experiments are presented as percentage values of LD control ± SEM. $P < 0.05$ was considered statistically significant.

Results

Effect of seasonal changing photoperiod on body weight

The body weight trajectory of ND animals was inversely related to the seasonal change in ambient photoperiod (Fig. 2). Beginning with an average body weight of 32.3 ± 3.4 g in October, ND body weight decreased by 17.3% to a minimum of 26.7 ± 2.1 g in January, followed by a weight gain of 53.9% to a body weight of 41.1 ± 3.9 g in April Control group animals kept in constant LD photoperiod (16 : 8 h light : dark) maintained an average body weight of 38.3 ± 3.6 g throughout the 6 months of the experiment. As a result, mean body weights of ND and LD animals differed by 12 g in January ($P < 0.01$), and were also significantly different in November ($P < 0.05$).

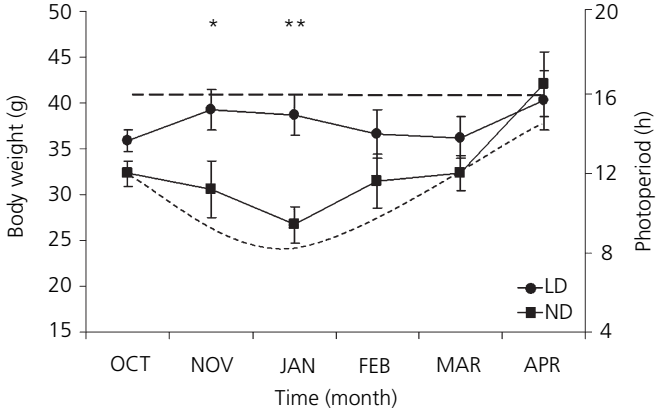

FIG. 2. Body weight of Siberian hamsters kept in constant long day (LD) (16 : 8 h light : dark; dashed line) or dynamic natural-day (ND) photoperiod (day length depending on ambient light during winter; dotted line) over 6 months from October until April (means ± SEM, n = 6 per time point). Photoperiod ranged from a minimum of 8.07 h light in January to a maximum of 14.19 h light in April. **P < 0.01; *P < 0.05, ND versus LD.

Effect of natural photoperiod on gene expression of PC1/3 and PC2

PC1/3 and PC2 mRNA were detected in various areas of the hamster hypothalamus with region-specific intensity differences (Fig. 3). Gene expression of both PC1/3 and PC2 was observed in ARC, paraventricular nucleus (PVN) and ventromedial nucleus (VMH), although gene expression in the PVN and VMH was close to the limit of detection and consequently was not quantified. In addition, PC1/3 mRNA was observed in the LH. Autoradiographs of PC1/3 and PC2 in the ARC revealed similar expression patterns to previously observed POMC mRNA distribution in this area (10). In addition, high concentrations of PC2 mRNA were observed in a small group of neurones within the dorsal medial posterior part of the arcuate nucleus (dmpARC).

Gene expression of PC1/3 within the ARC (Fig. 4A) and LH (Fig. 4B) revealed a significant overall effect of photoperiod ($P < 0.05$ for both regions) with higher levels of mRNA in ND (versus LD controls). However, PC1/3 mRNA levels in the ARC and LH were not correlated with the profile of changing photoperiod in ND; there were no effects of time (month) and no time × photoperiod interaction. In the LH (Fig. 4B), the apparent reflection of ND photoperiod in trends to increased levels of PC1/3 mRNA from October until January followed by a decline to February were not statistically significant.

Gene expression of PC2 in the ARC (Fig. 4C) and the dmpARC (Fig. 4D) also revealed strong effects of photoperiod with higher levels of mRNA in ND ($P < 0.001$ for both

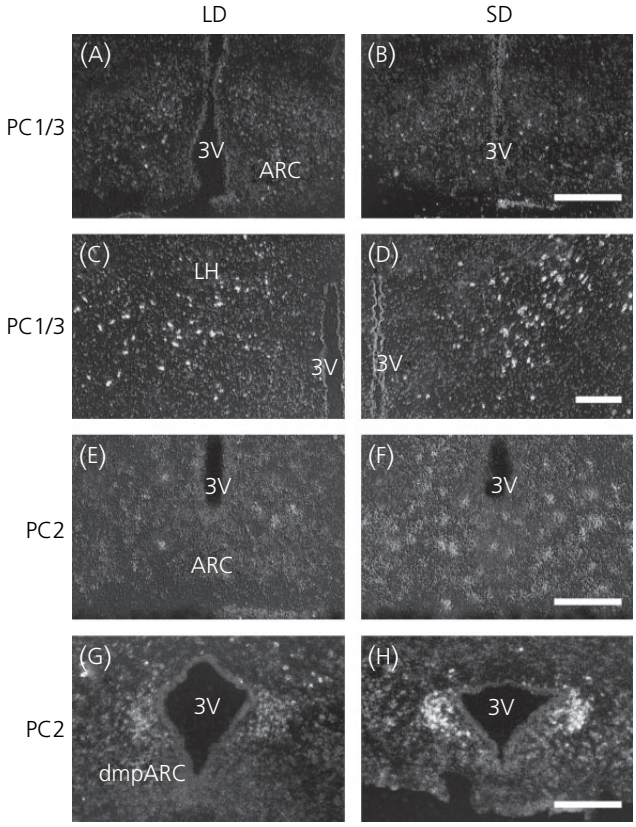

FIG. 3. Representative dark-field micrographs of autoradiographs showing gene expression of prohormone convertases 1/3 (PC1/3) and 2 (PC2) in quantified areas of the hypothalamus in long day (LD) and short day (SD) animals. Scale bars = 80 μm (A–B, E–H) and 100 μm (C–D).

regions). In addition, a seasonal pattern of PC2 gene expression in the ARC (Fig. 4C, quantified area excluding the dmpARC) was observed in ND hamsters (two-way ANOVA: $P < 0.01$ for effect of time; $P < 0.05$ for time × photoperiod interaction) with maximal mRNA levels observed in January (multiple comparison: $P < 0.05$). Although a similar temporal gene expression profile was apparent for gene expression of PC2 in the dmpARC (and for PC1/3 in LH), this could not be consolidated statistically (Fig. 4D).

Effect of transfer of hamsters from SD to LD on body weight

Body weights of the Siberian hamsters used in these experiments have been documented previously (29). Fourteen weeks in SD resulted in a 27% reduction in body weight, compared to LD controls. Transfer back to LD had little effect on body weight for the first 2 weeks but, thereafter, body weight increased significantly ($P < 0.001$) and achieved a level similar to that of LD controls by 6 weeks.

Effect of transfer of hamsters from SD to LD on gene expression of PC1/3 and PC2

Gene expression of PC1/3 in the ARC and LH did not change significantly after 14 weeks in SD (Fig. 4E,F, week 0). PC1/3 mRNA levels in the ARC and LH were unaffected by transfer from SD back to LD photoperiod (week 2, week 4, week 6) and were similar to those of LD controls. There were no effects of photoperiod or time, and no interaction. Neuroanatomical distribution patterns of PC1/3 mRNA analysed by emulsion autoradiography in the ARC (Fig. 3A–B) and LH (Fig. 3C–D) of SD and LD (week 0) also showed no apparent differences.

Photoperiod had no overall effect on PC2 gene expression in the ARC (Fig. 4G) or dmpARC (Fig. 4H) but PC2 gene expression revealed a significant effect of time ($P < 0.001$ for both regions), and a time × photoperiod interaction ($P < 0.001$ for both regions). Significantly higher levels of PC2 mRNA were found in the ARC ($P < 0.05$) and dmpARC ($P < 0.05$) of SD animals compared to LD controls after 14 weeks in SD photoperiod (week 0). This observation was corroborated by emulsion autoradiographs showing a higher content of silver grains with PC2 probes within the ARC (Fig. 3E–F) and dmpARC (Fig. 3G–H) of SD hamsters at time point week 0. Following the transfer from SD back to LD photoperiod, gene expression of PC2 in the ARC decreased to a nadir at week 4. A significant down regulation of gene expression was observed after transfer from SD back to LD at all three time points (week 2, week 4, week 6; $P < 0.05$, versus week 0 SD, respectively). Between 4 and 6 weeks after transfer back to LD, mRNA levels of PC2 increased significantly ($P < 0.05$). In the dmpARC, gene expression of PC2 was decreased after 2 weeks and remained significantly lower until 6 weeks (week 2, week 4, week 6; $P < 0.05$, versus week 0 SD, respectively) after transfer back to LD.

Effect of photoperiod on protein expression of PC1/3, PC2, POMC, ACTH, α-MSH, β-endorphin and orexin-A

Immunoreactive cells and fibres for PC1/3, PC2, POMC, ACTH, α-MSH, β-endorphin and orexin-A were observed in different hypothalamic areas of the Siberian hamster brain. Immunolocalised distribution patterns of PC1/3 and PC2 protein matched the mRNA pattern, except for a lack of PC2-ir in the dmpARC. Unlike the strong signal detected for PC2 mRNA in this region, little immunoreactivity for its protein could be observed (data not shown).

In the ARC, there was no effect of photoperiod on the number of counted PC1/3-ir cells (Fig. 5A,B, a-b); hamsters kept in LD had 167 ± 15 ir-cells and those in SD 153 ± 11 ir-cells within the investigated region of the ARC. However immunohistochemical staining of PC2 in the ARC showed 125% more ir-cells in SD (88 ± 19 ir-cells), leading to a significant difference ($P < 0.01$) compared to those counted in LD controls (39 ± 6 ir-cells) (Fig. 5A,B, c-d). POMC-ir in LD (178 ± 22 ir-cells) and SD (156 ± 10 ir-cells) revealed no significant difference in ir-cell number (Fig. 5A,B, e-f). ACTH-ir (LD, 105 ± 14; SD, 81 ± 9 ir-cells) as well as α-MSH-ir (LD, 47 ± 11; SD, 54 ± 13 ir-cells) levels in the ARC were also unaffected by photoperiod (Fig. 5A,B, g–h,k–l). By contrast, the density of α-MSH-ir fibres appeared greater in SD, but was not quantifiable (Fig. 5A,B, k–l). The neuroanatomical distribution pattern of β-endorphin-ir was similar to that of α-MSH-ir, but was mainly concentrated in cell bodies. Counting of β-endorphin-ir cells revealed 76%

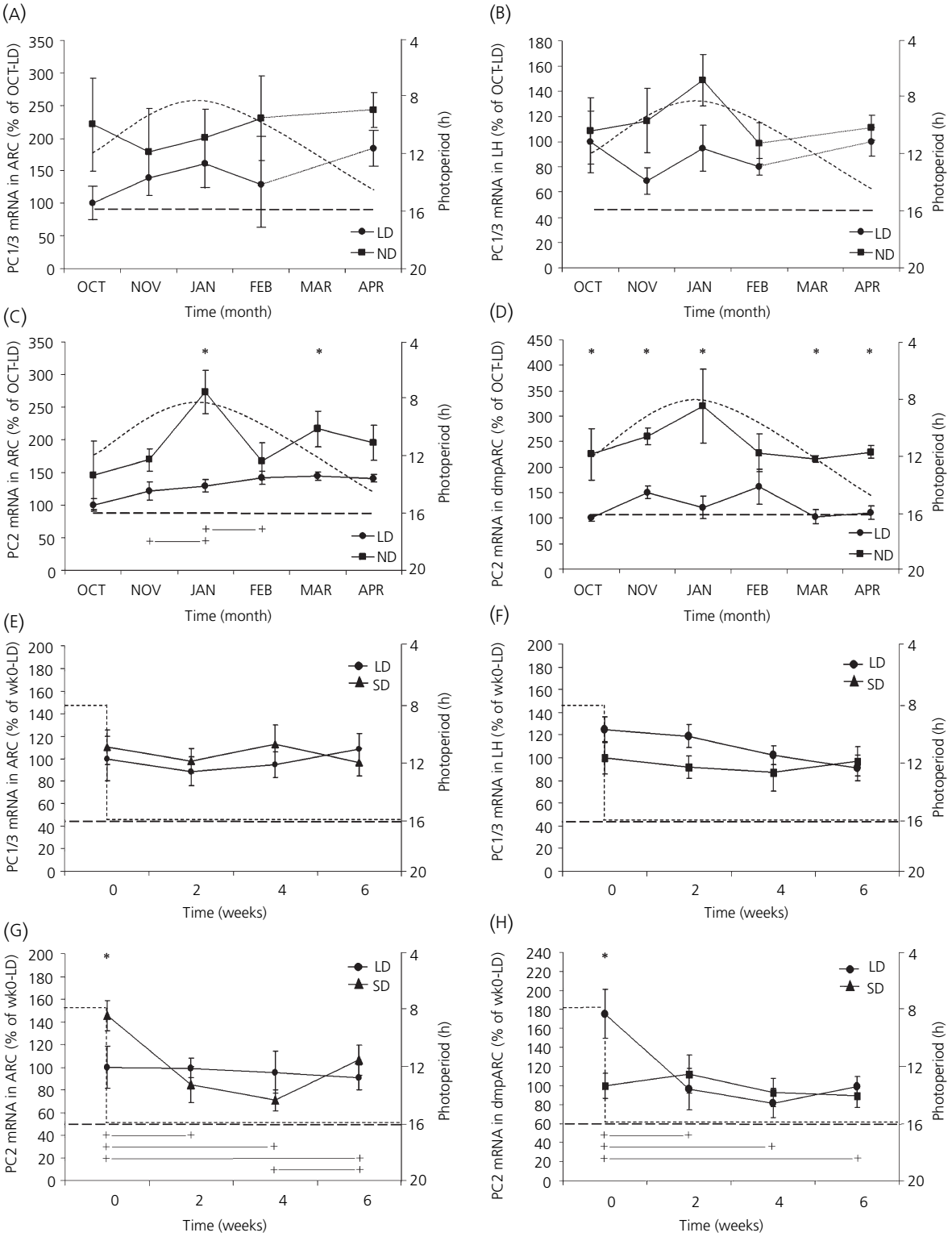

FIG. 4. Gene expression of prohormone convertases 1/3 (PC1/3) and 2 (PC2) in selected areas of the Siberian hamster hypothalamus. (A–D) Effect of changing photoperiod during winter on expression of PC1/3 (A, ARC; B, LH) and PC2 (C, ARC; D, dmpARC) genes. mRNA levels are expressed as mean percentages of LD controls in October (± SEM, n = 6 per time point). (E–H) PC1/3 (E, ARC; F, LH) and PC2 (G, ARC; H, dmpARC) gene expression after switch from SD (week 0) back to LD (week 2, week 4, week 6) photoperiod. mRNA levels are expressed as mean percentages of LD controls at week 0 (± SEM, n = 4 per group). LD is indicated by dashed lines, whereas dotted curves mark ND (A–D) or SD (E–H). Significances ($P < 0.05$) are marked by asterisks (*) for same time points but different photoperiods and crosses (+) for the same photoperiod (ND or SD, respectively) but at different time points.

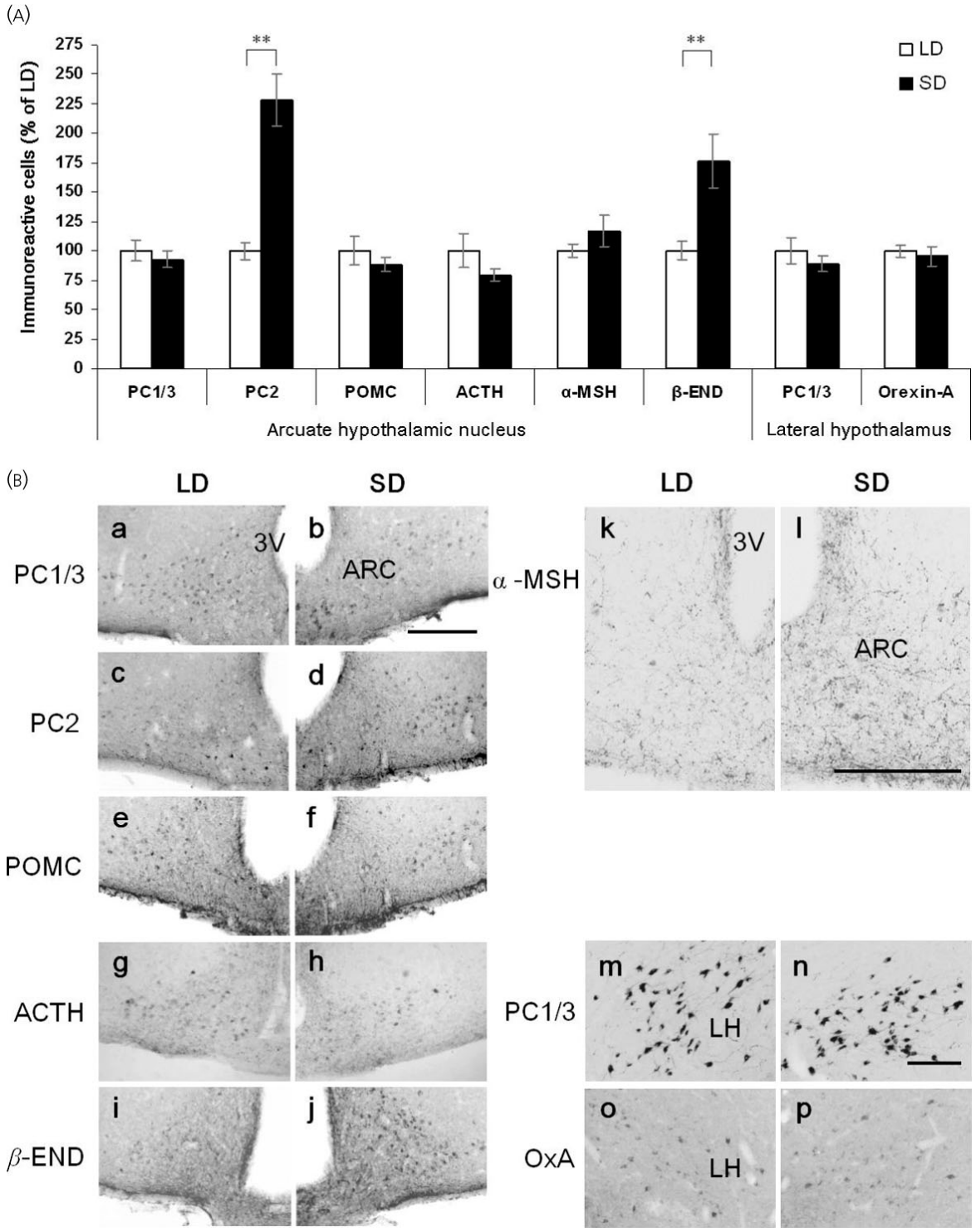

FIG. 5. (A) Quantitative analysis of immunoreactive (-ir) cells in selected areas of the Siberian hamster hypothalamus. Data are number of ir-cells expressed as percentage of long day (LD) controls (**$P < 0.01$, $n = 3$ per group). (B) Representative photomicrographs showing neuroanatomical distribution of immunoreactive cells in comparable hypothalamic areas of LD and short day (SD) animals. Colour inverted images of immunofluorescence stained sections (a–f, i–p) or peroxidase/substrate stained sections (g–h). 3V, Third ventricle; ARC, arcuate nucleus; LH, lateral hypothalamus. Scale bars = 100 μm (a–l) and 180 μm (m–p).

($P < 0.01$) more neurones in SD (74 ± 18 ir-cells) compared to LD (42 ± 9 ir-cells) (Fig. 5A,B, i–j). Quantification of PC1/3-ir (LD, 119 ± 16; SD, 104 ± 13 ir-cells) and orexin-A-ir (LD, 105 ± 14; SD, 97 ± 11 ir-cells) within the LH did not reveal differences between SD and LD controls (Fig. 5A,B, m–p).

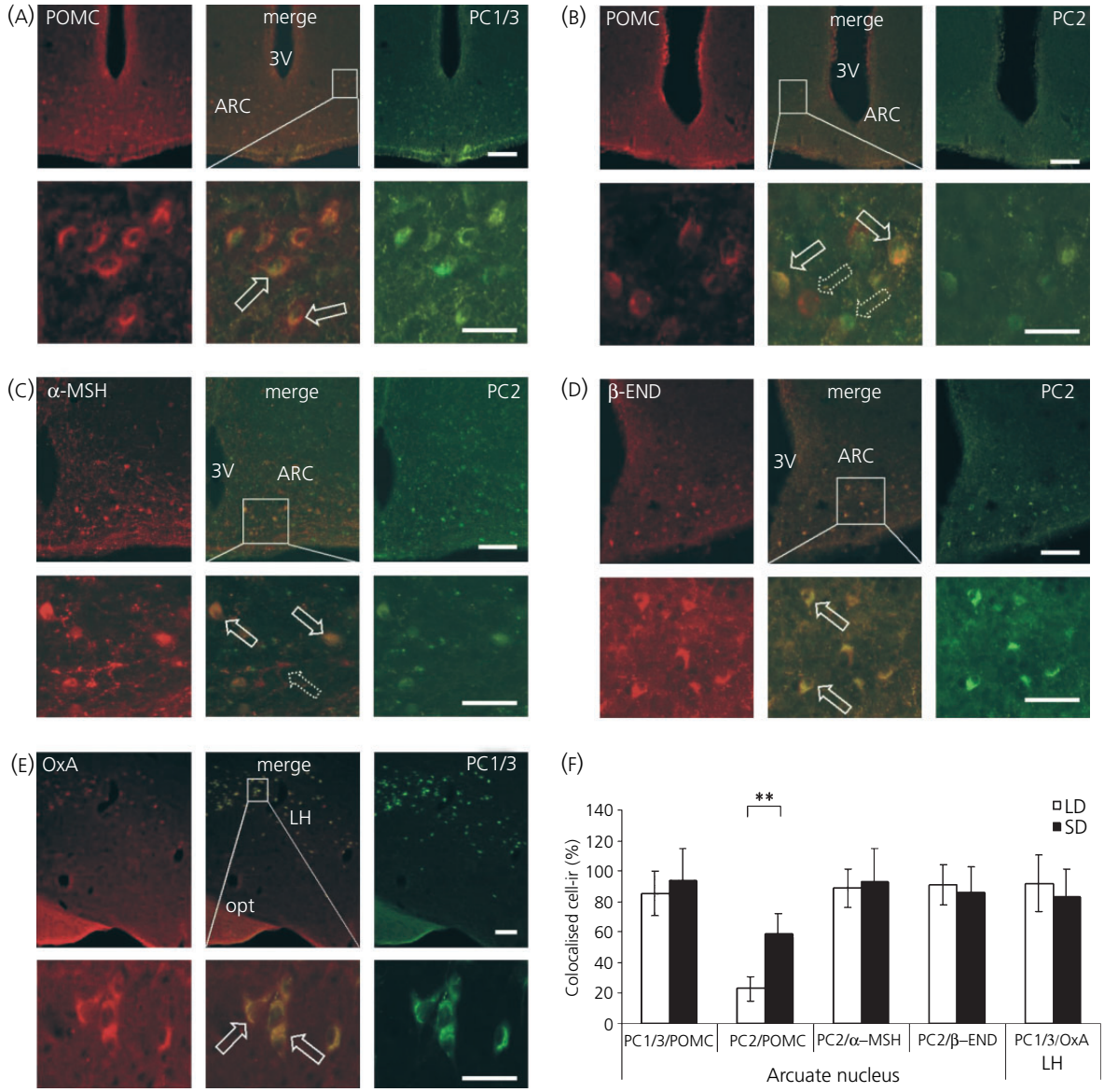

FIG. 6. (A–D) Photomicrographs showing immunofluorescence double staining of prohormone convertase 1/3 (PC1/3)-immunoreactivity (-ir) or prohormone convertase 2 (PC2)-ir with pro-opiomelanocortin (POMC)-ir and its derived neuropeptides in the arcuate nucleus and (E) PC1/3-ir and orexin-A-ir double staining in the lateral hypothalamus. Images derive from SD hamsters. For each panel, the upper row shows low magnification images and the lower row high magnification images of selected (boxed) areas. Merged images (centre) demonstrate colocalisation of immunoreactive products. Colocalisation is indicated by solid arrows, single cell-ir by dashed arrows. (F) Quantitative colocalisation analysis of prohormone convertase-ir (PC1/3 or PC2) and neuropeptide-ir. Values are expressed as mean percentages (± SEM) of counted POMC-ir, α-MSH-ir, β-endorphin-ir and orexin-A-ir cells in long day (LD) and short day (SD) (n = 3 per group). 3V, Third ventricle; ARC, arcuate nucleus; LH, lateral hypothalamus; opt, optical tract. Scale bars, low magnification images = 100 μm; high magnification images = 40 μm.

Effect of photoperiod on colocalisation of PC1/3 and PC2 with POMC, α-MSH, β-endorphin and orexin-A immunoreactivity

Dual fluorescence immunohistochemistry in the ARC showed no significant differences between the proportion of POMC-ir cells colocalised with PC1/3-ir cells in SD and LD. In both LD (87.5 ± 21%) and SD (94.1 ± 14.7%), nearly all POMC-ir cells were also PC1/3-ir positive (Fig. 6A,F). By contrast, the overall level of PC2-ir colocalisation with POMC-ir was lower and revealed significantly ($P < 0.01$) more POMC-ir cells which also contained PC2-ir in SD (59.14 ± 12.9%) than in LD (22.9 ± 8%) (Fig. 6B,F). Colocalisation of PC2-ir cells with α-MSH and β-endorphin immunoreactivity (Fig. 6C,D) revealed a nearly complete match of these POMC derived neuropeptides and the cleavage mediating prohormone convertase in SD and LD (Fig. 6F; α-MSH, LD, 89.1 ± 12.6%; SD, 93.2 ± 21.5%; β-endorphin, LD, 90.9 ± 13.5%; SD, 86.4 ± 16.3%). In the LH, there was no effect of photoperiod on the colocalisation of orexin-A-ir and PC1/3-ir (Fig. 6E,F); the neuropeptide product of prepro-orexin was localised with the majority of PC1/3-ir cells in this area in both LD (92 ± 18.4%) and SD (83.2 ± 18.7%).

Discussion

Seasonal body weight in mammals is regulated by a complex interaction of neuropeptides in a hypothalamic network of neurones that integrates environmental photoperiod inputs. Most of these energy balance-regulating neuropeptides are derived from larger biologically inactive precursors and have to undergo post-translational processing by endoproteolytic cleavage. The present study presents evidence substantiating the hypothesis that an important part of the photoperiod-driven regulation of POMC product biosynthesis is mediated by post-translational processing through PC1/3 and PC2, and thus provides valuable information over and above the control of precursor gene expression at a transcriptional level.

Neuroanatomical distribution patterns of PC1/3 and PC2 transcripts in the hamster hypothalamus match with previously described localisations in other rodent species such as rats and mice (21, 30). Hamsters kept in ND and SD displayed typical physiological adaptations to shortening or short photoperiod, including change of coat colour, reduction of reproductive tissue, reduced food intake and body weight loss. These photoperiod-induced physiological changes were not accompanied by temporal change in PC1/3 mRNA levels. Gene expression of PC1/3 in ARC and LH was higher overall in ND (versus LD) but this effect was not observed after 14 weeks in SD (versus LD) artificial photoperiod, suggesting some impact of prior photoperiodic history. At present, there is no clear explanation for this unexpected difference between ND and SD because gene expression of PC1/3 in summer ND (May to September) was not measured. Furthermore, short-term change of photoperiod induced by transfer from SD to LD was also without discernible effect on gene expression of PC1/3 in ARC and LH, suggesting that, on a transcriptional level, PC1/3 is not directly regulated by photoperiodic inputs. However, previous observations have demonstrated a regulatory effect of the adipose tissue hormone, leptin, on gene expression of PC1/3 in LH and ARC because reduced PC1/3 mRNA levels observed in obese *ob*/*ob* mice were up-regulated in response to leptin injection (31). Although PC1/3 gene expression appears to be sensitive to leptin in this natural knockout model, contrary to expectation, in Siberian hamsters, PC1/3 gene expression appears to be independent of seasonal modulation of leptin, despite the effect of photoperiod on this hormone (32). This suggests that the adipose tissue signal may be responsible for the maintenance of basal PC1/3 gene expression level.

By contrast to PC1/3, gene expression of PC2 in the ARC and dmpARC broadly paralleled the profile of changing ambient ND photoperiod in winter resulting in elevated mRNA when photoperiod was shortest. This photoperiod dependency was substantiated by up-regulated PC2 gene expression in hamsters kept in SD for 14 weeks. After transfer from SD to LD, mRNA levels of PC2 decreased rapidly and, within 2 weeks, levels were similar to those in LD. This acute regulatory change in PC2 gene expression preceded body weight loss and is therefore unlikely to be a secondary effect of metabolic and physiological changes. The photoperiod-driven gene expression profile suggests that PC2 may be an important part of a molecular neuroendocrine mechanism that is closely related to the integration of photoperiod information and the mediation of seasonal responses. Previous studies demonstrated a photoperiod-dependent differential gene expression of the neuropeptide precursor POMC in the ARC with lower mRNA levels in SD (11, 33). Initially, this observation appears paradoxical because down-regulation of POMC would most likely result in lower levels of its derived neuropeptide, α-MSH, whereas photoperiod-induced changes in metabolism and physiology such as reduced food intake and body weight loss would appear to require a higher concentration of the anorexic peptide, α-MSH. Artificial square-wave photoperiod transformation did not affect gene expression of PC1/3 and, consequently, cleavage activity of PC1/3 most likely results in unaltered levels of larger POMC derivates such as ACTH and β-lipotrophin, which are generated by PC1/3 cleavage. By contrast, increased gene expression of PC2 in SD is likely to increase proteolytic activity of PC2 at specific cleavage sites resulting in higher levels of smaller peptides such as α-MSH, β-MSH, γ-MSH, β-endorphin and corticotrophin- like intermediate peptide.

Despite reported decreased gene expression of POMC in SD, protein distribution in neurones of the ARC remained unaltered by photoperiod, suggesting that gene expression may not be the primary regulator of POMC product biosynthesis. Gene expression of PC1/3 in SD (versus LD) animals was also unaffected by photoperiod and was reflected in similar levels of PC1/3 protein in SD and LD acclimated hamsters. The regulation of PC2 transcript by photoperiod in the ARC was also reflected at a translational level because there was more PC2 protein detected in SD than LD animals. Similar levels of PC1/3 and POMC protein in SD and LD are reflected in unaltered ACTH-ir, with ACTH peptide known to be a direct result of POMC cleavage by PC1/3 (34). Although inhibitory properties of ACTH on food intake (35) would presume an accumulation of this peptide in SD animals, our results imply a minor role in regulation of seasonal body weight. By contrast, increased PC2 protein in SD animals was accompanied by higher levels of α-MSH-ir fibres and β-endorphin-ir cells, in line with previous studies demonstrating that α-MSH production varies directly in accordance with the expression of PC2 (36). Similar observations were reported for the maturation of β-endorphin (37). Interestingly, the fate of β-endorphin after its cleavage from β-lipotrophin is more extensive than that of α-MSH, and the implications of the observed immunoreactive protein levels are worthy of further consideration. The initially generated β-endorphin$_{1-31}$ is further processed to β-endorphin$_{1-27}$ and β-endorphin$_{1-26}$ (Fig. 1), which are considered to be opiate receptor antagonists opposing the effects of β-endorphin$_{1-31}$ (38). Whereas proteolytic processing of β-endorphin$_{1-27}$ is solely mediated by PC2 activity (39) and removal of the terminal basic residue of β-endorphin$_{1-27}$ by carboxypeptidase's E yields β-endorphin$_{1-26}$ (40), the cleavage of β-lipotrophin to β-endorphin$_{1-31}$ by PC2 is contentious. *In vivo* studies scrutinising β-endorphin$_{1-31}$ levels by radioimmunoassay in PC2-deficient mouse hypothalamus reported increased β-endorphin$_{1-31}$ levels despite PC2 inactivity, suggesting that β-endorphin$_{1-31}$ is likely to be a PC2 substrate rather than a direct product (18). In contrast, *in vitro* studies performed on AtT-20 anterior pituitary cells overexpressing

PC2 demonstrated enhanced conversion of β-lipotrophin to β-endorphin$_{1-31}$ (41). Another experiment performed *in vivo* in the hypothalamus of mice lacking functional PC2 found the processing of β-lipotrophin to β-endorphin$_{1-31}$ diminished by two-thirds. This result suggests that a minor part of the proteolytic conversion from β-lipotrophin to β-endorphin$_{1-31}$ could be mediated by a supplementary processing of the β-lipotrophin substrate by PC1/3 (42). The polyclonal antibody against β-endorphin used in the present study reacts with epitopes of all three β-endorphin forms (1-31, 1-27, 1-26) and hence displays immunoreactivity of total β-endorphin. However, in the hypothalamus, β-endorphin$_{1-31}$ constitutes more than 60% of the total β-endorphin-ir, in contrast to less than 30% β-endorphin$_{1\text{-}27\ +\ 1\text{-}26}$-like immunoreactivity (43). Our results corroborate these findings because PC2 up-regulation in SD results in higher concentrations of total β-endorphin. Current opinions on the physiological function of β-endorphin are conflicting; pharmacological studies generally indicate a short-term stimulatory effect of opioids on food intake (44, 45), but longer term regulation of energy balance has not been reported (46, 47), although β-END$^{-/-}$ mice (48) are characterised by an obese phenotype. This latter finding may support our observation of increased β-endorphin protein levels in states of reduced feeding behaviour and negative energy balance in SD, and the time scale over which these changes are manifested. These characteristics are consistent with our results because seasonal regulation of energy balance is a long-term process rather than an acute induced inhibition of food intake. An opposing and antagonistic effect of the processed β-endorphin$_{1-27}$, evidently a cleavage product mediated exclusively by PC2 activity (39), on opioid receptors could be an interesting target for further experiments attempting to explain this observation. By contrast to immunoreactivity of β-endorphin, which is more confined to the cell body, α-MSH-ir was widely distributed throughout fibres and boutons of neurones in the ARC. Thus, the biological relevance of quantification of relative α-MSH protein content by counting of ir-neurones is questionable. Appraisal of SD and LD α-MSH-ir distribution patterns revealed more intense staining of α-MSH-ir fibres in SD and hence higher levels of protein in SD. This observation is supported by the fact that the concentrations of α-MSH and β-endorphin are closely correlated, in agreement with their production in equimolar amounts as products of the same precursor (49).

Therefore, it is unlikely that less α-MSH than β-endorphin is processed and the immunoreactivity patterns observed in the present study could reflect different rates of transport and routes of intracellular trafficking within the neuronal network. Visually apparent increased levels of α-MSH could be appropriate to the state of negative energy balance in SD (7, 50). Combined with increased expression of β-endorphin in SD, these findings suggest a complementary interaction between the melanocortin, α-MSH, and the opioid, β-endorphin, on seasonal regulation of energy homeostasis, rather than opposing effects.

Colocalisation of PC1/3-ir with POMC-ir in ARC showed almost complete coexpression. This observation implies that cleavage of POMC by PC1/3 is a fundamental process that provides the same relative amounts of PC1/3-cleaved POMC-derived peptides independent of changing photoperiod in SD. We substantiated this hypothesis by demonstrating levels of ACTH-ir that were nearly equal in SD and LD. Even though we did not scrutinise the proteolytic processing fate of β-lipotrophin, the intermediate precursor of β-endorphin, similar results would be expected because β-lipotrophin is cleaved by PC1/3 in a similar manner to ACTH. α-MSH and β-endorphin were almost completely colocalised with PC2 in SD and LD reflecting their derivation from larger intermediate POMC fragments by proteolytic PC2 processing. As a result of higher protein concentrations of PC2 in SD (versus LD), more α-MSH-ir and β-endorphin-ir was processed and could be observed in animals that were exposed to short photoperiod.

The precise involvement of the hypocretins, orexins A and B, in feeding behaviour remains uncertain. Whereas early studies demonstrated an orexigenic effect (51), more recent observations suggest a more complex influence of both neuropeptides on energy balance. In particular, the role of orexin-B remains controversial with only a weak effect on food intake (52). By contrast, the orexin-A-induced hyperphagia and effects (increase) on metabolic rate are more robust (53). However, the exact mechanism by which orexin-A exerts its orexigenic action is not fully elucidated. Orexin-A and orexin-B are highly specifically localised in the LH and are generated by proteolytic processing of the precursor peptide prepro-orexin (54), whose gene expression in the LH was previously colocalised with mRNA encoding for PC1/3 (31). To date, the exact post-translational enzymatic mechanism by which prepro-orexin cleavage is mediated is unknown and there is no evidence from studies performed *in vivo* of direct PC1/3 involvement. Immunohistochemical colocalisation of PC1/3-ir and orexin-A-ir in the present study suggests a close relationship between these two neuroendocrine components at a protein level. Interestingly, virtually all orexin-positive neurones in the LH also express dynorphin (55), whose precursor molecule pro-dynorphin has been reported to be processed by PC1/3 in studies performed *in vitro* (56). Hence pro-dynorphin could be another possible target of PC1/3 activity within the orexin-ir positive neurones of the LH. Current evidence indicates that gene expression of prepro-orexin, such as that of PC1/3 in LH, is unaffected by photoperiod (10, 11). Our observations of equivalent levels of PC1/3-ir and orexin-A-ir are consistent with these published studies in SD and LD. In addition, we recently demonstrated that photoperiod had no effect on the second prepro-orexin derived neuropeptide, orexin-B, because no differences of orexin-B-ir were found in LH of SD and LD acclimated hamsters (57). Combined, these observations suggest that PC1/3 does not play a major role in the seasonal regulation of post translational neuropeptide maturation processes in the LH and hence in seasonal energy balance.

Interestingly, despite distinct gene expression of PC2 in dmpARC, immunoreactive protein was not observed and consequently the function of PC2 mRNA within these neurones remains unclear. This phenomenon could reflect rapid protein denaturation in this nucleus or the ability of neuronal cells to transport mRNA and perform protein biosynthesis in remote locations away from cell bodies (58, 59). Thus, PC2 mRNA could be transported to, and protein

synthesis located in, regions and areas within the hypothalamus other than its origin in the dmpARC. Post-translational modification of proPC2 to PC2 represents another possible explanation for the failure to detect PC2-ir (60). However, because of the polyclonal structure of the PC antibodies, a cross reaction with epitope sequences of the proforms should be possible. Neuronal projections from the dmpARC to other nuclei and the integration of dmpARC neurones in the hypothalamic neuroendocrine network remain to be established. There is growing evidence that the dmpARC is a functionally important component of the neuroendocrine network that regulates energy balance during seasonal adaptation; previous studies have identified a number of photoperiod regulated genes in this area (29, 61, 62). One of the identified neuropeptides within this subdivision of the ARC is the precursor proVGF, which is cleaved by PC1/3 and PC2 into biological active energy balance regulating peptides (63, 64). By contrast to VGF, where gene expression is increased in the dmpARC in SD but decreased in the ARC, gene expression of PC2 was up-regulated in both hypothalamic areas in SD. Interestingly, VGF-ir in the ARC is, like PC2-ir, also characterised by the apparent absence of protein in the dmpARC despite abundant mRNA expressed in this subnucleus (P. Barrett, unpublished data). Therefore PC2 might be transported away from its site of synthesis in the dmpARC very quickly to perform subsequent post-translational processing of proVGF at a different location of the CNS. ProVGF mRNA in the dmpARC suggests a possible target of post-translational PC2 activity as mRNA levels of proVGF are also significantly increased in SD hamsters and respond promptly, like gene expression of PC2, following photoperiod manipulation.

Thus, our results demonstrate that decreasing photoperiod up-regulates PC2 gene expression and PC2 protein, whereas gene expression and protein of PC1/3 are unaffected by SD. We hypothesise that this intensifies proteolytic processing of POMC intermediate derivatives (ACTH and β-lipotrophin), and is the reason for higher concentrations of POMC-derived α-MSH and β-endorphin in short photoperiod despite apparently paradoxical findings showing down-regulated POMC gene expression in SD. By contrast, unaltered PC1/3 gene expression and protein in LH and ARC suggests that regulation by photoperiod is not accomplished via proteolytic processing at PC1/3 specific sites. Thus, regulation of proteolytic processing activity by photoperiod via coordinated expression of PC1/3 and PC2 at transcriptional and translational levels is critical for the maturation of neuropeptide precursors.

Interestingly, the proteolytic enzymes, PC1/3 and PC2 not only mediate post-translational modifications, but are also targets of post-translational modification. First, both enzymes are initially synthesised as inactive precursor molecules, and propeptide cleavage is therefore necessary to activate the enzymes. Second, interaction with small associated neuroendocrine proteins such as proSAAS with PC1/3 (65) and dimerisation of 7B2 with PC2 (66) leads to an inhibition of their enzymatic activities, making these proteins important factors in the intracellular endocrine pathway. In particular, the dependency of PC2 activity on the presence of 7B2 is highly complex because the neuroendocrine protein 7B2 has also been implicated in the activation of the zymogene proPC2 *in vivo* (67). This initially paradoxical observation reflects the complex dimension of interactions between small associated neuroendocrine proteins and the regulation of proteolytic capacity of prohormone convertases. Because the influence of these proteins on the proteolytic activity is evidently most distinct, future studies should focus on these factors to elucidate the exact mechanisms by which photoperiodic regulation of propeptide synthesis is mediated.

The photoperiod-driven regulatory mechanism on a post-translational level observed in the present study could be an additional universal control point for other energy balance related neuropeptide precursors such as proNPY, proTRH and CART. In addition, we provide further evidence for the dmpARC as an area with distinct photoperiod influenced neuroendocrine activity, suggesting that this subdivision of hypothalamic arcuate neurones is an important integral part of the seasonal energy balance regulation network.

Acknowledgements

This collaborative study was funded by the Scottish Executive Environment and Rural Affairs Department (to J. G. Mercer) and EC FP6 funding ('DIABESITY' contract no. LSHM-CT-2003-503041 to J. G. Mercer), Deutsche Forschungsgemeinschaft (German Research Foundation KL973/5; to M. Klingenspor), the National Genome Research Network (NGFN 01GS0483; to M. Klingenspor) and the Danish Research Agency (to R. M. H. Khorooshi). M. Helwig was recipient of a fellowship funded by the European Commission to attend the ObeSᵉchool European Union Marie Curie Training Site at the Rowett Research Institute.

Accepted 3 March 2006

References

1 Mercer JG. Regulation of appetite and body weight in seasonal mammals. *Comp Biochem Physiol* 1998; **119:** 295–303.
2 Morgan PJ, Ross AW, Mercer JG, Barrett P. Photoperiodic programming of body weight through the neuroendocrine hypothalamus. *J Endocrinol* 2003; **177:** 27–34.
3 Schwartz MW, Woods SC, Porte D Jr, Seeley RJ, Baskin DG. Central nervous system control of food intake. *Nature* 2000; **404:** 661–671.
4 Mercer JG, Tups A. Neuropeptides and anticipatory changes in behaviour and physiology: seasonal body weight regulation in the Siberian hamster. *Eur J Pharmacol* 2003; **480:** 43–50.
5 Klingenspor M, Dickopp A, Heldmaier G, Klaus S. Short photoperiod reduces leptin gene expression in white and brown adipose tissue of Djungarian hamsters. *FEBS Lett* 1996; **399:** 290–294.
6 Tups A, Helwig M, Khorooshi RM, Archer ZA, Klingenspor M, Mercer JG. Circulating ghrelin levels and central ghrelin receptor expression are elevated in response to food deprivation in a seasonal mammal (*Phodopus sungorus*). *J Neuroendocrinol* 2004; **16:** 922–928.
7 Fan W, Boston B, Kesterson R, Hruby V, Cone R. Role of melanocortinergic neurons in feeding and the agouti obesity syndrome. *Nature* 1997; **385:** 165–168.
8 McMinn JE, Wilkinson CW, Havel PJ, Woods SC, Schwartz MW. Effect of intracerebroventricular alpha-MSH on food intake, adiposity, c-Fos induction, and neuropeptide expression. *Am J Physiol Regul Integr Comp Physiol* 2000; **279:** R695–R703.
9 Cone RD. The central melanocortin system and energy homeostasis. *Trends Endocrinol Metab* 1999; **10:** 211–216.
10 Mercer JG, Moar KM, Ross AW, Hoggard N, Morgan PJ. Photoperiod regulates arcuate nucleus POMC, AGRP, and leptin receptor mRNA in the Siberian hamster hypothalamus. *Am J Physiol Regul Integr Comp Physiol* 2000; **278:** R271–R281.

11 Reddy AB, Cronin AS, Ford H, Ebling FJ. Seasonal regulation of food intake and body weight in the male Siberian hamster. Studies of hypothalamic orexin (hypocretin), neuropeptide Y (NPY) and pro-opiomelanocortin (POMC). *Eur J Neurosci* 1999; **11:** 3255–3264.

12 Atcha Z, Cagampang FR, Stirland JA, Morris ID, Brooks AN, Ebling FJ, Klingenspor M, Loudon AS. Leptin acts on metabolism in a photoperiod-dependent manner, but has no effect on reproductive function in the seasonally breeding Siberian hamster (*Phodopus sungorus*). *Endocrinology* 2000; **141:** 4128–4135.

13 Tanaka S. Comparative aspects of intracellular proteolytic processing of peptide hormone precursors: studies of proopiomelanocortin processing. *Zool Sci* 2003; **20:** 1183–1198.

14 Paquet L, Zhou A, Chang EY, Mains RE. Peptide biosynthetic processing. distinguishing prohormone convertases PC1 and PC2. *Mol Cell Endocrinol* 1996; **120:** 161–168.

15 Dey A, Xhu X, Carroll R, Turck CW, Stein J, Steiner DF. Biological processing of the cocaine and amphetamine-regulated transcript precursors by prohormone convertases, PC2 and PC1/3. *J Biol Chem* 2003; **278:** 15007–15014.

16 Miller R, Toneff T, Vishnuvardhan D, Beinfeld M, Hook VY. Selective roles for the PC2 processing enzyme in the regulation of peptide neurotransmitter levels in brain and peripheral neuroendocrine tissues of PC2 deficient mice. *Neuropeptides* 2003; **37:** 140–148.

17 Laurent V, Jaubert-Miazza L, Desjardins R, Day R, Lindberg I. Biosynthesis of proopiomelanocortin-derived peptides in prohormone convertase 2 and 7B2 null mice. *Endocrinology* 2004; **145:** 519–528.

18 Miller R, Aaron W, Toneff T, Vishnuvardhan D, Beinfeld MC, Hook VY. Obliteration of alpha-melanocyte-stimulating hormone derived from POMC in pituitary and brains of PC2-deficient mice. *J Neurochem* 2003; **86:** 556–563.

19 Benjannet S, Rondeau N, Day R, Chretien M, Seidah NG. PC1 and PC2 are proprotein convertases capable of cleaving proopiomelanocortin at distinct pairs of basic residues. *Proc Natl Acad Sci USA* 1991; **88:** 3564–3568.

20 Thomas L, Leduc R, Thorne BA, Smeekens SP, Steiner DF, Thomas G. Kex2-like endoproteases PC2 and PC3 accurately cleave a model prohormone in mammalian cells: evidence for a common core of neuroendocrine processing enzymes. *Proc Acad Sci USA* 1991; **88:** 5297–5301.

21 Schafer MKH, Day R, Cullinan WE, Chrétien M, Seidah NG, Watson SJ. Gene expression of prohormone an proprotein convertases in the rat CNS. A comparative in situ hybridisation analysis. *J Neurosci* 1993; **13:** 1258–1279.

22 Brobeck JR. Mechanism of the development of obesity in animals with hypothalamic lesions. *Physiol Rev* 1946; **26:** 541–559.

23 Watson SJ, Khachaturian H, Taylor L, Fischli W, Goldstein A, Akil H. Pro-dynorphin peptides are found in the same neurons throughout rat brain: immunocytochemical study. *Proc Natl Acad Sci USA* 1983; **80:** 891–894.

24 Zamir N, Skofitsch G, Bannon MJ, Jacobowitz DM. Melanin-concentrating hormone: unique peptide neuronal system in the rat brain and pituitary gland. *Proc Natl Acad Sci USA* 1986; **83:** 1528–1531.

25 de Lecea L, Kilduff TS, Peyron C, Gao X, Foye PE, Danielson PE, Fukuhara C, Battenberg EL, Gautvik VT, Bartlett FS, 2nd Frankel WN, van den Pol AN, Bloom FE, Gautvik KM, Sutcliffe JG. The hypocretins: hypothalamus-specific peptides with neuroexcitatory activity. *Proc Natl Acad Sci USA* 1998; **95:** 322–327.

26 Klingenspor M, Niggemann H, Heldmaier G. Modulation of leptin sensitivity by short photoperiod acclimation in the Djungarian hamster, *Phodopus sungorus*. *J Comp Physiol [B]* 2000; **170:** 37–43.

27 Morin LP, Wood RI. *A Sterotaxic Atlas of the Golden Hamster Brain*. San Diego, CA: Academic Press, 2001.

28 Simmens DM, Arriza JL, Swanson LW. A complete protocol for *in situ* hybridisation of messenger RNAs in brain and other tissues with radiolabeled single-stranded RNA probes. *J Histotechnol* 1989; **12:** 169–181.

29 Ross AW, Bell LM, Littlewood PA, Mercer JG, Barrett P, Morgan PJ. Temporal changes in gene expression in the arcuate nucleus precede seasonal responses in adiposity and reproduction. *Endocrinology* 2005; **146:** 1940–1947.

30 Seidah NG, Marcinkiewicz M, Benjannet S, Gaspar L, Beaubien G, Mattei MG, Lazure C, Mbikay M, Chretien M. Cloning and primary sequence of a mouse candidate prohormone convertase PC1 homologous to PC2, Furin, and Kex2: distinct chromosomal localization and messenger RNA distribution in brain and pituitary compared to. *Pc2, Mol Endocrinol* 1991; **5:** 111–122.

31 Nilaweera KN, Barrett P, Mercer JG, Morgan PJ. Precursor-protein convertase 1 gene expression in the mouse hypothalamus. differential regulation by ob gene mutation, energy deficit and administration of leptin, and co expression with prepro-orexin. *Neuroscience* 2003; **119:** 713–720.

32 Williams G, Cai XJ, Elliott JC, Harrold JA. Anabolic neuropeptides. *Physiol Behav* 2004; **81:** 211–222.

33 Mercer JG, Moar KM, Ross AW, Morgan PJ. Regulation of leptin receptor, POMC, and AGRP gene expression by photoperiod in the hypothalamic nucleus of the male Siberian hamster (*Phodopus sungorus*). *Appetite* 2000; **34:** 109–111.

34 Friedman TC, Loh YP, Birch NP. In vitro processing of proopiomelanocortin by recombinant PC1 (SPC3). *Endocrinology* 1994; **135:** 854–862.

35 Al-Barazanji KA, Miller JE, Rice SQ, Arch JR, Chambers JK. C-terminal fragments of ACTH stimulate feeding in fasted rats. *Horm Metab Res* 2001; **33:** 440–445.

36 Kato H, Kuwako K, Suzuki M, Tanaka S. Gene expression patterns of pro-opiomelanocortin-processing enzymes PC1 and PC2 during postnatal development of rat corticotrophs. *J Histochem Cytochem* 2004; **52:** 943–957.

37 Marcinikewicz M, Day R, Seidah NG, Chretien M. Ontogeny of the prohormone convertases PC1 and PC2 in the mouse hypophysis and their colocalization with corticotropin and alpha-melanotropin. *Proc Natl Acad Sci USA* 1993; **90:** 4922–4926.

38 Hammonds RG Jr, Nicolas P, Li CH. beta-endorphin-(1-27) is an antagonist of beta-endorphin analgesia. *Proc Natl Acad Sci USA* 1984; **81:** 1389–1390.

39 Zhou A, Bloomquist BT, Mains RE. The prohormone convertases PC1 and PC2 mediate distinct endoproteolytic cleavages in a strict temporal order during proopiomelanocortin biosynthetic processing. *J Biol Chem* 1993; **268:** 1763–1769.

40 Fricker LD. Carboxypeptidase E. *Annu Rev Physiol* 1988; **50:** 309–321.

41 Zhou A, Mains RE. Endoproteolytic processing of proopiomelanocortin and prohormone convertases 1 and 2 in neuroendocrine cells overexpressing prohormone convertases 1 or 2. *J Biol Chem* 1994; **269:** 17440–17447.

42 Allen RG, Peng B, Pellegrino MJ, Miller ED, Grandy DK, Lundblad JR, Washburn CL, Pintar JE. Altered processing of pro-orphanin FQ/nociceptin and pro-opiomelanocortin-derived peptides in the brains of mice expressing defective prohormone convertase 2. *J Neurosci* 2001; **21:** 5864–5870.

43 Millington WR, Smith DL. The posttranslational processing of beta-endorphin in human hypothalamus. *J Neurochem* 1991; **57:** 775–781.

44 Glass MJ, Billington CJ, Levine AS. Opioids and food intake: distributed functional neuronal pathways? *Neuropeptides* 1999; **33:** 360–368.

45 Kalra SP, Horvath TL. Neuroendocrine interactions between galanin, opioids, and neuropeptide Y in the control of reproduction and appetite. *Ann NY Acad Sci* 1998; **863:** 236–240.

46 de Zwaan M, Mitchell JE. Opiate antagonists and eating behaviour in humans: a review. *J Clin Pharmacol* 1992; **32:** 1060–1072.

47 Levine AS, Billington CJ. Opioids. Are they regulators of feeding? *Ann NY Acad Sci* 1989; **575:** 209–219.

48 Appleyard SM, Hayward M, Young JI, Butler AA, Cone RD, Rubinstein M, Low MJ. A role of endogenous opioids beta-endorphin in energy homeostasis. *Endocrinology* 2003; **144:** 1753–1760.

49 Bertagna X. Proopiomelanocortin-derived peptides. *Endocrinol Metab Clin North Am* 1994; **23:** 467–485.

50 Brown KS, Gentry RM, Rowland NE. Central injection in rats of alpha-melanocyte stimulating hormone analog: effects on food intake and brain Fos. *Regul Pept* 1998; **78:** 89–94.

51 Sakurai T, Amemiya A, Ishii M, Matsuzaki I, Chemelli RM, Tanaka H, Williams SC, Richarson JA, Kozlowski GP, Wilson S, Arch JR, Buckingham RE, Haynes AC, Carr SA, Annan RS, McNulty DE, Liu WS, Terrett JA, Elshourbagy NA, Bergsma DJ, Yanagisawa M. Orexins and orexin receptors: a family of hypothalamic neuropeptides and G protein-coupled receptors that regulate feeding behavior. *Cell* 1998; **92:** 696.

52 Edwards CM, Abusnana S, Sunter D, Murphy KG, Ghatei MA, Bloom SR. The effect of the orexins on food intake. comparison with neuropeptide Y, melanin-concentrating hormone and galanin. *J Endocrinol* 1999; **160:** R7–R12.
53 Haynes AC, Jackson B, Overend P, Buckingham RE, Wilson S, Tadayyon M, Arch JR. Effects of single and chronic intracerebroventricular administration of the orexins on feeding in the rat. *Peptides* 1999; **20:** 1099–1105.
54 Sakurai T, Moriguchi T, Furuya K, Kajiwara K, Nakamura T, Yanagisawa M, Goto K. Structure and function of human prepro-orexin gene. *J Biol Chem* 1999; **274:** 17771–17776.
55 Chou TC, Lee CE, Lu J, Elmquist JK, Hara J, Willie JT, Beuckmann CT, Chemelli RM, Sakurai T, Yanagisawa M, Saper CB, Scammell TE. Orexin (hypocretin) neurons contain dynorphin. *J Neurosci* 2001; **21:** RC168.
56 Dupuy A, Lindberg I, Zhou Y, Akil H, Lazure C, Chretien M, Seidah NG, Day R. Processing of prodynorphin by the prohormone convertase PC1 results in high molecular weight intermediate forms. Cleavage at a single arginine residue. *FEBS Lett* 1994; **337:** 60–65.
57 Khorooshi RM, Klingenspor M. Neuronal distribution of melanin-concentrating hormone, cocaine- and amphetamine-regulated transcript and orexin-B in the brain of the Djungarian hamster (*Phodopus sungorus*). *J Chem Neuroanatom* 2005; **29:** 137–148.
58 Lee SK, Hollenbeck PJ. Organization and translation of mRNA in sympathetic axons. *J Cell Sci* 2003; **116:** 4467–4478.
59 Koenig E, Giuditta A. Protein-synthesizing machinery in the axon compartment. *Neuroscience* 1999; **89:** 5–15.
60 Braks JA, Van Horssen AM, Martens GJ. Dissociation of the complex between the neuroendocrine chaperone 7B2 and prohormone convertase PC2 is not associated with proPC2 maturation. *Eur J Biochem* 1996; **238:** 505–510.
61 Barrett P, Ross AW, Balik A, Littlewood PA, Mercer JG, Moar KM, Sallmen T, Kaslin J, Panula P, Schuhler S, Ebling FJ, Ubeaud C, Morgan PJ. Photoperiodic regulation of histamine H3 receptor and VGF messenger ribonucleic acid in the arcuate nucleus of the Siberian hamster. *Endocrinology* 2005; **146:** 1930–1939.
62 Ross AW, Webster CA, Mercer JG, Moar KM, Ebling FJ, Schuhler S, Barrett P, Morgan PJ. Photoperiod regulation of hypothalamic retinoid signalling: association of retinoid X receptor gamma with body weight. *Endocrinology* 2004; **145:** 13–20.
63 Trani E, Giorgio A, Canu N, Amadoro G, Rinaldi AM, Halban PA, Ferri GL, Possenti R, Schinina ME, Levi A. Isolation and characterization of VGF peptides in rat brain. Role of PC1/3 and PC2 in the maturation of VGF precursor. *J Neurochem* 2002; **81:** 565–574.
64 Hahm S, Mizuno TM, Wu TJ, Wisor JP, Priest CA, Kozak CA, Boozer CN, Peng B, McEvoy RC, Good P, Kelley KA, Takahashi JS, Pintar JE, Roberts JL, Mobbs CV, Salton SR. Target deletion of the VGF gene indicates that the encoded secretory peptide precursor plays a novel role in the regulation of energy balance. *Neuron* 1999; **23:** 537–548.
65 Fricker LD, McKinzie AA, Sun J, Curran E, Qian Y, Yan L, Patterson SD, Courchesne PL, Richards B, Levin N, Mzhavia N, Devi LA, Douglass J. Identification and characterization of proSAAS, a granin-like neuroendocrine peptide precursor that inhibits prohormone processing. *J Neurosci* 2000; **20:** 639–648.
66 Mbikay M, Seidah NG, Chretien M. Neuroendocrine secretory protein 7B2: structure, expression and functions. *Biochem J* 2001; **357:** 329–342.
67 Westphal CH, Muller L, Zhou A, Zhu X, Bonner-Weir S, Schambelan M, Steiner DF, Lindberg I, Leder P. The neuroendocrine protein 7B2 is required for peptide hormone processing in vivo and provides a novel mechanism for pituitary Cushing's disease. *Cell* 1999; **96:** 689–700.

PHOTOPERIOD-DEPENDENT REGULATION OF CARBOXYPEPTIDASES D AND E AND EXOPROTEOLYTIC PROCESSING OF PRO-OPIOMELANORCORTIN IN THE SEASONAL SIBERIAN HAMSTER (*PHODOPUS SUNGORUS*)

HELWIG, M.[1, 2], LUDEWIG, P. S. [1], HELDMAIER, G.[1], MERCER, J.G.[2] and KLINGENSPOR, M.[3]

1. *Philipps-Universität Marburg, Faculty of Biology, Department of Animal Physiology, Marburg, Germany*
2. *The Rowett Research Institute, Division of Obesity and Metabolic Health, Aberdeen, Scotland, UK*
3. *Technische Universität München, Else Kröner-Fresenius Center, Molecular Nutritional Medicine, Freising-Weihenstephan, Germany*

Correspondence to:

Michael Helwig, Department of Animal Physiology, Philipps University Marburg, Karl von Frisch Str. 8, D-35043 Marburg, Germany

Tel: +49 6421 2823395

Fax: +49 6421 2828937

E-mail: helwigmi@staff.uni-marburg.de

Abstract

The production and maturation of bioactive peptides from biological inactive precursors underlies extensive post-translational processing including enzymatic cleavage by exo- and endoproteolytic peptidases. Endoproteolytic acting prohormone-convertases 1/3 and 2 (PC1/3, PC2) initially cut the precursors of many neuropeptides at specific dibasic amino acid sequences to generate intermediates with basic amino acid extensions on their C-termini. Consecutive related exopeptidases, carboxypeptidase D and E (CPD, CPE), are responsible for removing these amino acids before the peptides achieve biological activity. We investigated the effect of photoperiod on the post-translational processing of the neuropeptide precursor pro-opiomelanocortin (POMC) and its derived anorexigenic neuropeptides, alpha-melanocyte stimulating hormone (α-MSH) and β-endorphin (β-END), within key energy-balance regulating centres of the hypothalamus of the seasonal Siberian hamster (*Phodopus sungorus*). We thus compared hypothalamic protein distribution of CPD, CPE and POMC-derived neuropeptides α-MSH and β-END, using single and dual-fluorescence immunohistochemistry in short day (SD, 8h/16h light/dark) and long day (LD, 16h/8h light/dark) acclimatised hamsters. Furthermore we scrutinized the effect of leptin on the expression of both enzymes and neuropeptide substrates in either photoperiod. Immunoreactivity (-ir) of CPE was up regulated in SD along with increased total-α-MSH-ir and β-END-ir. Moreover administration of leptin induced a significant increase in CPD- and CPE-ir in SD. Our results suggest that exoproteolytic cleavage of POMC-derived neuropeptides is tightly regulated by photoperiod in the seasonal Siberian hamster. This in turn may yield higher levels of biological active anorexigenic neuropeptides in SD and may therefore be a key event in the regulation of seasonal energy balance.

Introduction

The maintenance of an appropriate body weight in seasonal mammals such as the Siberian hamster (*Phodopus sungorus*) is reliant on a precise adjustment of energy balance to prevailing environmental conditions (1). The major trigger that effects physiological adaptations such as an annual body weight trajectory is the seasonal change in ambient photoperiod. Siberian hamsters spontaneously reduce their food intake following transition to winter-like short-day photoperiod (6h: 18h light: dark) in anticipation to the coming shortage of food supplies (2,3). A significant proportion of studies focused on the central regulation of energy balance and considerably improved our understanding of the underling neuropeptidergic circuitries (4). It is well established that within the hypothalamus of Siberian hamsters, information on photoperiod gets integrated to peripheral energy balance related signals such as leptin which provides the CNS with information on the status of body fat stores (5-7). Subsequent processed information is encoded by a complex network of interacting orexigenic and anorexigenic neuropeptides generating the seasonally appropriate feeding behaviour (8). Among the so far identified peptidergic systems, pro-opiomelanocortin (POMC)-derived neuropeptides are putative candidates responsible for the seasonal decrease in food intake (9,10). It has been shown that adipocyte secreted leptin exerts its anorexigenic action in part by activation of hypothalamic arcuate nucleus POMC-expressing neurons (11). Downstream to the leptin signalling cascade, POMC-derived neuropeptides such as alpha-melanocyte stimulating hormone (α-MSH) activate the melanocortin-4 receptor resulting in a marked anorexigenic drive (12). Surprisingly differential seasonal gene expression of POMC is lacking (13,14). Initially POMC gets synthesised into a larger inactive polypeptide precursor undergoing extensive post-translational processing before its neuropeptide products achieve biological activity (15). Hence, based on the pro-hormone theory, gene expression of POMC is not the only means by which POMC-neuropeptide biosynthesis becomes modulated. The ultimate generation of bioactive POMC-derived α-MSH and beta-endorphin

(*β*-END) involves cleavage by pro-hormone convertases 1/3 (PC1/3) and 2 (PC2) (16,17) and carboxypeptidases D (CPD) and E (CPE) (18,19). Further diversification, amidation on the C terminus by peptidyl *α*-amidating monooxygenase (PAM), (20) and acetylation from desacetylated *α*-MSH is necessary for full maturation of *α*-MSH (21). Within the intracellular regulated secretory pathway (RSP), POMC-products are routed and processed in a tight temporal and spatial coordinated manner. During these post-translational processing events, POMC gets initially cleaved by neuroendocrine tissue specific PC1/3 yielding intermediated sized peptide fragments such as ACTH and β-Lipotropin (Fig. 1). Subsequently these fragments migrate through the trans-Golgi network (TGN) and are further cleaved by PC2 producing *α*-MSH, *β*-MSH*, γ*-MSH and *β*-END. Both, PC1/3 and PC2, cut their respective neuropeptide substrates at specific paired basic amino acid sequences consisting of lysine and arginine. Following this endoproteolytic cleavage the neuropeptides remain still inactive and are secreted from the TGN to the cytoplasm where they are stored in secretory vesicles until exocytosis. Prior to synaptic release exoproteolytic enzymes have been identified to remove the remaining C-terminal dibasic amino acid residues (22). This step is proposed to be a final activation event in neuropeptide biosynthesis from the inactive to the bioactive form. So far, two enzymes, carboxypeptidases D and E (CPD and CPE), have been isolated that meet the criterion of exo-proteases capable of removing the C-terminal dibasic amino acid residues within the RSP. Both, CPD and CPE, are highly concentrated in neuroendocrine tissue of the CNS, including the POMC expressing neurons of the hypothalamic arcuate nucleus (23). A critical involvement of carboxypeptidases in regulation of energy balance-related neuropeptide biosynthesis is highlighted by proteomic analysis in CPE deficient mice (Cpe^{fat}/ Cpe^{fat}). These mice are characterized by a severe maturity-onset obese phenotype (24) accompanied by low levels of mature anorexigenic *α*-MSH as demonstrated by quantitative mass-spectrometry (25). The absence of functional CPE in Cpe^{fat}/ Cpe^{fat} mice was believed to be lethal as prohormone processing by this exopeptidase is involved in the maturation of

numerous hormones. *Cpe*^{fat} mice, however, are viable with low levels of mature neuropeptides. In this mouse model CPD was discovered and it was established that this enzyme at least partially compensates for the loss of CPE (26). Together carboxypeptidases D and E are crucial for the final maturation of anorexigenic POMC-derived and other neuropeptides.

We previously demonstrated that in the Siberian hamster post-translational processing of POMC trough endoproteolytic prohormone convertases 1/3 (PC1/3) and 2 (PC2) is regulated by photoperiod (27). Consequently we detected higher levels of anorexigenic neuropeptides ACTH, α-MSH and β-END in SD. We hypothesize that this photoperiod-depended regulation of neuropeptide biosynthesis on an endoproteolytic level is continued by exoproteolytic cleavage through CPD and CPE. Therefore, in the present study we investigated the effect of photoperiod and leptin treatment on the expression of CPD and CPE within the arcuate nucleus of *P. sungorus*. To test our hypothesis we analyzed the hypothalamic protein content of CPD and CPE by immunohistochemistry in Siberian hamsters that were acclimated to either LD or SD for 14 weeks. Furthermore, we investigated the effect of intraperitoneal (i.p.) injected leptin on the immunoreactivity of both carboxypeptidases in the photoperiod paradigm (Fig. 2, experimental set-up). To assess a functional relationship between CPD/CPE and the POMC-derived neuropeptides *α*-MSH and *β*-END we determined the proportion of colocalization between both enzymes and their neuropeptide substrates by utilizing dual fluorescence immunohistochemistry.

Material and Methods

Animals and Experimental Procedure

All described procedures were in accordance with German animal welfare regulations, were licensed and had local ethical approval. Siberian hamsters (*Phodopus sungorus*) were drawn from the breeding colony established at the Faculty of Biology in Marburg (Germany). All animals were housed individually in Macrolon cages and had *ad libitum* access to food (Altromin, Lage, Germany) and water at all times. Body weights were assessed weekly. Photoperiods referred to in this article are defined as LD (long day, 16 : 8 h light-dark cycle) and SD (short day, 8 : 16 h light-dark cycle). Hamsters (n = 28) were born and reared in LD at 21-22 °C. Post weaning at 3 weeks of age, hamsters were divided into two groups, each containing 14 individuals matched for sex and body weight. Groups were further maintained in either LD or SD photoperiod with all other conditions unaltered. Following 14 weeks of acclimatization to the respective photoperiod, both groups were subdivided so that one half in each photoperiod (n = 7 /group) received a single intraperitoneal (i.p.) injection of recombinant mouse leptin (LD-L and SD-L; 4 mg/kg body weight; R&D Systems, Minneapolis) 120 min. before sacrifice, whereas the other group (n = 7 /group) received a control vehicle injection (LD-V and SD-V; 15 mM sterile HCl and 7.5 mM sterile NaOH). All animals were killed in the middle of the light phase by transcardiac perfusion with 0.9% saline containing heparin (1000 U/litre) and 4% paraformaldehyde (PFA) in 0.1 M phosphate-buffered saline (PBS, pH 7.4) under deep Ketamin/Rompun (Bayer, Germany) anesthesia. Brains were dissected, stored in 4% PFA-PBS solution (24 h, 4°C), followed by cryoprotection in 30% sucrose - 0.1 M PBS (48 h, 4°C), and were deep frozen in isopentane over dry ice (1 min). Brains were stored at -80°C until required.

Immunohistochemistry

Coronal sections (35 μm) of the brain spanning through the extend of the hypothalamus, corresponding to –1.6 to –4.52 mm relative to Bregma (28), were processed and collected in four series using a freezing microtome. Two series were used for quantification of hypothalamic CPD- and CPE-immunoreactivity (-ir) employing a single staining protocol. On the residual two series analysis of CPD-ir/CPE-ir and substrates/products α-MSH-ir/β-END-ir colocalization was performed utilizing of fluorescence double staining.

Single immunostaining

Endogenous peroxidase activity was inhibited in sections using 80% phosphate buffered saline (PBS), 10% methanol and 10% H_2O_2 for 15 min at RT. Free-floating sections were rinsed in PBS and 0.5 % Triton X-100 - 0.1 M PBS (0.5% PBS-T). Following pre-incubation in a blocking solution (BS) containing 0.5% PBS-T and 3% bovine serum albumin (BSA). Sections were incubated with primary polyclonal rabbit anti-CPD antibody (1:500) or anti-CPE (1:150) in BS overnight at 4 °C. Following washes in 0.5% PBS-T, sections were then incubated with a biotinylated secondary goat anti-rabbit antibody for 1 h (1:1000, in BS) and then treated with ABC signal enhancing solution (Vector Labs, Burlingame, USA) for 2 h. Using Vector SG Nickel-DAB substrate solution for peroxidase (SK-4700, Vector Labs, Burlingame, USA), the colour reaction resulted in dark-gray/blue precipitate. Sections were then rinsed in PBS, mounted on gelatin-coated slides, air-dried, dehydrated in graded alcohol, cleared in xylene and coverslipped with Enthelan (Merck, Germany). Quantification was performed by using a Zeiss Axioskop (Carl Zeiss, Jena, Germany) microscope (objective, 20X). Images were taken by a mounted Polaroid DMCe digital camera. Immunoreactive cells in three comparable sections of each individual animal were counted without knowledge of the experimental treatment. Cell bodies were counted in the hypothalamic arcuate nucleus approximating from -2.12 mm to -4.3 mm relative to Bregma, according to stereotaxic

coordinates from the rat brain (28). Total ir-cell number for each individual animal was calculated followed by the assessment of mean values for each experimental group.

Dual immunostaining

Free-floating sections were treated with blocking solution (BS) containing 3% bovine serum albumin (BSA) in 0.5 % Triton X-100 - 0.1 M PBS (0.5% PBS-T) for 1 h to block non-specific reactions. Then, sections were incubated with polyclonal rabbit anti-CPD (1:200) or anti-CPE (1:150) in BS overnight (4 °C). Following washes in 0.25% PBS-T, sections (containing anti-CPD) were incubated for 2h with unconjugated goat anti-rabbit Fab-fragment antibody (111-007-003, Jackson ImmunoResearch, West Grove, USA) diluted 1:60 in BS at room temperature (RT). Sections were rinsed briefly in 0.25% PBS-T and incubated with Cy3 (Ex_{max} 554 nm, Em_{max} 566 nm) conjugated donkey anti-goat secondary antibody in BS (1:250, 705-165-147, Jackson ImmunoResearch, West Grove, USA) for 2h at RT, rinsed again in 0.25% PBS-T and incubated with second primary polyclonal rabbit anti-*β*-endorphin (1:100, H-022-33, Phoenix Pharmaceuticals, Belmont, USA) in BS overnight at 4 °C. Sections were incubated with Alexa 488 dye (Ex_{max} 492 nm, Em_{max} 520 nm) conjugated goat anti-rabbit secondary antibody (1:250, Molecular Probes, Eugene, USA) in BS for 2 h at RT. Colocalization for α-MSH was performed with polyclonal sheep anti-α-MSH antibody (1:15.000, Chemicon, Temecula, USA) in BS overnight at 4 °C. Here the different primary antibody necessitated an intermediate step of Fab-fragment incubation. α-MSH was visualized by incubation with Fluorescein (Ex_{max} 494 nm, Em_{max} 520 nm) conjugated donkey anti-sheep secondary antibody (1:100, AP184F, Chemicon) in BS for 2 h at RT. Incubation with the second primary antibodies and secondary antibody matched the steps described above. Sections were then rinsed in PBS, mounted on gelatin-coated slides, air-dried, dehydrated in graded alcohol, cleared in xylene and coverslipped with Enthelan (Merck Biosciences, Darmstadt, Germany). Immunoreactive cell bodies were counted according to the described

protocol for single immunostaining. Images were merged by colour channel overlay using image processing software (Adobe Photoshop version 7.0). The anatomical localization of neuropeptides within the brain of Siberian hamsters was annotated according to the atlas of the rat brain (28).

Controls

Antibodies against CPD and CPE (rabbit polyclonal antisera; anti-CPD, AE160, against C-terminus; anti-CPE, against N-terminus) were kind gifts of Dr. Lloyd Fricker (Albert Einstein College of Medicine; Bronx, NY, USA). The specificity has been previously demonstrated and is described elsewhere (29,30). Antibodies against α-MSH and β-endorphin are commercially available (polyclonal sheep anti-α-MSH, AB5087, Chemicon; polyclonal rabbit anti-*β*-endorphin, H-022-33, Phoenix) and were used in a previous study (27). They have been tested for specificity by pre-incubation of the antibodies with their complementary peptide (α-MSH, 043-01, Phoenix; β-endorphin, 022-33, Phoenix), prior to application resulting in no staining. Additional negative controls were performed by incubation of sections lacking primary antisera.

Statistical analysis

Data were analysed by one- or two-way ANOVA followed by the Student-Newman-Keuls multiple comparison test, as appropriate using a statistical software package (SigmaStat, Jandel, Erkrath, Germany). Where data failed equal variance or normality tests they where analyzed by one-way ANOVA on ranks followed by Dunn's multiple comparison test. Data for single staining immunohistochemistry experiments are presented as percentage values of LD control ± SEM. Data for colocalization of CPD/CPE with *β*-endorphin/α-MSH by dual fluorescence immunostaining are presented as total number of counted immunoreactive cells ± S.D. A probability value of $P < 0.05$ was considered as statistically significant.

Results

Effect of photoperiod on hamster body weight

At week 0 animals weighed an average of 42.2 g (± 3.8 g, n = 28). Exposure of hamsters to SD for 14 weeks led to a substantial decrease of body weight to 30.9 g (± 2.9 g, n = 14) and resulted in a significant body weight differential of 33.3% compared to the body weight trajectory of LD hamsters (41.2 g ± 4.1 g, n = 14) (one-way ANOVA on ranks; H = 19,265; P <0,001).

Effect of photoperiod and leptin treatment on protein expression of CPD and CPE in the arcuate nucleus of the Siberian hamster

Using a peroxidase immunohistochemistry method immunoreactive cells and fibres for CPD and CPE could be observed in various specific nuclei of the hamster hypothalamus including the supraoptic hypothalamic nucleus (SON), paraventricular nucleus (PVN), ventromedial hypothalamic nucleus (VMH) and the arcuate nucleus (ARC, Fig. 3 A and B). The neuroanatomical distribution of CPD-immunoreactivity (-ir) generally corresponded with the expression pattern of CPE-ir within these hypothalamic nuclei (data not shown). Although, overall more CPD-ir compared to CPE-ir positive cells were observed in the specific hypothalamic nuclei of animals within the same treatment group (LD-V vs. LD-V). This difference was quantified by counting of CPD- and CPE-ir positive cells in the ARC and revealed significantly elevated (one-way ANOVA; F =13.119, P = 0.004) CPD-ir (LD-V, 71 ±14 ir-cells) than CPE-ir (LD-V, 50 ±14 ir-cells).

In the ARC there was no significant effect of photoperiod on the number of counted CPD-ir cells (Fig. 3 A); vehicle receiving controls kept in LD-V had 71 ±14 ir-cells and those in SD-V had 81 ±9 ir-cells within the investigated region of the ARC. Leptin treatment failed to induce a significant difference in CPD-ir of LD photoperiod acclimated individuals [LD-V

(71 ±14 ir-cells) vs. LD-L (84 ±11 ir-cells)]; however, there was a statistically significant increase of CPD-ir positive cells by 20% (pairwise multiple comparison; P = 0.010) in the ARC of SD-L hamsters (101 ±15 ir-cells) compared to those levels counted for CPD-ir in the respective vehicle treated animals in SD [SD-V (81 ±9 ir-cells)]. Furthermore two-way ANOVA statistical analysis revealed no significant interaction of photoperiod and leptin/vehicle treatment (F = 54. 33, P = 0.564).

Acclimation to SD induced an increase in arcuate nucleus CPE-ir (SD-V; 99 ±17 ir-cells) by 90% of the levels observed in LD (LD-V; 52 ±7 ir-cells; Fig. 3 B). This effect was statistically significant in the vehicle treated groups as revealed by two-way ANOVA (F = 157.611; P < 0.001). While leptin treatment in LD photoperiod [LD-V (52 ±7 ir-cells) vs. LD-L (65 ±13 ir- cells)] failed to induce a significant difference in CPE-ir, there was a significant effect of leptin treatment within the SD acclimated hamster group [SD-V (99 ±17 ir-cells) vs. SD-L (149 ±16 ir-cells); P < 0.001]. In addition there was a statistically significant interaction of photoperiod and leptin/vehicle treatment on CPE-ir (F = 8.468; P = 0.008).

Effect of photoperiod and leptin treatment on colocalization of CPD and CPE with α-MSH and β-endorphin immunoreactivity

Immunoreactivity of Carboxypeptidases D and E visualized by dual fluorescence staining corresponded to the observed neuroanatomical distribution within the hypothalamus obtained from the single staining experiment. By contrast, immunoreactivity of α-MSH and *β*-endorphin was mainly confined to the arcuate nucleus.

Quantification of *β*-endorphin-ir cell numbers within the ARC revealed significantly more *β*-END-ir in SD acclimated hamsters compared to those levels observed in LD [Fig. 4 A, two-way ANOVA; F = 46,841, P < 0,001; LD-V (57 ±9 ir-cells) vs. SD-V (84 ±14 ir-cells)]. The increase of *β*-END-ir observed in SD was accompanied by an increase of CPD-ir [LD-V (77 ±17 ir-cells) vs. SD-V (86 ±12 ir-cells)]. Leptin treatment failed to induce a

significant difference of *β*-END-ir in LD [pairwise multiple comparison, P = 0.081; LD-L (71 ±9 ir-cells)] but lead to a significant increase in SD [pairwise multiple comparison, P = 0.012; SD-L (101 ±10 ir-cells)] compared to those levels observed in the respective vehicle treated animals. Quantification of numbers of *β*-END-ir neurons positive to CPD-ir revealed a high degree of colocalization throughout the four experimental paradigms [LD-V (87.7%), LD-L (97.1%), SD-V (94.0%) and SD-L (93.0%)]. The observed number of CPD-ir cells, however, slightly exceeded the number of *β*-END-ir positive cells in all experimental groups. As a result there where also CPD-ir positive cells which were not *β*-END-ir positive. (Fig. 4 B, hatched arrows). Furthermore, CPD-ir was not exclusively restricted to perikarya but was distributed throughout fibre-like structures and agglomerated in grains outside of cell bodies as demonstrated by high magnification photomicrographs (Fig. 4 B, hatched arrows).

Counting of α-MSH-ir positive cells within the ARC revealed significantly more α-MSH-ir in SD acclimated hamsters compared to those levels observed in LD [Fig. 5 A, two-way ANOVA; F =157,611, P<0,001; LD-V (54 ±9 ir-cells) vs. SD-V (84 ±11 ir-cells)]. The increase of α-MSH-ir observed in SD was accompanied by an increase of CPE-ir [LD-V (56 ±11 ir-cells) vs. SD-V (111 ±20 ir-cells)]. Leptin treatment failed to induce a significant effect on α-MSH-ir expression in LD [pairwise multiple comparison, P = 0.053; LD-L (63 ±17 ir-cells)] but lead to a significant increase of α-MSH-ir cells in SD [pairwise multiple comparison, P < 0.001; SD-L (98 ±18 ir-cells)] compared to those levels observed in the respective vehicle treated animals. Colocalization of α-MSH-ir cells with CPE immunoreactivity revealed a nearly complete match of this POMC-derived neuropeptide and the cleavage mediating carboxypeptidase in all four experimental paradigms [LD-V (94.0%), LD-L (95.2%), SD-V (97.6%) and SD-L (96.9%)]. The observed number of CPE-ir cells in SD-L (109 ±17 ir-cells), however, significantly exceeded the number of α-MSH-ir positive cells (one-way ANOVA; SD-L, F=44.86, P<0,001). As a result in SD acclimated and vehicle treated animals hamsters there where 26.2% (29 ±7 ir-cells) and in leptin treated individuals

38.4% (59 ±10 ir-cells) of CPE-ir positive cells which were not α-MSH-ir positive (Fig. 5 B, hatched arrows). Similar to the distribution of CDP-ir, CPE-ir was found throughout fibres and dendrite-like structures of the hypothalamus and agglomerated in crystal like dots outside of perikarya as demonstrated by high magnification photomicrographs (Fig. 4 B, hatched arrows).

Discussion

It is well established that within neurons of the hypothalamic arcuate nucleus a complementary system of orexigenic and anorexigenic neuropeptides is instrumental in the regulation of body weight (4). In the Siberian hamster, however, POMC gene expression is not altered in respect of the anticipated seasonal body weight adaptation (13). Here we demonstrate that expression of exoproteolytic enzyme carboxypeptidase E in hypothalamic melanocortinergic neurons of the Siberian hamster is regulated by photoperiod. In addition we detected higher levels of CPE-ir associated with an elevated abundance of POMC-derived neuropeptides α-MSH and *β*-END in neurons of the ARC suggesting a photoperiod-dependent increase in post-translational enzymatic "activation" of anorexigenic POMC-derived neuropeptides in SD.

Hamsters kept in SD for 14 weeks decreased their body weight by 27% while hamsters in LD maintained a comparatively high body weight average over the same time period. Studies investigating the effect of photoperiod on the body weight trajectory of Siberian hamsters demonstrated that the observed decrease in body weight in SD for a substantial part is due to the associated inhibition of food intake (31). These observations strongly indicate an increased activity of biologically active anorexigenic neuropeptides in SD-acclimated Siberian hamsters and are in line with our previous and current findings showing higher levels of α-MSH and *β*-END-ir, both of which have been reported to potently suppress food intake (9,32). Our immunohistochemical studies revealed neuroanatomical distribution patterns of the corresponding "neuropeptide-activating" enzymes CPD-ir and CPE-ir similar to those observed in other rodent species such as rat and mice (26,33) with high concentrations of immunoreactivity in cells of the hypothalamic arcuate nucleus. Along with immunoreactivity of CPD, distribution of CPE-ir was localized to perikarya and somata but was also present in axon-like fibres of the neuronal hypothalamic network. These observations are consistent with the intracellular localization of both carboxypeptidases in the regulated secretory pathway

(RSP) including the trans-Golgi network (TNG) and axonal transported secretory vesicles. The shortening in photoperiod and associated loss of body weight in SD acclimated hamsters was not accompanied by a change of CPD-ir. Based on the enzymatic properties of CPD, which basically reassemble those of CPE, and similar neuroanatomical distribution it has been proposed that CPD is involved in the intracellular processing of neuropeptides. We conclude that enzymatic activity of CPD is of rather secondary importance in the photoperiod-depended activation of inactive melanocortinergic neuropeptides in the Siberian hamster. Although CPD has been reported to carry out exoproteolytic cleavage in CPE-deficient Cpe^{fat}/ Cpe^{fat} mice compensating for the loss of CPE our view is supported by the fact that levels of CPD-yielded mature neuropeptides in these mice are much lower compared to those found in wild type mice (34). Also, unlike CPE, CPD is wildly distributed throughout non-neuroendocrine cells of the central nervous system including glia and is not restricted to neuropeptidergic neurons (26). This fact is reflected in our observation showing that a relatively high proportion of CPD-ir cells do not colocalize with POMC-derived β-END-ir neurons of the ARC. In contrast to CPD, immunoreactivity of CPE was significantly increased in response to short photoperiod. Moreover, CPE-ir in SD is conspicuously accompanied by increased levels of α-MSH-ir within the same neurons of the ARC. It is well established that initial endoproteolytic cleavage of POMC by prohormone convertases yields intermediate sized peptides with C-terminal basic residues (35,36). Subsequently CPE has been reported to rapidly and specifically remove these terminal basic amino acid extensions (19,37). Together, observed overlapping spatial and temporal expression patterns of CPE-ir, α-MSH-ir and β-END-ir, as well as the enzyme specificity of carboxypeptidases for POMC-derived neuropeptides, strongly indicate a functional relation. Hence, we suggest that the observed regulatory change in CPE protein expression in SD is associated with a higher conversion of non-truncated to C-terminally cleaved and biological active neuropeptides. In the case of POMC-derived

anorexigenic α-MSH this enzymatic activation by CPE would be as anticipated for a catabolic peptide that is involved in establishing a seasonal body weight differential.

Moreover, we discovered a profound photoperiod-dependent effect of leptin treatment on the expression of both carboxypeptidases within neurons of the ARC. The hypothalamic melanocortin system plays a pivotal role in mediating the leptin-induced feedback inhibition of feeding. Leptin receptors (ObRs) are highly expressed in the hypothalamus including POMC-ergic neurons of the arcuate nucleus (38) and administration of leptin has been reported to induce POMC gene expression in this neurons (39). Therefore it is plausible that exogenous administration of leptin activates POMC-processing enzymes. Intriguingly, the observed increase in CPD-ir and CPE-ir positive cells 2h after leptin treatment was restricted to SD acclimated animals. This highly photoperiod-selective effect of leptin on the expression of carboxypeptidases follows the principle of a seasonal change in the central sensitivity to leptin in the Siberian hamster which has been the focus of a number of studies (5). It was demonstrated that hamsters in LD, which exhibit comparatively high blood plasma leptin levels, are resistant to the anorexigenic effect of this hormone due to a reversible impairment of intracellular signalling by a suppressor of cytokine signalling (SOCS3) (40). In SD, however, leptin signalling is fully restored and may therefore contribute to the observed regulatory change in carboxypeptidase expression. It remains to be identified whether the effect of leptin is a direct molecular one on a transcriptional level or indirect by either neuronal or via intermediate pathways. We believe that besides inducing the production of POMC-derived neuropeptides leptin may indirectly modulate the synthesis and activity of CPD and CPE by enhancing the level of non-cleaved prohormones which constitute the substrate of both enzymes. Our observations that enzymatic components of POMC-processing are regulated by leptin are corroborated by another study that investigated the effect of leptin on the post-translational modification of POMC-derived α-MSH by N-acetylation in mice (21). The authors of this study demonstrated that acetylation of α-MSH by an N-

acetyltransferase is rapidly increased following leptin treatment and this in turn yielded an enhanced biological activity of the neuropeptide. They also found a leptin-induced increase in the levels of total α-MSH which, as they concluded, presumably reflected an increased activity of proteolytic POMC-processing enzymes. Together, these observations are in line with our findings in the Siberian hamster showing increased levels of cleavage-mediating enzymes CPD/CPE as well as increased levels of POMC-derived α-MSH and *β*-END following leptin treatment.

One could argue that the authors of this study did not perform colocalization of CPD with α-MSH or CPE with *β*-END. This, however, is not necessarily a prerequisite to assess a functional relationship between the carboxypeptidases and their POMC-derived peptide substrates. Firstly, CPD has been reported to be expressed in nearly the same population of neurons as CPE (26) and secondly α-MSH and *β*-END are produced from the same precursor in equimolar amounts (23). Hence, both carboxypeptidases will colocalize with α-MSH as well as *β*-END. Moreover, antibodies used in this study were raised against total α-MSH and *β*-END and do not distinguish between the inactive and C-terminally truncated active form of neuropeptides. But, the observed increase in both, total amount of POMC-derived neuropeptides and CPE, within the same neurons strongly indicates an overall increased enzymatic turn-over from inactive to biological active anorexigenic α-MSH and *β*-END in SD. To our knowledge this study demonstrates for the first time a leptin-induced activation of carboxypeptidases in a physiological animal model and therefore strengthens the proposed capacity of post-translational processing in regulation of energy balance related neuropeptide maturation. In conclusion, our data provide further evidence that post-translational processing of neuropeptide precursors by proteases is an integral part of a regulatory mechanism that integrates photoperiod and peripheral leptin signalling to the central hypothalamic neuropeptidergic network. This in turn may contribute to establish the seasonal body weight differential in the Siberian hamster.

Acknowledgements

We would like to thank Dr Lloyd Fricker (Albert Einstein College of Medicine, New York, U.S.A.) for generously providing us with CPD and CPE antibodies and Sigrid Stöhr for her excellent technical assistance. M. Helwig was recipient of a fellowship funded by the European Commission to attend the ObeS^{e}chool European Union Marie Curie Training Site at the Rowett Research Institute. This collaborative study was also funded by the Scottish Government (to J. G. Mercer) and EC FP6 funding ('DIABESITY' contract no. LSHM-CT-2003-503041 to J. G. Mercer), Deutsche Forschungsgemeinschaft (German Research Foundation KL973/5; to M. Klingenspor), the National Genome Research Network (NGFN 01GS0483; to M. Klingenspor).

References

1. Mercer JG. Regulation of appetite and body weight in seasonal mammals Comp Biochem Physiol C Pharmacol Toxicol Endocrinol 1998; 119**:** 295-303.

2. Steinlechner S, Heldmaier G. Role of photoperiod and melatonin in seasonal acclimatization of the Djungarian hamster, Phodopus sungorus Int J Biometeorol 1982; 26**:** 329-337.

3. Steinlechner S, Buchberger A, Heldmaier G. Circadian rhythms of pineal N-acetyltransferase activity in the Djungarian hamster, Phodopus sungorus, in response to seasonal changes of natural photoperiod J Comp Physiol [A] 1987; 160**:** 593-597.

4. Schwartz MW, Woods SC, Porte D, Jr., Seeley RJ, Baskin DG. Central nervous system control of food intake Nature 2000; 404**:** 661-671.

5. Klingenspor M, Niggemann H, Heldmaier G. Modulation of leptin sensitivity by short photoperiod acclimation in the Djungarian hamster, Phodopus sungorus J Comp Physiol [B] 2000; 170**:** 37-43.

6. Tups A, Ellis C, Moar KM, Logie TJ, Adam CL, Mercer JG, Klingenspor M. Photoperiodic regulation of leptin sensitivity in the Siberian hamster, Phodopus sungorus, is reflected in arcuate nucleus SOCS-3 (suppressor of cytokine signaling) gene expression Endocrinology 2004; 145**:** 1185-1193.

7. Mercer JG, Tups A. Neuropeptides and anticipatory changes in behaviour and physiology: seasonal body weight regulation in the Siberian hamster Eur J Pharmacol 2003; 480**:** 43-50.

8. Morgan PJ, Ross AW, Mercer JG, Barrett P. Photoperiodic programming of body weight through the neuroendocrine hypothalamus J Endocrinol 2003; 177**:** 27-34.

9. McMinn JE, Wilkinson CW, Havel PJ, Woods SC, Schwartz MW. Effect of intracerebroventricular alpha-MSH on food intake, adiposity, c-Fos induction, and neuropeptide expression Am J Physiol Regul Integr Comp Physiol 2000; 279**:** R695-R703.

10. Cone RD. Anatomy and regulation of the central melanocortin system Nat Neurosci 2005; 8**:** 571-578.

11. Schwartz MW, Seeley RJ, Campfield LA, Burn P, Baskin DG. Identification of targets of leptin action in rat hypothalamus J Clin Invest 1996; 98**:** 1101-1106.

12. Schuhler S, Horan TL, Hastings MH, Mercer JG, Morgan PJ, Ebling FJ. Decrease of food intake by MC4-R agonist MTII in Siberian hamsters in long and short photoperiods Am J Physiol Regul Integr Comp Physiol 2003; 284**:** R227-R232.

13. Mercer JG, Moar KM, Ross AW, Hoggard N, Morgan PJ. Photoperiod regulates arcuate nucleus POMC, AGRP, and leptin receptor mRNA in Siberian hamster hypothalamus Am J Physiol Regul Integr Comp Physiol 2000; 278**:** R271-R281.

14. Reddy AB, Cronin AS, Ford H, Ebling FJ. Seasonal regulation of food intake and body weight in the male Siberian hamster: studies of hypothalamic orexin

(hypocretin), neuropeptide Y (NPY) and pro-opiomelanocortin (POMC) Eur J Neurosci 1999; 11**:** 3255-3264.

15. Nillni EA. Regulation of prohormone convertases in hypothalamic neurons: implications for prothyrotropin-releasing hormone and proopiomelanocortin Endocrinology 2007; 148**:** 4191-4200.

16. Pan H, Che FY, Peng B, Steiner DF, Pintar JE, Fricker LD. The role of prohormone convertase-2 in hypothalamic neuropeptide processing: a quantitative neuropeptidomic study J Neurochem 2006; 98**:** 1763-1777.

17. Steiner DF. The proprotein convertases Curr Opin Chem Biol 1998; 2**:** 31-39.

18. Song L, Fricker LD. Tissue distribution and characterization of soluble and membrane-bound forms of metallocarboxypeptidase D J Biol Chem 1996; 271**:** 28884-28889.

19. Fricker LD. Carboxypeptidase E Annu Rev Physiol 1988; 50**:** 309-321.

20. Pritchard LE, White A. Neuropeptide processing and its impact on melanocortin pathways Endocrinology 2007; 148**:** 4201-4207.

21. Guo L, Munzberg H, Stuart RC, Nillni EA, Bjorbaek C. N-acetylation of hypothalamic alpha-melanocyte-stimulating hormone and regulation by leptin Proc Natl Acad Sci U S A 2004; 101**:** 11797-11802.

22. Fricker LD, Snyder SH. Enkephalin convertase: purification and characterization of a specific enkephalin-synthesizing carboxypeptidase localized to adrenal chromaffin granules Proc Natl Acad Sci U S A 1982; 79**:** 3886-3890.

23. Mezey E, Kiss JZ, Mueller GP, Eskay R, O'Donohue TL, Palkovits M. Distribution of the pro-opiomelanocortin derived peptides, adrenocorticotrope hormone, alpha-melanocyte-stimulating hormone and beta-endorphin (ACTH, alpha-MSH, beta-END) in the rat hypothalamus Brain Res 1985; 328**:** 341-347.

24. Cawley NX, Zhou J, Hill JM, Abebe D, Romboz S, Yanik T, Rodriguiz RM, Wetsel WC, Loh YP. The carboxypeptidase E knockout mouse exhibits endocrinological and behavioral deficits Endocrinology 2004; 145**:** 5807-5819.

25. Che FY, Fricker LD. Quantitation of neuropeptides in Cpe(fat)/Cpe(fat) mice using differential isotopic tags and mass spectrometry Anal Chem 2002; 74**:** 3190-3198.

26. Dong W, Fricker LD, Day R. Carboxypeptidase D is a potential candidate to carry out redundant processing functions of carboxypeptidase E based on comparative distribution studies in the rat central nervous system Neuroscience 1999; 89**:** 1301-1317.

27. Helwig M, Khorooshi RM, Tups A, Barrett P, Archer ZA, Exner C, Rozman J, Braulke LJ, Mercer JG, Klingenspor M. PC1/3 and PC2 gene expression and post-translational endoproteolytic pro-opiomelanocortin processing is regulated by photoperiod in the seasonal Siberian hamster (Phodopus sungorus) J Neuroendocrinol 2006; 18**:** 413-425.

28. Paxinos G, Watson C. The Rat Brain in Stereotaxic Coordinates 2nd ed. Academic Press 1986.

29. Varlamov O, Leiter EH, Fricker L. Induced and spontaneous mutations at Ser202 of carboxypeptidase E. Effect on enzyme expression, activity, and intracellular routing J Biol Chem 1996; 271**:** 13981-13986.

30. Song L, Fricker LD. Tissue distribution and characterization of soluble and membrane-bound forms of metallocarboxypeptidase D J Biol Chem 1996; 271**:** 28884-28889.

31. Wade GN, Bartness TJ. Effects of photoperiod and gonadectomy on food intake, body weight, and body composition in Siberian hamsters Am J Physiol 1984; 246**:** R26-R30.

32. Low MJ, Hayward MD, Appleyard SM, Rubinstein M. State-dependent modulation of feeding behavior by proopiomelanocortin-derived beta-endorphin Ann N Y Acad Sci 2003; 994**:** 192-201.

33. Lynch DR, Braas KM, Hutton JC, Snyder SH. Carboxypeptidase E (CPE): immunocytochemical localization in the rat central nervous system and pituitary gland J Neurosci 1990; 10**:** 1592-1599.

34. Fricker LD. Neuropeptidomics to study peptide processing in animal models of obesity Endocrinology 2007; 148**:** 4185-4190.

35. Zhou A, Bloomquist BT, Mains RE. The prohormone convertases PC1 and PC2 mediate distinct endoproteolytic cleavages in a strict temporal order during proopiomelanocortin biosynthetic processing J Biol Chem 1993; 268**:** 1763-1769.

36. Zhou A, Mains RE. Endoproteolytic processing of proopiomelanocortin and prohormone convertases 1 and 2 in neuroendocrine cells overexpressing prohormone convertases 1 or 2 J Biol Chem 1994; 269**:** 17440-17447.

37. Day R, Lazure C, Basak A, Boudreault A, Limperis P, Dong W, Lindberg I. Prodynorphin processing by proprotein convertase 2. Cleavage at single basic residues and enhanced processing in the presence of carboxypeptidase activity J Biol Chem 1998; 273**:** 829-836.

38. Mercer JG, Hoggard N, Williams LM, Lawrence CB, Hannah LT, Trayhurn P. Localization of leptin receptor mRNA and the long form splice variant (Ob-Rb) in mouse hypothalamus and adjacent brain regions by in situ hybridization FEBS Lett 1996; 387**:** 113-116.

39. Schwartz MW, Seeley RJ, Woods SC, Weigle DS, Campfield LA, Burn P, Baskin DG. Leptin increases hypothalamic pro-opiomelanocortin mRNA expression in the rostral arcuate nucleus Diabetes 1997; 46**:** 2119-2123.

40. Tups A, Barrett P, Ross AW, Morgan PJ, Klingenspor M, Mercer JG. The suppressor of cytokine signalling 3, SOCS3, may be one critical modulator of seasonal body weight changes in the Siberian hamster, Phodopus sungorus J Neuroendocrinol 2006; 18**:** 139-145.

Figure legends

Fig. 1: Schematic representation of pro-opiomelanocortin (POMC) and its post-translational processing by endoproteolytic and exoproteolytic enzymes indicated by triangles. POMC gets initially cleaved by prohormone convertases 1 (PC1/3) and 2 (PC2) at paired basic amino acids R (Lysine) and K (Arginine) resulting in intermediate peptide fragments (upper panel). Subsequent cleavage of these peptide fragments by carboxypeptidases D (CPD) and E (CPE) results in bioactive neuropeptides (lower panel). α-MSH, α-melanocyte stimulating hormone; ACTH, adrenocorticotrophic hormone; *β*-End, *β*-endorphin; CLIP, corticotrophin-like intermediate peptide.

Fig. 2: Experimental setup: Two groups of adult Siberian hamsters where either exposed to short [short day (SD); 8:16-h light-dark cycle] or long photoperiod [long day (LD); 16:8-h light-dark cycle] and body weight was assessed weekly (means ± SEM, $n = 14$ per group). After 14 weeks both groups were subdivided so that one half of each photoperiod (n = 7 /group) received a single intraperitoneal (i.p.) injection of leptin (groups termed LD-L and SD-L) 120 min before sacrifice, whereas the other group (n = 7 /group) received a control vehicle injection (groups termed LD-V and SD-V).

Fig. 3: Quantitative analysis of CPD and CPE immunoreactive (-ir) cells within the arcuate nucleus (ARC) of the Siberian hamster hypothalamus. Data are number of ir-cells expressed as percentage of long day-vehicle controls (*$P < 0.05$, n = 7 per group). Lower panel: Representative photomicrographs showing neuroanatomical distribution of immunoreactive cells in comparable hypothalamic areas of long day (LD) and short day (SD) acclimatized animals. 3V, third ventricle; ARC, arcuate nucleus; ME, median eminence. Scale bar = 100 μm.

Fig. 4: A) Quantitative colocalization analysis of carboxypeptidase D (CPD) with *β*-endorphin (*β*-END). Values are presented as total number of counted immunoreactive cells (means ±S.D.) in SD and LD, either leptin or vehicle treated (n = 7 / group) B) Photomicrographs showing immunofluorescence double staining of CPD-immunoreactivity (-ir) with POMC derived *β*-END-ir in the arcuate nucleus of the Siberian hamster in SD. The upper row shows low magnification images and the lower row high magnification images of selected (boxed) areas. Merged images (centre) demonstrate colocalization of immunoreactive products. Colocalization is demonstrated by solid arrows, single cell-ir by dashed arrows. 3V, third ventricle; ARC, arcuate nucleus. Scale bars, low magnification images = 100 μm; high magnification images = 30 μm.

Fig. 5: A) Quantitative colocalization analysis of carboxypeptidase E (CPE) with α-melanocyte stimulating hormone (α-MSH). Values are presented as total number of counted immunoreactive cells (means ±S.D.) in SD and LD, either leptin or vehicle treated (n = 7 / group) B) Photomicrographs showing immunofluorescence double staining of (CPE)-immunoreactivity (-ir) with POMC derived α-MSH-ir in the arcuate nucleus of the Siberian hamster in SD. The upper row shows low magnification images and the lower row high magnification images of selected (boxed) areas. Merged images (centre) demonstrate colocalization of immunoreactive products. Colocalization is demonstrated by solid arrows, single cell-ir by dashed arrows. 3V, third ventricle; ARC, arcuate nucleus. Scale bars, low magnification images = 100 μm; high magnification images = 30 μm.

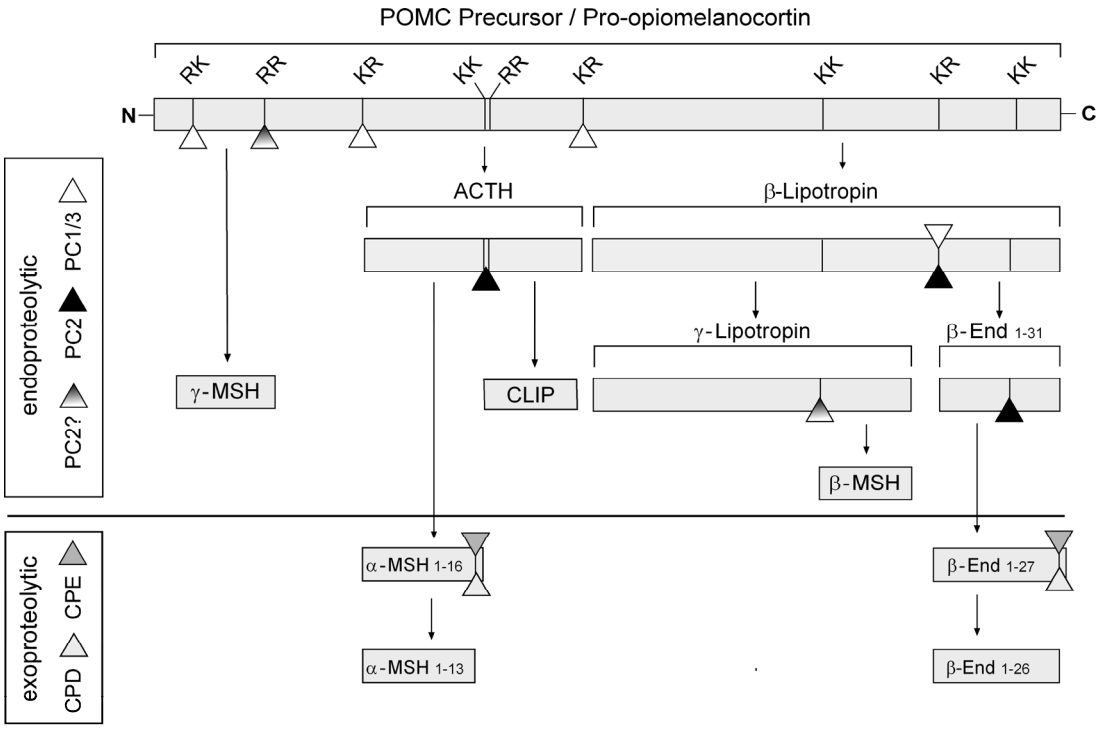
POMC Precursor / Pro-opiomelanocortin
RK
RR
KR
KK
RR
KR
KK
KR
KK
N
C
ACTH
β-Lipotropin
γ-MSH
CLIP
γ-Lipotropin
β-End 1-31
β-MSH
α-MSH 1-16
β-End 1-27
α-MSH 1-13
β-End 1-26
endoproteolytic
PC1/3
PC2
PC2?
exoproteolytic
CPE
CPD

Fig. 1

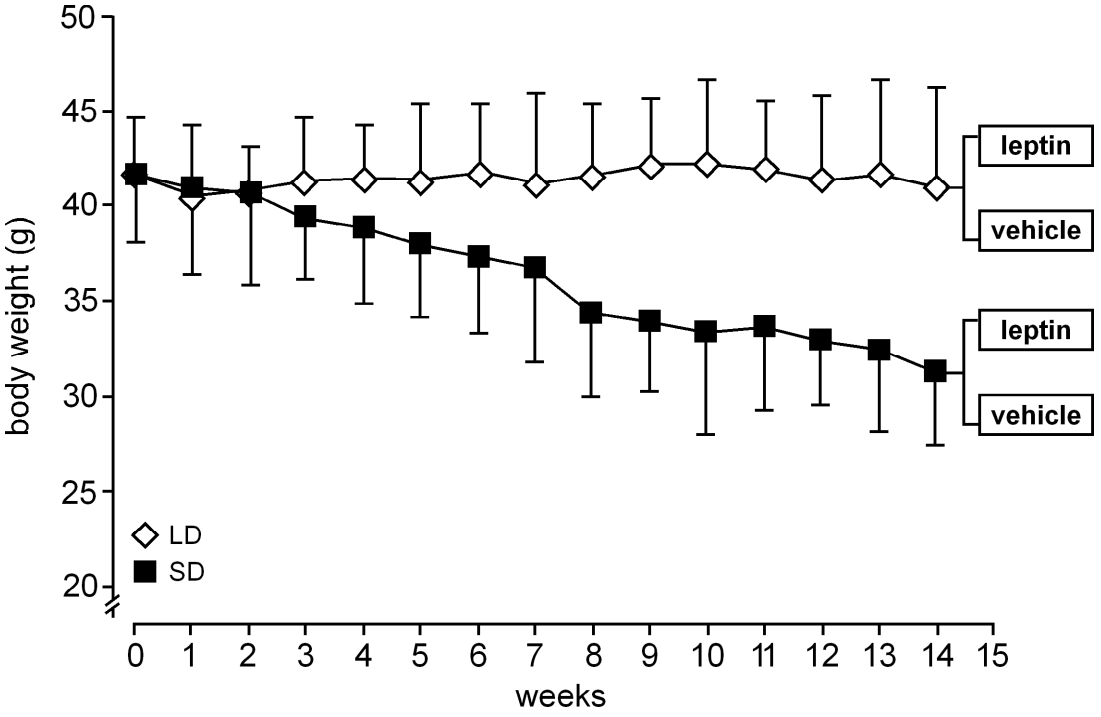
50
45
40
35
30
25
20
body weight (g)
LD
SD
leptin
vehicle
leptin
vehicle
0 1 2 3 4 5 6 7 8 9 10 11 12 13 14 15
weeks

Fig. 2

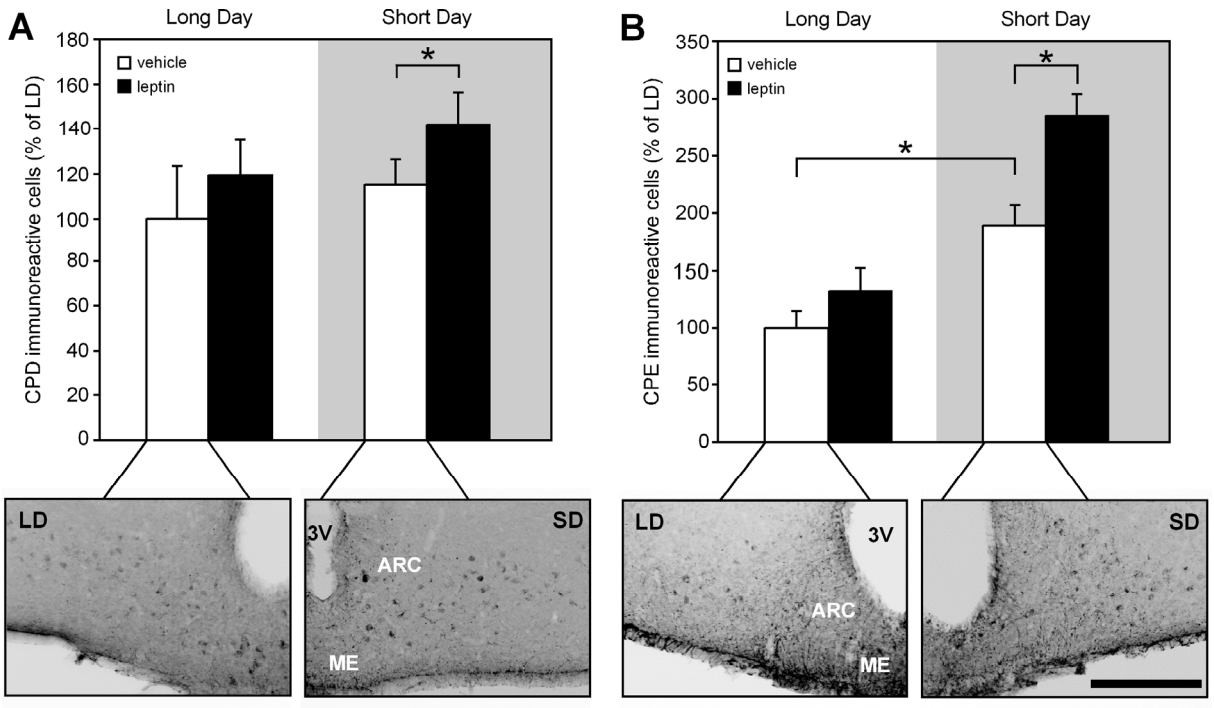
A
Long Day
Short Day
vehicle
leptin
CPD immunoreactive cells (% of LD)
180
160
140
120
100
80
60
40
20
0
*
LD
3V
ARC
ME
SD
B
Long Day
Short Day
vehicle
leptin
CPE immunoreactive cells (% of LD)
350
300
250
200
150
100
50
0
*
*
LD
3V
ARC
ME
SD

Fig. 3

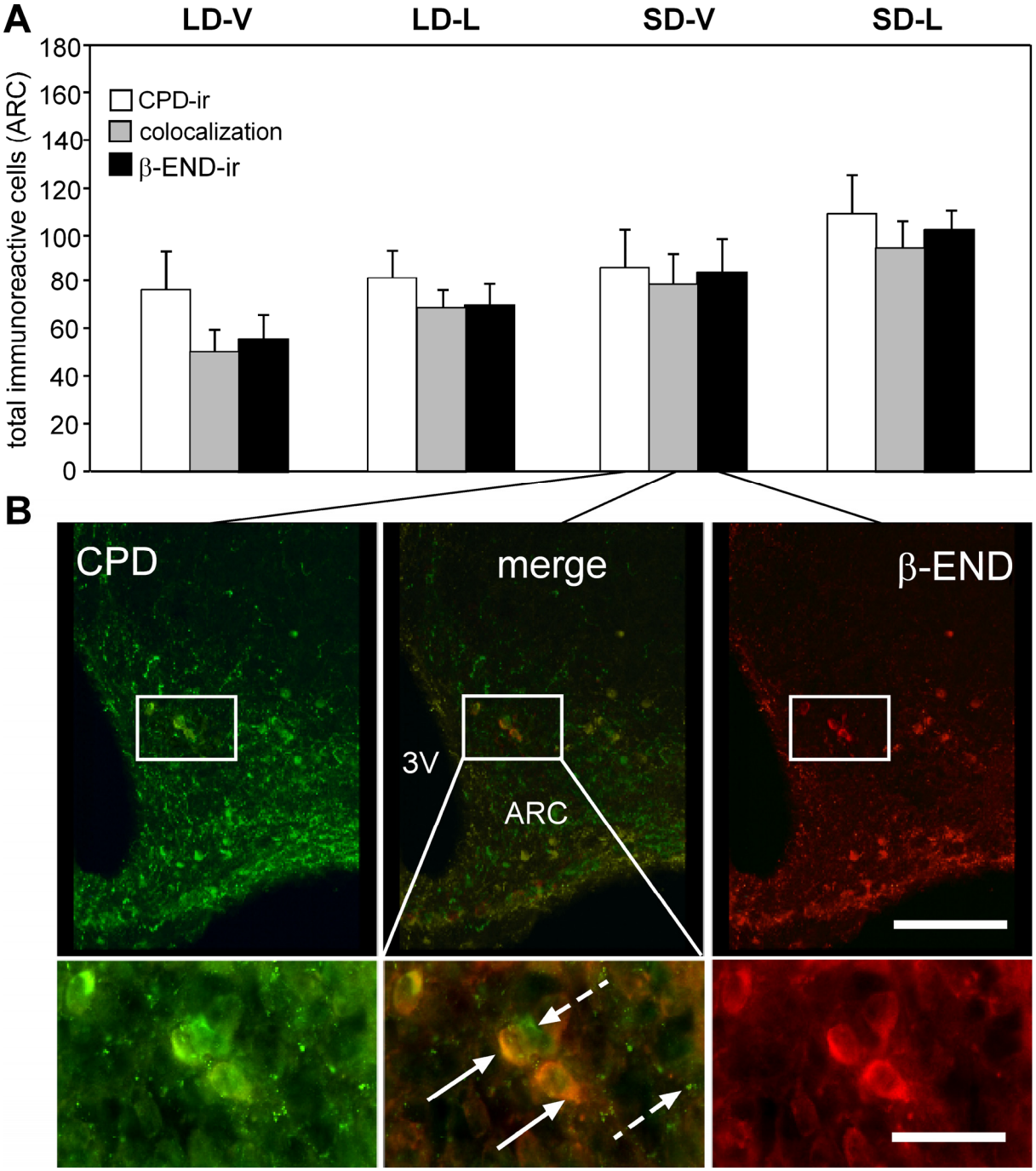
A
LD-V
LD-L
SD-V
SD-L
total immunoreactive cells (ARC)
180
160
140
120
100
80
60
40
20
0
CPD-ir
colocalization
β-END-ir
B
CPD
merge
β-END
3V
ARC

Fig. 4

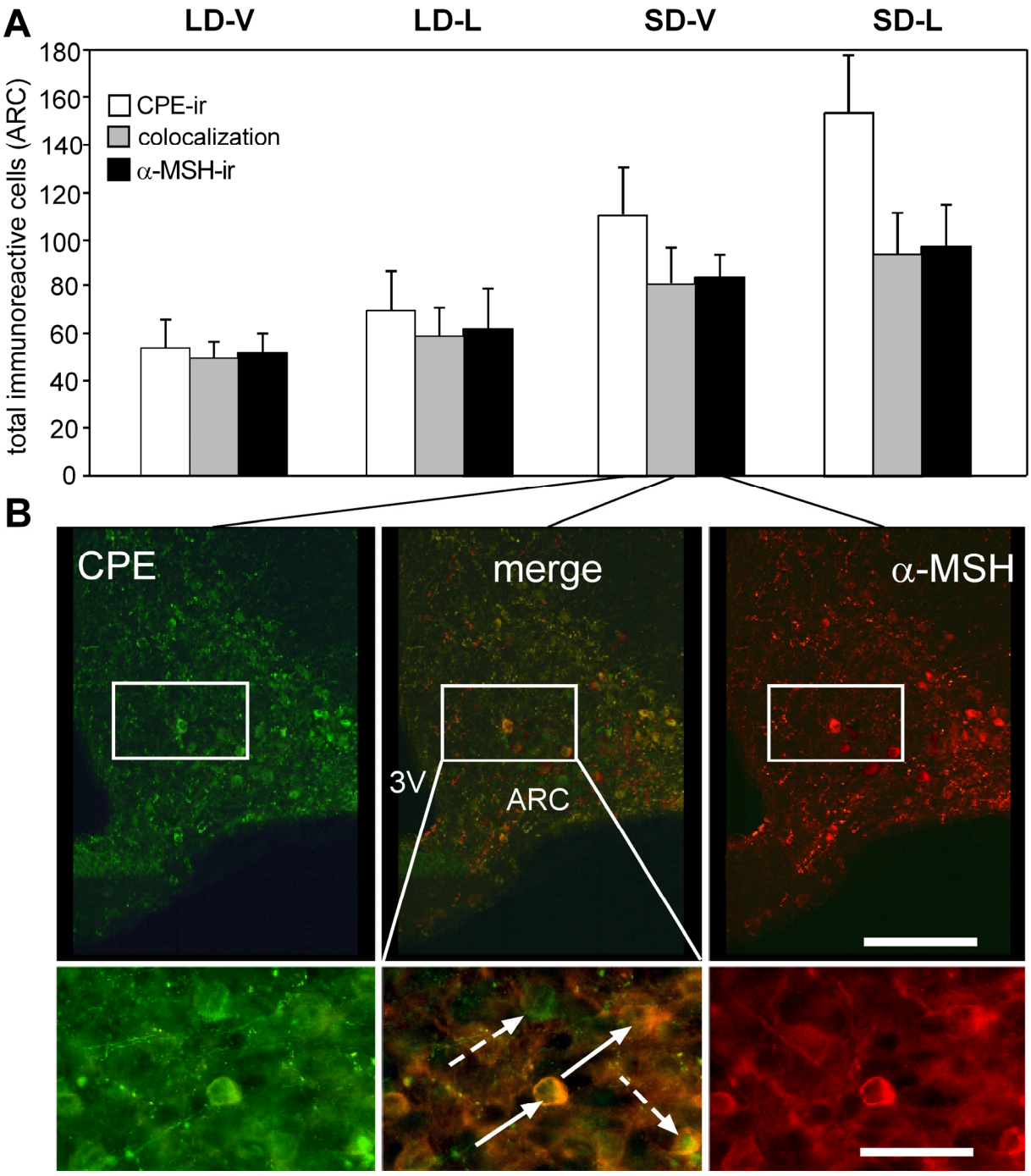
A
LD-V
LD-L
SD-V
SD-L
total immunoreactive cells (ARC)
180
160
140
120
100
80
60
40
20
0
CPE-ir
colocalization
α-MSH-ir
B
CPE
merge
α-MSH
3V
ARC

Fig. 5

General and Comparative Endocrinology 157 (2008) 142–147

Contents lists available at ScienceDirect

General and Comparative Endocrinology

journal homepage: www.elsevier.com/locate/ygcen

Seasonal regulation of cocaine- and amphetamine-regulated transcript in the arcuate nucleus of Djungarian hamster (*Phodopus sungorus*)

Reza Khorooshi [a,*], Michael Helwig [b], Achim Werckenthin [b], Nicole Steinberg [b], Martin Klingenspor [c]

[a] The Medical Biotechnology Center, Institute of Medical Biology, University of Southern Denmark, Winsloewparken 25, DK-5000 Odense C., Denmark
[b] Department of Animal Physiology, Biology Faculty, Philipps-University, Marburg, Germany
[c] Technische Universität München, Else Kröner-Fresenius Center, Molecular Nutritional Medicine, Freising-Weihenstephan, Germany

ARTICLE INFO

Article history:
Received 27 November 2007
Revised 7 April 2008
Accepted 14 April 2008
Available online 18 April 2008

Keywords:
CART
Photoperiod
Temperature
Food deprivation
Djungarian hamster

ABSTRACT

The hypothalamic neuropeptidergic system involved in the photoperiodic control of energy metabolism in seasonal mammals, is poorly understood. In the present study we examined whether distribution and number of the hypothalamic neuronal cell populations containing cocaine- and amphetamine-regulated transcript (CART) are influenced by different photoperiod and ambient temperature, or by food status in the Djungarian hamster (*Phodopus sungorus*). Hamsters bred and raised in long day photoperiod at room temperature (16 h light/8 h dark at 23 °C; LD) were transferred to short day photoperiod and moderate cold (8 h light/16 h dark at 16 °C; SD). After a 4 weeks acclimation period, uterus and body weight were decreased in SD as compared to controls maintained in LD. The number of CART-immunoreactive cells within the arcuate nucleus (ARC) was significantly higher in SD hamsters compared to LD control. This increase was restricted to the rostro to mid portion of the ARC, specifically in the hypothalamic retrochiasmatic area close to the rostral ARC and in the hypothalamic region lateral to the ARC and ventral to the ventromedial hypothalamic nuclei. In similar hypothalamic regions, food deprivation for 48 h significantly decreased the number of CART-immunoreactive cells in SD hamsters. Shortening of photoperiod combined with lowering of ambient temperature and food deprivation had no effect on the number of CART-immunoreactive cells in the lateral hypothalamic area. These findings suggest that photoperiod and ambient temperature influence energy metabolism potentially by alterations of the CART neuronal system in the rostral portion of the ARC in Djungarian hamsters.

1. Introduction

Djungarian hamsters (*Phodopus sungorus*) exhibit remarkable adaptations in physiology and behaviour in response to a seasonally changing environment. Transfer of hamsters from long day photoperiod (LD; 16 h light/8 h dark) to short day photoperiod (SD; 8 h light/16 h dark) leads to a decrease in daily food intake and an altered nocturnal feeding activity pattern (Ruf et al., 1991). In contrast, cold acclimated mammals increase food intake to compensate for higher energetic costs for thermoregulation (Bing et al., 1998; Leung and Horwitz, 1976). Furthermore, short photoperiod exposure induces reduction of body weight, impairment of reproductive activities and triggers moulting to a winter pelage (Morgan et al., 2003; Ruf et al., 1991). Lowering the ambient temperature facilitates responses to SD (Ruf et al., 1993). In addition, imposed food restriction during SD causes an additional reduction of body weight, which after refeeding of hamsters returns to a seasonally programmed "set-point" similar to that in control hamsters fed *ad lib* during SD (Steinlechner et al., 1983). Together these findings emphasize the importance of photoperiod and temperature in the regulation of energy homeostasis in seasonal animals such as the Djungarian hamsters (Adam et al., 2000; Klingenspor et al., 1996, 2000; Mercer et al., 2000; Mercer and Speakman, 2001). The manipulation of photoperiod and ambient temperature influences central regulatory pathways in the hypothalamus that are encoded by several neuropeptides and hormones acting within the central nervous system to affect and regulate energy metabolism.

Recent advances in understanding the involvement of hypothalamic neuropeptides in the photoperiodic regulation of energy balance have emerged from studies demonstrating the altered gene expression of neuropeptides in hamsters. In this context, the manipulation of photoperiod has been demonstrated to modulate the hypothalamic mRNA levels of neuropeptide Y-, pro-opiomelanocortin-, cocaine- and amphetamine-regulated transcript (CART) and agouti related peptide but not orexin and melanin-concentrating hormone (MCH) in hamsters (Adam et al., 2000; Mercer et al., 2000; Reddy et al., 1999). However, the result of gene expression profile for several neuropeptides has either been controversial or not expected. For instance findings concerning the gene expression profile of CART in the hypothalamic arcuate nucleus (ARC) in response to changes in photoperiod are controversial. In contrast to

* Corresponding author.
E-mail address: rkhorooshi@health.sdu.dk (R. Khorooshi).

0016-6480/$ - see front matter © 2008 Elsevier Inc. All rights reserved.
doi:10.1016/j.ygcen.2008.04.007

the study demonstrating that changes in photoperiod had no effect on CART-mRNA expression (Robson et al., 2002), there is evidence demonstrating increased CART-mRNA expression in the ARC in response to SD acclimation (Mercer et al., 2003; Mercer and Tups, 2003). Up to the present most studies scrutinizing the biological function of CART within the neuroendocrine homeostatic regulating network implicated to be a potent anorexigenic acting factor (Stanley et al., 2001). CART mediates catabolic responses such as decreased food intake and increased energy expenditure resulting in a loss of body mass. However, the effect of CART-peptides on the neuronal mechanism controlling energy balance in response to the changes in photoperiod, ambient temperature and food status in seasonal hamsters is unknown. The expression of CART peptide and mRNA was localized in neurons of the lateral hypothalamic area (LHA) and the paraventricular hypothalamic nuclei (PVN) (Khorooshi and Klingenspor, 2005; Kristensen et al., 1998; Robson et al., 2002; Vrang et al., 1999a). CART is an anorexigenic neuropeptide, since food deprivation of animals induces decreased CART gene expression in the ARC, and intracerebroventricular administration of CART causes a dose dependent inhibition of food intake (Thim et al., 1998; Vrang et al., 1999b, 2000). Aim of the present study was to investigate the distribution and number of hypothalamic CART-immunoreactive cells in response to different photoperiod, ambient temperature and food status.

2. Materials and methods

2.1. Animals

Female Djungarian hamsters were housed individually in Macrolon cages, raised in LD (at 23 °C) and had free access to standard rodent chow (Altromin 7014) and water. At 7 months of age, they were divided in two groups, each containing ten hamsters. One group of hamsters was kept in LD, whereas the other was transferred to SD (at 16 °C). The comparatively lower ambient temperature was chosen in order to accelerate acclimation to declining photoperiod. The body weight of hamsters was measured at weekly intervals. After 4 weeks, half of the hamsters in each group were fasted for a period of 48-h.

2.2. Tissue preparation

At the end of the experiment the pelage color and body weight were assessed and all hamsters were killed in CO_2 atmosphere between 10:00 and 14:00 h. The uteri were rapidly removed and weighed. Brains were extracted, fixed in 4% paraformaldehyde (48 h, 4 °C), cryoprotected in 20% sucrose in 0.1 M phosphate-buffered saline (PBS, pH 7.4) for 24 h at 4 °C and hypothalamic areas were cut on a cryostat into 30 μm coronal sections. Free-floating sections were stored in PBS at 4 °C prior to immunohistochemical procedures. All procedures were in accordance with German animal welfare regulation.

2.3. Immunostaining

The endogenous peroxidase activity was inhibited in sections using 80% PBS, 10% methanol and 10% H_2O_2 for 15 min at room temperature (RT). Free-floating sections were rinsed in PBS and in PBS containing 0.5% Triton X-100 (PBS-TX). Following pre-incubation in blocking solution containing PBS-TX and 3% BSA, sections were incubated with primary rabbit anti-CART (55–102; Phoenix Europe GmbH; H-003-62) antibody diluted 1:350 in blocking solution overnight at 4 °C. Following washing in PBS-TX, sections were then incubated with peroxidase-conjugated goat anti-rabbit antibody (Jackson Immunoresearch, 111-035-144) diluted 1:500 in blocking solution for 1 h at RT. Using Substrate SG (Vector kit) the color reaction resulted in dark-gray/blue immunostaining. Sections were then rinsed in PBS, mounted on gelatin-coated slides, air-dried, dehydrated in graded alcohol, cleared in xylene and coverslipped with Enthelan (Merck).

2.4. Specificity test

The specificity of primary antibodies was tested in an earlier study (Khorooshi and Klingenspor, 2005).

2.5. Counting of cells and statistical analysis

Sections from each brain were arranged in the rostro-caudal extension according to Paxinos Atlas of Rat brain (Paxinos and Watson, 1998). Using a Zeiss microscope (objective, 20×), CART-immunoreactive cell bodies in the ARC and LHA were counted by two students blinded to the experimental protocol. The mean values of both countings were calculated and either presented as the mean of total number of cells found in 7–8 sections or as the number of cells in four representative hypothalamic sections at levels corresponding to bregma −1.8, −2.5, −3.3, and −4.1 mm. Data were analyzed by ANOVA using SPSS 11.5 statistical software Data are presented as means ± SEM, and differences were considered significant if $p \leqslant 0.05$.

3. Result

3.1. Body weight, uterus weight and pelage color

After acclimation for 4 weeks, body weight in SD hamsters was decreased by 5% in comparison to LD control (Fig. 1A). Food deprivation for 48 h resulted in approximately 15% body weight reduction in either group (Fig. 1B).

SD induced down-regulation of body weight was accompanied by the initiation of gonadal regression indicated by a trend towards decreased weight of uteri ($P = 0.0910$, Fig. 1C). In contrast to body weight and gonadal status no change was detected in the pelage color of hamsters acclimated to SD for 4 weeks.

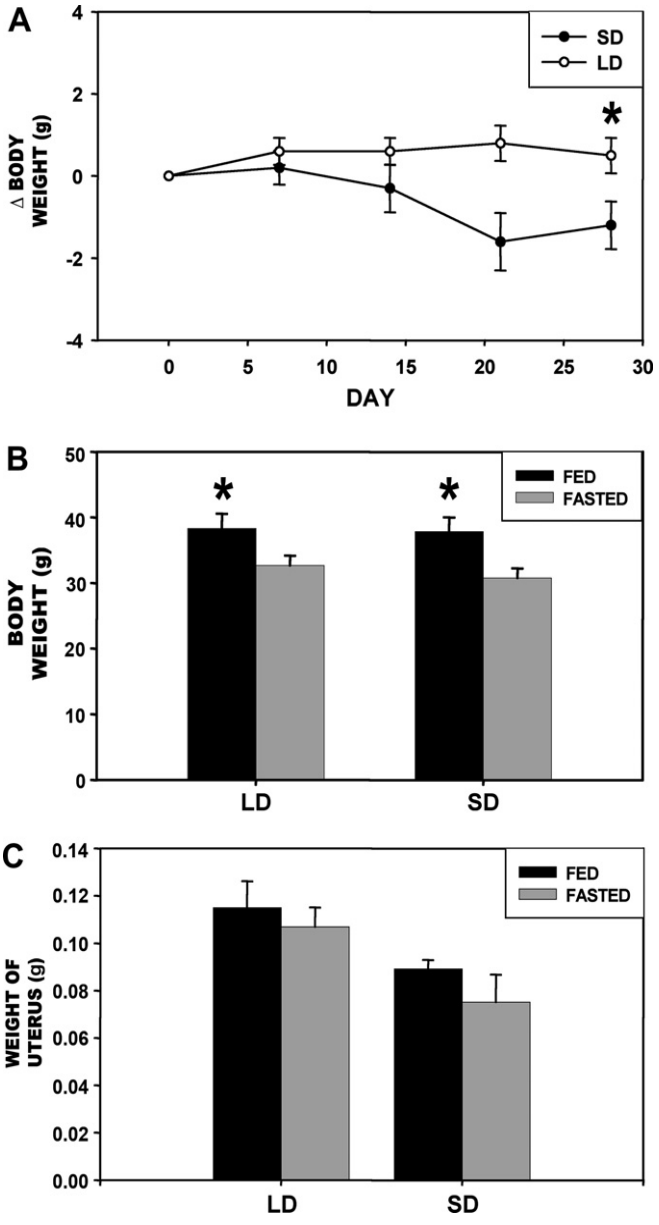

Fig. 1. Body weight (A and B) and uterus weight (C) in adult female Djungarian hamsters transferred to SD at 16 °C at day 0 or maintained in LD at 23 °C.

3.2. CART-immunoreactivity

As described earlier, CART-immunoreactive cells and fibers were distributed throughout the hypothalamus (Khorooshi and Klingenspor, 2005). In addition to the ARC, small CART-immunoreactive cell bodies were also localized in the peri-ARC that in the present study refers to the hypothalamic retrochiasmatic area (RCH) close to the rostral ARC and in the hypothalamic region lateral to the ARC and ventral to the ventromedial hypothalamic nuclei (VMH) (Fig. 2). Small CART-immunoreactive cells in the hypothalamus were also detected in the periventricular nucleus (Pe) and ventral premammillary nucleus (PMV) (Fig. 2). The densest and largest hypothalamic CART-immunoreactive cell-accumulation, was observed in the zona incerta (ZI), dorsomedial hypothalamic nuclei (DMH), and LHA (Fig. 2). Fibers and axon terminals immunoreactive for CART were distributed with various densities in several hypothalamic nuclei including the PVN. The most conspicuous staining of fibers and axon terminals immunoreactive for CART was observed in the external zone of the median eminence (ME).

3.3. The effect of photoperiod, ambient temperature and food status on CART-immunoreactivity

The transition from LD to SD resulted in a twofold increase of counted CART-immunoreactive cells in the ARC and peri-ARC (Fig. 3). Further analysis resolving the regional distribution of CART-immunoreactive cells in the rostro-caudal extension revealed a restriction of increased CART-immunoreactive cells in SD to the rostro to mid portion of the ARC, specifically the peri-ARC (Fig. 4).

In fasted SD hamsters the mean number of CART-immunoreactive cells in the ARC and peri-ARC was decreased significantly compared to SD fed *ad lib*. hamsters (Fig. 4). In fasted SD hamsters the number of CART-immunoreactive cells diminished to the level observed in LD hamsters either fed *ad lib*. or fasted (Fig. 4). Furthermore, the decrease in cell number detected in fasted SD hamsters was restricted to the rostro to mid portion of the ARC, specifically in the peri-ARC (Fig. 4).

No significant difference in the number of CART-immunoreactive cells was detected between hamsters fed *ad lib.* or fasted in LD and SD in the LHA (Fig. 5).

4. Discussion

In the current study the distribution and number of the hypothalamic neuronal cell populations containing CART-immunoreactivity in the hypothalamus of hamsters exposed to different photoperiod, ambient temperature and food status was investigated. Despite free access to food, body weight of SD hamsters was lower compared to control hamsters maintained in LD. Moreover, uterus weight was reduced in SD hamsters, a change that may announce the initiation of reproductive quiescence in these animals. As expected, due to an insufficient exposure of hamsters to SD duration, we found no changes in pelage color.

After 30 days in SD, the Djungarian hamsters had an elevated number of CART-immunoreactive cells in the ARC. The present finding is consistent with results demonstrating increased CART gene expression in the ARC of SD acclimatised hamsters (Adam et al., 2000; Mercer et al., 2003) and is contradictory to a former study where no significant difference in CART-mRNA expression

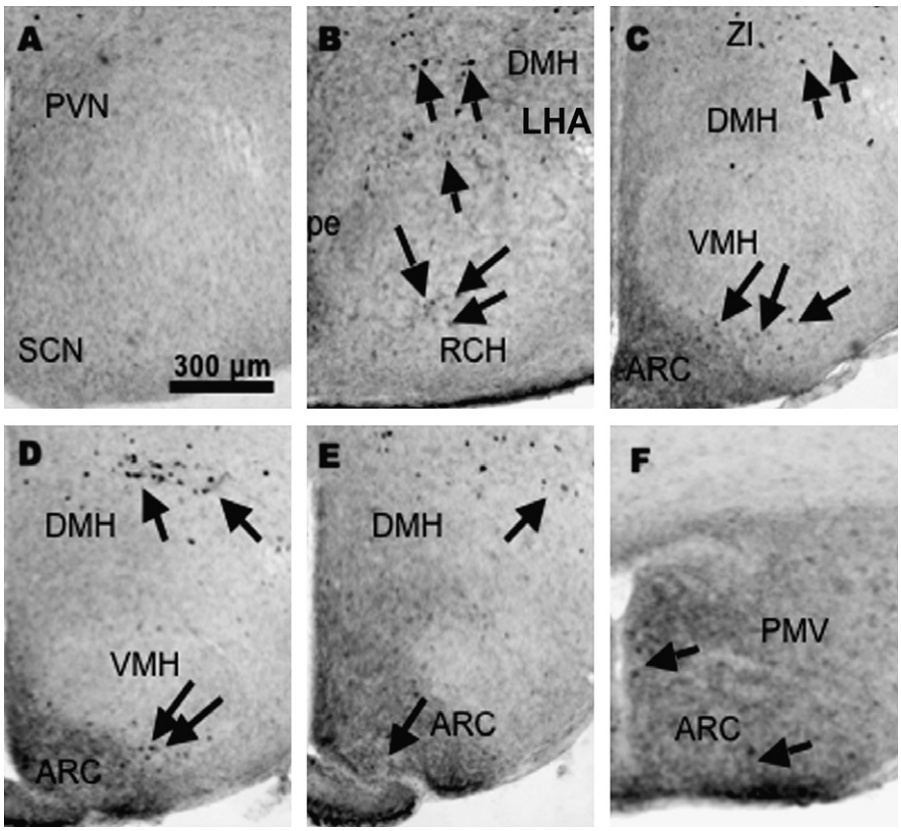

Fig. 2. Distribution of CART-immunoreactivity in the hypothalamus of Djungarian hamsters. Sections immunostained with CART antibody are organized from rostral (A) to caudal (F). Arrows showing CART-immunoreactive cells in the in the RCH (B), DMH and ZI (B–E) and ARC (C–F). Most CART-containing neurons of the ARC are concentrated in its ventrolateral part (C and D). ARC, arcuate nucleus; LHA, lateral hypothalamic area; Pe, periventricular nucleus; PMV, ventral premammillary nucleus; PVN, paraventricular nucleus of the hypothalamus; RCH, retrochiasmatic area; SCN, suprachiasmatic nucleus; ZI, zona incerta.

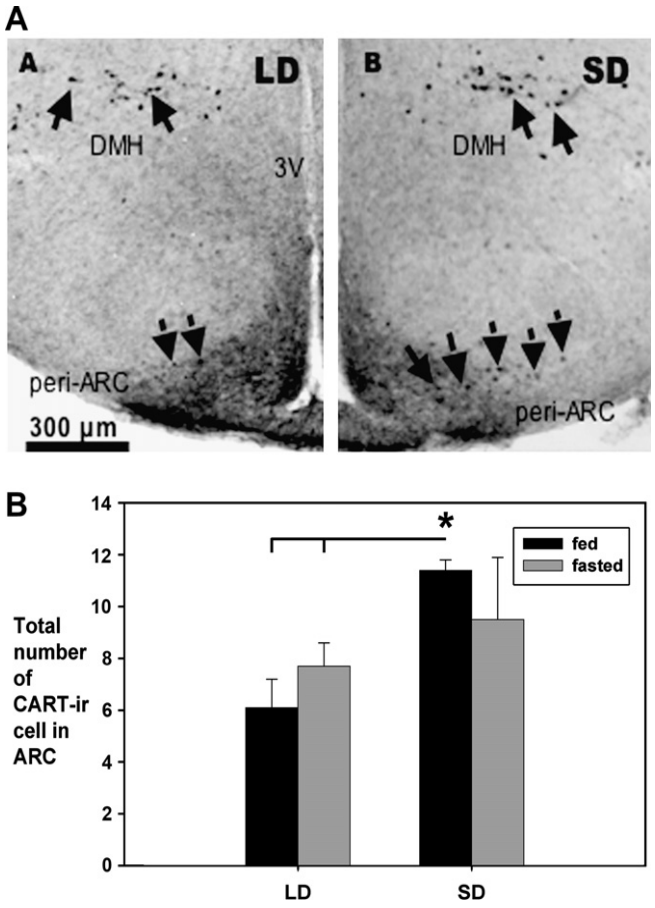

Fig. 3. (A) CART-immunoreactive cells (arrows) were more abundant in the ARC of SD hamsters. (B) Quantitative analysis of CART-immunoreactive cell numbers in the entire rostro-caudal extension of the ARC.

between SD and LD hamsters was reported (Robson et al., 2002). However, the results are consistent with the hypothesis that seasonal regulation of energy homeostasis may be mediated through the CART neuronal system. Interestingly the distribution pattern of the CART-immunoreactive cell bodies in SD hamsters matches the distribution pattern of CART neurons co-expressing Fos-immunoreactivity in the ARC and peri-ARC of rats after leptin injection (Elias et al., 1998, 1999). CART containing neurons in these regions project to several areas including the spinal sympathetic preganglionic neurons, the PVN, and the LHA (Elias et al., 1998, 1999, 2000; Elmquist, 2001) which are known to be involved in the control of energy balance. Thus, one pathway used by leptin to directly activate neuroendocrine pathways involved in energy balance is via CART-immunoreactive neurons in these regions. However, plasma leptin levels of SD hamsters are decreased, and these animals display lower food intake and body weight. It therefore appears unlikely that increased CART-immunoreactivity in SD is mediated by direct action of leptin on cells located in these regions. Acclimation to short photoperiod, however, renders hamsters more sensitive to leptin as compared to long photoperiod (Klingenspor et al., 2000). Hence, it is more likely that the changing photoperiod alters feeding behaviour by a modulation of the neuronal sensitivity to peripheral leptin. This is supported by recent findings demonstrating the molecular identity of seasonal leptin sensitivity triggered by the central leptin signaling cascade (Mercer and Tups, 2003; Tups et al., 2004). Suppressor of cytokine signaling molecule which inhibits leptin signaling seems to be a major mediator of these changes in leptin sensitivity (Mercer and Tups, 2003; Tups et al., 2004). The current findings also raise the possibility that the same CART containing neurons in the rostral–mid extension of the ARC and peri-ARC that are conveying the effect of leptin in non-photoperiodic animals, may be involved in mediating the effect of leptin in the regulation of feeding in the seasonal Djungarian hamster.

As expected, fasting for a period of 48-h led to an decrease in body weight. Similarly, food deprivation caused a reduction of the CART-immunoreactive cell number measured in the rostro to mid portion of the ARC in SD hamsters. In fasted SD hamsters the number of CART-immunoreactive cells was decreased to the level observed in LD fed *ad lib* hamsters indicating that the CART neuronal system conveys similar signals related to food intake in these different physiological states. In addition, food deprivation in LD had no effect on the number of CART-immunoreactive cells in the ARC. Together these findings raise the hypothesis that hamsters in LD experience similar anorexigenic signaling mediated by CART like SD hamsters in negative energy balance.

Our result on CART-immunoreactivity is compatible with those studies demonstrating reduced CART-mRNA in response to food restriction (Kristensen et al., 1998; Robson et al., 2002). Food status is therefore part of the regulatory mechanism that induces a pronounced effect on the CART-immunoreactivity in hamsters. This compensatory mechanism in part involves leptin, which due to the food deprivation is reduced. Leptin acts on CART containing neurons to activate catabolic pathways. It is therefore likely that the reduced number of CART-immunoreactive cells in the present study is due to the lower level of plasma leptin.

Considering anatomical localization of CART containing neurons, together with the number of CART-immunoreactive cells in *ad lib* and fasted hamsters, we suggest that CART neurons in the rostral–mid ARC, and specifically the peri-ARC, play an important role in photoperiodic programmed- and compensatory regulation of the energy balance. Also considering increased number of CART-immunoreactive cell bodies during SD, lower food intake in hamsters during SD and decreased CART-immunoreactivity due to food deprivation, the present results provides further evidence substantiating the anorexigenic function of CART. In the current study, we also quantified CART-immunoreactivity in the LHA, a hypothalamic structure implicated in the regulation of feeding. The number of CART-immunoreactive cells in the LHA appeared to be unaffected in response to either the change in photoperiod or fasting. This is consistent with former experiments demonstrating that gene-expression of CART was not affected by changes of photoperiod in hamsters (Robson et al., 2002). A role for CART in the LHA has not been yet defined. However, a neuroanatomical relation between the suprachiasmatic nuclei, the circadian pacemaker, and MCH-containing neurons of the LHA was reported (Abrahamson et al., 2001). It is also known that CART containing cells in the LHA co-express MCH (Elias et al., 2001). Considering former neuroanatomical findings together with our present results, it is most likely that CART-containing neurons in the LHA either contribute to the balance between anorexigenic and orexigenic system or relay photoperiodic information emerging from the SCN to other brain structures.

We cannot exclude the possibility that exposing SD hamsters to additional lower ambient temperature enhances the seasonal changes in CART expression within the ARC. However, gene expression of CART between LD and SD hamsters (Mercer et al., 2003) was induced by changes in photoperiod in constant ambient temperature.

In conclusion, our finding suggests that the CART neuronal system in rostral portion of the ARC plays an important role in the regulation of energy balance in Djungarian hamsters.

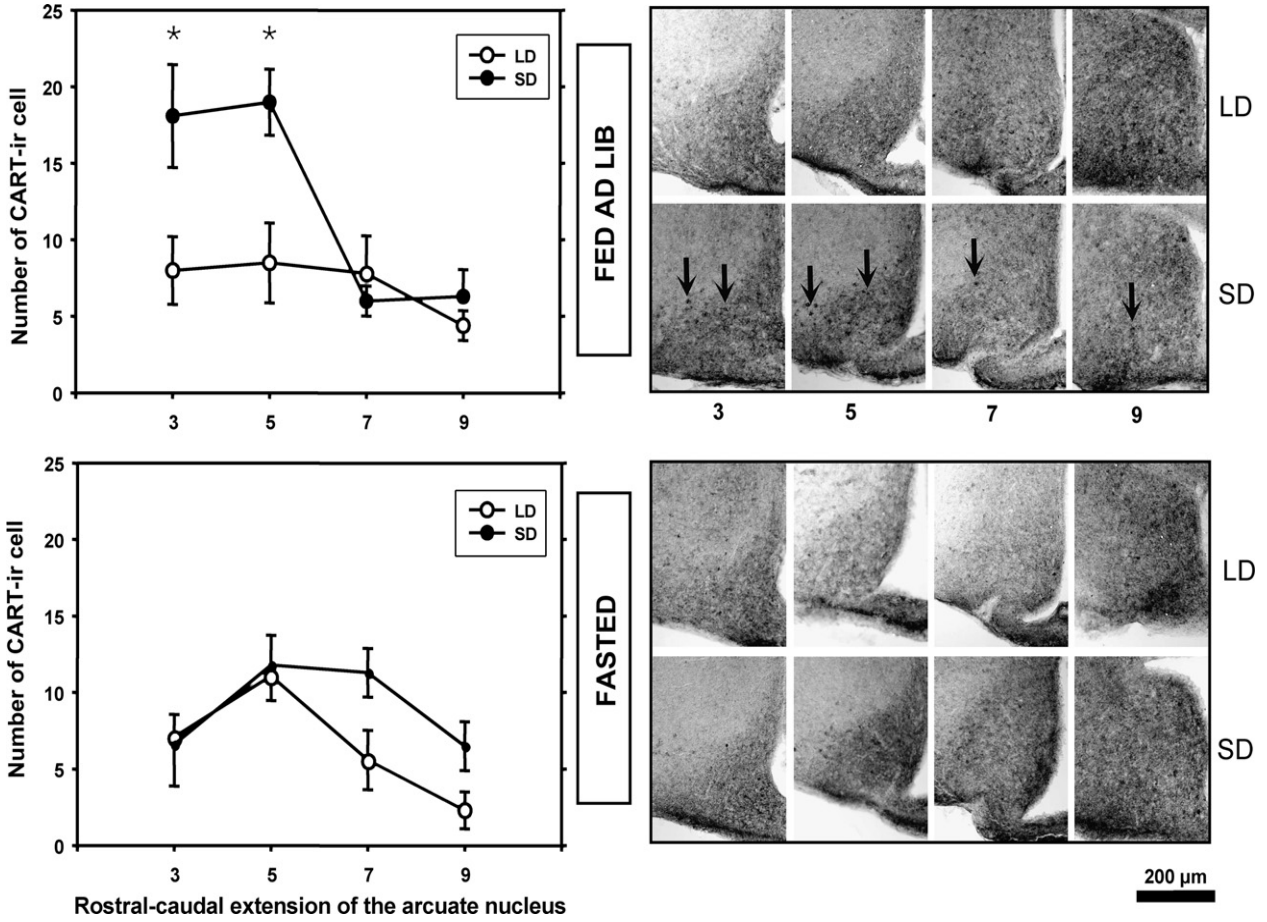

Fig. 4. Quantitative analysis of the CART-immunoreactive cell number (left) and photomicrographs of CART-immunoreactive cells (right) in the ARC of LD- and SD-hamsters either fed *ad lib* or fasted for a period of 48 h. Numbers (3, 5, 7, and 9) each highlighting a representative and comparable section in the rostro (3) to caudal (9) extension of the ARC.

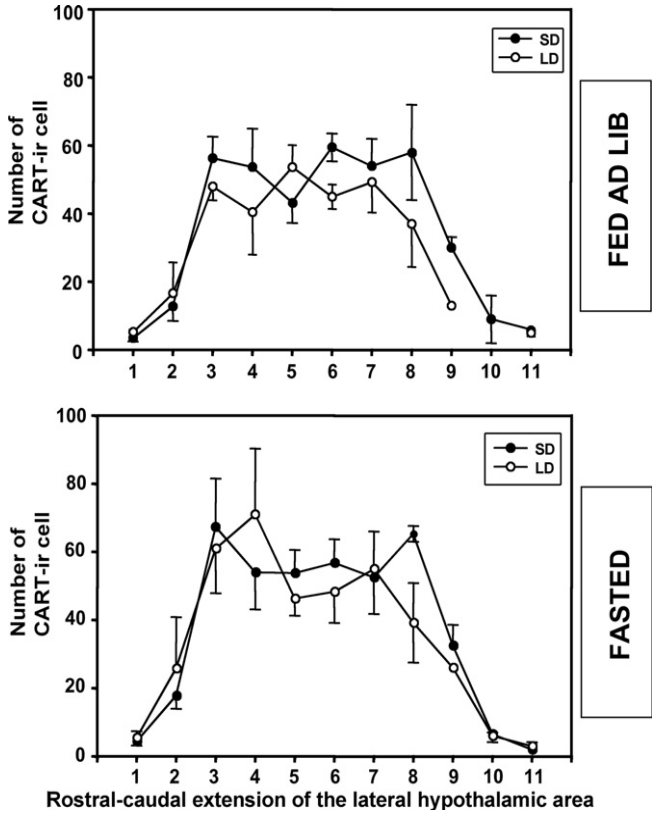

Fig. 5. Quantitative analysis of CART-immunoreactive cell numbers in the LHA of LD- and SD-hamsters either fed *ad lib* (top) or fasted (bottom) for a period of 48 h. Numbers (1–11) representing rostro (1) to caudal (11) extension of the LHA.

Acknowledgment

This study was supported by Deutsche Forschungsgemeinschaft (DFG, KL973-5) and Danish Research Agency.

References

Abrahamson, E.E. et al., 2001. The suprachiasmatic nucleus projects to posterior hypothalamic arousal systems. Neuroreport 12, 435–440.

Adam, C.L. et al., 2000. Photoperiod regulates growth, puberty and hypothalamic neuropeptide and receptor gene expression in female Siberian hamsters. Endocrinology 141, 4349–4356.

Bing, C. et al., 1998. Hyperphagia in cold-exposed rats is accompanied by decreased plasma leptin but unchanged hypothalamic NPY. Am. J. Physiol. 274, R62–R68.

Elias, C.F. et al., 1999. Leptin differentially regulates NPY and POMC neurons projecting to the lateral hypothalamic area. Neuron 23, 775–786.

Elias, C.F. et al., 2000. Chemical characterization of leptin-activated neurons in the rat brain. J. Comp. Neurol. 423, 261–281.

Elias, C.F. et al., 1998. Leptin activates hypothalamic CART neurons projecting to the spinal cord. Neuron 21, 1375–1385.

Elias, C.F. et al., 2001. Characterization of CART neurons in the rat and human hypothalamus. J. Comp. Neurol. 432, 1–19.

Elmquist, J.K., 2001. Hypothalamic pathways underlying the endocrine, autonomic, and behavioral effects of leptin. Physiol. Behav. 74, 703–708.

Khorooshi, R.M., Klingenspor, M., 2005. Neuronal distribution of melanin-concentrating hormone, cocaine- and amphetamine-regulated transcript and orexin B in the brain of the Djungarian hamster (*Phodopus sungorus*). J. Chem. Neuroanat. 29, 137–148.

Klingenspor, M. et al., 1996. Short photoperiod reduces leptin gene expression in white and brown adipose tissue of Djungarian hamsters. FEBS Lett. 399, 290–294.

Klingenspor, M. et al., 2000. Modulation of leptin sensitivity by short photoperiod acclimation in the Djungarian hamster, *Phodopus sungorus*. J. Comp. Physiol. [B] 170, 37–43.

Kristensen, P. et al., 1998. Hypothalamic CART is a new anorectic peptide regulated by leptin. Nature 393, 72–76.

Leung, P.M., Horwitz, B.A., 1976. Free-feeding patterns of rats in response to changes in environmental temperature. Am. J. Physiol. 231, 1220–1224.

Mercer, J.G. et al., 2003. Early regulation of hypothalamic arcuate nucleus CART gene expression by short photoperiod in the Siberian hamster. Regul. Pept. 111, 129–136.

Mercer, J.G. et al., 2000. Photoperiod regulates arcuate nucleus POMC, AGRP, and leptin receptor mRNA in Siberian hamster hypothalamus. Am. J. Physiol. Regul. Integr. Comp. Physiol. 278, R271–R281.

Mercer, J.G., Speakman, J.R., 2001. Hypothalamic neuropeptide mechanisms for regulating energy balance: from rodent models to human obesity. Neurosci. Biobehav. Rev. 25, 101–116.

Mercer, J.G., Tups, A., 2003. Neuropeptides and anticipatory changes in behaviour and physiology: seasonal body weight regulation in the Siberian hamster. Eur. J. Pharmacol. 480, 43–50.

Morgan, P.J. et al., 2003. Photoperiodic programming of body weight through the neuroendocrine hypothalamus. J. Endocrinol. 177, 27–34.

Paxinos, G., Watson, C., 1998. The Rat Brain in Stereotaxic Coordinates. Academic Press, London.

Reddy, A.B. et al., 1999. Seasonal regulation of food intake and body weight in the male Siberian hamster: studies of hypothalamic orexin (hypocretin), neuropeptide Y (NPY) and pro-opiomelanocortin (POMC). Eur. J. Neurosci. 11, 3255–3264.

Robson, A.J. et al., 2002. Cocaine and amphetamine-regulated transcript mRNA regulation in the hypothalamus in lean and obese rodents. J. Neuroendocrinol. 14, 697–709.

Ruf, T. et al., 1991. Daily torpor in the Djungarian hamster (*Phodopus sungorus*): interactions with food intake, activity, and social behaviour. J. Comp. Physiol. [B] 160, 609–615.

Ruf, T. et al., 1993. Cold exposure and food restriction facilitate physiological responses to short photoperiod in Djungarian hamsters (*Phodopus sungorus*). J. Exp. Zool. 267, 104–112.

Stanley, S.A. et al., 2001. Actions of cocaine- and amphetamine-regulated transcript (CART) peptide on regulation of appetite and hypothalamo-pituitary axes in vitro and in vivo in male rats. Brain Res. 893, 186–194.

Steinlechner, S. et al., 1983. The seasonal cycle of body weight in the Djungarian hamster: photoperiodic control and influence of starvation and melatonin. Oecologia 60, 401–405.

Thim, L. et al., 1998. Purification and characterisation of a new hypothalamic satiety peptide, cocaine and amphetamine regulated transcript (CART), produced in yeast. FEBS Lett. 428, 263–268.

Tups, A. et al., 2004. Photoperiodic regulation of leptin sensitivity in the Siberian hamster, *Phodopus sungorus*, is reflected in arcuate nucleus SOCS-3 (suppressor of cytokine signaling) gene expression. Endocrinology 145, 1185–1193.

Vrang, N. et al., 1999a. Neurochemical characterization of hypothalamic cocaine-amphetamine-regulated transcript neurons. J. Neurosci. 19, RC5.

Vrang, N. et al., 2000. Central administration of cocaine-amphetamine-regulated transcript activates hypothalamic neuroendocrine neurons in the rat. Endocrinology 141, 794–801.

Vrang, N. et al., 1999b. Recombinant CART peptide induces c-Fos expression in central areas involved in control of feeding behaviour. Brain Res. 818, 499–509.

PHOTOPERIODIC REGULATION OF SATIETY MEDIATING NEUROPEPTIDES IN THE BRAINSTEM OF THE SEASONAL SIBERIAN HAMSTER (*PHODOPUS SUNGORUS*)

HELWIG, M.[1, 2], ARCHER, Z.A.[1], HELDMAIER, G.[2], TUPS, A. [3], MERCER, J.G.[1] and KLINGENSPOR, M.[4]

1. *The Rowett Research Institute, Division of Obesity and Metabolic Health, Aberdeen, Scotland, UK*
2. *Philipps-Universität Marburg, Faculty of Biology, Department of Animal Physiology, Marburg, Germany*
3. *University of Otago, Centre for Neuroendocrinology and Department of Anatomy & Structural Biology, Dunedin, New Zealand*
4. *Technische Universität München, Else Kröner-Fresenius Center, Molecular Nutritional Medicine, Freising-Weihenstephan, Germany*

Correspondence to:

Michael Helwig, Department of Animal Physiology, Faculty of Biology, Philipps-Universität Marburg, Karl von Frisch Str. 8, D-35043, Marburg, Germany

Tel: +49 6421 2823395

Fax: +49 6421 2828937

E-mail: helwigmi@staff.uni-marburg.de

Abstract:

Central regulation of energy balance in seasonal mammals such as the Siberian hamster is dependent on the precise integration of short-term satiety information arising from gastrointestinal tract (GIT) with long-term signals on the status of available energy reserves (e.g. leptin) and prevailing photoperiod. Within the central nervous system, the brainstem nucleus of the solitary tract (NTS) and the parabrachial nucleus (PB) are major relay nuclei that transmit information from the GIT to higher forebrain centres. We extended studies on the seasonal programming of the hypothalamus to examine the effect of photoperiod on neuropeptidergic circuitries of this gut-brain axis in the caudal brainstem. In the NTS and PB we performed gene expression and immunoreactivity studies on selected brainstem satiety-related neuropeptides and receptors: alpha-melanocyte stimulating hormone (alpha-MSH), melanocortin 3-receptor (MC3-R), melanocortin 4-receptor (MC4-R), growth hormone secretagogue–receptor (GHS-R), cocaine- and amphetamine-regulated transcript (CART), pre-proglucagon (PPG), glucagon-like peptide 1 (GLP-1), cholecystokinin (CCK), peptide YY (PYY), galanin (GAL), neurotensin (NT), and corticotrophin-releasing hormone (CRH). Gene expression of PPG and MC4-R, and immunoreactivity (-ir) of CCK and GLP-1, in the NTS were up-regulated after 14 weeks in long-day photoperiod (LD; 16 light: 8h dark) compared to short days (SD; 8 light: 16h dark), whereas CRH–ir and NT-ir were increased in SD. We suggest that brainstem neuroendocrine mechanisms are involved in the long-term regulation of body weight in the Siberian hamster by a photoperiod-related modulation of satiety signalling that contributes to seasonally appropriate feeding behaviour.

Introduction:

Energy homeostasis of seasonal mammals such as the Siberian hamster (*Phodopus sungorus*) is regulated by a complex neuroanatomical network that integrates information on prevailing climatic conditions (in this case photoperiod) with the status of energy reserves to generate appropriate physiological and behavioural adaptations. The responsible external stimulus is represented by the trajectory of the ambient light/dark phases between summer (long day) and winter (short day) (1,2). The changing photoperiod triggers seasonal adaptations including an annual reproductive activity cycle, changes in pelage colour and insulation, and altered food intake and body weight. In the central nervous system (CNS), retinal input is conveyed to the suprachiasmatic nucleus (SCN), the superior authority of the circadian clock system embedded in the hypothalamic network, and is converted subsequently into the durational pineal melatonin signal, carrying the photoperiodic message (2,3). The drive to reduce food intake and the associated loss of body weight in short days persists even when food is provided *ad lib*, demonstrating the powerful impact of photoperiod on the long-term regulation of energy balance in seasonal mammals. The focus of most studies addressing photoperiodic aspects of seasonal energy homeostasis has been on the mechanisms involved in the integration of long-term adiposity signals like leptin into hypothalamic neuroendocrine circuits (4). However, regulation of energy balance is also dependent on integration of short-term information on ingestive status encoded by gut-derived "satiety" hormones such as postprandially-released cholecystokinin (CCK) and peptide YY (PYY) (5,6). The communication between the gastrointestinal tract (GIT) and the CNS takes place not only via direct binding of these peptides to their receptors in the hypothalamus, but also via a gut-brain axis involving caudal brainstem areas receiving visceral sensory afferents from the vagus nerve (Fig. 1).

The nucleus of the solitary tract (NTS) is a complex neuroanatomical integrator of food intake related visceral information. Interestingly, many neuropeptide/receptor substrates

involved in the regulation of energy balance in the hypothalamus are also present in the NTS including the melanocortin system [melanocortin-3 receptor (MC3-R), melanocortin-4 receptor (MC4-R), pro-opiomelanocortin (POMC), alpha-melanocyte stimulating hormone (alpha-MSH) (7)], which is presumed to mediate a major part of the catabolic effects of leptin. Furthermore, a distinct population of neurons restricted to the NTS is known to express the neuropeptide precursor, preproglucagon (PPG) (8). Posttranslational processing of PPG gives rise to neuropeptides including glucagon-like peptide 1 (GLP-1), glucagon-like peptide 2 (GLP-2) and oxyntomodulin, all of which have been shown to inhibit food intake after intracerebroventricular (i.c.v.) administration (9). Investigation of axonal projections by anterograde labelling identified the hypothalamus as the major target of PPG containing NTS neurons (10). Within the hypothalamus, GLP-1 and -2 exert their anorexic effect by binding to their respective receptors. In contrast to the hypothalamus, the NTS neuroendocrine systems seem to promote a direct response to food intake by inducing a meal dependent sense of satiety, leading to an acute rather than a chronic energy balance modulation.

From the NTS, processed satiety information is subsequently conveyed either directly to the long-term hypothalamic energy balance network or via the parabrachial nucleus (PB), which serves as a significant relay area situated in the dorsolateral pons. Neuroanatomical mapping of a number of peptides has highlighted the complex neurochemical architecture of this brain area (11). It was demonstrated that parabrachial CCK, corticotrophin releasing hormone (CRH), galanin (GAL), and neurotensin (NT) all modulate the activity of neurons with descending projections to higher forebrain centres. This modulation affects the amygdala and the hypothalamus and hence influences autonomic functions such as feeding behaviour (12,13). In turn, cervical stimulation of the afferent vagus nerve led to a substantial change in expression of the above mentioned neuropeptides, demonstrating the close relationship between visceral information transduction and the expression of these neuropeptides within the PB (12). Extensive studies, including lesioning of the PB, peripheral leptin treatment and

i.c.v. peptide injections designed to elucidate the physiological function of neuropeptides localized in the PB, demonstrated the anorexigenic properties of CCK (14), CRH (15) and NT (16), whereas GAL (17) exhibited an orexigenic effect on feeding. In this regard the PB is a key brain site modulating visceral sensory GIT information ascending from the NTS prior to its relay to higher forebrain centres. The latter centres are capable of modifying signals that are then integrated into the long-term neuroendocrine hypothalamic energy balance circuitry.

Intriguingly, receptors for both leptin (18) and melatonin (19,20), have been localized in the brainstem of many species, suggesting that short-term satiety signals from the GIT can be modulated at the level of the brainstem in response to long-term photoperiod and adiposity signals before they are integrated and processed by higher homeostatic forebrain centres.

Therefore, in the present study, we tested the hypothesis that transduction of satiety-related information by specific neuropeptide components in the caudal brainstem is seasonally affected. SD acclimatised hamsters display a substantial reduction in food intake. One way this could be accomplished is by modulating the response to satiety signals in brainstem areas that process ingestion-related visceral information. We localized mRNA transcripts of important neuropeptides and receptors regulating energy balance by in situ hybridisation, and investigated changes in gene expression of cocaine- and amphetamine-regulated transcript (CART), GAL, growth hormone secretagogue–receptor (GHS-R), MC3-R, MC4-R and PPG in the NTS in response to altered photoperiod (LD, 16h light: 8h dark vs. SD, 8h light: 16h dark). We then extended our analysis to the protein level using immunohistochemical methods. We quantified immunoreactivity of CCK, PYY, GLP-1 and alpha-MSH in the NTS, and CRH, NT, CCK and GAL in the PB in SD and LD hamsters. Furthermore, we investigated whether peripheral administration of leptin affects the expression of neuropeptides in the NTS and PB in different photoperiods.

Materials & Methods:

Animals

All described procedures were in accordance with German animal welfare regulations, or were licensed under the UK Home Office Animals (Scientific Procedures) Act, 1986, and had local ethical approval.

Siberian hamsters (*Phodopus sungorus*) were drawn from breeding colonies established at the Rowett Research Institute in Aberdeen (Scotland) or the Biology Faculty in Marburg (Germany). All animals were housed individually and had *ad libitum* access to food (Aberdeen: Labsure pelleted diet, Special Diet Services, Witham, Essex, UK; Marburg: Standard breeding chow diet, 7014, Altromin, Lage, Germany) and water at all times. Body weights were assessed weekly. Photoperiods referred to in this article are defined as LD (long day, 16 : 8 h light-dark cycle) and SD (short day, 8 : 16 h light-dark cycle).

Experimental Procedure

To investigate changes in brainstem mRNA expression induced by alteration of photoperiod, Siberian hamsters (n = 40, male, Aberdeen colony) were born and reared in LD at 21-22 C. At 4-6 months of age they were divided into two groups of 20 and matched for body weight. One group was transferred to SD whereas the other was maintained in LD photoperiod. After 14 weeks of acclimatisation to photoperiod, hamsters were killed by cervical dislocation in the middle of the light phase. Brains were immediately dissected, frozen on dry ice and stored at -80° C until required.

The effect of photoperiod and leptin treatment on brainstem peptide expression at the protein level was investigated by fluorescence immunohistochemistry. Siberian hamsters (n=16, Marburg colony, matched for weight and sex) were born and reared in LD at 23°C. At 4–6 months of age, hamsters were allocated to two weight-matched groups of 8 animals, one of

which was transferred into SD for 14 wk. At the end of the experiment, the two groups were subdivided so that one half in each photoperiod (n = 4/group) received a single intraperitoneal (i.p.) injection of recombinant mouse leptin (4 mg/kg body weight; R&D Systems, Minneapolis, MN) 2 hours before sacrifice, whereas the other group (n=4/group) received a control vehicle injection (15 mM sterile HCl and 7.5 mM sterile NaOH). All animals were killed in the middle of the light phase by transcardiac perfusion with 4% paraformaldehyde (PFA) in PBS under deep Ketamin/Rompun (Bayer, Germany) anesthesia.

Brainstem gene expression

Brainstem mRNA levels for a panel of energy-balance-related neuropeptides and receptors were quantified using *in situ* hybridization on 20 µm coronal brain sections as described in detail elsewhere (21). Sections were collected throughout the extent of the brainstem onto a set of 8 slides with 13 sections mounted on each slide. Accordingly, slides spanned a medullary region including the nucleus of the solitary tract approximating from rostral minus 8.24 mm to caudal minus 6.24 mm relative to Bregma, according to the atlas of the mouse brain (22). One slide from each animal was hybridised with a rodent-specific riboprobe complementary to partial fragments of CART, GAL, GHS-R, MC3-R, MC4-R, and PPG generated from cloned cDNA as described previously (23-26). Sections were fixed, acetylated, and hybridised overnight at 58 °C using ^{35}S-labelled antisense riboprobes. Slides were treated with RNase A to remove unhybridised probe and then desalted with a final high stringency wash in 0.1 x saline-sodium citrate (SSC) at 60 °C for 30 min. Hybridised slides were apposed to Kodak BioMax MR film. The levels of brainstem mRNAs were analysed and quantified by computerized densitometry (Image Pro-Plus software, Version 5.5.1; Media Cybernetics, Wokingham, Berkshire, UK) of *in situ* hybridisation autoradiograms. This determined the intensity and area of the hybridisation signal on the basis of set parameters; the integrated intensity was then computed using standard curves generated from ^{14}C

autoradiographic microscales (Amersham, Bucks, UK). Image analysis was performed on representative sections, by an observer blind to the respective treatment groups, on three or four comparable sections spanning the NTS. A control was performed by hybridising sections with corresponding equal length sense riboprobes, resulting in no signal.

Immunohistochemistry:

Brains were dissected and transferred into a 4% PFA-PBS solution (8h, 4°C), followed by cryoprotection in 30% sucrose (48h, 4°C), and were deeply frozen in isopentane on dry ice (1 min). Coronal sections (35 μm) of two distinct areas of the brainstem, the parabrachial nucleus (PB) and the nucleus of the solitary tract (NTS), approximating from -5.02 mm to -5.68 mm (PB) and -6.24 mm to -8.24 mm (NTS) relative to Bregma, according to the atlas of the mouse brain, were processed on a cryostat and collected in four series. Free-floating sections were treated with blocking solution (BS) containing 3% bovine serum albumin (BSA) in 0.5% PBS-Triton X-100) for 1h to block non-specific reactions. Then, sections of the two areas were incubated with polyclonal rabbit antibodies as follows: slices of the PB with anti- CCK(26-33), (1:200, H-069-04, Phoenix Pharmaceuticals Inc; Belmont, USA), anti- CRF (1:100, H-019-06, Phoenix), anti-GAL (1:200, H-026-13, Phoenix), and anti-NT (1:200, H-048-03, Phoenix), and slices of the NTS with anti-CCK(26-33), (1:200, H-069-04, Phoenix), anti- GLP-1(7-37) (1:300, H-028-13, Phoenix), and anti-PYY (1:200, H-059-03, Phoenix) in BS overnight (4°C). Following washes in 0.25% PBS-T, sections were incubated with green fluorochrome Alexa 488 (Ex_{max} 492 nm, Em_{max} 520 nm) conjugated goat anti-rabbit secondary antibody (1:250, Molecular Probes, Eugene, USA) in BS for 2h at 4°C. Immunohistochemistry for α-MSH in the NTS was performed with polyclonal sheep anti-α-MSH antibody (1:10,000, Chemicon) in BS overnight at 4°C. α-MSH-ir was visualized by incubation with Fluorescein (Ex_{max} 494 nm, Em_{max} 520 nm) conjugated donkey anti-sheep secondary antibody (1:100, AP184F, Chemicon) in BS for 2 h at RT. All sections were then

rinsed in PBS, mounted on gelatin-coated slides, air-dried, dehydrated in graded alcohol, cleared in xylene and coverslipped with Enthelan (Merck Biosciences, Darmstadt, Germany).

Immunoreactive cells were counted in three comparable sections of the parabrachial nucleus and four sections of the nucleus of the solitary tract of each individual animal without knowledge of the experimental treatment. Total ir-cell number for each individual animal from the respective regions was calculated followed by the assessment of mean values for each experimental group. Sections were examined under a conventional epifluorescent Zeiss Axioskop (Carl Zeiss, Jena, Germany) microscope. Images were taken by a mounted Polaroid DMCe digital camera. The anatomical localization of neuropeptides within the brain of Siberian hamsters was annotated according to the atlas of the mouse brain (22).

Statistical analysis

Data were analyzed by two-way analysis of variance (*ANOVA*) or one-way *ANOVA* followed by Student's-Newman-Keuls multiple-comparison test, where appropriate, using SigmaStat statistical software (Jandel Corp., Erkrath, Germany). Where data failed equal variance or normality tests they were analyzed by Mann Whitney rank sum test or one-way *ANOVA* on ranks followed by Dunn's multiple-comparison test. Data are presented as percentage values of LD control ± SEM. A probability value of $P < 0.05$ was considered as statistically significant.

Results:

Effect of photoperiod on hamster body weight

Experiment 1: Beginning with an average body weight of 40.5 g (± 3.6 g, n = 40) at week 0, body weight in SD hamsters decreased by 24.2% to a nadir of 30.8 g (± 3.8 g, n = 20) at week 14, whereas body weight of LD controls did not change (40.3 g ± 4.3 g, n = 20) over this period (Fig. 2). Mean body weights of SD and LD animals were significantly different after 14 weeks (one-way *ANOVA*, $P < 0.01$).

Experiment 2: At week 0 animals weighed 41.4 g (± 3.3 g, n = 16). SD exposure for 14 weeks led to a substantial decrease of body weight to 31.1 g (± 3.6 g, n= 8) and caused a significant body weight differential of 24.9% compared to the body weight of LD hamsters (40.7 g ± 5.5 g, n = 8) at the same time point (one-way *ANOVA*, $P < 0.01$).

Effect of photoperiod on gene expression of CART, GAL, GHS-R, MC3-R, MC4-R and PPG in the NTS

Messenger-RNA of all selected genes was detected within the NTS (Fig. 3). In addition to region-specific gene expression in the NTS, mRNA of PPG and CART was also observed in the dorsal part of the medullary reticular nucleus, the inferior olive and peripheral parts of the hypoglossal nucleus (12n), respectively, but was not quantified. Expression patterns were similar to those previously observed in the brainstem of other rodent species (8,27-31). Gene expression of pre-proglucagon (Fig. 3A) in the NTS revealed a strong effect of photoperiod with decreased levels of PPG mRNA in SD (one-way *ANOVA*, $P < 0.001$). Gene expression of MC4-R (Fig. 3B) within the NTS also revealed a significant effect of photoperiod (one-way *ANOVA*, $P < 0.001$) with decreased levels in SD (versus LD controls). There was no effect of photoperiod on CART, GAL, GHS-R or MC3-R mRNA in the NTS (Fig. 3C-F).

Effect of photoperiod and leptin administration on protein expression of α-MSH, CCK, PYY and GLP-1 in the NTS

Immunoreactive cells and fibers for α-MSH, CCK, PYY and GLP-1 were observed and quantified in the medial part of the NTS of the Siberian hamster brain (Fig. 4). GLP-1 distribution patterns by immunoreactivity corresponded with the mRNA patterns for the precursor PPG (Fig. 3A). GLP-1-ir perikarya were visualized from the central to the caudal portion of the medial part of the NTS. Quantification of GLP-1-ir cells (Fig. 4A) revealed a significant effect (two-way *ANOVA*, F = 13.28, P = 0.031) of photoperiod with a decreased number of ir-cells in SD-V (short day, vehicle) (34 ± 6 ir-cells) compared to LD-V (long day, vehicle) (50 ± 4 ir-cells) in the NTS. In both photoperiod groups, administration of leptin (LD-L and SD-L) had no effect on the number of GLP-ir cells (LD-L, 54 ± 4; SD-L 42 ± 7 ir-cells). Levels of α-MSH-ir (LD-V, 61 ± 5; SD-V, 69 ± 7 ir-cells) were unaffected by photoperiod and there was no effect of leptin treatment (α-MSH; LD-L, 67 ± 4; SD-L, 74 ± 10 ir-cells) (Fig. 4B). There was an effect of photoperiod on the number of CCK-ir cells counted in the NTS (two-way *ANOVA*, F = 23,15, P = 0.004); LD-V hamsters had 72 ± 8 ir-cells whereas SD-V animals had 52 ± 6 ir-cells within the investigated region of the NTS. Leptin administration in LD (80 ± 6 ir-cells, LD-L) and SD (58 ± 6 ir-cells, SD-L) had no effect on the number of CCK-ir cells (Fig. 4C). PYY-ir (LD-V, 38 ± 6; SD-V, 33 ± 5 ir-cells) (Fig. 4D) was unaffected by photoperiod, and there was no effect of leptin treatment (PYY: LD-L, 36 ± 4; SD-L, 39 ± 6 ir-cells).

Effect of photoperiod and leptin administration on protein expression of CCK, CRH, GAL, and NT in the PB

Immunoreactive cells of all candidate peptides were detected and localized to the parabrachial nucleus of the Siberian hamster brain with region-specific distribution patterns within the PB subnuclei. The neuroanatomical distribution pattern of CRH-ir cells was mainly confined to

the *internal part of the lateral parabrachial nucleus* (LPBI) and to the adjacent *medial parabrachial nucleus* (MPB). Quantification of immunohistochemical staining of CRH (Fig. 5A) showed 45% more ir-cells in SD-V (106 ± 7 ir-cells), leading to a significant difference (two-way *ANOVA*, F = 8,173 P = 0.012) compared to those counted in LD-V (71 ± 7 ir-cells). Within the investigated subnuclei this differential was mainly manifested by an increased CRH-ir cell number in the MPB. Intraperitoneal administration of leptin 2h prior to tissue sampling led to a significant reduction in CRH-ir cells (two-way *ANOVA*, F = 11,64 P = 0.025) in the SD-L group (69 ± 9 ir-cells) resulting in similar levels to those observed in LD-V. However, there was no effect of leptin on CRH-ir in LDs (67 ± 5 ir-cells). There was a significant effect of photoperiod on the number of NT-ir cells (Fig. 5B); numbers were elevated in SD (SD-V, 88 ± 8) compared to LD (LD-V, 67 ± 5). There was no effect of leptin on NT-ir in SD (SD-L, 100 ± 7 ir-cells). Quantification of CCK-ir (Fig. 5C) did not reveal an effect of photoperiod (LD-V, 55 ± 3; SD-V, 50 ± 6 ir-cells) or of leptin administration in either photoperiod (LD-L, 49 ± 3; SD-L, 56 ± 7 ir-cells). We found no significant changes in GAL immunoreactivity within the parabrachial nucleus. Neither acclimation to LD (LD-V, 36 ± 4 ir-cells) or SD (SD-V, 31 ± 3) nor leptin administration in either photoperiod (LD-L, 33 ± 5; SD-L, 30 ± 2 ir-cells) had a significant effect on GAL-ir in the parabrachial nucleus (Fig. 5D).

Discussion:

The questions addressed in this study are a) are brainstem neuroendocrine feedback and relay mechanisms influenced by photoperiod? and b) if this is the case, is the alteration consistent with the seasonal feeding behavior of the Siberian hamster? We initially tested the response to altered photoperiod of a number of major satiety-related genes expressed in the NTS including CART, GAL, GHS-R, MC3-R, MC4-R and PPG, all of which have been demonstrated to be involved in the mediation of central satiety signaling. Of the six genes investigated in this study, PPG and MC4-R were differentially expressed at the transcriptional level in response to altered photoperiod. Messenger-RNA levels of both genes were elevated in LD (Fig. 3A and B), whereas photoperiod did not affect gene expression for CART, GAL, GHS-R or MC3-R (Fig 3C-F). Pre-proglucagon and MC4-R are both components of the brain anorexigenic neuropeptide system that potently inhibits food intake. The precursor PPG, however, does not exhibit anorexigenic properties itself, but undergoes extensive post-translational processing giving rise to the bioactive neuropeptides, GLP-1, GLP-2 and oxyntomodulin. We found higher PPG gene expression accompanied by elevated GLP-1-ir in LD (Fig. 4A). PPG-derived neuropeptides are produced in equimolar amounts from the PPG precursor (8), we conclude that other PPG-derived peptides should thus also be augmented in LD. Hence, our observations probably represent an overall elevated activity of the brainstem PPG-system in neurons of the NTS in LD. Hypothalamic sites involved in regulation of food intake are densely innervated by brainstem PPG-expressing neurons (32). Since the NTS is the only CNS site of PPG-expression, the observed increase in PPG mRNA and GLP-1-ir should consequently lead to augmented ligand availability in the hypothalamus of LD hamsters. This increase, however, appears to run contrary to elevated seasonal body weight in LD as GLP-1 and other PPG-derived peptides have been demonstrated to potently suppress food intake when injected i.c.v. into the lateral ventricle (33). However, the exact mechanism by which the brainstem PPG system mediates anorexia is not fully understood. In this context,

there are only two other studies that have investigated the regulation of PPG gene expression in the brainstem (34,35). Both demonstrated a leptin-mediated effect to be a decisive regulating factor of brainstem PPG expression. Their results, however, are contradictory. While Goldstone *et al.* (34) demonstrated an increase of hypothalamic GLP-1 peptide content following i.p. leptin administration in food-restricted mice, Vrang *et al.* (35) observed significantly increased brainstem PPG mRNA levels in obese Zucker rats with defective leptin receptor signalling. These results contrast to each other in respect of functional leptin signalling as a positive regulator of GLP-1 expression. The adipocyte hormone, leptin, is generally secreted in proportion to fat content and inhibits food intake via the hypothalamic leptin receptor, Ob-Rb (36). There is strong evidence that the caudal brainstem is also a target for the food intake inhibitory effect of leptin since receptors are also expressed in this area (37). We, however, found no change in brainstem GLP-1-ir in either photoperiod after i.p. leptin administration.

MC4-R is one part of the melanocortin system that includes pro-opiomelanocortin (POMC) and the POMC-derived peptides, α-MSH and β-endorphin. It has been demonstrated that activation of brainstem MC4-R by binding of MTII, a stable MC4-R ligand, potently inhibits food intake when MTII is injected into the fourth ventricle (38). Therefore, we performed immunohistochemistry for α-MSH, the physiological agonist of MC4-R, to extend our analysis of the brainstem melanocortin system. The observed up-regulation of MC4-R gene expression in LD, however, was not accompanied by higher levels of α-MSH-ir (Fig. 4B) indicating that photoperiod may be modulating the responsiveness of the melanocortin system by regulation of MC4-R rather than its agonist, α-MSH. According to the present opinion on the physiological functions of the brainstem preproglucagon and melanocortin systems our results represent a hyperactivity of anorexigenic neuropeptidergic components in LD. The overall higher body weight in LD acclimated Siberian hamsters, compared to SD animals, however, suggests that increased expression of putative satiety-mediating genes in the NTS in

LDs is likely to be the result rather than the direct cause of higher food intake. Interestingly, in the pregnant rat model of hyperphagia, it has been reported that α-MSH fails to reduce food intake when injected into the brain, suggesting that pregnancy is an α-MSH resistant state (39). A similar state may exist in the LD Siberian hamster, which also appears to be leptin-insensitive at both behavioural and molecular levels (40,41).

The expression of PPG and MC4-R in brainstem neurons is stimulated by direct neural and/or PYY- and CCK-induced postprandial activation of vagal afferent fibres (42). Both CCK and PYY are secreted by the intestine in response to food intake, reflecting increased gastrointestinal activity, and act centrally to induce a sense of satiety. CCK and PYY are also centrally expressed in neurons of numerous brain sites including the NTS and PBN (43,44). We therefore performed immunohistochemical analysis to evaluate the amount of CCK and PYY within the NTS and PBN and assess the relationship with observed changes in caudal PPG and MC4-R brainstem gene expression. We found significantly higher levels of CCK-ir in neurons of the NTS in LD (Fig. 4C), while PYY-ir was unaffected (Fig. 4D). Although there is no substantial evidence that centrally expressed CCK is regulated by peripherally secreted CCK, it was reported that expression and release of CCK in the hypothalamus is increased in direct response to food intake (45,46). Within the NTS, CCK acts as a neurotransmitter and/or neuromodulator to mediate satiety and suppress food intake (47). Together these findings suggest that the photoperiod-associated changes in CCK-ir observed in this study may directly reflect differential feeding activity in the photoperiod paradigm with higher levels of CCK in LD. Interestingly, food intake inhibition by CCK is in part mediated by activation of the brainstem melanocortin system; intraperitoneal CCK administration leads to increased cFOS expression in 30% of POMC-ir cells in the NTS, suggesting that POMC-derived α-MSH contributes to the satiety effects of CCK (48). In the Siberian hamster, however, there is evidence of a differential sensitivity to peripherally injected CCK (49); CCK is ten-fold more effective in suppressing food intake when administered to SD-

acclimatized Siberian hamsters than in LD controls. This observation implies a contribution of CCK to the seasonally changing feeding behavior of *P. sungorus*. The extent to which seasonally-differential CCK sensitivity is mediated by brainstem neuroendocrine systems and the relationship between peripherally-secreted CCK and centrally-expressed CCK still needs to be determined. PYY, which is also peripherally secreted postprandially from L-cells of the ileum, is centrally expressed in neurons of the brainstem too. Our study showed no differential PYY-ir within the boundaries of the NTS in response to altered photoperiod and leptin treatment, indicating little potential for centrally expressed PYY to mediate a photoperiod-related neuroendocrine response.

Although CCK produced by NTS neurons is transported via axonal efferents to the PBN (50), there was no discernible effect of photoperiod on the expression of CCK-ir within the PBN. Pre-procholecystokinin mRNA (ppCCK) has been reported to be mainly confined to neurons of the superior lateral subnucleus of the PBN (51), in line with the observed CCK-ir within this specific sub-nucleus in the present study. Interestingly 80-90% of these neurons are known to project to the ventromedial hypothalamus, a key site in regulation of long-term energy homeostasis (52). Hence it seems plausible that CCK in the PBN occupies a major position in transmitting visceral-ascending information on short-term satiety to the hypothalamus. Our data indicate that CCK-encoded increased satiety information from the NTS is seasonally "damped" at the level of the PBN as we found levels of CCK-ir in LD comparable to those observed in SD. This in turn may lead to an attenuation of anorexigenic input to hypothalamus in LD and would be in line with the observed weight gain of hamsters in this photoperiod. Contrary, we found an up regulation of CRH-ir (Fig. 5A) and NT-ir **(**Fig. 5B) in the PBN in SD, both neuropeptides that exert an anorexigenic effect on feeding behavior in the hypothalamic neuroendocrine circuitries (53,54). Their function in regulation of food intake within the PBN, however, is unknown. Intrinsic CRH-positive neurons (55) can be found in the PBN as well as CRH-ir fibers originating in the lateral hypothalamus (56) and

the NTS (57), suggesting that, within the PBN, CRH contributes to the linkage of ascending visceral information to higher forebrain centers. The involvement of parabrachial CRH in energy balance regulation is further substantiated by studies showing a significant decrease in long-term feeding and body weight after stimulation of brainstem CRH receptors (58). Similar observations have been reported regarding the anorexigenic actions of neurotensin in the brainstem. Neurotensin containing neurons of the PBN project to the lateral hypothalamus, and administration of NT to the brainstem leads to a significant decrease in food intake (59). Together the neuroanatomical distribution within key sites of the ascending neuroendocrine gut-brain axis indicates a crucial role of CRH and NT in satiety signalling. The proposed involvement of the PBN in long-term energy balance regulation is also strengthened by the photoperiod-induced response of CRH-expressing neurons to stimulation by adiposity hormone leptin (Fig. 5A). Interestingly, the significant decrease in parabrachial CHR-ir represents the opposite response that might have been predicted from consideration of hypothalamic systems (60). Based on the anorexigenic actions of brainstem CRH and NT, we suggest that, within the PBN, these neuropeptides may be responsible for a photoperiod-depended modulation of gut-brain signalling, which leads to an amplification of satiety input to the hypothalamus in SD. This in turn could partly explain the long-term voluntary decrease in food intake and body weight despite reduced digestive activity and expected sense of hunger in SD.

How can changing photoperiod provoke the differential expression of gut-brain signalling components observed in this study? Certainly, pineal melatonin is the major mediator of photoperiodic information to the CNS in mammals (2). Interestingly, the highest density of melatonin binding sites in the CNS of many rodent species is the brainstem, particular the area postrema (AP) that lies in close neuroanatomical and functional proximity to the NTS (3,20). Binding of melatonin to the AP, however, seems to be highly species specific and little binding was reported in Siberian hamsters (19). Besides transmission via

melatonin, information on photoperiod gets processed and relayed directly by neural components of the circadian clock system including the SCN and raphe nuclei (61). Efferent projections of the raphe nuclei have been recognized as a significant source of neuropeptidergic input to the NTS, and influence brainstem regulation of gastric functions (62). Besides this direct neural signal feed-in on photoperiod, descending projections to the brainstem from hypothalamic nuclei involved in regulation of energy balance have been identified (63,64). It is therefore likely that information on photoperiod gets also indirectly conveyed from the hypothalamus to the caudal brainstem and influences processing of satiety signals and ingestive behavior on a long-term basis.

Our data provides evidence of a photoperiod-regulated expression of neuroendocrine components in the brainstem of a seasonal animal. We found an up-regulation of NTS preproglucagon and melanocortin systems accompanied by increased levels of CCK-ir in LD. However, in the parabrachial nucleus, CCK-ir was unaltered and immunoreactivity of the anorexigenic neuropeptides, CRH and NT, was up-regulated in SD. Together these observations strengthen the hypotheses that incoming information on satiety is differentially processed and relayed in the brainstem in response to altered photoperiod. This in turn may contribute to the pronounced seasonal feeding behaviour exhibited by *P. sungorus*.

Acknowledgements:

We thank Sigrid Stöhr for her excellent technical assistance. M. Helwig was recipient of a fellowship funded by the European Commission to attend the ObeS^{e}chool European Union Marie Curie Training Site at the Rowett Research Institute. This collaborative study was also funded by the Scottish Government (to J. G. Mercer) and EC FP6 funding ('DIABESITY' contract no. LSHM-CT-2003-503041 to J. G. Mercer), Deutsche Forschungsgemeinschaft (German Research Foundation KL973/5; to M. Klingenspor), the National Genome Research Network (NGFN 01GS0483; to M. Klingenspor).

References

1. Mercer JG, Tups A. Neuropeptides and anticipatory changes in behaviour and physiology: seasonal body weight regulation in the Siberian hamster Eur J Pharmacol 2003; 480**:** 43-50.

2. Steinlechner S, Heldmaier G. Role of photoperiod and melatonin in seasonal acclimatization of the Djungarian hamster, Phodopus sungorus Int J Biometeorol 1982; 26**:** 329-337.

3. Morgan PJ, Mercer JG. Control of seasonality by melatonin Proc Nutr Soc 1994; 53**:** 483-493.

4. Morgan PJ, Ross AW, Mercer JG, Barrett P. Photoperiodic programming of body weight through the neuroendocrine hypothalamus J Endocrinol 2003; 177**:** 27-34.

5. Dhillo WS, Bloom SR. Gastrointestinal hormones and regulation of food intake Horm Metab Res 2004; 36**:** 846-851.

6. Murphy KG, Bloom SR. Gut hormones and the regulation of energy homeostasis Nature 2006; 444**:** 854-859.

7. Joseph SA, Pilcher WH, nett-Clarke C. Immunocytochemical localization of ACTH perikarya in nucleus tractus solitarius: evidence for a second opiocortin neuronal system Neurosci Lett 1983; 38**:** 221-225.

8. Larsen PJ, Tang-Christensen M, Holst JJ, Orskov C. Distribution of glucagon-like peptide-1 and other preproglucagon-derived peptides in the rat hypothalamus and brainstem Neuroscience 1997; 77**:** 257-270.

9. Tang-Christensen M, Larsen PJ, Goke R, Fink-Jensen A, Jessop DS, Moller M, Sheikh SP. Central administration of GLP-1-(7-36) amide inhibits food and water intake in rats Am J Physiol 1996; 271**:** R848-R856.

10. Vrang N, Hansen M, Larsen PJ, Tang-Christensen M. Characterization of brainstem preproglucagon projections to the paraventricular and dorsomedial hypothalamic nuclei Brain Res 2007; 1149**:** 118-126.

11. Block CH, Hoffman GE. Neuropeptide and monoamine components of the parabrachial pontine complex Peptides 1987; 8**:** 267-283.

12. Saleh TM, Cechetto DF. Peptide changes in the parabrachial nucleus following cervical vagal stimulation J Comp Neurol 1996; 366**:** 390-405.

13. Nagase H, Nakajima A, Sekihara H, York DA, Bray GA. Regulation of feeding behavior, gastric emptying, and sympathetic nerve activity to interscapular brown adipose tissue by galanin and enterostatin: the involvement of vagal-central nervous system interactions J Gastroenterol 2002; 37 Suppl 14**:** 118-127.

14. Becskei C, Grabler V, Edwards GL, Riediger T, Lutz TA. Lesion of the lateral parabrachial nucleus attenuates the anorectic effect of peripheral amylin and CCK Brain Res 2007; 1162**:** 76-84.

15. de Castro E Silva, Fregoneze JB, Johnson AK. Corticotropin-releasing hormone in the lateral parabrachial nucleus inhibits sodium appetite in rats Am J Physiol Regul Integr Comp Physiol 2006; 290**:** R1136-R1141.

16. Elias CF, Kelly JF, Lee CE, Ahima RS, Drucker DJ, Saper CB, Elmquist JK. Chemical characterization of leptin-activated neurons in the rat brain J Comp Neurol 2000; 423**:** 261-281.

17. Nagase H, Nakajima A, Sekihara H, York DA, Bray GA. Regulation of feeding behavior, gastric emptying, and sympathetic nerve activity to interscapular brown adipose tissue by galanin and enterostatin: the involvement of vagal-central nervous system interactions J Gastroenterol 2002; 37 Suppl 14**:** 118-127.

18. Mercer JG, Moar KM, Hoggard N. Localization of leptin receptor (Ob-R) messenger ribonucleic acid in the rodent hindbrain Endocrinology 1998; 139**:** 29-34.

19. Weaver DR, Rivkees SA, Reppert SM. Localization and characterization of melatonin receptors in rodent brain by in vitro autoradiography J Neurosci 1989; 9**:** 2581-2590.

20. Williams LM, Hannah LT, Hastings MH, Maywood ES. Melatonin receptors in the rat brain and pituitary J Pineal Res 1995; 19**:** 173-177.

21. Simmons DM, Arriza JL, Swanson LW. A complete protocol for in situ hybridization of messenger RNAs in brain and other tissues with radiolabeled single-stranded RNA probes J Histotechnol 1989; 12**:** 169-181.

22. Paxinos G, Franklin K. The Mouse Brain in Stereotaxic Coordinates Academic Press 2002.

23. Adam CL, Moar KM, Logie TJ, Ross AW, Barrett P, Morgan PJ, Mercer JG. Photoperiod regulates growth, puberty and hypothalamic neuropeptide and receptor gene expression in female Siberian hamsters Endocrinology 2000; 141**:** 4349-4356.

24. Goldstone AP, Mercer JG, Gunn I, Moar KM, Edwards CM, Rossi M, Howard JK, Rasheed S, Turton MD, Small C, Heath MM, O'Shea D, Steere J, Meeran K, Ghatei MA, Hoggard N, Bloom SR. Leptin interacts with glucagon-like peptide-1 neurons to reduce food intake and body weight in rodents FEBS Lett 1997; 415**:** 134-138.

25. Mercer JG, Ellis C, Moar KM, Logie TJ, Morgan PJ, Adam CL. Early regulation of hypothalamic arcuate nucleus CART gene expression by short photoperiod in the Siberian hamster Regul Pept 2003; 111**:** 129-136.

26. Vrontakis ME, Yamamoto T, Schroedter IC, Nagy JI, Friesen HG. Estrogen induction of galanin synthesis in the rat anterior pituitary gland demonstrated by in situ hybridization and immunohistochemistry Neurosci Lett 1989; 100**:** 59-64.

27. Dun SL, Ng YK, Brailoiu GC, Ling EA, Dun NJ. Cocaine- and amphetamine-regulated transcript peptide-immunoreactivity in adrenergic C1 neurons projecting to the intermediolateral cell column of the rat J Chem Neuroanat 2002; 23**:** 123-132.

28. Calingasan NY, Ritter S. Presence of galanin in rat vagal sensory neurons: evidence from immunohistochemistry and in situ hybridization J Auton Nerv Syst 1992; 40**:** 229-238.

29. Zigman JM, Jones JE, Lee CE, Saper CB, Elmquist JK. Expression of ghrelin receptor mRNA in the rat and the mouse brain J Comp Neurol 2006; 494**:** 528-548.

30. Kishi T, Aschkenasi CJ, Lee CE, Mountjoy KG, Saper CB, Elmquist JK. Expression of melanocortin 4 receptor mRNA in the central nervous system of the rat J Comp Neurol 2003; 457**:** 213-235.

31. Dun SL, Castellino SJ, Yang J, Chang JK, Dun NJ. Cocaine- and amphetamine-regulated transcript peptide-immunoreactivity in dorsal motor nucleus of the vagus neurons of immature rats Brain Res Dev Brain Res 2001; 131**:** 93-102.

32. Vrang N, Hansen M, Larsen PJ, Tang-Christensen M. Characterization of brainstem preproglucagon projections to the paraventricular and dorsomedial hypothalamic nuclei Brain Res 2007; 1149**:** 118-126.

33. Tang-Christensen M, Larsen PJ, Goke R, Fink-Jensen A, Jessop DS, Moller M, Sheikh SP. Central administration of GLP-1-(7-36) amide inhibits food and water intake in rats Am J Physiol 1996; 271**:** R848-R856.

34. Goldstone AP, Morgan I, Mercer JG, Morgan DG, Moar KM, Ghatei MA, Bloom SR. Effect of leptin on hypothalamic GLP-1 peptide and brain-stem pre-proglucagon mRNA Biochem Biophys Res Commun 2000; 269**:** 331-335.

35. Vrang N, Larsen PJ, Jensen PB, Lykkegaard K, Artmann A, Larsen LK, Tang-Christensen M. Upregulation of the brainstem preproglucagon system in the obese Zucker rat Brain Res 2008; 1187**:** 116-124.

36. Schwartz MW, Seeley RJ, Campfield LA, Burn P, Baskin DG. Identification of targets of leptin action in rat hypothalamus J Clin Invest 1996; 98**:** 1101-1106.

37. Mercer JG, Moar KM, Findlay PA, Hoggard N, Adam CL. Association of leptin receptor (OB-Rb), NPY and GLP-1 gene expression in the ovine and murine brainstem Regul Pept 1998; 75-76**:** 271-278.

38. Zheng H, Patterson LM, Phifer CB, Berthoud HR. Brain stem melanocortinergic modulation of meal size and identification of hypothalamic POMC projections Am J Physiol Regul Integr Comp Physiol 2005; 289**:** R247-R258.

39. Augustine RA, Ladyman SR, Grattan DR. From feeding one to feeding many: hormone-induced changes in bodyweight homeostasis during pregnancy J Physiol 2008; 586**:** 387-397.

40. Tups A, Ellis C, Moar KM, Logie TJ, Adam CL, Mercer JG, Klingenspor M. Photoperiodic regulation of leptin sensitivity in the Siberian hamster, Phodopus sungorus, is reflected in arcuate nucleus SOCS-3 (suppressor of cytokine signaling) gene expression Endocrinology 2004; 145**:** 1185-1193.

41. Tups A, Barrett P, Ross AW, Morgan PJ, Klingenspor M, Mercer JG. The suppressor of cytokine signalling 3, SOCS3, may be one critical modulator of seasonal body weight changes in the Siberian hamster, Phodopus sungorus J Neuroendocrinol 2006; 18**:** 139-145.

42. Blevins JE, Chelikani PK, Haver AC, Reidelberger RD. PYY(3-36) induces Fos in the arcuate nucleus and in both catecholaminergic and non-catecholaminergic neurons in the nucleus tractus solitarius of rats Peptides 2008; 29**:** 112-119.

43. Hokfelt T, Cortes R, Schalling M, Ceccatelli S, Pelto-Huikko M, Persson H, Villar MJ. Distribution patterns of CCK and CCK mRNA in some neuronal and non-neuronal tissues Neuropeptides 1991; 19 Suppl**:** 31-43.

44. Hermanson O, Larhammar D, Blomqvist A. Preprocholecystokinin mRNA-expressing neurons in the rat parabrachial nucleus: subnuclear localization, efferent projection, and expression of nociceptive-related intracellular signaling substances J Comp Neurol 1998; 400**:** 255-270.

45. Schick RR, Yaksh TL, Roddy DR, Go VL. Release of hypothalamic cholecystokinin in cats: effects of nutrient and volume loading Am J Physiol 1989; 256**:** R248-R254.

46. Schick RR, Reilly WM, Roddy DR, Yaksh TL, Go VL. Neuronal cholecystokinin-like immunoreactivity is postprandially released from primate hypothalamus Brain Res 1987; 418**:** 20-26.

47. Blevins JE, Stanley BG, Reidelberger RD. Brain regions where cholecystokinin suppresses feeding in rats Brain Res 2000; 860**:** 1-10.

48. Fan W, Ellacott KL, Halatchev IG, Takahashi K, Yu P, Cone RD. Cholecystokinin-mediated suppression of feeding involves the brainstem melanocortin system Nat Neurosci 2004; 7**:** 335-336.

49. Bartness TJ, Morley JE, Levine AS. Photoperiod-peptide interactions in the energy intake of Siberian hamsters Peptides 1986; 7**:** 1079-1085.

50. Herbert H, Saper CB. Cholecystokinin-, galanin-, and corticotropin-releasing factor-like immunoreactive projections from the nucleus of the solitary tract to the parabrachial nucleus in the rat J Comp Neurol 1990; 293**:** 581-598.

51. Hermanson O, Larhammar D, Blomqvist A. Preprocholecystokinin mRNA-expressing neurons in the rat parabrachial nucleus: subnuclear localization, efferent projection, and expression of nociceptive-related intracellular signaling substances J Comp Neurol 1998; 400**:** 255-270.

52. Fulwiler CE, Saper CB. Cholecystokinin-immunoreactive innervation of the ventromedial hypothalamus in the rat: possible substrate for autonomic regulation of feeding Neurosci Lett 1985; 53**:** 289-296.

53. Grill HJ, Markison S, Ginsberg A, Kaplan JM. Long-term effects on feeding and body weight after stimulation of forebrain or hindbrain CRH receptors with urocortin Brain Res 2000; 867**:** 19-28.

54. Sahu A, Carraway RE, Wang YP. Evidence that neurotensin mediates the central effect of leptin on food intake in rat Brain Res 2001; 888**:** 343-347.

55. Cummings S, Elde R, Ells J, Lindall A. Corticotropin-releasing factor immunoreactivity is widely distributed within the central nervous system of the rat: an immunohistochemical study J Neurosci 1983; 3**:** 1355-1368.

56. Kelly AB, Watts AG. The region of the pontine parabrachial nucleus is a major target of dehydration-sensitive CRH neurons in the rat lateral hypothalamic area J Comp Neurol 1998; 394**:** 48-63.

57. Herbert H, Saper CB. Cholecystokinin-, galanin-, and corticotropin-releasing factor-like immunoreactive projections from the nucleus of the solitary tract to the parabrachial nucleus in the rat J Comp Neurol 1990; 293**:** 581-598.

58. Grill HJ, Markison S, Ginsberg A, Kaplan JM. Long-term effects on feeding and body weight after stimulation of forebrain or hindbrain CRH receptors with urocortin Brain Res 2000; 867**:** 19-28.

59. de BR, Suaudeau C. Anorectic effect of calcitonin, neurotensin and bombesin infused in the area of the rostral part of the nucleus of the tractus solitarius in the rat Peptides 1988; 9**:** 729-733.

60. Gardner JD, Rothwell NJ, Luheshi GN. Leptin affects food intake via CRF-receptor-mediated pathways Nat Neurosci 1998; 1**:** 103.

61. Fite KV, Wu PS, Bellemer A. Photostimulation alters c-Fos expression in the dorsal raphe nucleus Brain Res 2005; 1031**:** 245-252.

62. Tache Y, Yang H, Kaneko H. Caudal raphe-dorsal vagal complex peptidergic projections: role in gastric vagal control Peptides 1995; 16**:** 431-435.

63. Blevins JE, Schwartz MW, Baskin DG. Evidence that paraventricular nucleus oxytocin neurons link hypothalamic leptin action to caudal brain stem nuclei controlling meal size Am J Physiol Regul Integr Comp Physiol 2004; 287**:** R87-R96.

64. Zheng H, Patterson LM, Phifer CB, Berthoud HR. Brain stem melanocortinergic modulation of meal size and identification of hypothalamic POMC projections Am J Physiol Regul Integr Comp Physiol 2005; 289**:** R247-R258.

Figure legends:

Fig. 1: Brainstem neuroendocrine pathways involved in energy balance regulation. A: Humoral signals encoding energy status are transduced by peripherally adipocyte-secreted leptin. Neuronal afferences emerge from the gastrointestinal tract (*vagus n*. via PYY/CCK) and the tongue and pharynx (*glossopharyngeal n.*). Retinal information on seasonal photoperiod is processed in the SCN and relayed over pineal melatonin to be integrated in remote brainstem centers. A-B: Coronal detail drawings of the hindbrain at the level of the parabrachial nucleus (B) and nucleus of the solitary tract (C). *ARC, arcuate hypothalamic nucleus; AP, area postrema; Cb, cerebellum; CC, central canal; CCK, cholecystokinin; DMN; dorsomedial hypothalamic nucleus; PB, parabrachial nucleus; PVN, paraventricular hypothalamic nucleus; py, pyramidal tract; PYY, peptide YY; SCN, suprachiasmatic nucleus.*

Fig. 2: Effect of 14 week exposure to short [short day (SD); 8:16-h light-dark cycle] and long photoperiod [long day (LD); 16:8-h light-dark cycle] on body weight of adult male Siberian hamsters (means ± SEM; *n*=20 per group).

Fig. 3: Neuropeptide and receptor gene expression in the brainstem nucleus of the solitary tract of Siberian hamsters kept in long or short day photoperiod (n = 20 per group) for 14 weeks. A: pre-proglucagon, B: melanocortin 4 receptor, C: cocaine- and amphetamine regulated transcript, D: galanin, E: growth hormone secretagogue receptor, F: melanocortin 3 receptor. Lower panels of each graph show representative autoradiographs of coronal brainstem sections. Values are expressed as percentages of values in LD hamsters. Means ± SEM; ***, $P < 0.001$. 12n, hypoglossal nucleus; *Cb, cerebellum; IO, inferior olive; MdD, medullary reticular nucleus, dorsal part; SolM nucleus of the solitary tract, medial part.* Scale bar = 2.1 mm.

Fig. 4: Effect of photoperiod and/or i.p. leptin administration on neuropeptides in the nucleus of the solitary tract quantified by analysis of Immunoreactive (-ir) cells. Values are expressed as percentages of –ir cells in LD control hamsters. A: glucagon-like peptide-1, B: cholecystokinin, C: alpha-melanocyte-stimulating hormone, D: peptide YY. White bars: saline injected, black bars: leptin treated, white background: long day, grey background: short day. A-B: Lower panels showing representative photomicrographs of immunofluorescence CCK-ir (A) and GLP-1-ir (B) in the NTS. Boxed: High magnification images of selected areas. Means ± SEM; *, $P < 0.05$. *CC, central canal; SolM, nucleus of the solitary tract, medial part.* Scale bars, low magnification images = 100 μm; high magnification images = 70 μm.

Fig. 5: Effect of photoperiod and/or i.p. leptin administration on neuropeptides in the parabrachial nucleus quantified by analysis of Immunoreactive (-ir) cells. Values are expressed as percentages of –ir cells in LD control hamsters. A: corticotrophin releasing hormone, B: neurotensin, C: cholecystokinin, D: galanin. White bars: saline injected, black bars: leptin treated, white background: long day, grey background: short day. A-B: Lower panels showing representative photomicrographs of immunofluorescence CRH-ir (A) and NT-ir (B) in the PB. Means ± SEM; *, $P < 0.05$. *LPBD, lateral parabrachial nucleus, dorsal part; LPBI, lateral parabrachial nucleus, internal part; MPB, medial parabrachial nucleus,* Scale bar = 70 μm.

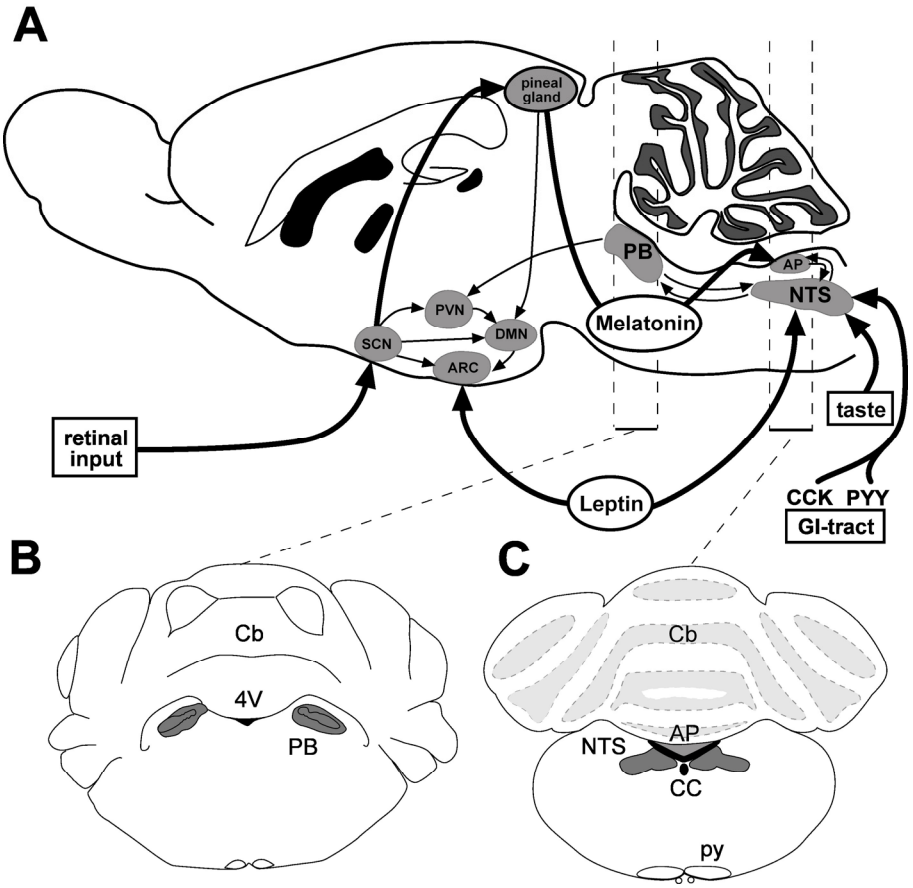
A
pineal gland
PB
AP
NTS
PVN
DMN
SCN
ARC
Melatonin
retinal input
taste
Leptin
CCK PYY
GI-tract
B
Cb
4V
PB
C
Cb
AP
NTS
CC
py

Fig. 1

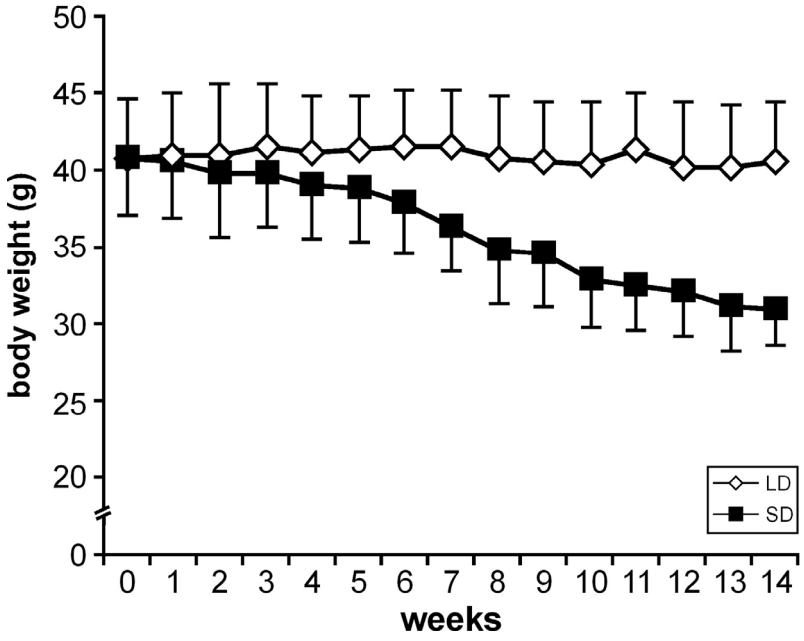
body weight (g)
50
45
40
35
30
25
20
0
0 1 2 3 4 5 6 7 8 9 10 11 12 13 14
weeks
LD
SD

Fig. 2

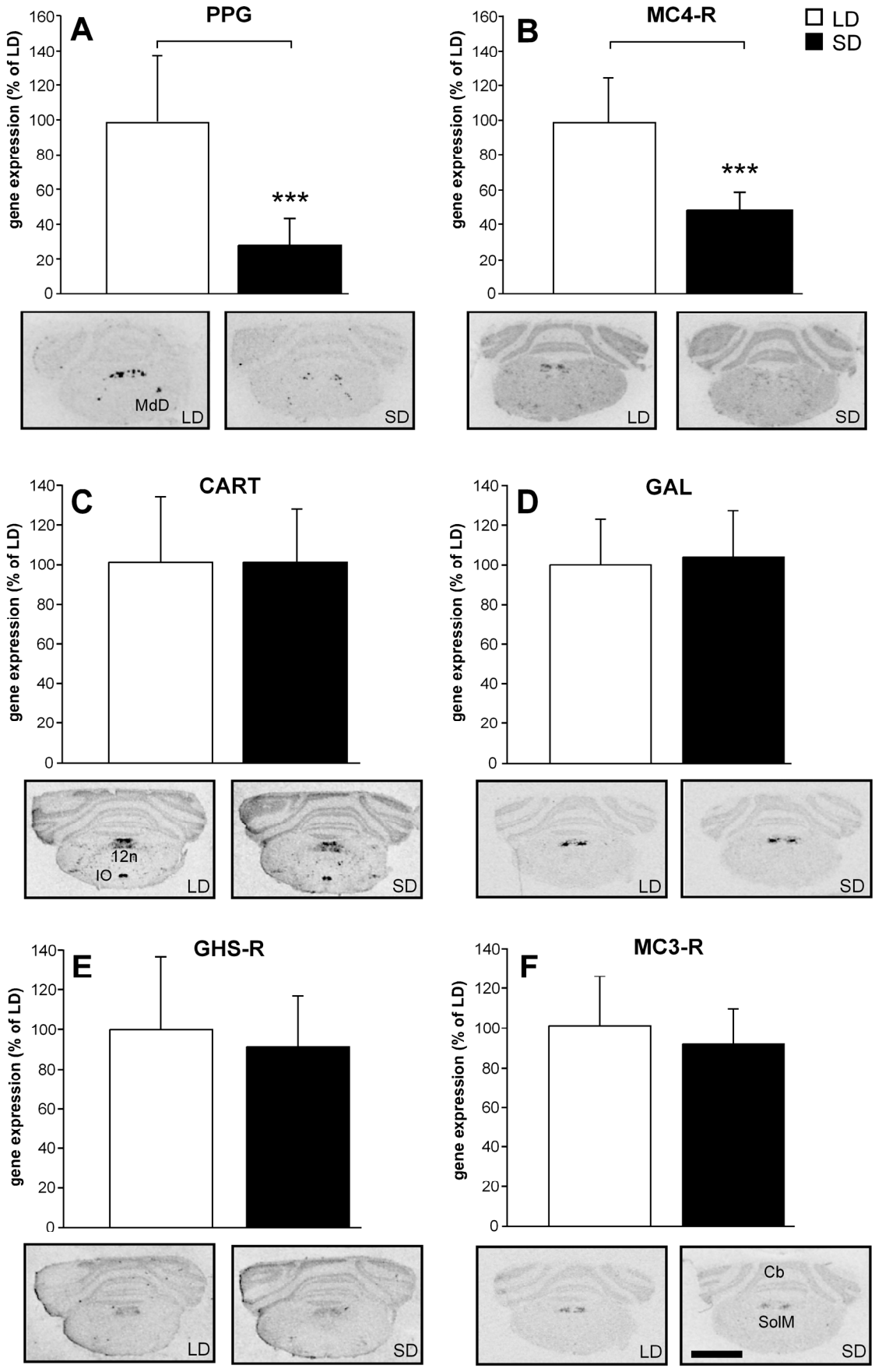
A
PPG
gene expression (% of LD)
***
MdD
LD
SD
B
MC4-R
LD
SD
***
LD
SD
C
CART
12n
IO
LD
SD
D
GAL
LD
SD
E
GHS-R
LD
SD
F
MC3-R
Cb
SolM
LD
SD

Fig. 3

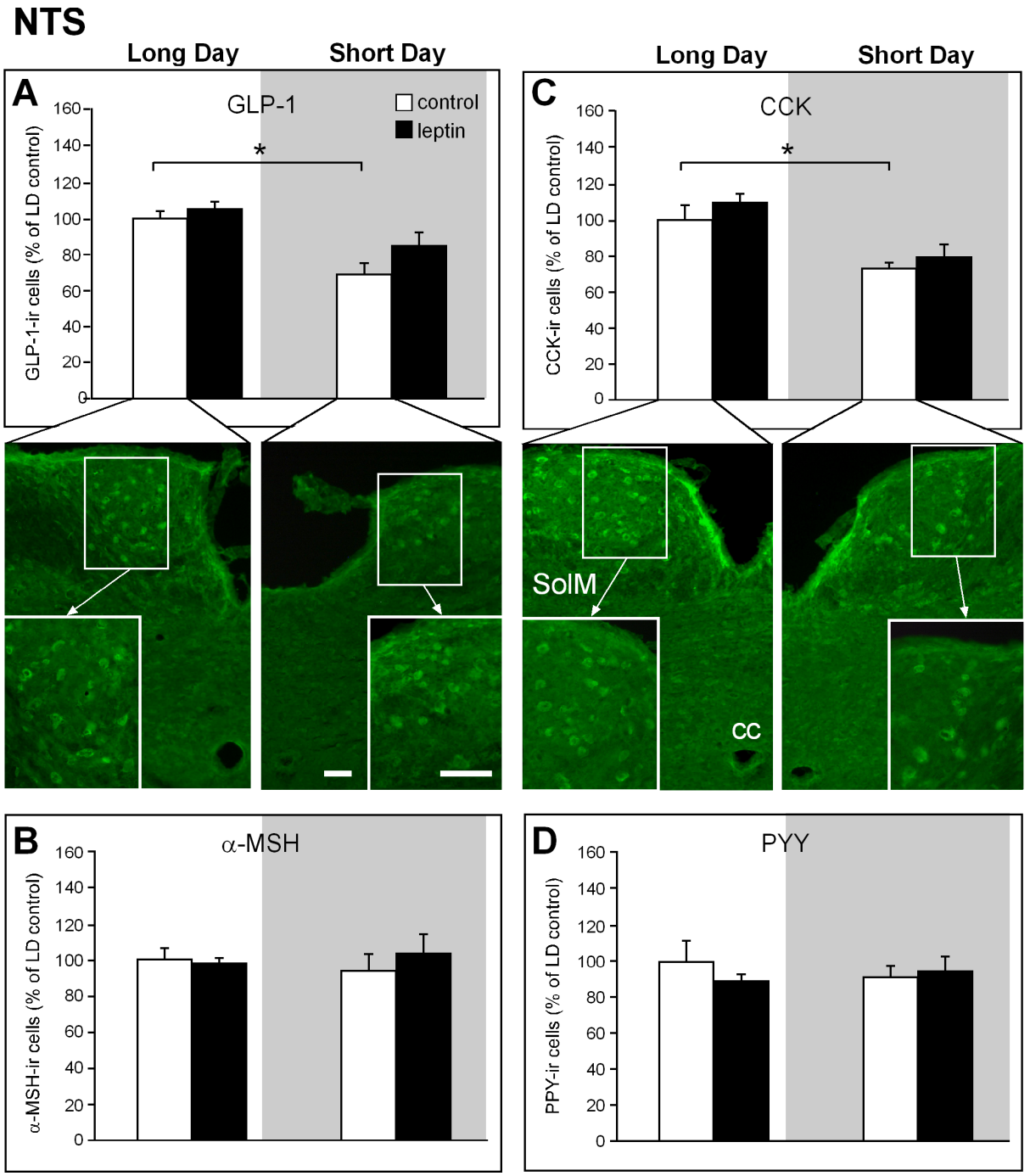
NTS
Long Day
Short Day
A
GLP-1
control
leptin
GLP-1-ir cells (% of LD control)
C
CCK
CCK-ir cells (% of LD control)
SolM
cc
B
α-MSH
α-MSH-ir cells (% of LD control)
D
PYY
PPY-ir cells (% of LD control)

Fig. 4

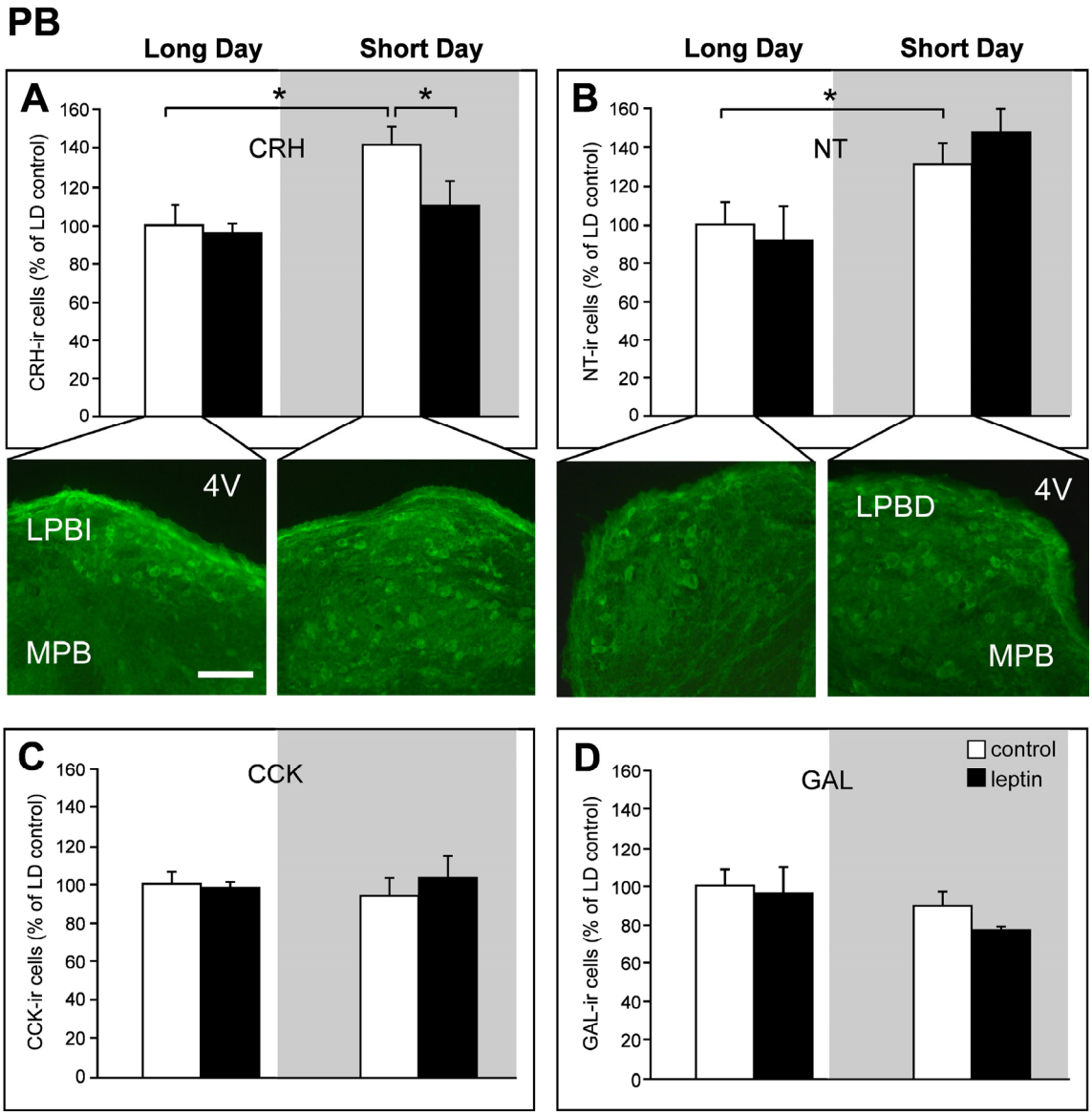
PB
Long Day
Short Day
A
CRH
CRH-ir cells (% of LD control)
4V
LPBI
MPB
B
NT
NT-ir cells (% of LD control)
LPBD
4V
MPB
C
CCK
CCK-ir cells (% of LD control)
D
GAL
GAL-ir cells (% of LD control)
control
leptin

Fig. 5

Am J Physiol Regul Integr Comp Physiol 291: R643–R650, 2006.
First published April 6, 2006; doi:10.1152/ajpregu.00807.2005.

Photoperiodic regulation of insulin receptor mRNA and intracellular insulin signaling in the arcuate nucleus of the Siberian hamster, *Phodopus sungorus*

Alexander Tups,[1,2] Michael Helwig,[1,2] Sigrid Stöhr,[2] Perry Barrett,[1] Julian G. Mercer,[1] and Martin Klingenspor[2]

[1]*Division of Obesity and Metabolic Health, Rowett Research Institute, Aberdeen Centre for Energy Regulation and Obesity, Aberdeen, Scotland, and* [2]*Department of Animal Physiology, Philipps University Marburg, Marburg, Germany*

Submitted 15 November 2005; accepted in final form 25 March 2006

Tups, Alexander, Michael Helwig, Sigrid Stöhr, Perry Barrett, Julian G. Mercer, and Martin Klingenspor. Photoperiodic regulation of insulin receptor mRNA and intracellular insulin signaling in the arcuate nucleus of the Siberian hamster, *Phodopus sungorus. Am J Physiol Regul Integr Comp Physiol* 291: R643–R650, 2006. First published April 6, 2006; doi:10.1152/ajpregu.00807.2005.—During the last 5 years it has been well established that photoperiod-induced changes in body weight in the seasonal hamster, *Phodopus sungorus*, are accompanied by a marked seasonal cycle in leptin sensitivity. In the present study, we investigated the possible involvement of insulin signaling in seasonal body weight regulation. We analyzed the expression pattern and relative intensity of insulin receptor (IR), phosphatidylinositol 3-kinase (PI3-kinase), and protein tyrosine phosphatase 1B (PTP1B) mRNAs by in situ hybridization in the brains of juvenile female hamsters acclimated to either long- (LD) or short-day length (SD) for 8 wk, with or without superimposed food deprivation for 48 h. Furthermore, the hypothalamic concentration and distribution of phospho-AKT, a marker of PI3-kinase activity was determined by immunoblotting and immunohistochemistry. Eight weeks of acclimation to SD led to a substantial downregulation of IR, PTP1B gene expression, and phospho-AKT concentration in this brain region, whereas PI3-kinase mRNA was unchanged. Food deprivation induced a decrease in PTP1B and a trend toward lowered IR gene expression in LD but not in SD. Additionally, a striking increase in PTP1B gene expression in the thalamus was observed after food deprivation in both photoperiods. The direction of change in neuronal insulin signaling contrasts to the central catabolic nature of this pathway described in other species. SD-induced reduction in insulin signaling may be due to decline in body fat stores mediated by enhanced central leptin sensitivity. Increased anorexigenic tone of leptin may overwrite central insulin signaling to prevent catabolic overdrive.

protein tyrosine phosphatase 1B; body weight regulation; hypothalamus; thalamus

SEASONAL MAMMALS LIKE THE Siberian hamster, *Phodopus sungorus* (also known as the Djungarian hamster), undergo an anticipatory seasonal cycle in energy balance in response to the annual change in photoperiod. Acclimation to a short-day (SD) photoperiod induces alterations in physiology, such as a reduction of food intake, energy expenditure, and body weight, which are reversible after transfer back to long-day (LD) photoperiod. During the complete cycle, precise adjustment of seasonally-appropriate parameters regulating energy balance requires cross talk between peripheral adiposity signals and the brain (25, 42). To date, only two molecules have been identified (leptin and insulin) that meet the criteria proposed for adiposity signals (30). The seasonal cycle in body weight is associated with a correlation of these hormones in proportion to body fat mass. Leptin and insulin are transported into the brain from the bloodstream where they bind to their receptors and, in particular, those in the arcuate nucleus, a key neuronal center for control of energy homeostasis. Activation of signal transduction pathways distal to their receptors integrates these peripheral signals into a neuronal response. Leptin and insulin exhibit similarities in their central effects (both display catabolic actions), and accumulating evidence suggests that cross talk between these hormones, particularly at the level of their central intracellular signal transduction, leads to synergistic action in the regulation of energy balance (11, 30, 41).

The insulin receptor (IR) is a tetrameric complex composed of two α- and β-subunits. Although not related to the leptin receptor, the IR shares the feature of possessing intrinsic tyrosine-protein-kinase activity leading to activation of downstream signaling pathways (39). Cellular interaction of leptin and insulin signaling is most likely to occur via a pathway involving phosphatidylinositol 3-kinase (PI3-kinase) (28, 31, 41). Upon insulin binding, PI3-kinase is activated by IR substrate proteins that have been phosphorylated by the IR (16, 27). PI3-kinase catalyzes the phosphorylation of phosphatidylinositol 4,5-bisphosphate to phosphatidylinositol 3,4,5-trisphosphate, which, in turn, activates downstream targets like AKT (also known as protein kinase B), a pivotal molecule for most of insulin's effects (14, 30).

Inhibitory molecules, such as the suppressor of cytokine signaling 3 (SOCS3) and several protein tyrosine phosphatases [(PTPs) PTPα, LAR, CD45, PTPε, and PTP1B], are thought to deactivate insulin signaling, whereas some of them (SOCS3 and PTP1B) even exhibit synergistic effects in terms of inhibition of both leptin and IR signaling (2, 26). Among these molecules, substantial evidence supports PTP1B as being the central player in controlling insulin action. PTP1B knockout in mice and knockdown by antisense oligonucleotides in diabetic rodents leads to enhanced insulin sensitivity (10, 17, 36, 46). These animals maintain euglycemia (in the fed state) with one-half the level of insulin observed in wild-type littermates and, surprisingly, are resistant to diet-induced obesity. These attributes make this phosphatase a very attractive candidate for obesity and type 2 diabetes research.

Our knowledge of insulin signaling pathways and the molecules involved is derived from studies investigating insulin's action in the periphery. The only study investigating the

Address for reprint requests and other correspondence: A. Tups, Dept. of Animal Physiology, Philipps Univ. Marburg, Karl von Frisch Str. 8, D-35043 Marburg, Germany (e-mail: tups@staff.uni-marburg.de).

The costs of publication of this article were defrayed in part by the payment of page charges. The article must therefore be hereby marked "*advertisement*" in accordance with 18 U.S.C. Section 1734 solely to indicate this fact.

peripheral effect of insulin on seasonal body weight regulation in *P. sungorus* was compromised by the adverse response to streptozotocin treatment (5). Although recent studies reported blockade of intracerebroventricular (ICV) insulin actions on both food intake and hepatic glucose production by ICV pretreatment with PI3-kinase inhibitors (28, 31), the details of central insulin signal transduction remain limited.

Recent studies have unmasked a seasonal cycle in sensitivity to the adipocyte-derived hormone leptin in *P. sungorus* (3, 19, 37). We proposed that SOCS3 plays an important role in mediating seasonal modifications in leptin sensitivity, suggesting that the underlying molecular mechanism is centered on intracellular signal transduction of leptin receptors in the arcuate nucleus, the brain region with strongest density of SOCS3 gene expression (43).

The close association of leptin and insulin signaling raises the question of whether modifications in insulin signal transduction within the arcuate nucleus are implicated in seasonal body weight regulation. In the present study, we investigated this idea by analyzing (in situ hybridization) hypothalamic IR, PTP1B, and PI3-kinase gene expression in juvenile female hamsters that had been acclimated to either SD or LD for a period of 8 wk. Furthermore, we investigated phosphorylation of AKT in the hypothalamus, detected with phosphospecific antibodies by immunoblotting and immunohistochemistry, and determined the effect of photoperiod on the hypothalamic content of this pivotal insulin signaling molecule.

MATERIALS AND METHODS

All procedures involving animals were licensed under the Animals (Scientific Procedures) Act of 1986 and received approval from the Ethical Review Committee at the Rowett Research Institute. Siberian hamsters were drawn from the Rowett breeding colony (1, 21, 23) and were gestated and suckled in a LD photoperiod (16:8-h light-dark cycle). All Siberian hamsters were weaned at 3 wk of age and were individually housed at weaning. Where specified, hamsters were transferred into a SD photoperiod (8:16-h light-dark cycle) but with all other environmental conditions unaltered; rooms were maintained at 22°C. Food (Labsure pelleted diet; Special Diet Services, Witham, Essex, UK) and water were available ad libitum, or, where specified, hamsters were food deprived for 48 h. For verification of SD acclimation, body weight was measured once a week and uterine tract size was inspected by two examiners at the end of the study. All animals were killed in the middle of the light phase by either cervical dislocation (for in situ hybridization and immunoblotting) or by transcardial perfusion with 4% paraformaldehyde under deep pentobarbital sodium anesthesia (for immunohistochemistry). Brains were processed differently for each analytical end point. For in situ hybridization, brains were rapidly removed and frozen on dry ice. For immunoblotting, fresh hypothalami were excised with anatomical precision and frozen in liquid nitrogen. For immunohistochemistry, brains were treated as stated below.

Experimental Procedure

For all experiments, juvenile female hamsters (weaned at 3 wk of age) were used, which were either maintained in LD photoperiod for 8 wk ($n = 19$) or transferred to SD photoperiod for the same period ($n = 19$) postweaning. For analysis of IR, PTP1B, and PI3-kinase gene expression by in situ hybridization in either photoperiod, six food-deprived (48 h) and six ad libitum-fed control animals were killed. For detection of phospho-AKT by immunoblotting or immunohistochemistry, respectively, three or four brains from ad libitum-fed hamsters from each photoperiod were used. PTP1B mRNA in ad libitum-fed animals was analyzed in archived brain sections from an earlier experiment performed under identical conditions (43).

Hypothalamic Gene Expression

mRNA levels were quantified by in situ hybridization in 20-μm coronal hypothalamic sections by using techniques described in detail elsewhere (23). Riboprobes complementary to IR, PI3-kinase, and PTP1B were generated from cloned cDNA from the hypothalamus of the Siberian hamster. cDNA synthesis was performed by using a cDNA synthesis kit (Invitrogen, Carlsbad, CA), according to the manufacturer's instructions. Primers for amplification of the three fragments were designed using Primer Select (Table 1; Lasergene, DNA-Star Software). The IR amplicons were generated by PCR with 35 cycles of 94°C for 1 min, 55°C for 1 min 40 s, and 72°C for 2 min, and a final extension at 72°C for 10 min. For the amplification of PI3-kinase and PTP1B, the annealing temperature was adjusted to 50°C for PI3-kinase and 59°C for PTP1B. DNA fragments were ligated into pGEM-T-Easy [(IR and PI3-kinase), Promega, Madison, WI] or pPCR-Script Amp SK^+ [(PTP1B) Stratagene, La Jolla, CA] transformed into *Escherichia coli* DH5α and sequenced. For cRNA synthesis of antisense riboprobes by in vitro transcription SP6-polymerase (IR and PI3-kinase; Invitrogen) or T3-polymerase (PTP1B; Invitrogen) were used. To generate the sense control for all three riboprobes, cRNA synthesis was performed by T7-polymerase.

As previously described (23), forebrain sections (20 μm) were collected throughout the extent of the arcuate nucleus (ARC) onto a set of eight slides with six or seven sections mounted on each slide. Accordingly, slides spanned the hypothalamic region approximating from −2.7 to −1.46 mm relative to Bregma according to the atlas of the mouse brain (33). One slide from each animal was hybridized. Briefly, slides were fixed, acetylated, and hybridized overnight at 58°C using ^{35}S-labeled cRNA probes ($1–2 \times 10^7$ cpm/ml). Slides were treated with RNase A, desalted with a final high-stringency wash (30 min) in 0.1 × SSC at 60°C, dried, and apposed to Kodak Biomax MR Film (Kodak, Rochester, New York, NY). Autoradiographic images were quantified using the Image-Pro Plus system. Corresponding sections of individual animals were matched according to the atlas of the mouse brain. Three to four sections from the ARC of each animal spanning from −2.54 to −1.94 mm relative to Bregma were

Table 1. *Oligonucleotides used for cloning of the respective candidate genes for in situ hybridisation*

Probes	Primers	Oligonucleotide Sequence	Fragment Size, bp	GenBank Accession No., rat/mouse
Insulin receptor	Forward	5′-CTGCGGCCCGATGCTGAGA-3′	229	8393620
	Reverse	5′-CCCTTGCCCCCTTTCCGATAGTAA-3′		
PI3-Kinase	Forward	5′-AACGCGAAGGCAACGAGAAGGAA-3′	219	6981357
	Reverse	5′-AACGCGAAGGCAACGAGAAGGAA-3′		
PTP1B	Forward	5′-TGGCCACAGCAAGAAGAAAAGGAG-3′	409	50872126
	Reverse	5′-TGAGCCCCATGCGGAACC-3′		

PI3-kinase, phosphatidylinositol 3-kinase; PTP1B, protein tyrosine phosphatase 1B.

analyzed. Data were manipulated using a standard curve generated from ^{14}C autoradiographic microscales (Amersham Pharmacia Biotech), and the integrated intensities of the hybridization signals were computed.

Immunohistochemistry

For immunohistochemistry, animals were anesthetized with Euthatal (Rhone Merieux, Harlow, UK), transcardially perfused with 0.9% saline containing heparin (1,000 U/l), and followed by 4% paraformaldehyde in 0.1 M phosphate buffer (pH 7.4). Brains were removed and postfixed in the same fixative overnight at 4°C. On the next morning, brains were transferred to 30% sucrose in 0.1 M phosphate buffer for dehydration and cryoprotection. When brains had sunk, they were frozen in isopentane, cooled on dry ice for 1 min, and sectioned coronally at 35 μm throughout the extent of the hypothalamus (additionally the nucleus tractus solitarius region of the hindbrain was cut) on a freezing microtome, collected in four series, and stored in cryoprotectant at 4°C. Free-floating sections were incubated in 1% H_2O_2, 10% methanol diluted in H_2O for 15 min to quench endogenous peroxide followed by incubation in blocking solution (5% BSA, 0.5% Triton X-100 in phosphate buffer) for 45 min. Sections were incubated overnight at 4°C with anti-phospho-AKT primary antibody (Ser473, IHC-specific; cat. no. 9277, Cell Signaling Technology) diluted in blocking solution (1:100). On the next day, sections were incubated with a biotinylated secondary goat anti-rabbit antibody for 1 h (1:1,000, in blocking solution containing 3% BSA), and then treated with ABC (Vector Laboratories, Burlingame, CA) solution for 2 h. Between steps, sections were washed in phosphate buffer containing 0.25% Triton X-100. Finally, the signal was developed by nickel-DAB solution (Vector Laboratories), giving a gray/black precipitate. Section images were captured by using a Polaroid DMCe digital camera mounted on a Zeiss Axioskop (Jena, Germany).

Immunoblotting

For immunoblotting, hypothalami were immediately excised with anatomical precision from freshly prepared brains, weighed, and rapidly frozen in liquid nitrogen. With the use of a glass homogenizer, tissues were homogenized in buffer containing phosphatase and protease inhibitors (in mM: 10 HEPES pH 7.9, 1.5 $MgCl_2$, 10 KCl, 0.5 DTT, 0.5 PMSF, 20 NaF, and 1 Na_3VO_4) and incubated on ice for 10 min. For detection of phospho-AKT, the cytoplasmic fraction was separated from the nuclear part by centrifugation for 15 min at 3,300 *g*. The protein content of the supernatant containing the cytoplasmic fraction was determined by the Bradford assay, and equal amounts of protein were loaded into each lane. Immunoblotting analysis was performed by standard method (18). Samples were separated on 12.5% SDS-PAGE and, after transfer to nitrocellulose membrane, stained with red Ponceau dye to ensure accurate protein loading and transfer. Phospho-AKT was detected with a polyclonal rabbit antibody specific for immnunoblotting (Ser473, 1:1,000, cat. no. 9271; Cell Signaling Technology). Goat anti-rabbit-IgG-HRPO conjugate (DAKO-Cytomation, Glostrup, Denmark) was used as the secondary antibody (1:10,000). Immunodetection was performed by enhanced chemiluminescence using reagent. Autoradiographs were quantified densitometrically using Scion-Image software. For technical validation, the immunoblot was repeated twice.

Statistical Analysis

Data were analyzed by one- or two-way ANOVA followed by Student-Newman-Keuls multiple comparison test, as appropriate, using SigmaStat statistical software (Jandel, Erkrath, Germany). Where data failed equal variance or normality tests they were analyzed by one-way ANOVA on ranks followed by Dunn's multiple comparison test. Results are presented as means ± SE, and differences were considered significant if $P < 0.05$.

RESULTS

Distribution of IR, PI3-Kinase, and PTP1B Gene Expression in the Hamster Brain

The species-specific probes to IR, PI3-kinase, and PTP1B mRNA had an identity of 95, 91, and 90% in nucleic acid sequence to *Rattus norvegicus* or *Mus musculus*, respectively (for GenBank accession nos., see Table 1). Within the investigated brain region, neuroanatomical structures that hybridized the three riboprobes are listed in Table 2 along with their estimated relative intensities (see also, Fig. 1). Of particular interest were the localized and intense hybridization signals of IR, PI3-kinase, and PTP1B in the ARC. PTP1B gene expression in the thalamus was relatively uniform and could not be attributed to individual thalamic nuclei. For all three candidate genes, sense probes synthesized from the cloned cDNA generated a low-intensity nonspecific signal (Fig. 1*D*).

Effect of Photoperiod and/or Food Deprivation on Insulin Signaling Components

Effect of photoperiod and food deprivation on IR gene expression. Body weight change at 8 wks postweaning was similar to an identical experiment reported earlier (43). Over the 8-wk period, SD hamsters gained 10.2 ± 1.3 g, while hamsters in LD gained 14.2 ± 1.2 g. Uterine tract size was reduced in SD acclimated hamsters compared with controls.

In juvenile female hamsters acclimated to SD photoperiod for 8 wk, IR gene expression was decreased significantly compared with hamsters maintained in LD for the same period (two-way ANOVA; $F = 5.909$; $P < 0.05$; Fig. 1*A*). Although there was a trend to decreased IR gene expression in response to food deprivation in LD, this difference was not significant, and there was no significant interaction between photoperiod and food deprivation. IR gene expression in structures analyzed outside the ARC was unaffected by either photoperiod or feeding status.

SD-induced downregulation of IR to about 40% of the expression level in LD hamsters was confirmed by repeating the experiment with 11–12 ad libitum-fed female hamsters in each photoperiod [8 wk postweaning, (one-way ANOVA on ranks; $H = 8.37$; $P < 0.001$; data not shown)].

Effect of photoperiod and food deprivation on PI3-kinase gene expression. There was no effect of photoperiod, feeding status, or interaction of both parameters on PI3-kinase mRNA

Table 2. *Distribution of mRNA in the investigated brain region*

	Probe (rel. density in LD ad lib.)		
Structure	IR	PI3-Kinase	PTP1B
CA1-3	+++	+++	+++
dentategyrus	+++	+++	+++
habenular nucleus	+++		+++
choroid plexus	++	+++	+
cerebral cortex		+++	+
piriform cortex	++	+	++
amygdala	+	+	+
optic tract	++	+	+
arcuate nucleus	++	++	++
thalamus			++

LD, long-day line; IR, insulin receptor.

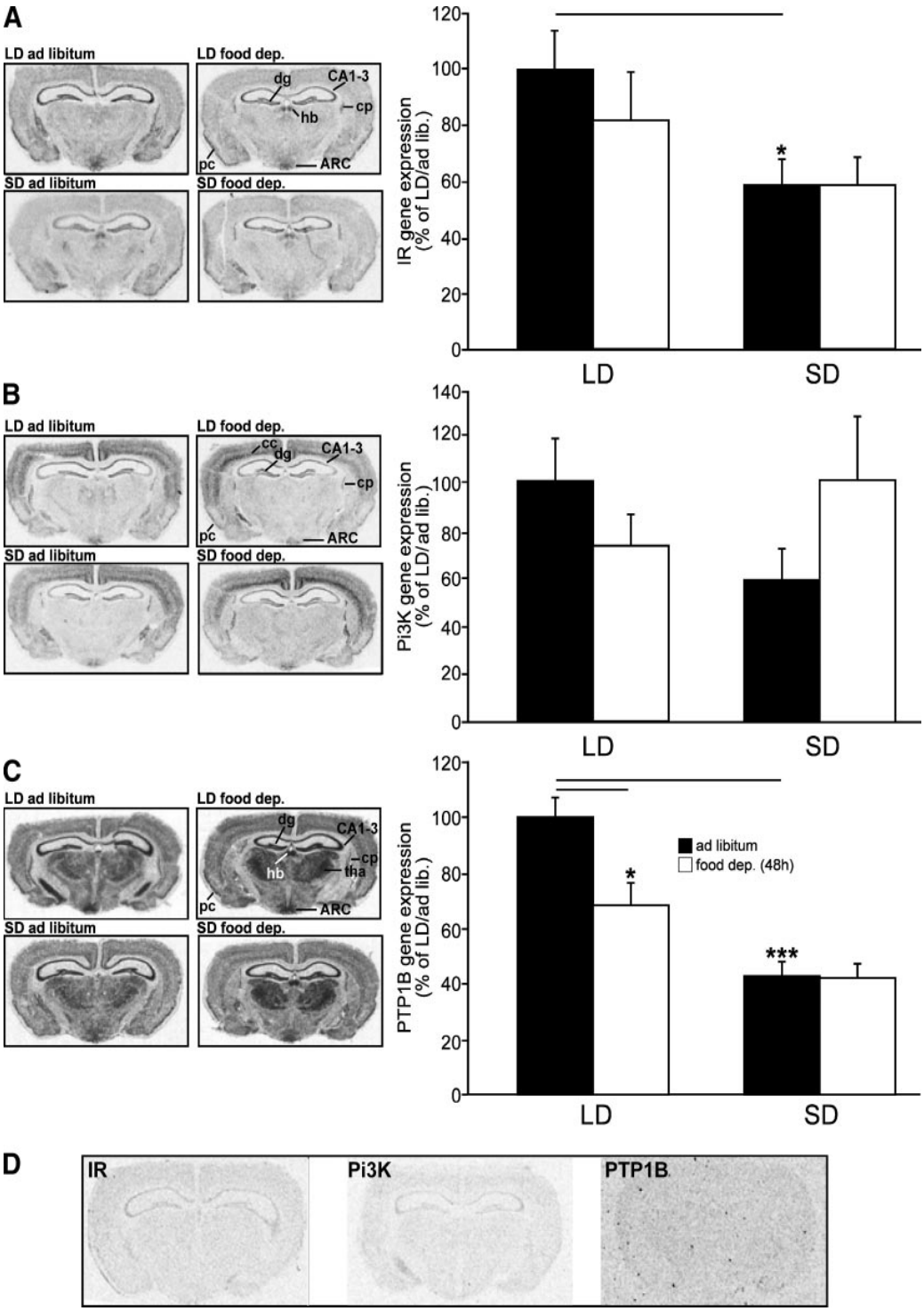

Fig. 1. Gene expression of insulin receptor (IR; *A*), phosphatidylinositol 3-kinase (PI3-kinase; *B*), and PTP1B (protein tyrosine phosphatase 1B; *C*) in juvenile female hamsters fed ad libitum or food deprived for 48 h in long- (LD) or short day length [8-wk acclimation (SD)] detected by in situ hybridization to antisense ^{35}S-labeled riboprobes or the respective sense controls (*D*). *Left*: autoradiographs of representative coronal brain sections of animals either fed ad libitum or food deprived for 48 h (food dep.) in either photoperiod. *Right*: bar chart of quantified gene expression in the arcuate nucleus from 3–4 sections of each animal (n = 6 animals/group). Values are expressed as %values in LD hamsters fed ad libitum. Means ± SE, *$P < 0.05$, ***$P < 0.001$; ARC, arcuate nucleus; CA 1–3, CA 1–3 region; cc, cerebral cortex; cp, choroid plexus; dg, dentate gyrus; hb, habenular nucleus; pc, piriform cortex; tha, thalamus.

in any of the brain regions examined (Fig. 1*B*), although the latter almost achieved significance with $P = 0.061$.

Effect of photoperiod and food deprivation on PTP1B gene expression. A highly significant reduction of PTP1B mRNA levels in the ARC was observed (Fig. 1*C*) in response to SD acclimation (two-way ANOVA, $F = 52.24$; $P < 0.001$) and to food deprivation (two-way ANOVA, $F = 7.74$; $P < 0.05$). Additionally, there was a significant interaction between photoperiod and feeding status (two-way ANOVA, $F = 7.14$; $P < 0.05$). Multiple group-wise comparisons revealed a sig-

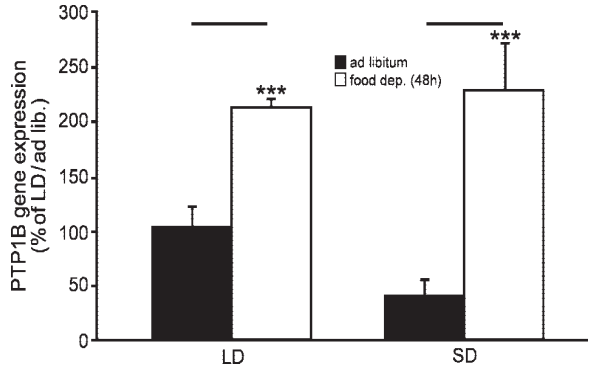

Fig. 2. PTP1B gene expression in the thalamus of juvenile female Siberian hamsters. Hamsters were either fed ad libitum or food deprived for 48 h (n = 6) LD or SD. Values are expressed as %values in LD hamsters fed ad libitum. Means ± SE; ***$P < 0.001$.

nificant reduction of ARC PTP1B gene expression induced by food deprivation in LD but not in SD (Fig. 1*C*). There was also a highly significant increase in PTP1B gene expression in the thalamus in response to food deprivation (two-way ANOVA, $F = 39.73$; $P < 0.0001$) but not in response to photoperiod (Fig. 1*C* and Fig. 2). PTP1B gene expression was unaffected by photoperiod or feeding status in other analyzed structures.

Effect of photoperiod on the phosphorylation of AKT. As a marker for PI3-kinase activity we determined the hypothalamic content of phosphorylated AKT. As shown in Fig. 3*A*, a single conspicuous and specific band of the expected size (60 kDa) for phospho-AKT could be determined in hypothalamic lysates of the Siberian hamster. Exposure of juvenile female hamsters to SD for 8 wk led to a striking reduction of phospho-AKT in the hypothalamus compared with LD hamsters as revealed by quantification of the immunoblot (Fig. 3*B*).

With the use of immunohistochemistry, phospho-AKT positive cells were detected in the ARC. The very specific signal was conspicuously confined to this brain region (Fig. 3*C*) and appeared to be located within the entire cell (Fig. 3*D*). Beyond the ARC, phospho-AKT immunoreactive cells were only present in the nucleus tractus solitarius of the hindbrain (data not shown). The differences revealed by immunoblotting were investigated at a neuroanatomical level by immunohistochemistry. As mentioned above, phospho-AKT immunoreactivity was restricted to the ARC and photoperiod-induced differences were confined to this region (Fig. 3*C*). Thus the changes observed by immunoblotting of total lysates were due to localized changes in the ARC. Consistently, in all four analyzed animals from each photoperiod, phospho-AKT immunoreactivity was substantially lower in SD compared with LD.

DISCUSSION

Over the last 5 years, accumulating evidence has revealed a seasonal alteration in central leptin signaling in *P. sungorus* reflected by increased leptin sensitivity in SD and the establishment of central leptin resistance in LD (3, 19, 37, 43). Leptin exhibits conspicuous similarities in its central effects with insulin, the second hormone besides leptin that meets the criteria for an "adiposity signal". Growing evidence in the literature suggests convergence of central leptin and insulin signaling at the level downstream of their respective receptors

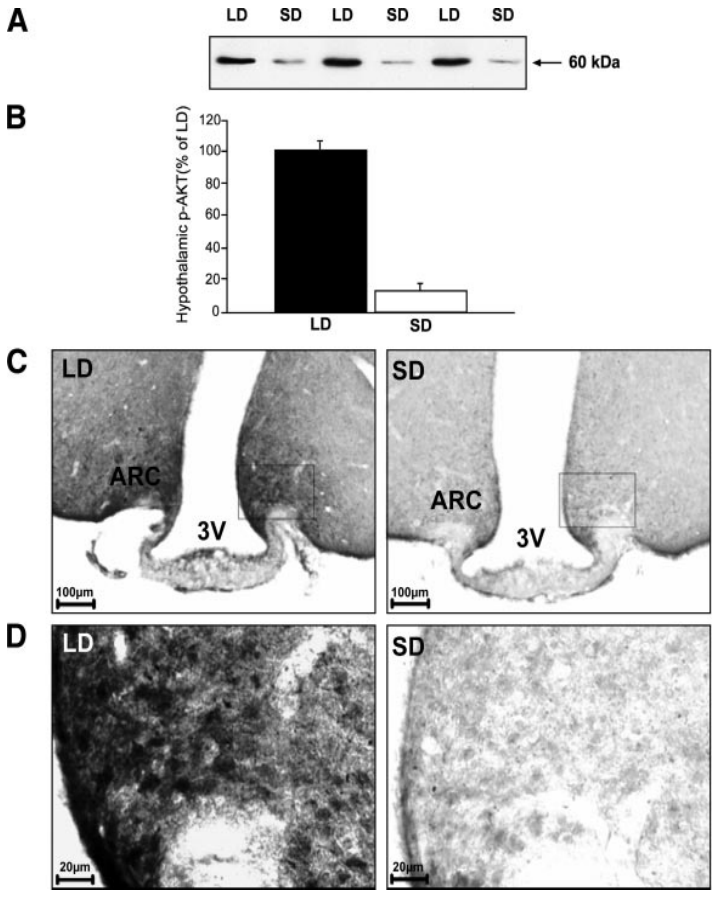

Fig. 3. SD induced downregulation of phospho-AKT in the hypothalamus of juvenile female hamsters acclimated to LD or SD for 8 wk. *A*: a confined specific band for *phospho*-AKT by immunoblotting in the hypothalamus of 3 animals from each photoperiod. *B*: densitometric analysis of the immunoblot shown in *A* (means ± SE). *C*: phospho-AKT in the ARC detected by immunohistochemistry. Shown are photomicrographs of coronal sections of one (from a group of 4 animals in each photoperiod) representative animal in each photoperiod. Boxed areas are region from which high resolution images are shown in *D*. 3V: third ventricle.

(30, 41). The present study was designed to investigate seasonal alterations in central signal transduction of insulin. Here we report downregulation of central IR gene expression in response to SD in the seasonal hamster *P. sungorus*. This was associated with a marked reduction of hypothalamic phospho-AKT either due to reduced phosphorylation of the total AKT pool or a chronic decline of total AKT protein abundance. These changes were accompanied by diminished gene expression of PTP1B, the main inhibitor of insulin signaling.

The neuroanatomical gene expression pattern of IR and PI3-kinase is consistent with those reported in rats and mice, respectively (13, 20). Expression was mainly confined to the ARC, a key neuronal center for the integrated regulation of body weight. This together with the fact that IR gene expression was profoundly downregulated by SD photoperiod in this area indicates that insulin signaling may be involved in the seasonal body weight cycle exhibited by *P. sungorus*.

Seasonally induced alterations in circulating insulin levels were reported in the related species *P. campbelli* (22). In adult male hamsters after a 20-wk acclimation, SD plasma insulin levels fell to about 20% of the level in LD controls (22).

In *P. sungorus*, presumed elevation of insulin levels in LD coincident with increased IR gene expression in the ARC suggests a causal link. Entry of insulin into specific brain areas across the blood-brain barrier is well established (4, 39). Although regional uptake of insulin into the brain does not directly correlate with the localization of the IR [the pons-medulla is the region with the greatest insulin passage K_i:0.764 μl/g min, but it only contains relatively few insulin IRs, (4)], intriguingly, the second largest flux of circulating insulin into the brain is located within the hypothalamus (K_i:0.731 μl/g min), substantiating the importance of regional density of IR molecules in this area. Although it is well documented that brain insulin is probably largely of peripheral origin, the possibility of local insulin synthesis cannot be excluded and remains controversial. It has been reported that the concentrations of insulin in the cerebrospinal fluid and the entry of insulin into the hypothalamus positively correlate with feeding status, which may provide a link between the seasonal alterations in IR gene expression and the marked seasonal body weight cycle that is reflected by alterations in food intake (12, 32, 40). An important association of brain IR and feeding status is also substantiated by the trend to decreased IR gene expression in the ARC in LD hamsters in response to food deprivation (48 h). This effect could not be observed in SD, suggesting that these animals exhibit a basal IR gene expression level.

Considering the potent anorexigenic action of central insulin, SD-induced downregulation of circulating insulin signaling in the brain appears to be paradoxical. Recent studies demonstrated that third cerebral ventricle (ICV) administration of insulin decreases food intake and body weight (35, 41, 44, 45). Furthermore, diminished insulin signaling, as it was achieved by neuronal knockout, or knockdown of the IR (by administration of antisense oligonucleotides against the IR) or neuronal-specific reduction of insulin signaling distal to its receptor (by ICV treatment with PI3-kinase inhibitors), led to hyperphagia and an increase in body weight (7, 29, 31). In Siberian hamsters, however, diminished hypothalamic signal transduction of this hormone (as exemplified by reduction of IR mRNA and phospho-AKT protein) occurs in SD, at times when body weight is low and food intake is comparatively reduced. The finding that both IR gene expression and insulin signaling via phospho-AKT are downregulated in SD hamsters contrasts to studies undertaken in other rodent species subjected to extreme genetical or pharmacological modifications. Clearly, *P. sungorus* reveals adaptive physiological responses, and seasonal cycles in body weight may not exclusively rely on the fundamental catabolic action of insulin described in the other studies mentioned above. Conceivably, reduced insulin signaling in SD may be the result rather than the trigger of an increased catabolic tone mediated by enhanced leptin sensitivity in this photoperiod. Reduced central insulin signaling possibly prevents a catabolic overdrive which would have resulted from additive actions of both hormones. This hypothetical scenario may be critical for the survival of Siberian hamsters in harsh winter conditions, times when food is limited. Nevertheless, our study supports central insulin signaling mediated via PI3-kinase since both IR and phospho-AKT were consistently coregulated in response to photoperiod within the ARC.

Beside the PI3-kinase pathway, other pathways (JAK-STAT and ERK) (8, 9) have been implicated in peripheral insulin signaling. Convergence of both insulin and leptin signal transduction upon the level of these other pathways beyond signaling through PI3-kinase is plausible.

The role of PTP1B as a central player in modulating insulin signal transduction is intriguing, but may be challenged by the fact that gene expression of this inhibitory molecule is reduced in SD when insulin signaling is minimal. Assuming that the reduction of PTP1B mRNA is reflected at the protein level, lowered content of this inhibitor in the ARC would be expected to result in increased insulin signaling. Nevertheless, the hypothalamic phospho-AKT content was substantially reduced in this photoperiod. We did not investigate functional interactions of the insulin signaling components. Although the regulation of the expression levels in response to SD and food deprivation for 48 h of both IR and PTP1B are almost identical, indicating strong interaction, it is possible that changes in brain PTP1B gene expression may not be exclusively associated with insulin signaling. The intriguing finding that PTP1B gene expression is massively induced by food deprivation in the thalamus, a region that in Siberian hamsters does not express either IR or the long form of the leptin receptor (with full signal transduction capacity), indicates that PTP1B may be involved in signaling of other feeding-status regulatory hormones whose identities are presently unknown. Interestingly, Purvis et al. (34) demonstrated that neurotoxic lesions of the midline thalamus (reuniens nucleus) inhibited SD-induced loss of body weight in *P. sungorus*. This implies a possible regulatory role of PTP1B in mediating seasonal changes in body weight within this neuroanatomical structure.

PTP1B has also been associated with intracellular signaling of the second "adiposity signal," leptin. This factor exhibits its inhibitory effects on leptin signaling most likely via deactivation of the Janus kinase 2, an enzyme associated with the leptin receptor (15). Seasonal modulation of leptin signaling by PTP1B may be plausible. Supporting evidence for this hypothesis is contributed by the identical neuroanatomical expression patterns of both PTP1B and leptin receptor mRNA within the ARC of the Siberian hamster (24). Moreover, the mRNA of SOCS3, a possible key modulator in the mediation of the seasonal cycle in leptin sensitivity, reveals a very similar hypothalamic neuroanatomical expression pattern like PTP1B

mRNA and in response to SD ARC, SOCS3, and PTP1B gene expression are diminished to a strikingly similar extent (43). PTP1B and SOCS3 may exhibit potent synergistic actions in terms of inhibition of insulin and leptin signaling. The complementary deactivatory attributes of both molecules are unlikely to be primarily displayed on the level of the PI3-kinase (due to the lack of increased PI3-kinase activity in SD); it is rather plausible that intracellular signaling is modified by additional recruitment of the JAK-STAT or ERK signaling pathways. Diminished inhibition of leptin signaling in SD on the level of the JAK-STAT pathway is also supported by the very recent finding of a substantial increase of phospho-STAT3 positive neurons within the hypothalamus in response to a single intraperitoneal leptin injection (Tups A, unpublished observations). These data substantiate the close association of leptin and insulin signaling within the hypothalamus. The decline of insulin signaling in SD may be primarily the response to the reduced fat mass and the metabolic modifications in SD. The apparent paradoxically reduced anorexigenic drive of insulin implicated by marked diminished insulin signaling may be antagonized by increased activation of the JAK-STAT pathway induced by enhanced leptin sensitivity in SD. This concept is corroborated by a very recent study performed by Sahu and Metlakunta (38) who showed that, in rats under chronic central leptin infusion for 16 days, the JAK-STAT pathway remains sensitive to exogenous leptin administration, whereas, under these circumstances, leptin treatment fails to induce PI3-kinase activity. Furthermore, in a human neuronal cell line, Benomar et al. (6) demonstrated that indeed both insulin and leptin are able to induce the JAK-STAT pathway and coadministration of both hormones further elevated STAT3 phosphorylation. In contrast, PI3-kinase signaling, despite being induced by both hormones individually, is not further enhanced by the presence of both insulin and leptin. Thus convergence of both insulin and leptin signaling within the hypothalamus and partial redundancy of their signal transduction cascades may be a central requirement for the dynamic regulation of energy homeostasis.

In summary, we provide evidence that seasonal body weight regulation is associated with modulations in ARC insulin signal transduction. The direction of change in neuronal insulin signaling, however, contrasts to the central catabolic nature of this pathway described in other species. Reduced insulin signaling in SD may result from enhanced leptin signaling in SD as a consequence of reduced body fat stores. IRs and leptin receptors are both expressed in the ARC of Siberian hamsters but intracellular signaling of both hormones is inverse, making it unlikely that both hormones exhibit synergistic body weight regulatory effects in the hypothalamus. We cannot, however, rule out possible inverse cross talk of both hormones. Beyond PI3-kinase, insulin and leptin share further signal transduction pathways. This cross talk of insulin and leptin within the hypothalamus, distal of their respective receptors, remains an enigma whose resolution will certainly enable us to better understand the complex mechanisms maintaining energy homeostasis and that may be perturbed in obesity.

GRANTS

This collaborative study was funded by the Scottish Executive Environment and Rural Affairs Department (to J. G. Mercer), the German Research Foundation (Grant DFG Kl 973/5 to M. Klingenspor), and the National Genome Research Network (Grant 01GS0483; to M. Klingenspor). A. Tups received a fellowship from the European Commission to attend the ObeS°chool EU Marie Curie Training Site (Grant HPMT-2001–00410) at the Rowett Research Institute and was a fellow of the Boehringer Ingelheim Fonds (Heidesheim, Germany).

REFERENCES

1. **Adam CL, Moar KM, Logie TJ, Ross AW, Barrett P, Morgan PJ, and Mercer JG.** Photoperiod regulates growth, puberty and hypothalamic neuropeptide and receptor gene expression in female Siberian hamsters. *Endocrinology* 141: 4349–4356, 2000.
2. **Asante-Appiah E and Kennedy BP.** Protein tyrosine phosphatases: the quest for negative regulators of insulin action. *Am J Physiol Endocrinol Metab* 284: E663–E670, 2003.
3. **Atcha Z, Cagampang FR, Stirland JA, Morris ID, Brooks AN, Ebling FJ, Klingenspor M, and Loudon AS.** Leptin acts on metabolism in a photoperiod-dependent manner, but has no effect on reproductive function in the seasonally breeding Siberian hamster (*Phodopus sungorus*). *Endocrinology* 141: 4128–4135, 2000.
4. **Banks WA and Kastin AJ.** Differential permeability of the blood-brain barrier to two pancreatic peptides: insulin and amylin. *Peptides* 19: 883–889, 1998.
5. **Bartness TJ, McGriff WR, and Maharaj MP.** Effects of diabetes and insulin on photoperiodic responses in Siberian hamsters. *Physiol Behav* 49: 613–620, 1991.
6. **Benomar Y, Roy AF, Aubourg A, Djiane J, and Taouis M.** Cross down-regulation of leptin and insulin receptor expression and signaling in a human neuronal cell line. *Biochem J* 388: 929–939, 2005.
7. **Bruning JC, Gautam D, Burks DJ, Gillette J, Schubert M, Orban PC, Klein R, Krone W, Muller-Wieland D, and Kahn CR.** Role of brain insulin receptor in control of body weight and reproduction. *Science* 289: 2122–2125, 2000.
8. **Carvalheira JB, Ribeiro EB, Folli F, Velloso LA, and Saad MJ.** Interaction between leptin and insulin signaling pathways differentially affects JAK-STAT and PI3-kinase-mediated signaling in rat liver. *Biol Chem* 384: 151–159, 2003.
9. **Carvalheira JB, Torsoni MA, Ueno M, Amaral ME, Araujo EP, Velloso LA, Gontijo JA, and Saad MJ.** Cross talk between the insulin and leptin signaling systems in rat hypothalamus. *Obes Res* 13: 48–57, 2005.
10. **Elchebly M, Payette P, Michaliszyn E, Cromlish W, Collins S, Loy AL, Normandin D, Cheng A, Himms-Hagen J, Chan CC, Ramachandran C, Gresser MJ, Tremblay ML, and Kennedy BP.** Increased insulin sensitivity and obesity resistance in mice lacking the protein tyrosine phosphatase-1B gene. *Science* 283: 1544–1548, 1999.
11. **Gerozissis K.** Brain insulin and feeding: a bi-directional communication. *Eur J Pharmacol* 490: 59–70, 2004.
12. **Gerozissis K, Rouch C, Nicolaidis S, and Orosco M.** Brain insulin response to feeding in the rat is both macronutrient and area specific. *Physiol Behav* 65: 271–275, 1998.
13. **Horsch D and Kahn CR.** Region-specific mRNA expression of phosphatidylinositol 3-kinase regulatory isoforms in the central nervous system of C57BL/6J mice. *J Comp Neurol* 415: 105–120, 1999.
14. **Kanai F, Ito K, Todaka M, Hayashi H, Kamohara S, Ishii K, Okada T, Hazeki O, Ui M, and Ebina Y.** Insulin-stimulated GLUT4 translocation is relevant to the phosphorylation of IRS-1 and the activity of PI3-kinase. *Biochem Biophys Res Commun* 195: 762–768, 1993.
15. **Kaszubska W, Falls HD, Schaefer VG, Haasch D, Frost L, Hessler P, Kroeger PE, White DW, Jirousek MR, and Trevillyan JM.** Protein tyrosine phosphatase 1B negatively regulates leptin signaling in a hypothalamic cell line. *Mol Cell Endocrinol* 195: 109–118, 2002.
16. **Keller SR and Lienhard GE.** Insulin signalling: the role of insulin receptor substrate 1. *Trends Cell Biol* 4: 115–119, 1994.
17. **Klaman LD, Boss O, Peroni OD, Kim JK, Martino JL, Zabolotny JM, Moghal N, Lubkin M, Kim YB, Sharpe AH, Stricker-Krongrad A, Shulman GI, Neel BG, and Kahn BB.** Increased energy expenditure, decreased adiposity, and tissue-specific insulin sensitivity in protein-tyrosine phosphatase 1B-deficient mice. *Mol Cell Biol* 20: 5479–5489, 2000.
18. **Klingenspor M, Ebbinghaus C, Hulshorst G, Stohr S, Spiegelhalter F, Haas K, and Heldmaier G.** Multiple regulatory steps are involved in the control of lipoprotein lipase activity in brown adipose tissue. *J Lipid Res* 37: 1685–1695, 1996.

19. **Klingenspor M, Niggemann H, and Heldmaier G.** Modulation of leptin sensitivity by short photoperiod acclimation in the Djungarian hamster, Phodopus sungorus. *J Comp Physiol* 170: 37–43, 2000.
20. **Marks JL, Porte D Jr, Stahl WL, and Baskin DG.** Localization of insulin receptor mRNA in rat brain by in situ hybridization. *Endocrinology* 127: 3234–3236, 1990.
21. **Mercer JG, Ellis C, Moar KM, Logie TJ, Morgan PJ, and Adam CL.** Early regulation of hypothalamic arcuate nucleus CART gene expression by short photoperiod in the Siberian hamster. *Regul Pept* 111: 129–136, 2003.
22. **Mercer JG, Lawrence CB, Beck B, Burlet A, Atkinson T, and Barrett P.** Hypothalamic NPY and prepro-NPY mRNA in Djungarian hamsters: effects of food deprivation and photoperiod. *Am J Physiol Regul Integr Comp Physiol* 269: R1099–R1106, 1995.
23. **Mercer JG, Moar KM, Logie TJ, Findlay PA, Adam CL, and Morgan PJ.** Seasonally inappropriate body weight induced by food restriction: effect on hypothalamic gene expression in male Siberian hamsters. *Endocrinology* 142: 4173–4181, 2001.
24. **Mercer JG, Moar KM, Ross AW, Hoggard N, and Morgan PJ.** Photoperiod regulates arcuate nucleus POMC, AGRP, and leptin receptor mRNA in Siberian hamster hypothalamus. *Am J Physiol Regul Integr Comp Physiol* 278: R271–R281, 2000.
25. **Mercer JG and Tups A.** Neuropeptides and anticipatory changes in behaviour and physiology: seasonal body weight regulation in the Siberian hamster. *Eur J Pharmacol* 480: 43–50, 2003.
26. **Myers MG Jr.** Leptin receptor signalling and the regulation of mammalian physiology. *Recent Prog Horm Res* 59: 287–304, 2004.
27. **Myers MG Jr, Sun XJ, and White MF.** The IRS-1 signalling system. *Trends Biochem Sci* 19: 289–293, 1994.
28. **Niswender KD, Morrison CD, Clegg DJ, Olson R, Baskin DG, Myers MG Jr, Seeley RJ, and Schwartz MW.** Insulin activation of phosphatidylinositol 3-kinase in the hypothalamic arcuate nucleus: a key mediator of insulin-induced anorexia. *Diabetes* 52: 227–231, 2003.
29. **Niswender KD, Morrison CD, Clegg DJ, Olson R, Baskin DG, Myers MG Jr, Seeley RJ, and Schwartz MW.** Insulin activation of phosphatidylinositol 3-kinase in the hypothalamic arcuate nucleus: a key mediator of insulin-induced anorexia. *Diabetes* 52: 227–231, 2003.
30. **Niswender KD and Schwartz MW.** Insulin and leptin revisited: adiposity signals with overlapping physiological and intracellular signalling capabilities. *Front Neuroendocrinol* 24: 1–10, 2003.
31. **Obici S, Zhang BB, Karkanias G, and Rossetti L.** Hypothalamic insulin signalling is required for inhibition of glucose production. *Nat Med* 8: 1376–1382, 2002.
32. **Orosco M, Gerozissis K, Rouch C, and Nicolaidis S.** Feeding-related immunoreactive insulin changes in the PVN-VMH revealed by microdialysis. *Brain Res* 671: 149–158, 1995.
33. **Paxinos G and Franklin K.** *The Mouse Brain in Stereotaxic Coordinates*. San Diego: Academic, 2002.
34. **Purvis CC and Duncan MJ.** Discrete thalamic lesions attenuate winter adaptations and increase body weight. *Am J Physiol Regul Integr Comp Physiol* 273: R226–R235, 1997.
35. **Richardson RD, Ramsay DS, Lernmark A, Scheurink AJ, Baskin DG, and Woods SC.** Weight loss in rats following intraventricular transplants of pancreatic islets. *Am J Physiol Regul Integr Comp Physiol* 266: R59–R64, 1994.
36. **Rondinone CM, Trevillyan JM, Clampit J, Gum RJ, Berg C, Kroeger P, Frost L, Zinker BA, Reilly R, Ulrich R, Butler M, Monia BP, Jirousek MR, and Waring JF.** Protein tyrosine phosphatase 1B reduction regulates adiposity and expression of genes involved in lipogenesis. *Diabetes* 51: 2405–2411, 2002.
37. **Rousseau K, Atcha Z, Cagampang FR, Le Rouzic P, Stirland JA, Ivanov TR, Ebling FJ, Klingenspor M, and Loudon AS.** Photoperiodic regulation of leptin resistance in the seasonally breeding Siberian hamster (*Phodopus sungorus*). *Endocrinology* 143: 3083–3095, 2002.
38. **Sahu A and Metlakunta AS.** Hypothalamic phosphatidylinositol 3-kinase-phosphodiesterase 3B-cyclic AMP pathway of leptin signalling is impaired following chronic central leptin infusion. *J Neuroendocrinol* 17: 720–726, 2005.
39. **Schulingkamp RJ, Pagano TC, Hung D, and Raffa RB.** Insulin receptors and insulin action in the brain: review and clinical implications. *Neurosci Biobehav Rev* 24: 855–872, 2000.
40. **Schwartz MW, Figlewicz DP, Baskin DG, Woods SC, and Porte D Jr.** Insulin in the brain: a hormonal regulator of energy balance. *Endocr Rev* 13: 387–414, 1992.
41. **Schwartz MW and Porte D Jr.** Diabetes, obesity, and the brain. *Science* 307: 375–379, 2005.
42. **Steinlechner St HGBH.** The seasonal cycle of body weight in the djungarian hamster: photoperiodic control and the influence of starvation and melatonin. *Oecologia* 60: 401–405, 1983.
43. **Tups A, Ellis C, Moar KM, Logie TJ, Adam CL, Mercer JG, and Klingenspor M.** Photoperiodic regulation of leptin sensitivity in the Siberian hamster, Phodopus sungorus, is reflected in arcuate nucleus SOCS-3 (suppressor of cytokine signalling) gene expression. *Endocrinology* 145: 1185–1193, 2004.
44. **Woods SC, Lotter EC, McKay LD, and Porte D Jr.** Chronic intracerebroventricular infusion of insulin reduces food intake and body weight of baboons. *Nature* 282: 503–505, 1979.
45. **Woods SC, Seeley RJ, Porte D Jr, and Schwartz MW.** Signals that regulate food intake and energy homeostasis. *Science* 280: 1378–1383, 1998.
46. **Zinker BA, Rondinone CM, Trevillyan JM, Gum RJ, Clampit JE, Waring JF, Xie N, Wilcox D, Jacobson P, Frost L, Kroeger PE, Reilly RM, Koterski S, Opgenorth TJ, Ulrich RG, Crosby S, Butler M, Murray SF, McKay RA, Bhanot S, Monia BP, and Jirousek MR.** PTP1B antisense oligonucleotide lowers PTP1B protein, normalizes blood glucose, and improves insulin sensitivity in diabetic mice. *Proc Natl Acad Sci USA* 99: 11357–11362, 2002.

Journal of Neuroendocrinology, 2004, Vol. 16, 922–928 doi:10.1111/j.1365-2826.2004.01251.x

Circulating Ghrelin Levels and Central Ghrelin Receptor Expression are Elevated in Response to Food Deprivation in a Seasonal Mammal *(Phodopus sungorus)*

A. Tups,*† M. Helwig,† R. M. H. Khorooshi,† Z. A. Archer,* M. Klingensport† and J. G. Mercer*
*Division of Energy Balance and Obesity, Rowett Research Institute, Aberdeen Centre for Energy Regulation and Obesity (ACERO), Aberdeen, UK.
†Department of Animal Physiology, Philipps University Marburg, Marburg, Germany.

Key words: energy balance, photoperiod, seasonal body weight regulation, leptin.

Abstract

Ghrelin is an endogenous ligand for the growth hormone secretagogue receptor (GHSR). However, the functional interaction of ligand and receptor is not very well understood. We demonstrate that GHSR mRNA is up-regulated after food deprivation (48 h) in the hypothalamic arcuate nucleus and ventromedial nucleus of the seasonal Siberian hamster, *Phodopus sungorus*. This increase is accompanied by a two-fold elevation of circulating ghrelin concentration. Chronic changes in feeding state imposed by food restriction over a period of 12 weeks during long day-length induced increased GHSR gene expression, whereas food restriction for 6 weeks had no effect. *Phodopus sungorus* reveals remarkable seasonal changes in body weight, fat mass and circulating leptin levels. Ghrelin is generally regarded as having opposing effects on appetite and body weight with respect to those exhibited by leptin. However, our study revealed that seasonal adaptations were not accompanied by changes in either GHSR gene expression or circulating ghrelin concentration. Therefore, we suggest that ghrelin only plays a minor role in modulating long-term seasonal body weight cycles. Our findings imply that ghrelin predominantly acts as a short-term regulator of feeding.

Ghrelin, a 28-amino-acid gut peptide, has been identified as an endogenous ligand of the growth hormone secretagogue receptor (GHSR) and shown to stimulate growth hormone (GH) secretion (1, 2). However, accumulating evidence suggests that its major physiological role may be related to the regulation of energy homeostasis (3–5). Ghrelin is produced by the stomach and circulating plasma ghrelin concentrations are dynamically related to feeding state (6, 7). Thus, in man, it has been demonstrated that circulating ghrelin levels are decreased in chronic (obesity) and acute (feeding) states of positive energy balance. By contrast, plasma ghrelin levels are increased by fasting and in patients with anorexia nervosa (7–10). Furthermore, peripheral and central (intracerebroventricular) ghrelin administration in mice and rats caused weight gain by either reducing fat utilization or by a dose-dependent increase in food intake (5). Ghrelin modifies energy homeostasis independent of its GH-releasing activity, as demonstrated by studies performed in GH-deficient rats (4). Ghrelin undergoes post-translational processing where the hydroxyl group of one of its serine residues is acylated by *n*-octanoic acid (1, 11). Acylation of this peptide is regarded to be essential for its endocrine actions because it facilitates transport across the blood–brain barrier and is essential for binding to GHSR (12–14).

GHSR was originally cloned in 1996 from the pituitary of several species, including humans and the rat (15, 16). The name GHSR derived from a class of synthetic molecules, the growth hormone secretagogues (GHSs) which represent the first identified ligands of this receptor. GHSR is a G-protein-coupled receptor (15) and is encoded by a single gene across different species (17). In the rat, central GHSR mRNA expression is confined to the hypothalamus and the pituitary gland (18).

Recently, a link between feeding status and GHSR mRNA expression was demonstrated. Total hypothalamic mRNA of GHSR was increased after food deprivation (48 h) in the rat (19). However, whether the anatomical localization of mRNA changes according to feeding status within the hypothalamus is unknown. It may be important to establish whether feeding-induced mRNA changes occur in distinct hypothalamic nuclei that are important centres in the modulation of body weight.

Correspondence to: Alexander Tups, Biology Faculty, Department of Animal Physiology, Philipps University Marburg, Karl von Frisch Str. 8, D-35043 Marburg, Germany (e-mail: alextups@gmx.de).

In the present study, we localized GHSR mRNA within the hypothalamus via *in situ* hybridization and investigated changes in the expression profile of GHSR mRNA within distinct hypothalamic nuclei. Moreover, we determined serum levels of total circulating ghrelin. We performed our studies in the seasonal Siberian hamster (*Phodopus sungorus*, also known as Djungarian hamster), which represents a unique model for the investigation of energy homeostasis. *Phodopus sungorus* reveals a remarkable natural body weight cycle determined by the prevailing photoperiod and reflected in changes of circulating leptin levels (20–22). Short day exposure (SD), either as a gradual change (natural conditions) or as an abrupt change (laboratory conditions), leads to a progressive reduction in body weight. This animal model allowed us to investigate the functional role of circulating ghrelin and its centrally expressed receptor in relation to chronically changed body weight induced by photoperiod. Effects of food deprivation on the interplay of this feeding related gut hormone and its receptor were analysed and, beyond that, the impact of food restriction and of the anorexigenic cytokine leptin on GHSR gene expression was studied, both in animals with a naturally high body weight and in animals that are reaching their body weight nadir induced by SD exposure.

Materials and methods

Animals

Procedures involving animals were licensed under the Animals (Scientific Procedures) Act of 1986 and received approval from the Ethical Review Committee at the Rowett Research Institute. All experimental animals were drawn from the Rowett breeding colony of Siberian hamsters (23–25), and were gestated and suckled in long day (LD) 16 : 8 h light/dark cycle. All hamsters were weaned at 3 weeks of age, and were individually housed either at weaning or, in the case of adult animals, at least 2 weeks before food deprivation. Where specified, hamsters were maintained from weaning in a short day (SD) 8 : 16 h light/dark cycle, but with all other environmental conditions unaltered. Food (Labsure pelleted diet; Special Diet Services, Witham, Essex, UK) and water were available *ad libitum* unless specified, and rooms were maintained at 22 °C. All animals were killed by cervical dislocation in the middle of the light phase, trunk blood was collected and brains were rapidly removed and frozen on dry ice.

Experimental procedure

To investigate acute changes in GHSR mRNA expression induced by food deprivation (48 h), archived brain sections were used from juvenile female LD hamsters weaned in LD and then held in LD (n = 12) or SD (n = 12) photoperiods. Eight weeks after weaning, half of the animals (n = 6) in each photoperiod were deprived of food while the remainder continued to feed *ad libitum* (26).

Chronic changes in GHSR gene expression following food restriction for 6 and 12 weeks, respectively, were examined by analysing archived brain sections of three groups of juvenile female hamsters. One group was maintained in LD (LD-ADLIB), the second was transferred to SD (SD-ADLIB) and the third group was also maintained in LD (LD-REST) but was food restricted so that the body weight trajectory was matched with that of the SD group (26).

In another experiment, the effect of leptin on GHSR gene expression was investigated. Archived brain sections (26) of juvenile female hamsters which had received a single intraperitoneal leptin injection 15, 30, 60 or 120 min before cervical dislocation were analysed. Control groups were injected with vehicle (26).

Serum ghrelin concentration was investigated in a second food deprivation experiment, which was carried out exactly as above with a new group of hamsters (n = 24). This repeated study was performed due to insufficient blood sampled from the first set of animals. To substantiate the results obtained from juvenile female hamsters, we also determined serum ghrelin concentration in adult male hamsters. Twenty adult male LD hamsters, aged 5–6 months, were divided into two groups, one of which was deprived of food for 48 h whereas the other group continued to feed *ad libitum*.

Radioimmunoassay

Serum concentrations of total immunoreactive ghrelin were measured using the commercially available radioimmunoassay kit from Phoenix Pharmaceuticals, Inc. (catalogue no. RK 031-31, Belmont, CA, USA).

Hypothalamic gene expression

Messenger RNA levels were quantified by *in situ* hybridization in 20-μm coronal hypothalamic sections, using techniques previously described in detail (24). A riboprobe complementary to GHSR (type 1a and b) was generated from cloned cDNA from the hypothalamus of rat. cDNA synthesis was performed by reverse transcription (cDNA synthesis Kit, Invitrogen, Carlsbad, CA, USA), according to the manufacturer's instructions. The 449-bp (Genebank NM032075) fragment of rat GHSR was amplified by polymerase chain reaction (PCR) with 35 cycles of 94 °C for 30 s, 60 °C for 30 s and 68 °C for 1 min and finally one cycle at 72 °C for 10 min. For the amplification, the primers 5′-GCGCTCTTCGTGGTGGGCATCT-3′ and 5′-GTGGCGCGGCATTCGTTGGT-3′ were used. The DNA fragments were ligated into PCR-script Amp cloning vector (Stratagene, Basingstoke, UK) and transformed into JM 109 cells (Promega, Southampton, UK). Automated sequencing was performed to verify the sequence of interest.

As previously described (24), 20-μm forebrain sections were collected throughout the extent of the arcuate nucleus and the caudal part of the ventromedial nucleus (VMH), to which GHSR gene expression is confined, onto a set of eight slides with six or seven sections mounted on each slide. Accordingly, slides spanned the hypothalamic region approximating from −2.7 mm to −1.25 mm relative to Bregma according to the atlas of the mouse brain (27). One slide from each animal was hybridized. Briefly, slides were fixed, acetylated, and hybridized overnight at 58 °C using [^{35}S]-labelled cRNA probes (1–2 × 10^7 c.p.m./ml). Slides were treated with RNase A, desalted, with a final high stringency wash (30 min) in 0.1 × SSC at 60 °C, dried and apposed to Kodak Biomax MR Film (Kodak, Rochester, NY, USA). Autoradiographic images were quantified using the Image-Pro Plus system. Equivalent sections of individual animals were matched according to the atlas of the mouse brain. Four sections from the arcuate nucleus and 3 sections from VMH of each animal spanning from −2.54 mm to 0.94 mm relative to Bregma were analysed. Integrated optical densities were calculated using a standard curve generated from ^{14}C autoradiographic microscales (Amersham Pharmacia Biotech, UK Ltd, Bucks, UK).

Statistical analysis

Data were analysed by one- or two-way analysis of variance (ANOVA) followed by the Student–Newman–Keuls multiple comparison test, as appropriate, using SigmaStat statistical software (Jandel Corp., Erkrath, Germany). Where data failed normality tests, they were analysed by one-way ANOVA on ranks followed by Dunn's multiple comparison test. Data are presented as mean ± SEM. $P < 0.05$ was considered to be statistically significant.

Results

Localization of GHSR mRNA and protein in the hamster hypothalamus

The riboprobe complementary to rat GHSR mRNA hybridized within the hypothalamus of the Siberian hamster to the arcuate nucleus and the VMH (Fig. 1), as well as to the paraventricular (PVN) and suprachiasmatic nucleus (SCN) (data not shown). Differential gene expression was not observed in the PVN or SCN in any of the experiments reported below. A sense probe synthesized from the cloned

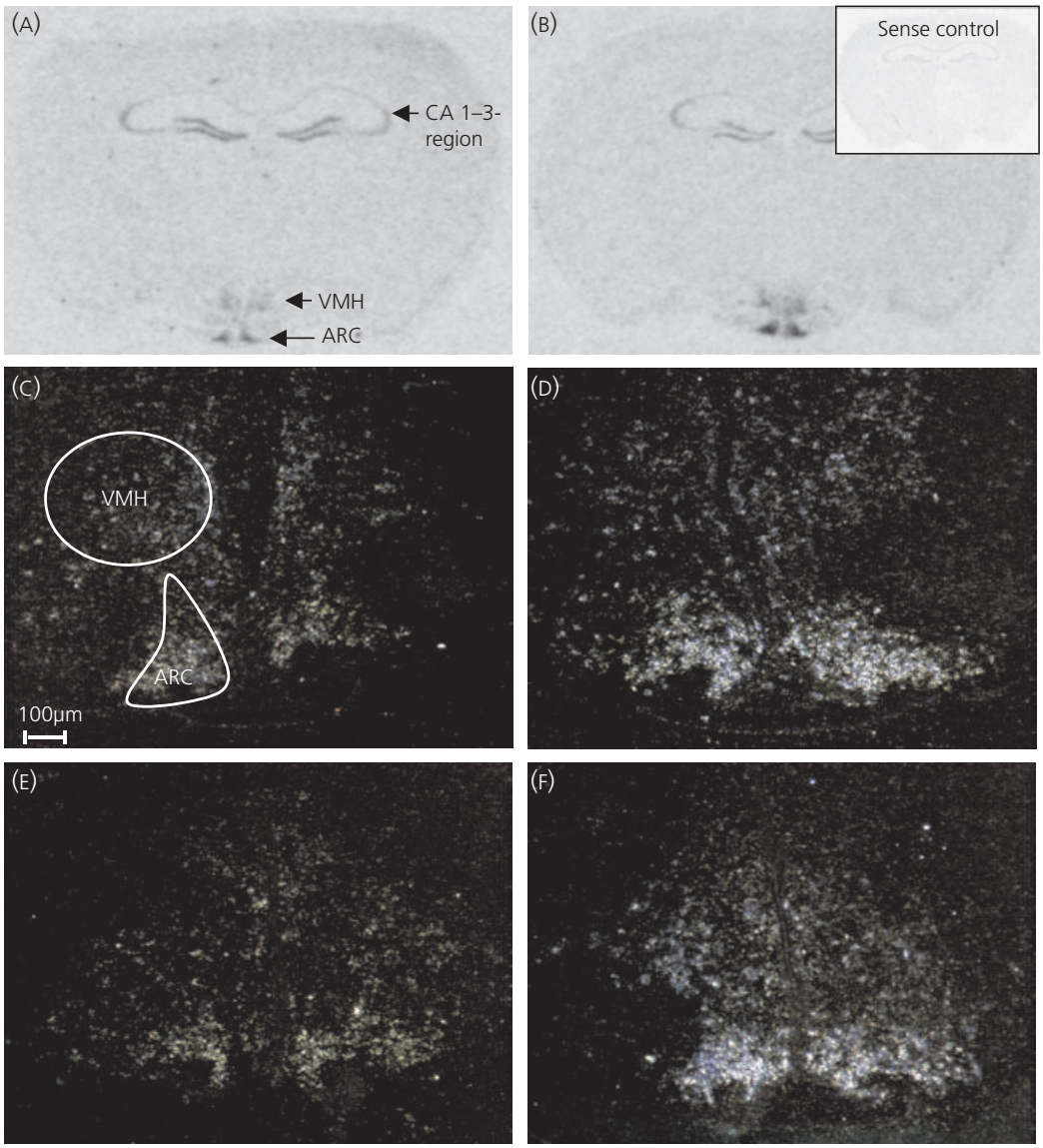

FIG. 1. Autoradiographs of LD female Siberian hamster brain sections (20 µm coronal sections; 8 weeks post weaning) either *ad libitum* fed (A) or 48-h food deprived (B) following *in situ* hybridization to an antisense ^{35}S-labelled riboprobe to growth hormone secretagogue receptor mRNA (inset depicting sense control). Also shown are representative sections of animals from each photoperiod. (C) to (F) Dark field photomicrographs showing high resolution images of the respective hypothalamic regions in LD (C,D) and SD (E,F) depicting induction of GHSR gene expression after food deprivation (C,E: *ad libitum*; D,F: food deprived). ARC, Arcuate nucleus; CA 1–3, CA 1–3 region; VMH, ventromedial hypothalamus.

rat cDNA generated a low intensity nonspecific signal (data not shown).

Effect of food deprivation(48 h) on GHSR gene expression in LD and SD hamsters

As described previously (26), SD hamsters gained 10.9 ± 1.0 g body weight, while hamsters in LD gained 16.8 ± 0.8 g during the 8 weeks following weaning. Food deprivation for 48 h led to a loss in body weight of 13.4 ± 2.3% in LD hamsters and 17.9 ± 2.3% in SD hamsters.

We found no difference in hypothalamic arcuate nucleus and VMH GHSR mRNA expression between LD and SD *ad libitum* fed hamsters, although there was a trend to increased gene expression in the arcuate nucleus and VMH in SD, which came close to, but did not achieve, statistical significance. However, food deprivation for 48 h led to a marked increase in GHSR gene expression in the arcuate nucleus (two-way ANOVA; $F = 18.17$; $P < 0.001$; Figs 1 and 2A) and VMH (two-way ANOVA; $F = 4.99$; $P < 0.05$; Figs 1 and 2B) irrespective of photoperiod.

Effect of chronic food restriction on GHSR gene expression in LD and SD hamsters

This experiment investigated changes in GHSR gene expression related to chronic manipulation of feeding state. As described previously (26), the body weight trajectory of LD-REST hamsters was matched to the body weight traject-

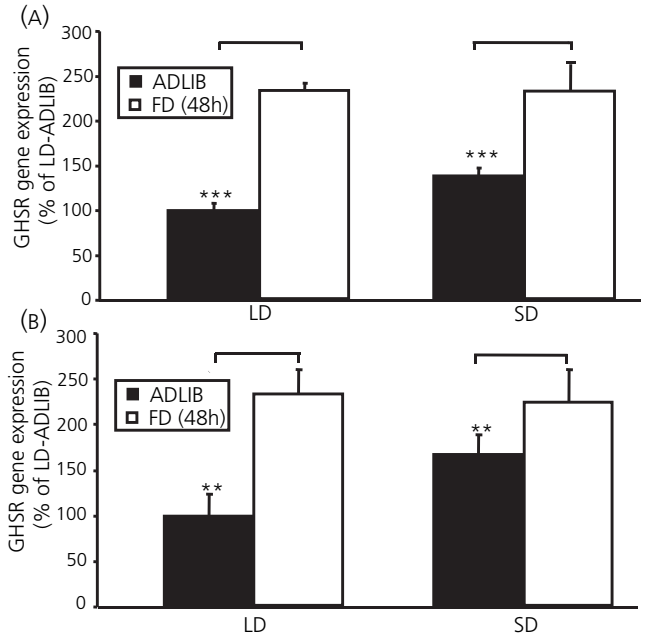

FIG. 2. Growth hormone secretagogue receptor (GHSR) gene expression in the hypothalamic arcuate nucleus (A) and in the ventromedial hypothalamus (B) of juvenile female Siberian hamsters. Hamsters were either *ad libitum* fed (ADLIB) or food deprived for 48 h (FD) (n = 6) in long (LD) or short day-length (SD). Values are expressed as percentages of values in LD hamsters fed *ad libitum*. Data are mean ± SEM. **P < 0.01, ***P < 0.001.

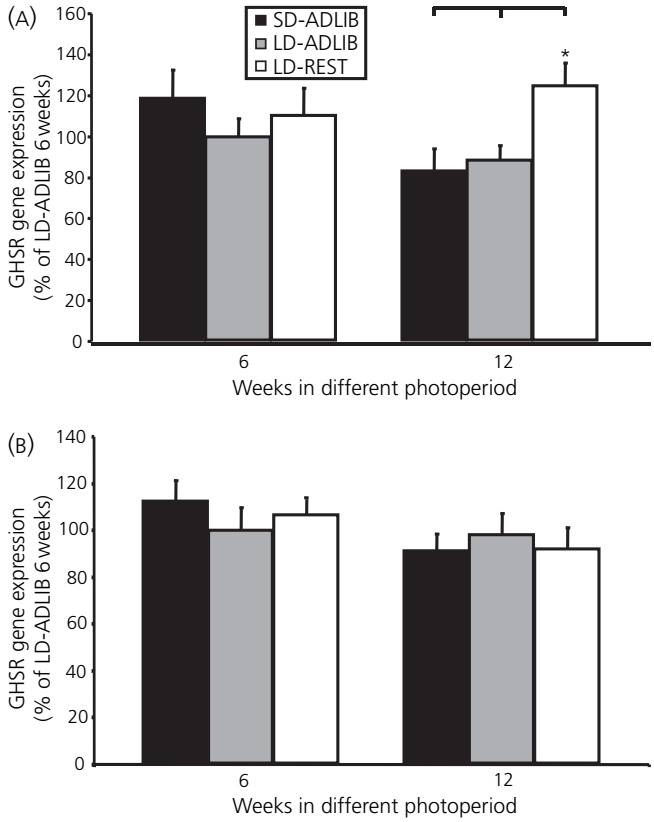

FIG. 3. Growth hormone secretagogue receptor (GHSR) gene expression in the hypothalamic arcuate nucleus (A) and in the ventromedial hypothalamus (B) of juvenile female Siberian hamsters (n = 9–12 in each group), fed *ad libitum* in long (LD-ADLIB) or short day-length (SD-ADLIB) for either 6 or 12 weeks, or held in long day-length with restricted food from day 0 post weaning onwards to mimic short-day-length body weight trajectory (LD-REST). Values are expressed as percentages of values in LD hamsters fed *ad libitum* (6 weeks). Data are mean ± SEM, *P < 0.05

ory of SD hamsters, whereas LD hamsters which continued to feed *ad libitum* gained significantly more weight than the remaining two groups (approximately 30% after 12 weeks).

Neither SD acclimation nor food restriction for 6 weeks had significant effects on arcuate nucleus (Fig. 3A) GHSR gene expression. By contrast, after 12 weeks, the LD-REST group showed significantly elevated arcuate nucleus GHSR gene expression compared to the LD-ADLIB and SD-ADLIB animals (one-way ANOVA on ranks; H = 5.39; P < 0.01). GHSR gene expression in the VMH (Fig. 3B) after either food restriction period was not different from the respective *ad libitum* fed groups.

Effect of leptin injection on GHSR gene expression

There was no effect of leptin injection on GHSR gene expression in the arcuate nucleus in either LD or SD hamsters over the 15–120 min time course postinjection compared to the vehicle-injected controls. Furthermore, GHSR gene expression of LD and SD vehicle injected hamsters was not different (Fig. 4).

Serum ghrelin concentration

In this repetition of the first experiment, over the 8-week postweaning period, SD hamsters gained 10.7 ± 1.0 g, while hamsters in LD gained 15.4 ± 1.1 g. Following food deprivation, LD hamsters lost 18.4 ± 2.4%, and SD hamsters 20.4 ± 3.2%, of their initial body weight before food deprivation. These values are similar to those observed previously (26).

Serum ghrelin levels recorded in the Siberian hamster are within the range measured in different mammalian species (28–30). No significant effect of photoperiod on serum ghrelin concentration was observed, although there was a trend for higher levels in SD. In food-deprived juvenile female hamsters, serum ghrelin concentration was significantly elevated in comparison to *ad libitum* fed hamsters (Fig. 5). This increase was observed in both LD and SD hamsters with a slightly greater elevation in SD (Fig. 5). The overall effect of feeding status was highly significant (two-way ANOVA; F = 9.20; P < 0.001). A similar increase in serum ghrelin concentration was also apparent in adult male LD hamsters after 48 h of food deprivation (LD-ADLIB: 795.2 ± 83.5 pg/ml, LD-FD: 1510.6 ± 189.0 pg/ml; n = 10 in each group, *t*-test; −3.31; P < 0.001).

Discussion

In this report, we demonstrate, for the first time, a marked elevation of GHSR gene expression in the arcuate nucleus and VMH in response to food deprivation for 48 h. By contrast chronic food restriction imposed to match SD body weight trajectory in LD hamsters (LD-REST) for 6 weeks

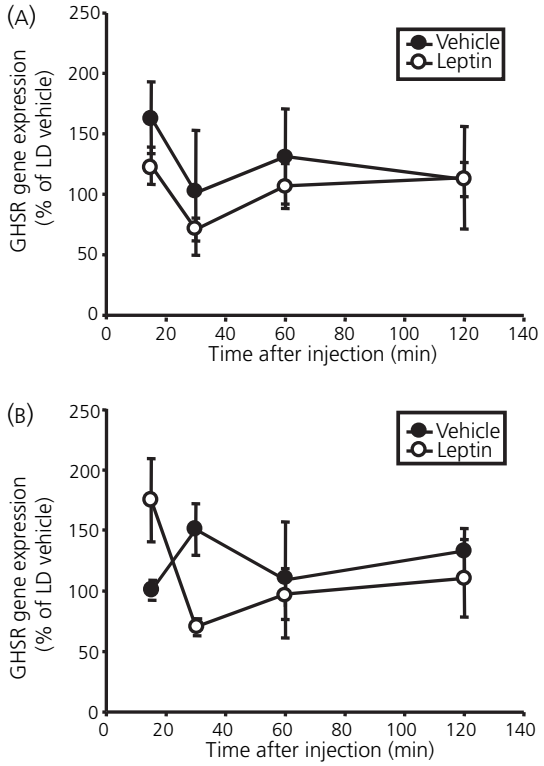

FIG. 4. Time-dependent effect of leptin injection on Growth hormone secretagogue receptor (GHSR) gene expression in the hypothalamic arcuate nucleus of juvenile female hamsters held in short (A) or long (B) day-length for 8 weeks (n = 3). Leptin was injected intraperitoneally at different time-points (15, 30, 60 and 120 min) before preparation of the brains; values are expressed as percentages of values in LD 15 min vehicle. Data are mean ± SEM.

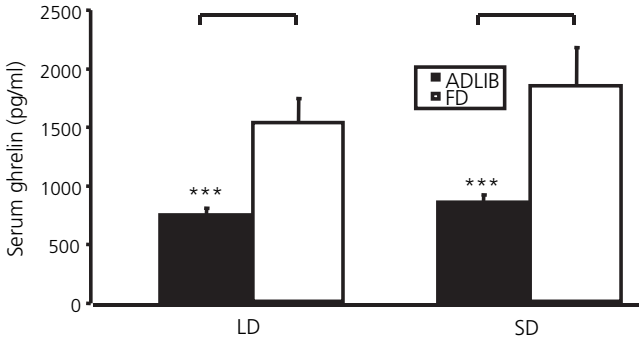

FIG. 5. Serum ghrelin levels in juvenile female Siberian hamsters 8 weeks post weaning. Hamsters were either *ad libitum* fed (ADLIB) or food deprived for 48 h (FD) (n = 4–6) in long (LD) or short day-length (SD). Data are mean ± SEM. ***P < 0.001.

had no effect and after 12 weeks led to only a slight increase in GHSR gene expression. Remarkably, the distinct photoperiod induced changes in body weight of *P. sungorus* did not affect GHSR gene expression within the examined hypothalamic regions. The arcuate nucleus and the VMH are both regarded to be key centres for the central integration of peripheral signals that convey energy homeostasis (31). Across different mammalian species, including the seasonal hamster *P. sungorus*, it is well established that body weight regulatory hormones such as leptin are processed in these hypothalamic nuclei to transduce their bioenergetic information into a central response. Recently, GHSR was demonstrated to be the primary ghrelin receptor that is able to modulate appetite in mice (32). We demonstrate that an increase of GHSR gene expression following food deprivation (48 h) is associated with a two-fold elevation of serum ghrelin levels. In addition to the fact that hypothalamic differential GHSR gene expression is confined to the arcuate nucleus and VMH, this implies that the orexigenic function of ghrelin would appear to depend on signal processing in these hypothalamic nuclei.

Ad libitum fed LD acclimated hamsters adjust their body weight corresponding to a postulated 'set-point' encoded by unknown neuronal mechanisms. In the present study, LD-REST hamsters were manipulated to a much lower body weight than imposed by this 'set point'. By contrast, SD hamsters defend a body weight that is appropriate to the lowered 'set-point' induced by SD acclimation. In terms of appetite, SD-ADLIB and LD-REST hamsters, despite having the same body weight, are in different satiety states due to their photoperiodic history. Therefore, LD-REST hamsters are expected to exhibit a permanently increased appetite, reflecting the drive to regain their individual body weight to the desired LD 'set point'. Indeed after 12 weeks of food restriction, GHSR gene expression in the arcuate nucleus of LD-REST hamsters was significantly elevated by approximately 50% compared to LD-ADLIB hamsters, but food restriction for 6 weeks had no effect. This discrepancy may be explained by the respective body weight differentials established between LD-ADLIB and LD-REST hamsters in these studies. In juvenile female hamsters, 6 weeks of food restriction led to a body weight differential of 6.3 g between LD-ADLIB (27.7 ± 2.6 g) and LD-REST (21.4 ± 1.4 g), whereas 12 weeks of food restriction caused a body weight differential of 8.6 g between LD-ADLIB (30.6 ± 2.6 g) and LD-REST (22.0 ± 1.0 g) (26). The larger body weight differential established after 12 weeks of food restriction may be indicative for stronger appetite in these hamsters. Interestingly, imposed food restriction in LD-REST hamsters led to a more dramatic decrease of circulating leptin levels after 12 weeks compared to 6 weeks [6 weeks: LD-ADLIB: 26.3 ± 0.8, LD-REST: 15.4 ± 3.2 ng/ml, SD-ADLIB: 10.8 ± 1.5; 12 weeks: LD-ADLIB: 26.7 ± 8.1; LD-REST: 3.8 ± 0.6 and SD-ADLIB: 9.1 ± 2.4 ng/ml (26)]. Only after 12 weeks were serum leptin levels in LD-REST hamsters clearly decreased even below the level measured in SD-ADLIB hamsters. Thus, leptin may exert an inhibitory effect on GHSR gene expression that is released only in catabolic states associated with extremely low serum leptin levels. The inhibitory potential of leptin on ghrelin sensitivity may be fully exploited in *ad libitum* fed hamsters. This may be one reason why leptin injections had no effect on GHSR gene expression in *ad libitum* fed hamsters with normal leptin levels. Hewson *et al.* (33) demonstrated that leptin alters ghrelin sensitivity only in food deprived rats, in which ghrelin and ghrelin mimetics were able to increase the number of cells expressing Fos protein in the arcuate nucleus. Our observed increase in GHSR gene expression and the accompanied elevation in circulating ghrelin concentration,

after 48 h of food deprivation, although being in a different species, may be a general mechanism through which ghrelin sensitivity could be altered in this catabolic state. This may be mediated by the abrupt decline of circulating leptin levels induced by food deprivation (26). Clearly, the increase in gene expression after 12 weeks of food restriction was less profound than that exhibited following food deprivation for 48 h. Together with the finding that GHSR gene expression in the VMH was not at all affected by chronic food restriction but clearly induced by acute food deprivation, our data support the hypothesis that ghrelin is primarily involved in the short-term regulation of appetite and body weight.

Across different species, including man, a negative correlation between circulating ghrelin and leptin has been described (10, 28, 34); obesity is associated with high leptin and low ghrelin levels. However, in *P. sungorus*, ghrelin levels were not negatively correlated with body weight. Although LD and SD hamsters exhibited a body weight differential of 15% after 8 weeks acclimation to the opposite photoperiod, no changes in serum ghrelin concentration could be detected. As published previously (26), serum leptin levels in LD hamsters are elevated by two- to three-fold in LD compared to SD. Thus, the lack of SD photoperiod-induced changes of both GHSR gene expression as well as circulating ghrelin levels implies that in seasonal body weight regulation, leptin may not counteract ghrelin. Barazzoni *et al*. (34) demonstrated that, in lean rats, subcutaneous leptin infusion prevented the rise in serum ghrelin levels in response to moderate caloric restriction. However, our results in *P. sungorus* suggest that leptin has no effect on serum ghrelin levels in the ad libitum fed state.

Long-term changes in serum leptin concentrations induced by photoperiod in the female juvenile hamster do not affect central expression of GHSR or ghrelin serum concentration, suggesting that ghrelin does not play a major role in seasonal body weight regulation. To generalize this conclusion, further photoperiod experiments in adult male and female hamsters are required. As such, ghrelin does not appear to be a functional antagonist to leptin (at least for the regulation of long-term body weight changes) but perhaps a signal regulating responses to short-term changes in energy homeostasis, such as food deprivation. The data obtained from the seasonal species *P. sungorus* contribute additional information to the poorly understood interaction of leptin and ghrelin. This discrepancy implies that the interaction of the important feeding related hormones leptin and ghrelin, an interesting enigma in body weight regulation, certainly requires further investigation.

Acknowledgements

This collaborative study was funded by the Scottish Executive Environment and Rural Affairs Department (J. G. Mercer), EC FP6 funding (contract no. LSHM-CT-2003-503041 to J. G. Mercer), the German Research Foundation (DFG Kl 973/5; M. K.) Danish Research Agency (R. K.) and the Neuronet Marburg (NGFN 01GS0118 to M. K.). A. Tups received a fellowship from the European Commission to attend the ObeS°chool EU Marie Curie Training Site (HPMT-2001-00410) at the Rowett Research Institute and is in receipt of funding from Boehringer Ingelheim Fonds (Heidesheim, Germany).

Accepted 24 October 2004

References

1 Kojima M, Hosoda H, Date Y, Nakazato M, Matsuo H, Kangawa K. Ghrelin is a growth-hormone-releasing acylated peptide from stomach. *Nature* 1999; **402:** 656–660.
2 Takaya K, Ariyasu H, Kanamoto N, Iwakura H, Yoshimoto A, Harada M, Mori K, Komatsu Y, Usui T, Shimatsu A, Ogawa Y, Hosoda K, Akamizu T, Kojima M, Kangawa K, Nakao K. Ghrelin strongly stimulates growth hormone release in humans. *J Clin Endocrinol Metab* 2000; **85: 4908–4911.**
3 Kalra SP, Bagnasco M, Otukonyong EE, Dube MG, Kalra PS. Rhythmic, reciprocal ghrelin and leptin signaling: new insight in the development of obesity. *Regul Pept* 2003; **111:** 1–11.
4 Nakazato M, Murakami N, Date Y, Kojima M, Matsuo H, Kangawa K, Matsukura S. A role for ghrelin in the central regulation of feeding. *Nature* 2001; **409:** 194–198.
5 Tschöp M, Smiley DL, Heiman ML. Ghrelin induces adiposity in rodents. *Nature* 2000; **407:** 908–913.
6 Ariyasu H, Takaya K, Tagami T, Ogawa Y, Hosoda K, Akamizu T, Suda M, Koh T, Natsui K, Toyooka S, Shirakami G, Usui T, Shimatsu A, Doi K, Hosoda H, Kojima M, Kangawa K, Nakao K. Stomach is a major source of circulating ghrelin, and feeding state determines plasma ghrelin-like immunoreactivity levels in humans. *J Clin Endocrinol Metab* 2001; **86:** 4753–4758.
7 Cummings DE, Purnell JQ, Frayo RS, Schmidova K, Wisse BE, Weigle DS. A preprandial rise in plasma ghrelin levels suggests a role in meal initiation in humans. *Diabetes* 2001; **50:** 1714–1719.
8 Muccioli G, Tschop M, Papotti M, Deghenghi R, Heiman M, Ghigo E. Neuroendocrine and peripheral activities of ghrelin: implications in metabolism and obesity. *Eur J Pharmacol* 2002; **440:** 235–254.
9 Shiiya T, Nakazato M, Mizuta M, Date Y, Mondal MS, Tanaka M, Nozoe S, Hosoda H, Kangawa K, Matsukura S. Plasma ghrelin levels in lean and obese humans and the effect of glucose on ghrelin secretion. *J Clin Endocrinol Metab* 2002; **87:** 240–244.
10 Tschop M, Weyer C, Tataranni PA, Devanarayan V, Ravussin E, Heiman ML. Circulating ghrelin levels are decreased in human obesity. *Diabetes* 2001; **50:** 707–709.
11 Kojima M, Hosoda H, Kangawa K. Purification and distribution of ghrelin. the natural endogenous ligand for the growth hormone secretagogue receptor. *Horm Res* 2001; **56** (Suppl. 1)**:** 93–97.
12 Muccioli G, Papotti M, Locatelli V, Ghigo E, Deghenghi R. Binding of 125I-labeled ghrelin to membranes from human hypothalamus and pituitary gland. *J Endocrinol Invest* 2001; **24:** RC7–RC9.
13 Banks WA, Tschop M, Robinson SM, Heiman ML. Extent and direction of ghrelin transport across the blood–brain barrier is determined by its unique primary structure. *J Pharmacol Exp Ther* 2002; **302:** 822–827.
14 Hosoda H, Kojima M, Matsuo H, Kangawa K. Ghrelin and des-acyl ghrelin: two major forms of rat ghrelin peptide in gastrointestinal tissue. *Biochem Biophys Res Commun* 2000; **279:** 909–913.
15 Howard AD, Feighner SD, Cully DF, Arena JP, Liberator PA, Rosenblum CI, Hamelin M, Hreniuk DL, Palyha OC, Anderson J, Paress PS, Diaz C, Chou M, Liu KK, McKee KK, Pong SS, Chaung LY, Elbrecht A, Dashkevicz M, Heavens R, Rigby M, Sirinathsinghji DJ, Dean DC, Melillo DG, Van Der Ploeg LH. A receptor in pituitary and hypothalamus that functions in growth hormone release. *Science* 1996; **273:** 974–977.
16 McKee KK, Palyha OC, Feighner SD, Hreniuk DL, Tan CP, Phillips MS, Smith RG, Van Der Ploeg LH, Howard AD. Molecular analysis of rat pituitary and hypothalamic growth hormone secretagogue receptors. *Mol Endocrinol* 1997; **11:** 415–423.
17 Petersenn S, Rasch AC, Penshorn M, Beil FU, Schulte HM. Genomic structure and transcriptional regulation of the human growth hormone secretagogue receptor. *Endocrinology* 2001; **142:** 2649–2659.
18 Guan XM, Yu H, Palyha OC, McKee KK, Feighner SD, Sirinathsinghji DJ, Smith RG, Van Der Ploeg LH, Howard AD. Distribution of mRNA encoding the growth hormone secretagogue receptor in brain and peripheral tissues. *Brain Res Mol Brain Res* 1997; **48:** 23–29.
19 Kim MS, Yoon CY, Park KH, Shin CS, Park KS, Kim SY, Cho BY, Lee HK. Changes in ghrelin and ghrelin receptor expression according to feeding status. *Neuroreport* 2003; **14:** 1317–1320.

20 Atcha Z, Cagampang FR, Stirland JA, Morris ID, Brooks AN, Ebling FJ, Klingenspor M, Loudon AS. Leptin acts on metabolism in a photoperiod-dependent manner, but has no effect on reproductive function in the seasonally breeding Siberian hamster (*Phodopus sungorus*). *Endocrinology* 2000; **141:** 4128–4135.

21 Horton TH, Buxton OM, Losee-Olson S, Turek FW. Twenty-four-hour profiles of serum leptin in siberian and golden hamsters: photoperiodic and diurnal variations. *Horm Behav* 2000; **37:** 388–398.

22 Klingenspor M, Dickopp A, Heldmaier G, Klaus S. Short photoperiod reduces leptin gene expression in white and brown adipose tissue of Djungarian hamsters. *FEBS Lett* 1996; **399:** 290–294.

23 Adam CL, Moar KM, Logie TJ, Ross AW, Barrett P, Morgan PJ, Mercer JG. Photoperiod regulates growth, puberty and hypothalamic neuropeptide and receptor gene expression in female Siberian hamsters. *Endocrinology* 2000; **141:** 4349–4356.

24 Mercer JG, Moar KM, Logie TJ, Findlay PA, Adam CL, Morgan PJ. Seasonally inappropriate body weight induced by food restriction: effect on hypothalamic gene expression in male Siberian hamsters. *Endocrinology* 2001; **142:** 4173–4181.

25 Mercer JG, Ellis C, Moar KM, Logie TJ, Morgan PJ, Adam CL. Early regulation of hypothalamic arcuate nucleus CART gene expression by short photoperiod in the Siberian hamster. *Regul Pept* 2003; **111:** 129–136.

26 Tups A, Ellis C, Moar KM, Logie TJ, Adam CL, Mercer JG, Klingenspor M. Photoperiodic regulation of leptin sensitivity in the Siberian hamster, *Phodopus sungorus*, is reflected in arcuate nucleus SOCS-3 (suppressor of cytokine signaling) gene expression. *Endocrinology* 2004; **145:** 1185–1193.

27 Paxinos G, Franklin K. *The Mouse Brain in Stereotaxic Coordinates*. San Diego, CA: Academic Press, 2002.

28 Angeloni SV, Glynn N, Ambrosini G, Garant MJ, Higley JD, Suomi S, Hansen BC. Characterization of the rhesus monkey ghrelin gene and factors influencing ghrelin gene expression and fasting plasma levels. *Endocrinology* 2004; **145:** 2197–2205.

29 Levin BE, Dunn-Meynell AA, Ricci MR, Cummings DE. Abnormalities of leptin and ghrelin regulation in obesity-prone juvenile rats. *Am J Physiol Endocrinol Metab* 2003; **285:** E949–E957.

30 Meyer CW, Korthaus D, Jagla W, Cornali E, Grosse J, Fuchs H, Klingenspor M, Roemheld S, Tschop M, Heldmaier G, DeAngelis MH, Nehls M. A novel missense mutation in the mouse growth hormone gene causes semidominant dwarfism, hyperghrelinemia and obesity. *Endocrinology* 2004; **145:** 2531–2541.

31 Schwartz MW, Woods SC, Porte D Jr, Seeley RJ, Baskin DG. Central nervous system control of food intake. *Nature* 2000; **404:** 661–671.

32 Chen HY, Trumbauer ME, Chen AS, Weingarth DT, Adams JR, Frazier EG, Shen Z, Marsh DJ, Feighner SD, Guan XM, Ye Z, Nargund RP, Smith RG, Van Der Ploeg LH, Howard AD, MacNeil DJ, Qian S. Orexigenic action of peripheral ghrelin is mediated by neuropeptide Y (NPY) and agouti-related protein (AgRP). *Endocrinology* 2004; **145:** 2607–2612.

33 Hewson AK, Tung LY, Connell DW, Tookman L, Dickson SL. The rat arcuate nucleus integrates peripheral signals provided by leptin, insulin, and a ghrelin mimetic. *Diabetes* 2002; **51:** 3412–3419.

34 Barazzoni R, Zanetti M, Stebel M, Biolo G, Cattin L, Guarnieri G. Hyperleptinemia prevents increased plasma ghrelin concentration during short-term moderate caloric restriction in rats. *Gastroenterology* 2003; **124:** 1188–1192.

J Comp Physiol B (2007) 177:743–752
DOI 10.1007/s00360-007-0171-6

ORIGINAL PAPER

Functional characterisation of UCP1 in the common carp: uncoupling activity in liver mitochondria and cold-induced expression in the brain

Martin Jastroch · Julie A. Buckingham · Michael Helwig · Martin Klingenspor · Martin D. Brand

Received: 16 March 2007 / Revised: 18 May 2007 / Accepted: 21 May 2007 / Published online: 19 June 2007

Abstract Mammalian uncoupling protein 1 (UCP1) mediates nonshivering thermogenesis in brown adipose tissue. We previously reported on the presence of a UCP1 orthologue in ectothermic fish and observed downregulation of UCP1 gene expression in the liver of the common carp. Neither the function of UCP1, nor the mode of UCP1 activation is known in carp liver mitochondria. Here, we compared the proton conductance at 25°C of liver mitochondria isolated from carp either maintained at 20°C (warm-acclimated, WA) or exposed to 8°C (cold-acclimated, CA) water temperature for 7–10 days. Liver mitochondria from WA carp had higher state four rates of oxygen consumption and greater proton conductance at high membrane potential. Liver mitochondria from WA, but not from CA, carp showed a strong increase in proton conductance when palmitate (or 4-hydroxy-*trans*-2-nonenal, HNE) was added, and this inducible proton conductance was prevented by addition of GDP. This fatty acid sensitive proton leak is likely due to the expression of UCP1 in the liver of WA carp. The observed biochemical properties of proton leak strongly suggest that carp UCP1 is a functional uncoupling protein with broadly the same activatory and inhibitory characteristics as mammalian UCP1. Significant UCP1 expression was also detected in our previous study in whole brain of the carp. We here observed a twofold increase of UCP1 mRNA in carp brain following cold exposure, suggesting a role of UCP1 in the thermal adaptation of brain metabolism. In situ hybridization located the UCP1 gene expression to the optic tectum responsible for visual system control, the descending trigeminal tract and the solitary tract. Taken together, this study characterises uncoupling protein activity in an ectotherm for the first time.

Keywords Uncoupling protein 1 · Proton leak · *Cyprinus carpio* · 4-hydroxynonenal · Liver

Abbreviations

ADP	Adenosine 5′-(trihydrogen diphosphate)
BSA	Bovine serum albumin
CA	Cold-acclimated
DEPC	Diethylpyrocarbonate
DTT	Dithiothreitol
EDTA	Ethylenediaminetetraacetic acid
EGTA	Ethylene glycol bis (2-aminoethyl ether)-N,N,N′N′-tetraacetic acid
FCCP	Carbonyl cyanide p-trifluoro-methoxyphenylhydrazone
GDP	Guanosine 5′-diphosphate
HEPES	4-(2-Hydroxyethyl)-1-piperazineethanesulfonic acid
PBS	Phosphate buffered saline
SSC	Sodium chloride sodium citrate buffer
^{35}S-UTP	Uridine 5′-[α-^{35}S]thiotriphosphate
TEA	Triethanolamine
TPMP	Triphenylmethylphosphonium

Communicated by G. Heldmaier.

Electronic supplementary material The online version of this article (doi:10.1007/s00360-007-0171-6) contains supplementary material, which is available to authorized users.

M. Jastroch (✉) · M. Helwig · M. Klingenspor
Animal Physiology, Department of Biology,
Philipps University Marburg, Karl-von-Frisch-Str. 8,
Marburg 35032, Germany
e-mail: Jastroch@staff.uni-marburg.de

J. A. Buckingham · M. D. Brand
Medical Research Council Dunn Human Nutrition Unit,
Hills Road, Cambridge, CB2 2XY, UK

Tris–HCl	(Hydroxymethyl) aminomethane-hydrochloride
WA	Warm-acclimated

Introduction

Uncoupling protein 1 (UCP1) executes nonshivering thermogenesis in brown adipose tissue of newborn humans, small mammals and hibernating mammals. The protein catalyses proton leakage through the inner membrane of mitochondria in brown adipocytes, decreasing the proton motive force and resulting in increased oxygen consumption and heat generation without concomitant ATP generation (Nicholls and Locke 1984). Paralogous proteins have been identified in vertebrates (UCP2, UCP3 and avian UCP) and in plants (plant UCP) but their physiological role remains controversial (Brand and Esteves 2005). Further proteins were named UCP4 and UCP5 but typical UCP1-like biochemical properties of these other proteins have not yet been demonstrated and phylogenetic inference excludes them from the core UCP protein family (Cannon and Nedergaard 2004).

The thermogenic role of mammalian UCP1 has been clearly identified and until recently the phylogenetic distribution of UCP1 was broadly accepted as restricted to placental mammals (Jastroch et al. 2005). In placental mammals, signal transduction at the brown adipocyte leads to an immediate breakdown of triglycerides, releasing free fatty acids into the cytosol. These fatty acids not only activate uncoupling by UCP1 (Lowell 1998) but are also fed into the respiratory chain of brown adipocyte mitochondria and serve as fuel. Direct activation of uncoupling activity by fatty acids has only been unambiguously demonstrated for UCP1 (Cunningham et al. 1986). Proton transport of all uncoupling proteins can be potently inhibited with purine nucleoside di- and triphosphates, including ADP, GDP, ATP and GTP. The activatory role of fatty acids remains unclear. There are three competing models: (a) fatty acids are required cofactors facilitating transport of protons (Klingenberg and Winkler 1985); (b) cycling of fatty acids is required for proton transport (UCP1 transports fatty acid anion from the matrix to the intermembrane space, and this is followed by protonation and flip-flop of the acid back to the matrix) (Garlid et al. 1996) or (c) there is no mechanistic requirement for fatty acids but they overcome nucleotide inhibition by simple competitive kinetics (Rial et al. 2004; Shabalina et al. 2004).

As one feature common to all known UCPs proton transport resulting in mild uncoupling can be activated by exposure of mitochondria to superoxide, which is prevented in the presence of purine nucleotides. 4-hydroxy-trans-2-nonenal (HNE), a reactive alkenal that also activates UCPs, may be one mediator of this mild uncoupling in response to the superoxide pathway (Echtay et al. 2003; Considine et al. 2003). Based on this activation of UCPs by reactive oxygen species produced by the respiratory chain a general role of UCPs in protection from oxidative cell damage has been proposed.

A recent study demonstrates the expression of UCP1, UCP2 and UCP3 in the common carp (*Cyprinus carpio*), an ectothermic vertebrate, providing a departure point for further investigation on the evolution of UCP1-mediated thermogenesis in placental mammals and the general function of UCPs in vertebrates (Jastroch et al. 2005). Interestingly, UCP1 mRNA in carp liver is diminished in response to cold, in contrast to expression of mammalian UCP1 in brown adipose tissue, which is cold induced. In the present paper we measured proton conductance in liver mitochondria from carp to resolve the function of UCP1. No previous studies have demonstrated uncoupling activity of UCP1 in an ectothermic vertebrate like the common carp, and the functional characterisation will assist in understanding the general roles of UCPs in the animal kingdom.

Materials and methods

Animal experiments

Common carp (400–600 g body weight) were kept in a temperature-controlled recirculating water system (Living stream, Frigid units) maintained at 20°C for at least 2 weeks. Three individuals were transferred to a second system and water temperature was gradually lowered (2°C per day) to 8°C. It has been demonstrated that 48 h of exposure to 8°C diminishes UCP1 mRNA levels dramatically (Jastroch et al. 2005). In the present study, carp were cold-exposed at 8°C for 7–10 days before use to induce metabolic acclimatisation processes. Animals were killed within UK Home Office rules by stunning, puncture of the heart and cerebral dislocation.

Isolation of liver mitochondria

Mitochondria for proton conductance measurements were always isolated in parallel from two carp, one taken from the warm and the other from the cold water tank in order to control for possible day-by-day variability in the quality of mitochondrial preparations. The liver was removed and immediately placed in ice-cold isolation medium (250 mmol l^{-1} sucrose, 5 mmol l^{-1} Tris–HCl, 2 mmol l^{-1} EGTA pH 7.4) containing 1% (w/v) defatted BSA (Sigma). The tissue was minced with scissors and disrupted using a Dounce homogeniser with a medium-fitting pestle. The homogenate was centrifuged at 8,500*g* for 10 min at 4°C and the pellet was resuspended in isolation medium and spun at 1,047*g* for 10 min; the resulting supernatant was subjected to a high-speed spin cycle (11,630*g*, 10 min, and

4°C). The pellet was resuspended in medium without BSA. The high-speed spin cycle was repeated twice and the final pellet resuspended in a minimal volume of isolation medium. Protein concentration was determined using the biuret method with fatty acid-free bovine serum albumin as standard (Gornall et al. 1949).

Measurement of oxygen consumption and membrane potential

Oxygen consumption was measured using a Clark-type oxygen electrode (Rank Brothers Ltd, United Kingdom) maintained at 25°C and calibrated with air-saturated medium (120 mmol l^{-1} KCl, 5 mmol l^{-1} KH_2PO_4, 3 mmol l^{-1} HEPES, 1 mmol l^{-1} EGTA, and 0.3% (w/v) defatted BSA, pH 7.2), which was assumed to contain 479 nmol O ml^{-1} (Reynafarje et al. 1985). Prior to the first measurements, the RCR =*respiratory control ratio*, dividing state three respiration (ADP-induced) by state 4 (leak respiration) of liver mitochondria was measured to ascertain the integrity of the carp liver mitochondria during the mitochondrial isolation procedure. Simultaneously with oxygen consumption, membrane potential was measured using a $TPMP^+$ sensitive electrode (Brand 1995). Mitochondria were suspended at 1.5 mg ml^{-1} in 2.5 ml medium and incubated with 8 µM rotenone to inhibit complex I, with 4 µg ml^{-1} oligomycin to inhibit phosphorylation of ADP, and with 110 ng ml^{-1} nigericin to abolish ΔpH. The $TPMP^+$ electrode was calibrated with sequential additions up to 2.5 µmol l^{-1} $TPMP^+$. Succinate (6 mmol l^{-1}) was added to start the reaction. Oxygen consumption and membrane potential were titrated through sequential steady states by successive additions of malonate up to 1 mmol l^{-1} for skeletal muscle mitochondria and up to 4 mmol l^{-1} for liver mitochondria. Where indicated, 1 mmol l^{-1} GDP, 35 µmol l^{-1} HNE or 100 µmol l^{-1} sodium palmitate dissolved in ethanol were added at the beginning of each run. The equation to calculate the binding of palmitate to bovine serum albumin (BSA) at 37°C by Richieri and coworkers (Richieri et al. 1993) was used to estimate free palmitate levels in our measurements containing 0.3% BSA (50.1 µmol l^{-1}): Free palmitate (nmol l^{-1}) = 4.4n − 0.03 + 0.23 exp (1.16n), where n is the molar ratio of palmitate to albumin.

Northern blot analysis and in situ hybridisation of the carp brain

The carp skull was opened; the brain carefully removed and immediately snap frozen in liquid nitrogen. All brain samples were stored at −70°C. Prior to RNA extraction the whole brain was first powdered in liquid nitrogen. Isolation of total RNA and Northern blotting was performed as described previously (Jastroch et al. 2004). The blot was hybridised with a probe corresponding to the full-length cDNA sequence of carp UCP1 (Jastroch et al. 2005). The hybridised probe was then detected by phospor imaging (Storm 860, Molecular Dynamics), and relative expression levels quantified using ArrayVision 7.0 (Imaging Research).

Coronal and sagittal brain sections (20 µm) were processed using a cryosectioning microtome (Leica CM 3050) and transferred to precooled object slides. A riboprobe complementary to carp UCP1 was generated from a linearised cloned cDNA. 50 µl of the ^{35}S-UTP-labelled probe was mixed in a volume of 256 µl with 3.9 mg ml^{-1} tRNA, 20 µl 1M DTT, 74 µl DEPC-treated water and added to 1 ml dextran sulphate and 1.5 ml hybridisation buffer (1M NaCl, 3.4× Denhardts, 34 mmol l^{-1} Tris (pH 8), 3.4 mmol l^{-1} EDTA (pH 8)). Prior to hybridisation, the slides were fixed in 4% paraformaldehyde in PBS (137 mmol l^{-1} NaCl, 10 mmol l^{-1} phosphate, 2.7 mmol l^{-1} KCl, pH 7.4) for 20 min on ice followed by 2 × 5 min washes in 0.1 mol l^{-1} PBS, immersed in 250 ml, 0.1 mol l^{-1} TEA (2 min) and transferred to 0.1 mol l^{-1} TEA containing 625 µl of acetic anhydride for 10 min. Slides were dehydrated through a gradient of increasing concentration of ethanol (50, 70, 95 and 100%) for 3 min each step. For hybridisation, 50 µl of hybridisation cocktail was loaded on each slide and incubated for 16 h at 60°C. Post hybridisation, object slides were transferred to 4× SSC (150 mmol l^{-1} NaCl, 15 mmol l^{-1} Na_3-citrate), cover slides were removed, and washed four times for 5 min in 4× SSC. After incubation in RNase solution (0.5 mol l^{-1} NaCl, 10 mmol l^{-1} Tris (pH 8), 1 mmol l^{-1} EDTA, 2 µg ml^{-1} RNase) at 37°C for 30 min, washing was repeated in descending concentrations of SSC (2× SSC twice for 5 min each, 1× SSC for 10 min and 0.5× SSC for 10 min at room temperature plus 0.1× SSC incubation for 30 min at 60°C). Dried slides were exposed to BioMax MR Film (Kodak) for two weeks. A control was performed by hybridising sections with equal length sense riboprobes of UCP1 resulting in no signal.

Statistical analysis

Values are means ± SEM. For comparisons of warm-acclimated (WA) and cold-acclimated (CA) carp, unpaired Student's *t* tests were performed. Activation and inhibition of proton conductance was tested using one-way ANOVA and Tukey's post hoc test with the level of significance set to $P < 0.05$.

Results

Morphology of liver from WA and CA carp

Prior to tissue removal, we observed an altered morphological appearance of the carp liver at different acclimation

temperatures (Supplemental photograph). In CA carp, the liver appeared enlarged and enshrouded other organs (e.g. spleen, intestine) indicating that significant physiological adaptations occurred due to cold acclimation. In accordance with our observations, the positive effect of cold exposure on liver mass seems to be a common adaptational process in fish as it was also described in the eel (*Anguilla anguilla* L.) (Wodtke 1974) or in the canal catfish (Kent et al. 1988).

State 4 respiration and basal proton conductance of liver mitochondria from WA and CA carp

We first compared the values of resting (state 4) oxygen consumption and membrane potential in liver mitochondria from WA and CA carp (Fig. 1). The mitochondrial assays were done under standardised 25°C conditions so that effects of the acclimation procedures (which happen to be at different temperatures) could be directly compared.

When respiring on succinate, state 4 respiration of mitochondria from WA fish tended to be higher than from CA fish (9.77 ± 0.73 compared to 7.72 ± 0.36 nmol O min^{-1} mg^{-1} of protein, *t* test, $P = 0.065$, $n = 3$, Fig. 1). In contrast, the CA group trends towards higher state 4 potential (168.5 ± 2.6 vs. 162.2 ± 0.7 mV, *t* test, $P = 0.097$, $n = 3$, Fig. 1). Lower respiration rate and higher membrane potential shows that state 4 proton leakage in carp liver mitochondria is decreased in response to cold acclimation.

We next compared the full kinetic response at 25°C of proton leak (monitored as oxygen consumption rate) to stepwise changes in its driving force, membrane potential,

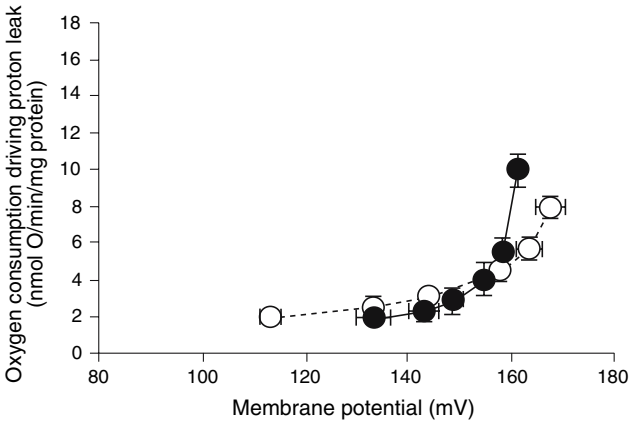

Fig. 1 Kinetics of basal proton conductance in liver mitochondria from CA and WA carp. Oxygen consumption driving proton leak in the absence of ATP synthesis is plotted against different membrane potentials imposed by malonate titration of succinate oxidation in isolated carp liver mitochondria to display the kinetic dependence of proton leak on its driving force, membrane potential, at 25°C. For details see "Materials and methods". *Filled circle* warm-acclimated (WA) carp; *open circle* cold-acclimated (CA) carp. Data are mean ± SEM of three (carp) independent experiments each performed in duplicate

in liver mitochondria from WA and CA carp (Fig. 1). As proton leak is a nonlinear function of membrane potential, to make comparisons between the two acclimation temperatures we compared the oxygen consumption driving proton leak at a common membrane potential. At the highest common potential of about 162 mV (the state 4 potential of mitochondria from WA carp), oxygen consumption was significantly ($P < 0.05$) decreased from 9.77 ± 0.73 in WA to 5.21 ± 0.56 nmol O min^{-1} mg^{-1} of protein in mitochondria from CA carp, indicating a twofold drop in the proton conductance of liver mitochondria from CA carp. However, this effect was only apparent at the highest membrane potentials.

Palmitate activation and GDP inhibition of proton conductance in carp liver mitochondria

Carp acclimated to 20°C express relatively high amounts of UCP1 mRNA in liver, whereas UCP1 mRNA levels are diminished after exposure to 8°C (Jastroch et al. 2005). The proton leak kinetics of UCPs have two major characteristics: activation by fatty acids (Locke et al. 1982), superoxide and alkenals (Echtay et al. 2003); (Considine et al. 2003) and inhibition by purine nucleoside di- or triphosphates (Nicholls and Locke 1984). We investigated if the kinetics of proton leak in carp liver mitochondria are affected by well characterized UCP1 activators and inhibitors, and whether the effects of these compounds are altered when UCP1 mRNA levels are diminished in response to cold acclimation.

Figure 2a shows that addition of palmitate (100 µmol l^{-1} total, which would result in about 11 nmol l^{-1} free palmitate according to (Richieri et al. 1993) in the presence of 0.3% BSA) increased the proton leakiness of liver mitochondria from WA carp. At the highest common potential of 154 mV, oxygen consumption was increased significantly from 3.63 ± 0.69 to 11.95 ± 1.44 nmol O min^{-1} mg^{-1} of protein, indicating a 3–4-fold stimulation of proton conductance (Fig. 2c). The increase in proton conductance was fully prevented by 1 mmol l^{-1} GDP (Fig. 2a, c), as expected if it was caused by palmitate activation of proton conductance through UCP1. In liver mitochondria from CA carp, palmitate had a negligible effect on proton conductance (Fig. 2b, d). Additionally, we observed that GDP without the addition of palmitate had no further effect on lowering proton conductance neither in the warm acclimated nor in the CA carp (data not shown). This experiment shows that GDP-sensitive fatty acid activation of proton conductance occurs in liver mitochondria from the common carp just as it does in UCP1-containing mitochondria from brown adipose tissue and implies that carp UCP1 is a functional fatty acid activated proton transporter. This conclusion is greatly strengthened by the lack of fatty acid and GDP effects in

J Comp Physiol B (2007) 177:743–752

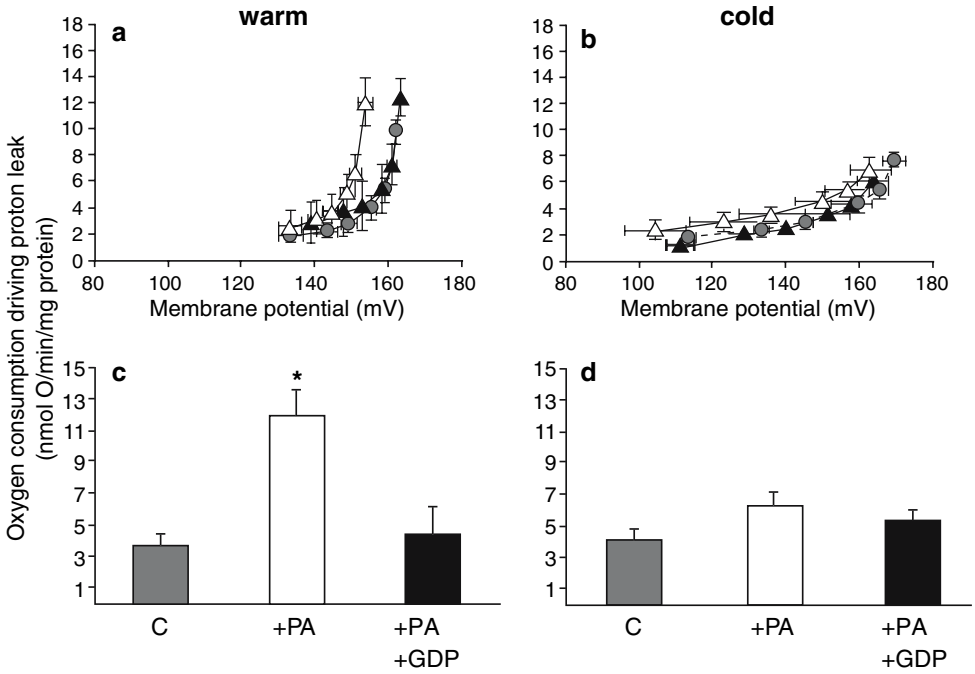

Fig. 2 Palmitate induced GDP-sensitive proton conductance in carp liver mitochondria. The kinetics of proton leak at 25°C were measured as described in Fig. 1. **a** and **b** show the kinetic curves; **c** and **d** show the derived rates of proton leak at the highest common potential (154 mV). Liver mitochondria were from (**a**, **c**) 20°C WA or (**b**, **d**) 8°C CA common carp. *Circle*, control; Δ, 100 µmol l^{-1} M palmitate; *filled triangle*, 100 µmol l^{-1} palmitate + 1 mmol l^{-1} GDP. All data are mean ± SEM of three independent experiments each performed in duplicate. *Asterisk* significant compared to control and GDP-inhibition ($P < 0.05$, one way ANOVA followed by Tukey's post hoc test); *C* control; *PA* palmitate

liver mitochondria from CA carp, in which UCP1 mRNA expression is lower (Jastroch et al. 2005).

HNE activation and GDP inhibition of proton conductance in carp liver mitochondria

HNE activates the proton conductance of mammalian UCP1, UCP2 and UCP3 (Echtay et al. 2003) and plant UCP (Smith et al. 2004). Figure 3a shows that addition of 35 µmol l^{-1} HNE to liver mitochondria from WA carp increased the proton conductance. At the highest common potential of about 151 mV, oxygen consumption driving proton leak was elevated 3–4-fold, from 3.06 ± 0.63 to 10.87 ± 1.13 nmol O min^{-1} mg^{-1} of protein (Fig. 3c). Although the proton conductance of mammalian adenine nucleotide translocase is also activated by HNE, activation of UCPs can be distinguished from this effect by its sensitivity to addition of GDP to inhibit specifically UCPs (Echtay et al. 2003). Figure 3a and c show that HNE-activated proton conductance could be partially inhibited with 1 mmol l^{-1} GDP. Once again, these effects were absent in liver mitochondria from CA carp (Fig. 3b, d), suggesting that they were caused by UCP1 and not by the adenine nucleotide translocase. Addition of both palmitate and HNE gave similar results to palmitate or HNE alone (Fig. 3e–h), suggesting no additivity or synergy of activation of carp UCP1 by fatty acids and alkenals under our assay conditions.

UCP1 in the brain of the common carp

In the studies reported above, we used mitochondria from carp liver to elucidate a possible function of UCP1. These experiments were based on the rationale that in liver we previously found the highest UCP1 gene expression of all carp tissues investigated (Jastroch et al. 2005) and the isolation of large amounts of coupled mitochondria was convenient. However, UCP1 mRNA is also expressed in carp brain (Jastroch et al. 2005). We therefore investigated in the carp brain the effect of cold acclimation on UCP1 expression and the neuroanatomical localisation of UCP1 mRNA.

Whereas UCP1 in carp liver is downregulated in the cold (Jastroch et al. 2005), UCP1 mRNA levels in the carp brain were upregulated about 2.4-fold in response to 7–10 days of cold acclimation (Fig. 4a). We furthermore scrutinised the neuroanatomical expression sites by in situ hybridisation. Figure 4b shows a representative autoradiograph of a sagittal brain section of a CA carp and the corresponding scheme adapted from the brain atlas of the goldfish (Canosa et al. 2004). A coronal section in the anterior part of the brain shows clear hybridisation of the UCP1 probe in the periventricular grey zone of the optic tectum (Fig. 4c). In the posterior region consisting of neuronal hindbrain structures, the descending trigeminal tract and the solitary tract show specific binding of the UCP1 probe (Fig. 4d).

Discussion

Our results demonstrate that the proton conductance of carp liver mitochondria can be stimulated by palmitate or HNE and inhibited by GDP. This regulated proton conductance was, however, only found in mitochondria isolated from carp acclimated to 20°C, but absent in carp acclimated to 8°C. We previously reported that UCP1 mRNA is most

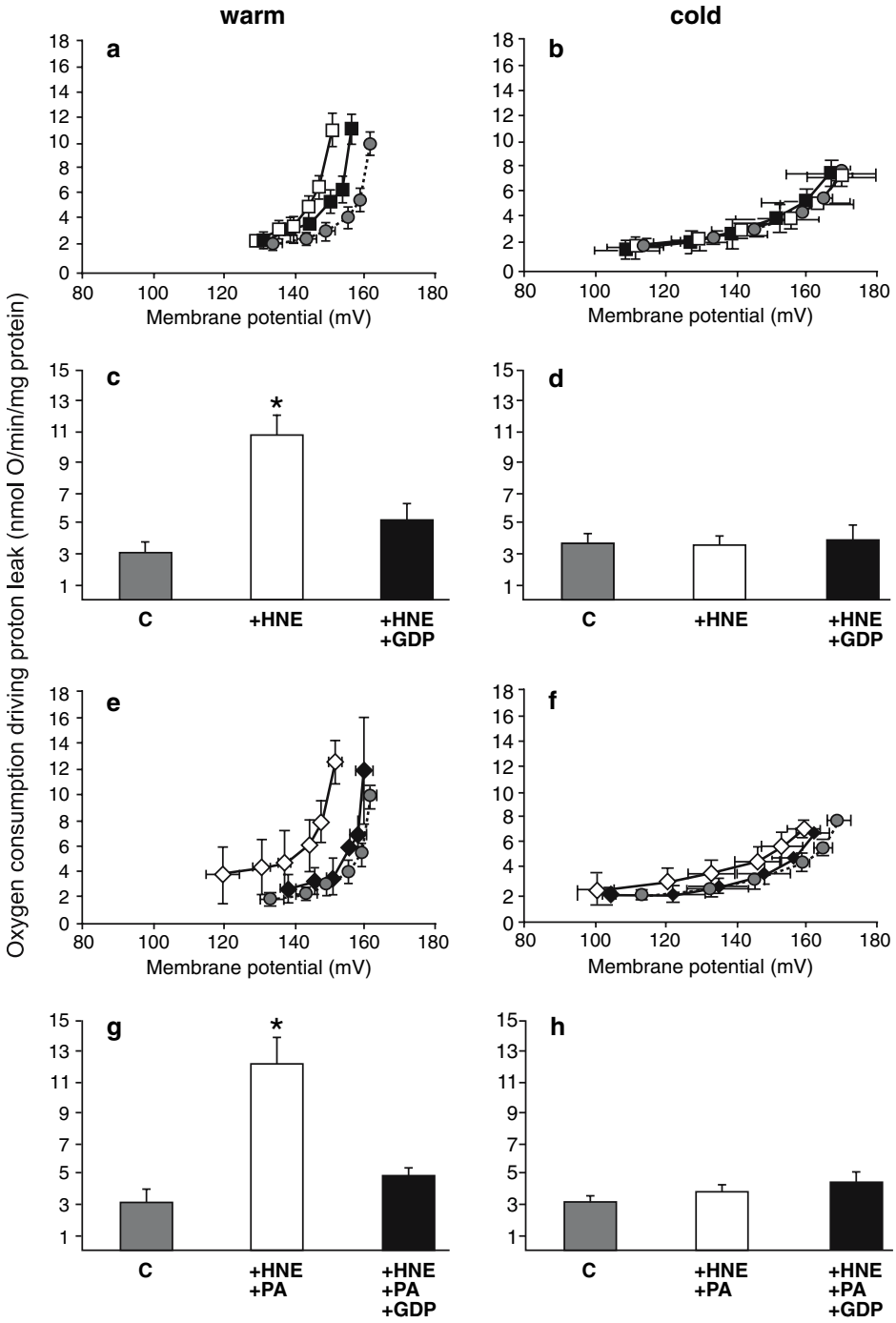

Fig. 3 HNE and palmitate induced GDP-sensitive proton conductance in carp liver mitochondria. The kinetics of proton leak at 25°C were measured as described in Fig. 1. **a**, **b**, **e**, **f** show the kinetic curves; **c**, **d**, **g**, **h** show the derived rates of proton leak at the highest common potential (151 mV). Liver mitochondria were from (**a**, **c**, **e**, **g**) 20°C WA or (**b**, **d**, **f**, **h**) 8°C CA common carp. *Circle*, control; *open square*, 35 μmol l^{-1} HNE; *filled square*, 35 μmol l^{-1} HNE + 1 mmol l^{-1} GDP; *open diamond*, 35 μmol l^{-1} HNE + 100 μmol l^{-1} palmitate; *filled diamond* 35 μmol l^{-1} HNE + 100 μmol l^{-1} palmitate + 1 mmol l^{-1} GDP. All data are mean ± SEM of three independent experiments except the treatment with "HNE and palmitate" which was performed twice in duplicate. *Asterisk* significant compared to control and GDP-inhibition ($P < 0.05$, one way ANOVA followed by Tukeys post hoc test); *C* control; *PA* palmitate

abundant in carp liver and strongly down regulated in response to cold (Jastroch et al. 2005). This coincidence strongly suggests that the observed GDP-sensitive induction of proton conductance by fatty acids and HNE is due the presence of UCP1 in liver mitochondria of WA carp. Unfortunately, available antibodies raised against mammalian UCP1 do not cross-react with the carp UCP1 orthologue. In future studies, the generation of a fish-specific UCP1 antibody and the use of UCP1 gene knockout or iRNA methodology is definitely required to further corroborate the function of carp UCP1. We have to consider that the rather weak expression of UCP2 in carp liver may also explain the presence of inducible proton conductance. However, a study investigating UCP2 expression in the liver of a temperate marine fish, the common eelpout *Zoarces viviparous*, shows an upregulation of UCP2 in response to cold (Mark et al. 2006). Based on the assumption that UCP2 expression is similarly regulated in the temperate carp, inducible proton conductance would therefore, be more pronounced in the CA carp which was not the case. Further

J Comp Physiol B (2007) 177:743–752

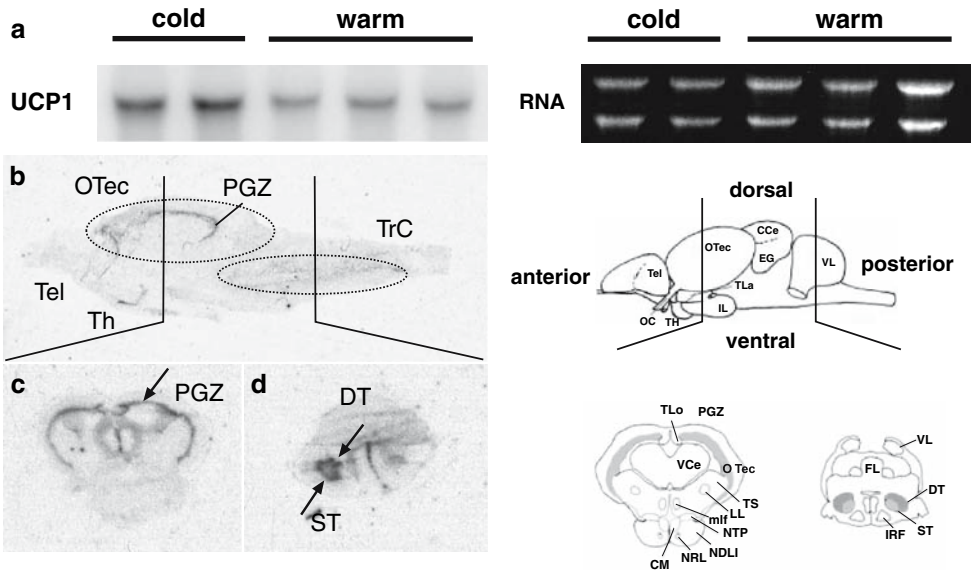

Fig. 4 Northern blot analysis of UCP1 in carp brain and autoradiographs of carp brain sections. **a** Twenty micrograms total RNA from the brain of WA or CA carp were hybridised with the carp UCP1 full-length cDNA (*left*). Loading of RNA was checked by ethidium–bromide staining of the agarose gel (*right*). **b** Sagittal section of carp brain, labelled according to the schematic representation (*right*) of whole goldfish brain anatomy modified from (Canosa et al. 2004). **c** Coronal and **d** sagittal sections located as indicated in **b**, labelled according to the schematic representation (*right*) of coronal and sagittal sections of the goldfish brain (10). *CCe* cerebellar body; *CM* mammilar body; *DT* descending trigeminal tract; *EG* eminentia granularis; *FL* facial lobe; *IL* inferior lobe; *IRF* inferior reticular formation; *LL* lateral lemniscus; *mlf* medial longitudinal fascicules; *NDLI* diffuse nucleus of the inferior lobe; *NRL* nucleus of the lateral recess; *NTP* posterior thalamic nucleus; *OC* optic chiasma; *OTec* optic tectum; *PGZ* periventricular grey zone of OTec; *ST* solitary tract; *Tel* telencephalon; *TH* thalamus; *TLA* lateral thalamus; *TLo* torus longitudinalis; *TrC* truncus cerebri; *TS* torus semicircularis; *VCe* cerebellar valve; *VL* vagal lobe. Terminology according to (10)

indication that we do not measure UCP2 activity is provided by studies of their mammalian species orthologues: the conserved central matrix loop of mammalian UCP1 is required for fatty acid activation which is absent for UCP2 and UCP3 (Jimenez-Jimenez et al. 2006).

The fatty acid induced uncoupling of mitochondrial proton conductance resembles the action of UCP1 in mammalian brown adipose tissue mitochondria. Even though the alkenal HNE activated carp UCP1 per se, palmitate activation of carp UCP1 required no further addition of metabolites of the superoxide activatory pathway, closely reflecting the situation reported for UCP1 in mammalian mitochondria (Klingenberg and Echtay 2001). Fatty acid induced uncoupling can also be mediated by other proton translocases like the adenine nucleotide transporter or the phosphate carrier protein but high GDP sensitivity is so far a common feature for UCPs. A recent study suggested a dual-site model of UCP1 regulation including fatty acids and reactive alkenals interacting at separate sites. It cannot be excluded, however, that endogenous alkenals are required for UCP1 activity as they are released continuously by oxidising natural membranes (Esteves et al. 2006). In contrast, all other members of the core UCP family so far investigated (UCP2, UCP3, potato UCP, penguin UCP) (Considine et al. 2003; Talbot et al. 2004; Echtay et al. 2002) experimentally required the addition of alkenals before they catalysed proton conductance in mitochondria (Brand et al. 2004).

Our study on UCP1 in carp emphasises the strength of parallel measurements of oxygen consumption and membrane potential for the quantification of proton leakage. In numerous studies, state 4 oxygen consumption alone has been taken as a surrogate for the proton leakiness of the mitochondrial inner membrane. Higher leak should result in an increased pump activity of the respiratory chain to maintain the membrane potential. The activation of UCP1 in brown adipose tissue decreases the membrane potential dramatically but the high oxidative capacity strongly defends this potential resulting in increased oxygen consumption. Thus, respiration of brown adipose tissue mitochondria can be induced several fold with palmitate and is a good index of UCP1 function. With carp liver mitochondria, activation of proton leak leads to little elevation of oxygen consumption (Figs. 1, 2), but simultaneous measurement of both oxygen consumption and membrane potential clearly resolves the increase of proton conductance. In these mitochondria of low oxidative capacity, oxygen consumption is not dramatically increased to defend the membrane potential but the membrane potential is rather decreased.

Among the teleost fish, the common carp is a "cold-inactive" species: winter-acclimatised carp have reduced activity and metabolism. Several studies demonstrate a recruitment of mitochondrial density and respiratory capacity during cold acclimation in skeletal muscle (Guderley 1990). In liver, however, no evidence has been reported that the respiratory capacity, using cytochrome c oxidase as a marker, is increased (Wodtke 1981). On the other hand the metabolic capacity of the Krebs cycle, as judged from liver citrate synthase activity, appears to be augmented during cold acclimation (Lucassen et al. 2006). In the "cold-inactive" species the requirement for ATP in vivo is strongly reduced which likely results in a depressed state 3 respiration of hepatocytes. In this situation the contribution of proton leak (state 4 respiration) to the cellular oxygen consumption would dominate. Accordingly, the observed reduction in proton leakage in CA carp mitochondria (Fig. 1) serves to save energy and increases the efficiency of mitochondrial ATP production. Our findings on the reduction of mitochondrial proton leak are consistent with physiological findings in other ectothermic vertebrates during metabolic depression. Basal proton leak rate is reduced in skeletal muscle mitochondria of hypometabolic frogs because of decreased activity of the electron transport chain (St Pierre et al. 2000), and it is reduced in hepatopancreas cells from aestivating snails compared to controls because of changes in mitochondrial proton conductance (Bishop and Brand 2000).

Alterations in proton conductance might be caused by alterations in membrane properties. In carp, the proportion of unsaturated fatty acids rapidly increases within less than a week in response to cold (Wodtke 1978; Trueman et al. 2000; Tiku et al. 1996). The influence of phospholipid fatty acid composition on proton conductance has been intensively discussed in the past. Whereas, a correlation between proton conductance and fatty acid composition is observed in mitochondria, the proton permeability of liposomes made from mitochondrial inner membranes does not depend on phospholipid composition (Porter et al. 1996; Brookes et al. 1997). Given an assay temperature of 25°C, we would expect higher membrane fluidity in accordance with homeoviscous adaptation in mitochondria of CA carp and perhaps a higher proton conductance due to a higher degree of unsaturation (Guderley 2004). In contrast, we observed a lower basal proton conductance in mitochondria from the CA group (Fig. 1). Liver mitochondria from CA carp were measured at an assay temperature of 25°C to allow comparisons of UCP1 function between WA and CA carp. Therefore, the biological relevance of lower proton conductance might be impaired, as the cold-exposed mitochondria might not work properly at a higher temperature. Anyway, the high temperature does not disrupt the mitochondrial inner membrane, as damaged mitochondria would lose proton motive force. Instead, the membrane potential was even higher as in the warm-acclimated liver mitochondria. Other studies investigating basal proton leak kinetics in fish found similar proton conductance in carp and goldfish liver mitochondria at 25°C (J Baca, K Dickson, JA Buckingham, J St Pierre and MD Brand, unpublished observations) whereas proton conductance of trout liver mitochondria at 20°C was about twice as high (Brookes et al. 1998).

What is the physiological function of carp UCP1? One might speculate that it either mediates thermogenesis, protects against oxidative stress by causing mild uncoupling, or has some role in fatty acid metabolism. To date, adaptive heat production has not been detected in the liver of ectotherms. Furthermore, the thermogenic function of UCP1 in mammalian brown adipose tissue is supported by high mitochondrial density, high respiratory capacity and high protein density of UCP1, features either lacking or not yet investigated in carp liver. Most fish are obligate ectotherms and recorded body temperatures always range within 1 or 2°C of ambient water temperature (Block 1994; Crawshaw 1976), but the possibility of local thermogenesis cannot be categorically excluded. One precedent is the brain heater organ of Scombroid fish (billfish, swordfish and butterfly mackerel) (Carey 1982). However, in Scombroid fish, counter-current heat exchangers and calcium cycling activity underlie local heat production and speculations on a thermogenic or thermocompensatory role of UCP1 in fish brain are not substantial.

In carp brain, we detected the highest abundance of UCP1 in the periventricular grey zone of the optic tectum containing nuclei of descending neurons into the optic tectum. The physiological role of the optic tectum is related to the control of sensory functions (e.g., the visual system). Descending nerve fibres control motor functions and metabolic homeostasis of the carp. Temperature compensation mechanisms in the neuronal system are suggested (Montgomery and Macdonald 1990) and in carp, rapid temperature drops even led to an increase of neuronal activity in the preoptic area (van den Burg et al. 2005). Under these conditions, peroxidation products are most likely increased and UCP1 might be required as a protective protein to prevent lipid peroxidation. Intriguingly, brain UCP1 mRNA levels were twofold increased after 7–10 days of cold acclimation in our study. For further studies, it would be of interest to cover the dynamic changes of UCP1 mRNA levels during cold acclimation in a time-course experiment as responses often occur in the earliest phase of cold stress.

If we focus on the activation of proton conductance in carp liver mitochondria by HNE, an involvement in the defense system against reactive oxygen species seems to be the most likely. The degree of activation correlates well with the previously reported UCP1 expression levels and

can be inhibited with GDP, leading to the conclusion that UCP1 is mediating HNE-activated proton conductance. Nevertheless, GDP inhibition could not be observed in rodent liver mitochondria (Echtay et al. 2003).

Considering the depressed metabolic state of CA carp during winter, reduced metabolism in the liver may result in decreased lipid peroxidation and less need for mild uncoupling. It has been hypothesised that the ability of superoxide and reactive alkenals to activate the proton conductance of all the major branches of the UCP core family suggests that the "ancestral" function of the UCPs was related to the response to radicals rather than to thermogenesis. In contrast, increased incorporation of polyunsaturated fatty acids in the phospholipids of mitochondrial membranes of CA carp should rather increase the risk for lipid peroxidation, a situation in which increased capacity for mild uncoupling would be of benefit. On this background it is currently difficult to judge whether the presence of fatty acid induced proton leak in WA carp, but not in CA fish, hints towards a role in the mitigation of superoxide production.

Fatty acid activation of proton conductance in carp UCP1 demonstrates that the biochemical properties of the common ancestor of the fish and mammalian protein already possessed the potential to be functional in the thermogenic machinery of brown adipose tissue later in mammalian evolution. We postulate that all orthologues of UCP1 upstream from the fish/mammal common ancestor will exhibit fatty acid activated proton conductance. Future studies on these proteins will help to define the onset point of UCP1-mediated adaptive thermogenesis. On the molecular level, the identification of orthologues earlier in the evolutionary tree will help to trace back the evolutionary origin of fatty acid sensitivity and will further extend our understanding of its biological significance.

Acknowledgments We thank Helen Boysen, Ian Goldstone and Sigrid Stöhr for excellent technical assistance, and the Department of Zoology, Cambridge University for providing us with their animal facilities. This study was funded by the Medical Research Council, the DAAD and the DFG (Grant KL 973/7).

References

Bishop T, Brand MD (2000) Processes contributing to metabolic depression in hepatopancreas cells from the snail *Helix aspersa*. J Exp Biol 203:3603–3612

Block BA (1994) Thermogenesis in muscle. Ann Rev Physiol 56:535–577

Brand MD (1995) Measurement of mitochondrial protonmotive force. In: Brown GC (ed) Bioenergetics: a practical approach. IRL Press, Oxford, pp 39–62

Brand MD, Affourtit C, Esteves TC, Green K, Lambert AJ, Miwa S, Pakay JL, Parker N (2004) Mitochondrial superoxide: production, biological effects, and activation of uncoupling proteins. Free Radic Biol Med 37:755–767

Brand MD, Esteves TC (2005) Physiological functions of the mitochondrial uncoupling proteins UCP2 and UCP3. Cell Metab 2:85–93

Brookes PS, Buckingham JA, Tenreiro AM, Hulbert AJ, Brand MD (1998) The proton permeability of the inner membrane of liver mitochondria from ectothermic and endothermic vertebrates and from obese rats: correlations with standard metabolic rate and phospholipid fatty acid composition. Comp Biochem Physiol B Biochem Mol Biol 119:325–334

Brookes PS, Hulbert AJ, Brand MD (1997) The proton permeability of liposomes made from mitochondrial inner membrane phospholipids: no effect of fatty acid composition. Biochim Biophys Acta 1330:157–164

Cannon B, Nedergaard J (2004) Brown adipose tissue: function and physiological significance. Physiol Rev 84:277–359

Canosa LF, Cerda-Reverter JM, Peter RE (2004) Brain mapping of three somatostatin encoding genes in the goldfish. J Comp Neurol 474:43–57

Carey FG (1982) A brain heater in the swordfish. Science 216:1327–1329

Considine MJ, Goodman M, Echtay KS, Laloi M, Whelan J, Brand MD, Sweetlove LJ (2003) Superoxide stimulates a proton leak in potato mitochondria that is related to the activity of uncoupling protein. J Biol Chem 278:22298–22302

Crawshaw LI (1976) Effect of rapid temperature change on mean body temperature and gill ventilation in carp. Am J Physiol 231:837–841

Cunningham SA, Wiesinger H, Nicholls DG (1986) Quantification of fatty acid activation of the uncoupling protein in brown adipocytes and mitochondria from the guinea-pig. Eur J Biochem 157:415–420

Echtay KS, Esteves TC, Pakay JL, Jekabsons MB, Lambert AJ, Portero-Otin M, Pamplona R, Vidal-Puig AJ, Wang S, Roebuck SJ, Brand MD (2003) A signalling role for 4-hydroxy-2-nonenal in regulation of mitochondrial uncoupling. EMBO J 22:4103–4110

Echtay KS, Roussel D, St Pierre J, Jekabsons MB, Cadenas S, Stuart JA, Harper JA, Roebuck SJ, Morrison A, Pickering S, Clapham JC, Brand MD (2002) Superoxide activates mitochondrial uncoupling proteins. Nature 415:96–99

Esteves TC, Parker N, Brand MD (2006) Synergy of fatty acid and reactive alkenal activation of proton conductance through uncoupling protein 1 in mitochondria. Biochem J 395:619–628

Garlid KD, Orosz DE, Modriansky M, Vassanelli S, Jezek P (1996) On the mechanism of fatty acid-induced proton transport by mitochondrial uncoupling protein. J Biol Chem 271:2615–2620

Gornall AG, Bardawill CJ, David MM (1949) Determination of serum proteins by means of the biuret reaction. J Biol Chem 177:751–766

Guderley H (1990) Functional significance of metabolic responses to thermal acclimation in fish muscle. Am J Physiol 259:R245–R252

Guderley H (2004) Metabolic responses to low temperature in fish muscle. Biol Rev Camb Philos Soc 79:409–427

Jastroch M, Withers K, Klingenspor M (2004) Uncoupling protein 2 and 3 in marsupials: identification, phylogeny, and gene expression in response to cold and fasting in *Antechinus flavipes*. Physiol Genomics 17:130–139

Jastroch M, Wuertz S, Kloas W, Klingenspor M (2005) Uncoupling protein 1 in fish uncovers an ancient evolutionary history of mammalian nonshivering thermogenesis. Physiol Genomics 22:150–156

Jimenez-Jimenez J, Ledesma A, Zaragoza P, Gonzalez-Barroso MM, Rial E (2006) Fatty acid activation of the uncoupling proteins requires the presence of the central matrix loop from UCP1. Biochim Biophys Acta 1757:1292–1296

Kent J, Koban M, Prosser CL (1988) Cold-acclimation-induced protein hypertrophy in channel catfish and green sunfish. J Comp Physiol [B] 158:185–198

Klingenberg M, Echtay KS (2001) Uncoupling proteins: the issues from a biochemist point of view. Biochim Biophys Acta 1504:128–143

Klingenberg M, Winkler E (1985) The reconstituted isolated uncoupling protein is a membrane potential driven H^+ translocator. EMBO J 4:3087–3092

Locke RM, Rial E, Nicholls DG (1982) The acute regulation of mitochondrial proton conductance in cells and mitochondria from the brown fat of cold-adapted and warm-adapted guinea pigs. Eur J Biochem 129:381–387

Lowell BB (1998) Adaptive thermogenesis: turning on the heat. Curr Biol 8:R517–520

Lucassen M, Koschnick N, Eckerle LG, Portner HO (2006) Mitochondrial mechanisms of cold adaptation in cod (*Gadus morhua* L.) populations from different climatic zones. J Exp Biol 209:2462–2471

Mark FC, Lucassen M, Portner HO (2006) Thermal sensitivity of uncoupling protein expression in polar and temperate fish. Comp Biochem Physiol D—Genomics Proteomics 1:365–374

Montgomery JC, Macdonald JA (1990) Effects of temperature on nervous system: implications for behavioral performance. Am J Physiol 259:R191–R196

Nicholls DG, Locke RM (1984) Thermogenic mechanisms in brown fat. Physiol Rev 64:1–64

Porter RK, Hulbert AJ, Brand MD (1996) Allometry of mitochondrial proton leak: Influence of membrane surface area and fatty acid composition. Am J Physiol 40:R1550–R1560

Reynafarje B, Costa LE, Lehninger AL (1985) O_2 solubility in aqueous media determined by a kinetic method. Anal Biochem 145:406–418

Rial E, Aguirregoitia E, Jimenez-Jimenez J, Ledesma A (2004) Alkylsulfonates activate the uncoupling protein UCP1: implications for the transport mechanism. Biochim Biophys Acta 1608:122–130

Richieri GV, Anel A, Kleinfeld AM (1993) Interactions of long-chain fatty acids and albumin: determination of free fatty acid levels using the fluorescent probe ADIFAB. Biochemistry 32:7574–7580

Shabalina IG, Jacobsson A, Cannon B, Nedergaard J (2004) Native UCP1 displays simple competitive kinetics between the regulators purine nucleotides and fatty acids. J Biol Chem 279:38236–38248

Smith AM, Ratcliffe RG, Sweetlove LJ (2004) Activation and function of mitochondrial uncoupling protein in plants. J Biol Chem 279:51944–51952

St Pierre J, Brand MD, Boutilier RG (2000) Mitochondria as ATP consumers: cellular treason in anoxia. Proc Nat Acad Sci USA 97:8670–8674

Talbot DA, Duchamp C, Rey B, Hanuise N, Rouanet JL, Sibille B, Brand MD (2004) Uncoupling protein and ATP/ADP carrier increase mitochondrial proton conductance after cold adaptation of king penguins. J Physiol 558:123–135

Tiku PE, Gracey AY, Macartney AI, Beynon RJ, Cossins AR (1996) Cold-induced expression of delta 9-desaturase in carp by transcriptional and posttranslational mechanisms. Science 271:815–818

Trueman RJ, Tiku PE, Caddick MX, Cossins AR (2000) Thermal thresholds of lipid restructuring and delta(9)-desaturase expression in the liver of carp (Cyprinus carpio L). J Exp Biol 203:641–650

van den Burg EH, Peeters RR, Verhoye M, Meek J, Flik G, Van der LA (2005) Brain responses to ambient temperature fluctuations in fish: reduction of blood volume and initiation of a whole-body stress response. J Neurophysiol 93:2849–2855

Wodtke E (1974) Effects of acclimation temperature on the oxidative metabolism of the eel (*Anguilla anguilla* L.). J Comp Physiol [B] 91:309–332

Wodtke E (1978) Lipid adaptation in liver mitochondrial membranes of carp acclimated to different environmental temperatures: phospholipid composition, fatty acid pattern and cholesterol content. Biochim Biophys Acta 529:280–291

Wodtke E (1981) Temperature adaptation of biological membranes Compensation of the molar activity of cytochrome c oxidase in the mitochondrial energy-transducing membrane during thermal acclimation of the carp (*Cyprinus carpio* L). Biochim Biophys Acta 640:710–720

Physiol Genomics 32: 161–169, 2008.
First published October 30, 2007; doi:10.1152/physiolgenomics.00183.2007.

CALL FOR PAPERS | *Comparative Genomics*

Marsupial uncoupling protein 1 sheds light on the evolution of mammalian nonshivering thermogenesis

M. Jastroch,[1] K. W. Withers,[2] S. Taudien,[3] P. B. Frappell,[4] M. Helwig,[1] T. Fromme,[1] V. Hirschberg,[1] G. Heldmaier,[1] B. M. McAllan,[5] B. T. Firth,[6] T. Burmester,[7] M. Platzer,[3] and M. Klingenspor[1]

[1]*Department of Animal Physiology, Faculty of Biology, Philipps-Universität Marburg, Marburg, Germany,* [2]*Department of Biological and Physical Sciences, University of Southern Queensland, Toowoomba, Queensland, Australia,* [3]*Genome Analysis, Leibniz-Institute for Age Research-Fritz Lipmann Institute, Jena, Germany;* [4]*Adaptational and Evolutionary Respiratory Physiology Laboratory, Department of Zoology, La Trobe University, Melbourne 3086, Victoria;* [5]*Physiology, School of Medical Sciences, The University of Sydney, Sydney, New South Wales;* [6]*Discipline of Anatomical Sciences, School of Medical Sciences, University of Adelaide, Adelaide, South Australia, Australia; and* [7]*Institute of Zoology, Biozentrum Grindel, University of Hamburg, Hamburg, Germany*

Submitted 10 August 2007; accepted in final form 20 October 2007

Jastroch M, Withers KW, Taudien S, Frappell PB, Helwig M, Fromme T, Hirschberg V, Heldmaier G, McAllan BM, Firth BT, Burmester T, Platzer M, Klingenspor M. Marsupial uncoupling protein 1 sheds light on the evolution of mammalian nonshivering thermogenesis. *Physiol Genomics* 32: 161–169, 2008. First published October 30, 2007; doi:10.1152/physiolgenomics.00183.2007.— Brown adipose tissue expressing uncoupling protein 1 (UCP1) is responsible for adaptive nonshivering thermogenesis giving eutherian mammals crucial advantage to survive the cold. The emergence of this thermogenic organ during mammalian evolution remained unknown as the identification of UCP1 in marsupials failed so far. Here, we unequivocally identify the marsupial *UCP1* ortholog in a genomic library of *Monodelphis domestica*. In South American and Australian marsupials, *UCP1* is exclusively expressed in distinct adipose tissue sites and appears to be recruited by cold exposure in the smallest species under investigation (*Sminthopsis crassicaudata*). Our data suggest that an archetypal brown adipose tissue was present at least 150 million yr ago allowing early mammals to produce endogenous heat in the cold, without dependence on shivering and locomotor activity.

marsupials; brown adipose tissue; cold acclimation

THE EVOLUTION OF BROWN ADIPOSE TISSUE (BAT) and its thermogenic uncoupling protein 1 (UCP1) is of major interest in the understanding of successful mammalian radiation. Adaptive nonshivering thermogenesis generated in BAT enables small eutherian mammals to maintain high body temperature independent of daily and seasonal temperature fluctuations (7). Although BAT was first described in 1551 (16), its thermogenic role was not recognized until the 1960s (10, 48), and it is now established that BAT contributes significantly to adaptive nonshivering thermogenesis of rodents, hibernators, and newborns (7). During cold exposure, sympathetic norepinephrine release activates BAT by stimulation of lipolysis and futile UCP1-dependent mitochondrial respiration, and recruitment of oxidative capacity. UCP1, a mitochondrial carrier protein, is located in the inner membrane of BAT mitochondria and provides the molecular basis for nonshivering thermogenesis (36). The protein increases proton conductance and uncouples oxidative phosphorylation from ATP synthesis by dissipating proton motive force as heat. All eutherian species investigated so far possess UCP1, with the exception of pigs where a naturally disrupted *UCP1* gene results in poor thermoregulation and sensitivity to cold exposure (3). The observation that UCP1-knockout mice are unable to defend their body temperature when exposed to the cold (17) confirms that UCP1 is crucial for adaptive nonshivering thermogenesis. In contrast to previous expectations, an ancient UCP1 ortholog was identified in the ectothermic teleost fish, but it is not expressed in adipose tissue and the physiological function might be other than heat production (28).

Marsupials are proficient thermoregulators and are capable of defending a stable body temperature during cold exposure (11, 15, 46). Evidence for nonshivering thermogenesis is a matter of debate in marsupial mammals, which separated from eutherians about 150 million yr ago (4). Since BAT is innervated by the sympathetic nervous system, norepinephrine released endogenously or injected into the animal leads to an increase in metabolic rate that is generally interpreted as a thermogenic response. In macropods the injection of norepinephrine led to an increase in thermogenesis (35, 37), a response attributed to skeletal muscle and not to BAT as found for eutherians (38, 52). It was suggested that adaptive nonshivering thermogenesis may be of major importance in Australian dasyurids as they belong to the smallest marsupials. Indeed, a thermogenic response to norepinephrine has been observed in *Sminthopsis crassicaudata* acclimated at 24°C (9). No thermogenic response to norepinephrine, however, was observed in *Antechinus stuartii* (41), nor in South American marsupials (12, 40). Despite evidence for nonshivering thermogenesis in some marsupials, no study has demonstrated the molecular basis nor the presence of adaptive nonshivering thermogenesis in response to cold.

Article published online before print. See web site for date of publication (http://physiolgenomics.physiology.org).

Address for reprint requests and other correspondence: M. Jastroch, Dept. of Animal Physiology, Faculty of Biology, Philipps-Universität Marburg, Karl-von-Frisch-Str. 8, 35043 Marburg, Germany (e-mail: Jastroch@staff.uni-marburg.de).

Nonshivering thermogenesis in eutherians is usually associated with BAT, but the presence of this specialized adipose organ remains controversial in marsupials. Morphological studies revealed BAT characteristics like multilocular fat droplets and vascularization in the interscapular adipose tissue of Bennett's wallaby pouch young (*Macropus rufogriseus rufogriseus*) (35). Another study investigating 38 different marsupial and one monotreme species precluded the presence of BAT in marsupials (18), by pointing out that morphological features of BAT also occurred in white adipose tissue during cold stress (33, 34). Reliance on morphological features only has led to the erroneous conclusion that birds possess BAT (39).

The discovery of UCP1 (19, 42) and the cloning of the cDNA sequence in rodents (2, 5) have stimulated work to identify UCP1 and its genomic presence in marsupials. Weak UCP1-like immunoreactivity has been seen in the interscapular fat deposit of *S. crassicaudata* (22); however, it is generally accepted that UCP1 antibodies cross-react with other mitochondrial carriers (43) or UCP2/3, both of which have been recently identified in marsupials (27). Previous studies suggested that UCP2/3 do not compensate for the lack of nonshivering thermogenesis mediated by UCP1, suggesting physiological roles other than heat production (17, 27).

Unequivocal detection of marsupial *UCP1* requires genomic or gene transcript sequence data. However, several attempts to identify the *UCP1* sequence have failed so far (27, 30, 31, 45). In this study we searched for the presence of BAT and UCP1 in one South American (*Monodelphis domestica*) and two Australian marsupial species (*S. crassicaudata* and *Antechinus flavipes*). Our approach was to search the genomic trace archives for UCP-like sequence fragments of *M. domestica* and characterize their physiological function.

MATERIALS AND METHODS

Isolation of genomic DNA of M. domestica and polymerase chain reactions. DNA was isolated from a tail tip of a female adult *M. domestica* using a standard phenol-chloroform extraction protocol as described previously (27). Following extraction, 50 ng of photometrically quantified DNA was used in subsequent polymerase chain reactions (PCR).

To define specific primers, we initially searched the *M. domestica* whole genome shotgun data provided by the National Center for Biotechnology Information (http://www.ncbi.nlm.nih.gov/Traces/trace.fcgi) for UCP-like sequence fragments using a consensus UCP1 coding sequence deduced from available eutherian sequences. The fragments were assembled according to the intron-exon structure of mouse *Ucp1*. Using the obtained trace alignments for primer definition, we generated primers (MWG Biotech, Ebersberg, Germany) to amplify a *UCP1*-like fragment ("forEx3": 5′-AGTGGCACAGCCTACAGATGT-3′; "revEx4": 5′-CTTGGAACGTCATC ATGTTTG-3′).

A second primer pair was deduced from *M. domestica* fragments displaying high identity to UCP2 ("forUCP2": 5′-GCCTACAAGACTATTGCCCGAGAGGAG-3′; "revUCP2": 5′-AAGCGGAGAAAGGAAGGCATGAACCC-3′).

Following 40 cycles of denaturation at 94°C for 1 min, annealing at 54°C (or 58°C for UCP2) for 1 min and extension at 72°C for 1 min (2 min for UCP2) were performed. A final extension at 72°C was applied for 10 min followed by rapid cooling to 4°C. The PCR product was gel-purified and ligated into a pGEMT-easy vector (Promega) for sequencing. Nested oligonucleotides were used for the screening of a genomic *M. domestica* bacterial artificial chromosome (BAC) library.

Sequence analysis of opossum BAC clones. High-density arrayed grids of the genomic opossum (*M. domestica*) BAC library VMRC-6 (Virginia Mason Research Center, distributed by BACPAC Resources, Oakland, CA; http://bacpac.chori.org) were screened by hybridization with radioactively end-labeled (T4-Polynucleotidekinase, Roche) oligonucleotides (13):

The *M. domestica* UCP1 specific primers were: md1.F 5′-GGGACTTTCCATGCCTACAA-3′, md2.R 5′-CAATAGCATTTCTTGCCACG-3′, md3.F 5′-AATAGCATCCGCAGAAGGAA-3′, md4.R 5′-CGTCCCTGGAAAGAGGAAAT-3′, and the *M. domestica* UCP2 specific primers were: md5.F 5′-CTCTTGCAGGTGGCATCC-3′, md6.R 5′-GACATTGGGCGAAGTTCCT-3′.

The identified BACs were verified by PCR using the probe oligos as primers. BACs VMRC6-66F14 (GenBank acc. no. AC171738, containing md*UCP*1) and VMRC6-60O3 (GenBank acc. no. AC171737, containing md1*UCP2* and md*UCP3*) were sequenced by a combination of shotgun and directed approaches (50). Base calling and assembly were performed by Phred/Phrap. Finishing was performed in accordance to the Human Genome Project standards with the support of external *M. domestica* whole genome shotgun data (http://www.ncbi.nlm.nih.gov/Traces/trace.fcgi).

Phylogenetic inference. The coding and amino acid sequences of *M. domestica UCP1*, *UCP2,* and *UCP3* were deduced from the corresponding genes. A comprehensive search for UCP sequences was performed in public databases (Ensembl genome browser, www.ensembl.org/NCBI, www.ncbi.nlm.nih.gov) by employing the basic local alignment search tool algorithm (1). An alignment of the UCP amino acid sequences was generated using ClustalX 1.81 (ftp://ftp-igbmc.u-strasbg.fr/pub/ClustalX) and adjusted by eye. Bayesian phylogenetic analyses were performed employing MrBayes 3.1.2 (http://mrbayes.csit.fsu.edu/) (44). The WAG model of amino acid substitution (51) with gamma distribution of rates was applied. Substitution rates were allowed to change across the tree under the covarion model (23). Prior probabilities for all trees were equal; starting trees were random. Two analyses were run in parallel for 1,000,000 generations. Trees were sampled every 100th generation, and posterior probabilities were estimated on the final 3,000 trees (burnin = 7,000). The tree was visualized using Treeview (http://taxonomy.zoology.gla.ac.uk/rod/treeview). The branch lengths are mean branch lengths of the consensus tree representing substitution rates.

Animal care and experimental protocol. The gray short-tailed opossums (*M. domestica*) were kindly donated by P. Giere and U. Zeller (Museum für Naturkunde, Humboldt-Universität zu Berlin, Germany). The opossums were held individually in the animal facility at the Philipps-Universität Marburg on a 12-h/12-h light/dark cycle (12:12 L:D) at an ambient temperature (T_a) of 24°C ± 2°C given water and fed cat food, curd mixed with fruit, and insects ad libitum. For cold acclimation experiments, two individuals were transferred into a separate chamber maintained at 12°C for 14 days.

Seven yellow-footed Antechinus (*A. flavipes*) were captured with Elliott traps in several subtropical habitats in Southeast Queensland (Australia) between January and March 2005. Fourteen fat-tailed dunnarts (*S. crassicaudata*) were obtained from a breeding colony at La Trobe University, Melbourne. Both species were housed individually in the animal facility of the University of Southern Queensland (12:12 L:D, lights on at 0700 h) at a T_a of 24°C ± 2°C. To investigate the effect of cold acclimation, seven *S. crassicaudata* and four *A. flavipes* were transferred to a climate chamber adjusted to 10°C for 17–22 days, whereas the other individuals remained at 24°C. Animals were given water and fed mealworms and cat food mix including calcium carbonate and vitamins ad libitum.

For cytochrome *c* oxidase (COX) activity assays, 10 *S. crassicaudata* were acclimated to 14 and 28°C at the University of Adelaide animal holding facilities in November 1990.

Experimental protocols for the use of Australian marsupials were approved by the Animal Ethics Committee of the University of

Southern Queensland, Queensland Environmental Protection Agency (permit number WISP02633304) and Environment Australia (export number WT2005-12380). Animal experiments involving *M. domestica* were performed in accordance with the German Animal Welfare Laws.

Tissue dissection. Two 22- and 25-day-old *M. domestica* embryos were euthanized and immediately frozen on dry ice and stored at −70°C prior to cryosectioning. All other individuals of *M. domestica, S. crassicaudata,* and *A. flavipes* were euthanized (carbon dioxide), and tissues were dissected. The samples were immediately snap frozen in liquid nitrogen. Frozen tissue samples were stored at −70°C until use. Liver, skeletal muscle, and adipose tissue of *S. crassicaudata* and *A. flavipes* were shipped from Australia in liquid nitrogen to Marburg, Germany.

In situ hybridization of M. domestica embryos. Sagittal body sections (20 μm) were processed using a cryosectioning microtome (Leica CM 3050) and were transferred to precooled object slides. A riboprobe complementary to *M. domestica* UCP1 (225 bp; primers forEx3, revEx4) and UCP2 (350 bp; forUCP2, revUCP2) was generated from a linearized cloned cDNA. Radioactive riboprobes using [^{35}S]UTP (1–2 × 10^7 cpm ml^{-1}), pre- and posthybridization procedures were performed as described previously (26). Controls were performed by hybridizing sections with equal-length sense riboprobes of UCP1 and UCP2.

RNA isolation and reverse transcriptase-PCR. Total RNA was isolated with TRIzol (GIBCO-BRL) according to the manufacturer's protocol. As an additional step, the RNA pellet was redissolved in a solution containing 6.3 mol/l guanidinium thiocyanate, 40 mmol/l sodium citrate pH 7, 0.8% sarcosyl, 8 mmol L^{-1} 2-mercaptoethanol, precipitated with 1 volume isopropanol, washed in 75% ethanol, and finally dissolved in DEPC-treated water. Total RNA was photometrically quantified at 260 nm and stored at −70°C. The isolated RNA was used for first strand cDNA synthesis (SUPERSCRIPT II, GIBCO/BRL) according to the manufacturer's protocol.

M. domestica UCP1 primers 5′-AGGTGAAGCCCAGACCATGGAT-3′ and 5′-GGCTGACACAAAGTGGCAAGGT-3′, comprising 6.7 kb of the *UCP1* gene and resulting in 550 bp cDNA sequence, were subjected to PCR with cDNAs of selected tissues. We performed 40 cycles of 94°C (1 min), 59°C (1 min), and 72°C (1 min) and terminated them by a 10 min extension at 72°C. The PCR products were gel-purified and ligated into a pJET vector (Fermentas). The full coding sequence of *S. crassicaudata* UCP1 including 5′- and 3′-untranslated region (UTR) was amplified using the smart RACE cDNA amplification kit (Clontech) combined with gene-specific primers deduced from *M. domestica* UCP13′-UTR:5′-CTACAGATGTGGTGAAAGTCAGAC-3′ and 5′-UTR:5′-GGCTGACACAAAGTGGCAAGGT-3′.

Subsequent sequencing was used to confirm the identity of the PCR products.

Northern blot analysis. RNA was separated by gel electrophoresis, transferred onto a nylon membrane, and hybridized as described previously (27). After hybridization, the blots were washed with 2× SSC/0.1% SDS for 20 min, 1× SSC/0.1% SDS for 10 min, 0.5× SSC/0.1% SDS for 10 min at room temperature, blots where then transferred to 0.1× SSC/0.1% SDS and washed for 10 min at 60°C. Signal intensities were then monitored by exposure to a PhosphorScreen (Molecular Dynamics). The hybridized probes were then detected by phosphor imaging (Storm 860, Molecular Dynamics), and signal intensities were quantified using ArrayVision 7.0 (Imaging Research). Ethidium bromide staining of total RNA served to normalize gel loading.

COX activity. COX activity of interscapular fat deposits of *S. crassicaudata* was measured polarographically at 25°C with a Hansa Tech oxygen electrode chamber as described previously (21, 32). These experiments were performed in 1990 after tissue transfer to Germany.

Statistical analysis. Values for COX activity and UCP1 mRNA are expressed as means ± SE. The Mann-Whitney *U*-test was applied for two-sample comparisons. Results were considered statistically significant at $P < 0.05$.

RESULTS AND DISCUSSION

Identification of UCP1 in M. domestica and S. crassicaudata. Following our trace archive search for UCP-like sequence fragments, a 346 bp fragment was amplified from genomic DNA of *M. domestica* containing a putative 121 bp intron. The 225 bp partial coding sequence displayed highest identity to eutherian UCP1 (76%) but lower similarity to eutherian UCP2 and UCP3 (69%). A second fragment was amplified using UCP2 primers exhibiting high identity to UCP2 of *A. flavipes* (92%, summarized in supplement 1).[1] A genomic *M. domestica* BAC library was screened using homologous primers deduced from the cloned UCP fragments. The isolated BAC clones were sequenced, analyzed, and aligned to the human reference sequence (Fig. 1).

The UCP-like gene of BAC VMRC6-66F14 is flanked by highly conserved orthologs of human ELMOD2 and human TBC1D9 and thereby resembling the region syntenic to the human UCP1 locus at chromosome 4. The two UCP genes on BAC VMRC6-60O3 found in juxtaposition as human UCP2 and UCP3 on chromosome 11 and were also enclosed by the orthologs of human DNAJB13 and DKFZP586P0123. The conserved synteny of the loci in vertebrates unequivocally identified the three *M. domestica* genes as UCP1, 2, and 3. Therewith, VMRC6-66F14 (GenBank AC171738) contains the *M. domestica* UCP1 and VMRC6-60O3 (GenBank AC171737) the UCP2 and UCP3 orthologs. Compared with the corresponding human UCP orthologs, the deduced amino acid sequence of *M. domestica* UCP2 exhibited highest identity (91%, 95% similarity), followed by *M. domestica* UCP3 (82%, 90% similarity), and *M. domestica* UCP1 (65%, 77% similarity).

Primers amplifying the *M. domestica* cDNA were also used to amplify a 250 bp UCP1 cDNA fragment of *S. crassicaudata*. Using 5′- and 3′-RACE-PCR, we identified 1,386 bp of UCP1 transcript including the full coding sequence (GenBank acc. no. EF622232). An alignment of the *S. crassicaudata* UCP1 coding sequence showed highest identity with *M. domestica* UCP1 (92%) and lower identity to eutherian and marsupial UCP2 and UCP3 (70–75%) (supplement 2).

Although an ancestral UCP1 ortholog appears in the vertebrate lineage as early as the divergence of ray-finned and lobe-finned fish 420 million yr ago (28), UCP1 disappears during evolution in the bird lineage (e.g., the chicken genome, unpublished observation) and became inactivated in pigs among eutheria (3). Biochemical studies suggest that fish UCP1 is an uncoupling protein with broadly the same activatory and inhibitory characteristics as mammalian UCP1 (26). The physiological relevance of ancient UCP1 in fish liver, despite of protein activity similar to the mammalian ortholog, may be other than heat production. Significant thermogenic uncoupling activity not only requires the presence of UCP1-mediated proton translocation but also a high mitochondrial oxidative capacity to achieve sufficient uncoupled respiration

[1] The online version of this article contains supplemental material.

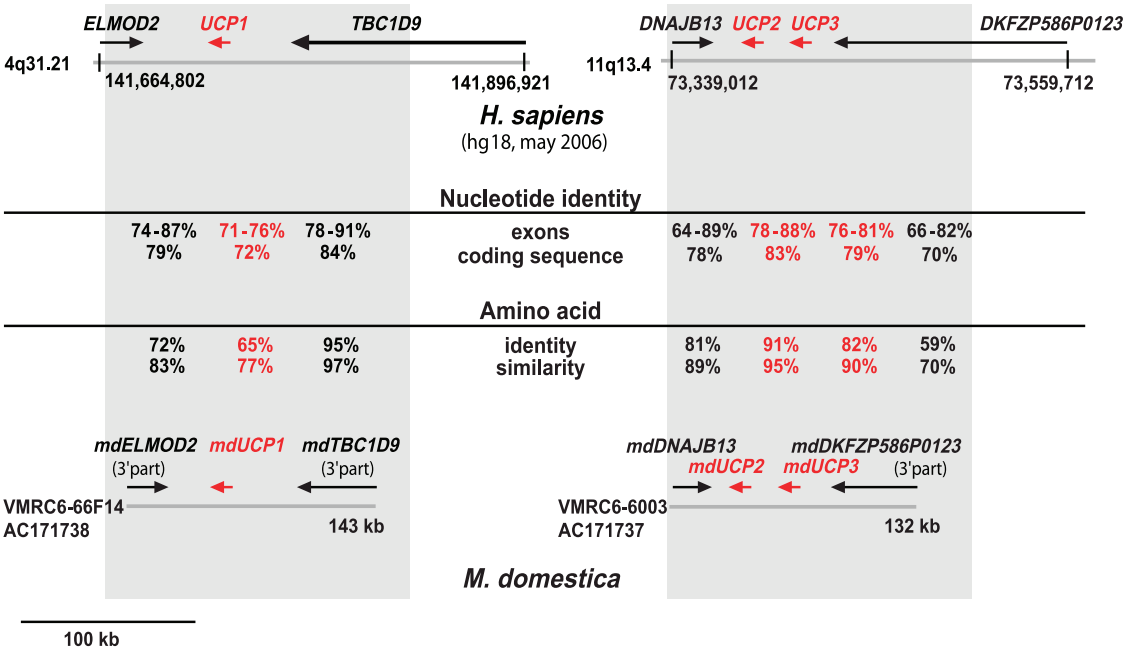

Fig. 1. Conservation of uncoupling protein (*UCP*) *1*, *UCP2*, *UCP3* and their flanking genes between human and opossum (*Monodelphis domestica*). The *top* scheme illustrates the genomic organization of the human *UCP1, 2,* and *3* locus; the *bottom* scheme the opossum orthologs. Nucleotide and amino acid identities between the orthologs are compared in the *middle* panel.

leading to relevant heat dissipation. The low oxidative capacity in fish hepatocytes can only contribute marginally to heat production compared with thermogenic brown adipocytes. Although fish UCP1 may already catalyze proton translocation, we must assume that during mammalian evolution this function was improved by natural selection. Our demonstration of marsupial *UCP1* in the present study is not only important because previous studies failed to demonstrate *UCP1* in marsupials, but distinct differences in the coding sequences may represent mutation events that improved the proton translocation function of marsupial and eutherian UCP1 (see supplement 2). Further experiments directly comparing different UCP1 orthologs in test systems will clarify if the proton transport activity increased during evolution and identify the functional residues.

Phylogenetic inference. For classification of the UCP sequences from *M. domestica* and *S. crassicaudata*, we generated a phylogenetic tree by a Bayesian method (24). Our comprehensive search for UCP sequences in public databases revealed 80 UCPs in the animal kingdom. The addition of further sequences, including UCP1 of *M. domestica* and *S. crassicaudata*, allowed a solid reconstruction of the UCP1, UCP2, and UCP3 clades (Fig. 2*A*, supplement 3). In contrast to previous studies (27, 29), this phylogenetic tree clearly resolves a monophyletic clade of all UCP1 proteins, including the fish UCP1 orthologs (Fig. 2*B*). The overall structure of the UCP1 clade reflects the phylogeny of the major vertebrate groups. A closer inspection of the UCP1 clade revealed that the branch length (substitution rate) between marsupials and eutherians is twice the length (0.4 expected mutations per site) of that between marsupials and amphibians (0.2 expected mutations per site). This is remarkable as marsupials are more distantly related to amphibians compared with eutherians. The large distance between marsupial and eutherian UCP1 sequences may indicate an accelerated evolution of UCP1 in eutherians in contrast to steady substitution rates found in the UCP2/3 clades. Eutherian UCP1 may have developed faster in response to so far unknown selection pressures. This would also explain why direct sequence comparisons result in a closer relationship of the fish and marsupial UCP1 sequences to UCP2/UCP3 than to eutherian UCP1.

Tissue-specific UCP gene expression in the South American marsupial M. domestica. Based on the identification of the *UCP1* gene in *M. domestica*, we investigated *UCP1* gene expression. We sampled cryosections of pouch embryos (22 and 25 days old) and sampled tissues of a juvenile (70 days old, post-nest vacation) and young adults (3 mo old).

Only in the juvenile we found dispersed adipose tissue deposits (brownish appearance) on the ribcage embedded in between pectoral muscle fibers (pectoral fat). Northern blotting analysis with a *UCP1* cDNA probe was insensitive, but using exon-spanning *M. domestica UCP1* primers comprising 6.7 kb of genomic sequence amplified a 550 bp cDNA fragment by PCR only in the pectoral fat (Fig. 3*A*), and subsequent sequencing clearly identified *UCP1* cDNA.

Hybridization techniques in all other individuals using a *M. domestica UCP1* cDNA probe demonstrated the lack of significant *UCP1* mRNA expression whereas *UCP2* mRNA was detectable (Fig. 3, *B* and *C*). In whole body cryosections of the embryos, *UCP2* mRNA was ubiquitously expressed with highest levels in spleen, heart, and liver (Fig. 3*B*). Nonspecific signals, as judged by comparison to the sense-control, occurred in calcified bone tissue. Northern blot analysis of selected tissues from the young adult revealed *UCP2* mRNA in all fat tissues, spleen, and intestine (Fig. 3*C*). Notably, *UCP1* mRNA expression in the interscapular fat, a typical BAT site in eutherians (in particular rodents), was undetectable.

Although the observed expression pattern in *M. domestica* is different from rodents, we have to consider that numerous eutherians do not possess significant amounts of BAT during their whole lifespan. In contrast to rodents and hibernators possessing

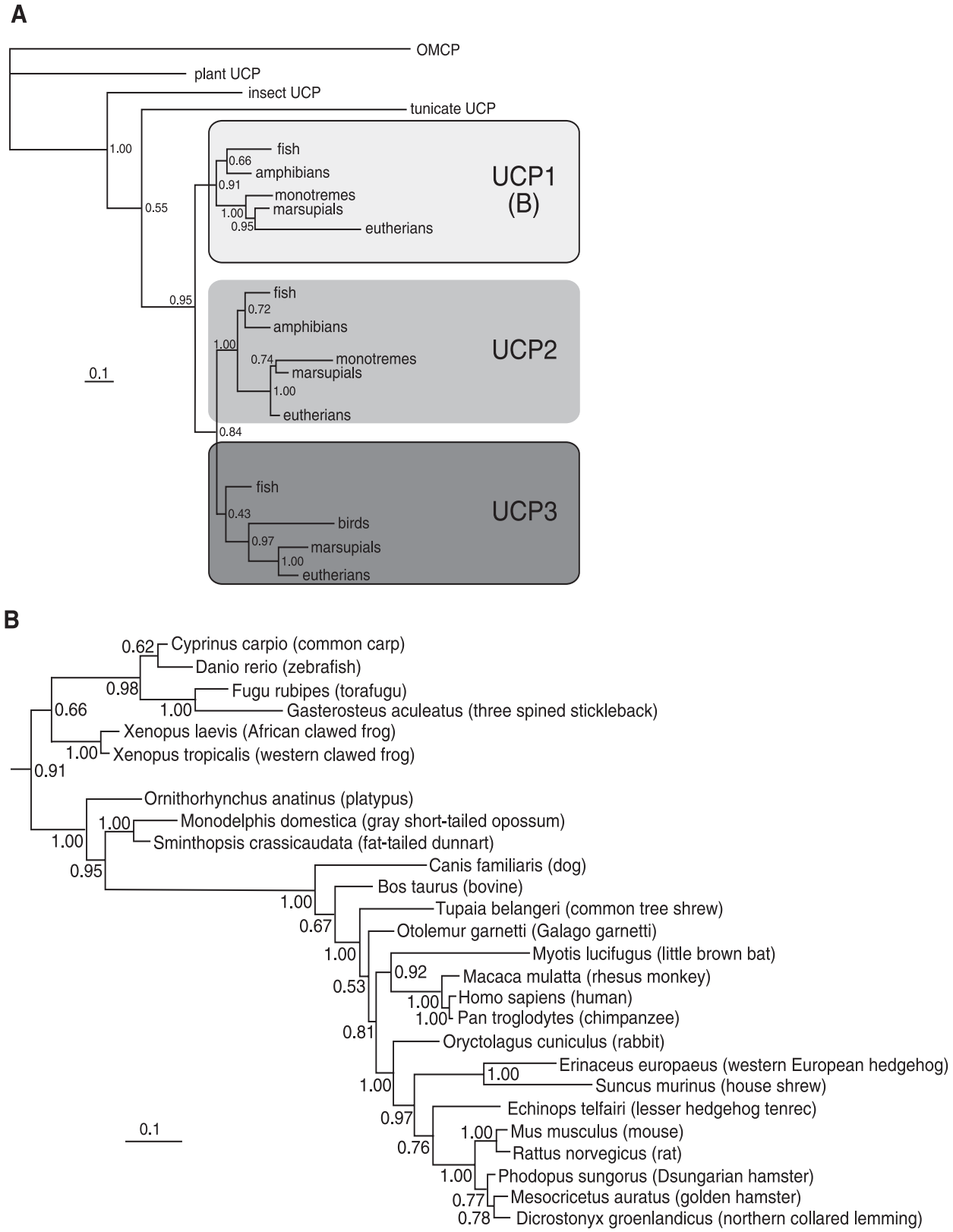

Fig. 2. Bayesian phylogeny of the core UCP family in vertebrates including marsupial UCP1 (*M. domestica* and *Sminthopsis crassicaudata*). An alignment of all available UCP sequences was analyzed by MrBayes 3.1.2, assuming a Whelan and Goldmann model of evolution. *A*: simplified tree resolving the phylogenetic relations of the core UCP family. The oxalacetate-malate carrier (OMCP) represents the out-group. *B*: detailed illustration of the UCP1 subgroup. Bayesian posterior probabilities are given at the branch nodes, and the scale bar indicates the substitution rate per aligned amino acid position. The complete phylogenetic tree can be found in supplement 3.

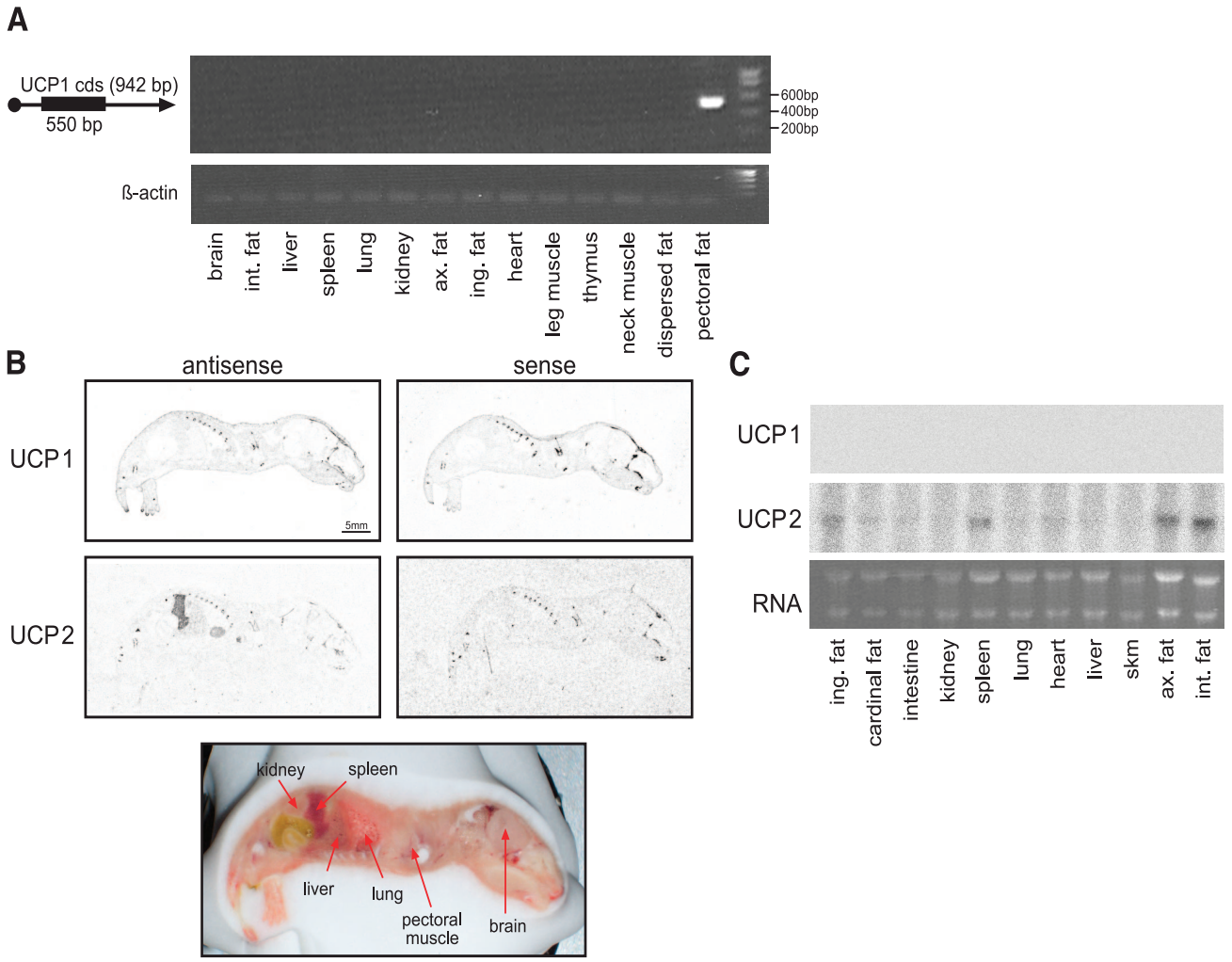

Fig. 3. Regulation of UCP1 and UCP2 gene expression in multiple tissues of the developing marsupial *M. domestica.* Homologous primers and radioactively labeled cDNA and riboprobes used. *A*: screening for UCP1 cDNA by PCR in multiple tissues of a 70-day-old juvenile. The 550 bp UCP1 fragment was amplified from adipose tissue embedded in the ribcage (pectoral fat). β-Actin mRNA served as a cDNA quality control. *B*: representative sagittal section showing whole body in situ hybridization of 22- to 25-day-old embryos. The UCP2 antisense riboprobe clearly hybridized with UCP2 mRNA in spleen, heart, and liver, while no UCP1 signals could be detected using an *M. domestica* UCP1 antisense riboprobe (*left*). All riboprobes hybridized artefactually with calcified bone as judged by comparison to sense controls (*right*). A photograph of a sagittal transection served to assign radioactive signals to organs. *C*: multiple tissue Northern blot analysis of 3-mo-old *M. domestica* including interscapular fat of warm-acclimated and cold-acclimated individuals (n = 4) and mouse BAT controls. Total RNA (10 μg) isolated from selected tissues was hybridized with a 225 bp UCP1 and a 350 bp UCP2 cDNA fragment of *M. domestica*. Total RNA from mouse BAT served as a control. Posthybridization for UCP1 was performed under less stringent conditions, detecting mouse UCP1. The *M. domestica* UCP2 probe detected mRNA in spleen, inguinal, and interscapular fat of *M. domestica*. Skm, skeletal muscle; int. fat, interscapular fat deposit; ing. fat, inguinal fat; ax. fat, axilliar fat.

BAT during their entire life, rabbits lose the ability to express *UCP1* 1 mo after birth (6), while in newborn bovine and lambs *UCP1* expression is of significance only 2 days after physiological birth (8). BAT, or at least *UCP1*, in marsupials may therefore only be of importance to overcome cold-stress around pouch or nest vacation. Increased responsiveness to norepinephrine coincides with pouch vacation in the wallaby and in the Eastern barred bandicoot *Perameles gunnii* (25, 35). Given the identification of marsupial *UCP1* in this study, these observations can be revisited and the contribution of BAT investigated.

Analysis of the UCP1 promoter region in M. domestica. Our experiments show a high specificity of marsupial *UCP1* expression in distinct adipose tissue sites. In rodents and humans, an enhancer box in the upstream promoter region contains condensed elements targeting *UCP1* expression to BAT and allows responsiveness to the cold (for review see Ref. 47). We searched a 10 kb genomic sequence upstream of the *UCP1* transcriptional start site of *M. domestica* for the presence of the enhancer box. Although we localized the enhancer box in all eutherians, including the ancient Afrotherian species *Echinops telfairii*, *M. domestica* lacks this distinct region, suggesting that the enhancer box first evolved in eutherian mammals (supplement 4). Despite the lack of the enhancer box, marsupial *UCP1* shows a remarkably high tissue-specificity targeting gene expression to distinct adipose tissue sites. The respective response elements may be dispersed across the promoter upstream region, and their presence cannot be categorically excluded.

Tissue-specific UCP gene expression in the Australian marsupials S. crassicaudata and A. flavipes. In *S. crassicaudata*, but not *A. flavipes*, we detected *UCP1* mRNA expression exclusively in the interscapular fat deposit, whereas no signal was detectable in liver and skeletal muscle (Fig. 4*A*). Probing with a *UCP2* fragment cloned from *Sminthopsis macroura* (27) detected highest *UCP2* mRNA levels in the

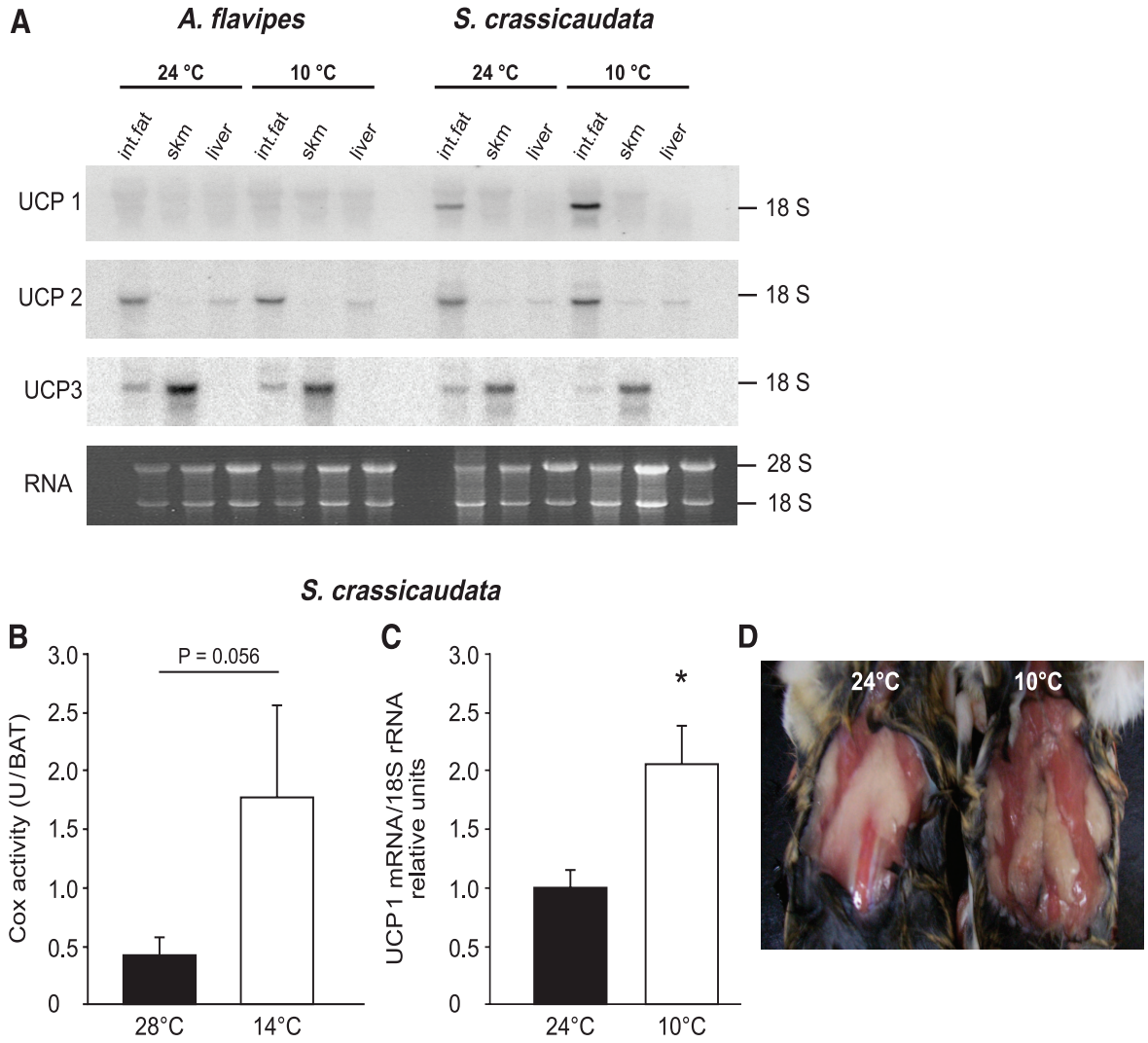

Fig. 4. *A*: UCP expression in selected tissues of the marsupials *S. crassicaudata* and *A. flavipes*. We hybridized 10 μg of total RNA with a *M. domestica* UCP1, *S. macroura UCP2,* and an *A. flavipes UCP3* cDNA probe. *B*: cytochrome c oxidase (COX) activity in interscapular adipose tissue homogenates of warm-acclimated and cold-acclimated *S. crassicaudata*. *C*: effect of cold exposure (10°C) on *UCP1* gene expression in *S. crassicaudata*. Radioactive intensities of specific signals are shown as relative units corrected by ethidium bromide staining of the 18S rRNA. The effects of cold acclimation was evaluated by Mann Whitney *U*-test; $*P < 0.05$. *D*: appearance of interscapular fat due to cold exposure. The photograph shows a dorsal view on the interscapular fat deposits of a warm-acclimated and a cold-acclimated *S. crassicaudata*.

interscapular fat region of *S. crassicaudata* and *A. flavipes,* whereas mRNA levels in liver and skeletal muscle were rather low (Fig. 4*A*). Cross-reactivity of the *UCP1* probe to *UCP2* could be excluded as the *UCP1* probe exhibited only 61–69% identity to *Sminthopsis* and *Antechinus* UCP2, respectively. Using an *A. flavipes UCP3* probe, we detected *UCP3* mRNA in skeletal muscle of both species confirming a previous study (27).

Here, we demonstrate that UCP1 is constitutively expressed in *S. crassicaudata*, the smallest marsupial under investigation, in contrast to a close dasyurid relative, *A. flavipes*. Previous studies in *Sminthopsis* and *Antechinus* species support the interdependence of nonshivering thermogenesis and marsupial UCP1. As would be likely to occur in the presence of brown adipose tissue, *Sminthopsis ssp.* elevate metabolic rate by 30% in response to 0.25 mg/kg norepinephrine at 24°C (*S. crassicaudata*) (9) or in response to cold exposure (*S. macroura*) (15). In contrast, *Antechinus ssp.* does not show a thermogenic response to norepinephrine (41). It is likely that the differences seen in UCP expression are a functional adaptation to reflect the significant life history differences between these species. *Sminthopsis ssp*. from arid Australia are exposed to pronounced seasonal fluctuations in environmental temperature, while the coastal *Antechinus ssp.* experiences less climatic fluctuations (14).

The lack of UCP1 in adult *A. flavipes* and *M. domestica* is a distinct difference to eutherian species of similar body mass (20). Conventional heating mechanisms like shivering in these marsupials may be adequate to defend body temperature in mild climates. This is, however, not the favored mode of thermogenesis during long-term cold exposure in eutherians, but the major mechanism when nonshivering is insufficient.

Effect of cold exposure on the marsupial interscapular fat deposit. Adaptive nonshivering thermogenesis in rodents requires the recruitment of oxidative capacity and UCP1 to increase heat production. In a preliminary study on *S. crassicaudata* in 1990, there was a strong trend toward increased COX activity in the interscapular fat deposit of cold-acclimated

individuals (Fig. 4*B*), but we were not able to detect *UCP1* mRNA using a rat *UCP1* cDNA probe. By using a marsupial *UCP1* probe in the present study, we demonstrated a significant upregulation of *UCP1* gene expression in response to cold. *UCP1* mRNA levels in cold-acclimated *S. crassicaudata* were twofold higher than in animals exposed to 24°C ($n = 7$, $P = 0.018$, Fig. 4*C*). Furthermore, appearance of the interscapular fat deposit changed from white in animals held at 24°C to brown in cold-acclimated *S. crassicaudata* (Fig. 4*D*), a transition that was absent in *M. domestica*.

Together with the absence of brownish color, *UCP1* mRNA expression was absent in the interscapular fat deposit in young adult *M. domestica* (3 mo old) even after cold exposure (supplement 5). Even posthybridization procedures under less stringent conditions revealed no signal in the interscapular fat of *M. domestica* but visualized cross-reactivity of the *M. domestica UCP1* cDNA probe to mouse UCP1. *M. domestica UCP2* mRNA levels remained unchanged in interscapular fat after cold exposure (supplement 4).

Despite some evidence for nonshivering thermogenesis in marsupials, no studies so far had investigated adaptiveness to the cold. In this study, cold-exposure elevated oxidative capacity and UCP1 expression in the interscapular fat of *S. crassicaudata* resembling adaptive molecular adjustments of eutherian BAT. Response of *S. crassicaudata UCP1* gene expression to cold exposure demonstrates different transcriptional control compared with *M. domestica*. Therefore, genomic *UCP1* promoter data of an Australian marsupial are required to identify *UCP1* response elements that are conserved during mammalian evolution.

Concluding Remarks

The successful radiation of eutherian mammals to cold environments was most likely facilitated by classical adaptive nonshivering thermogenesis depending on BAT and its crucial protein UCP1 (7). However, the origin and evolution of this thermogenic organ are unknown. Textbooks illustrate BAT as monophyletic trait of eutherians (49), and both UCP1 and BAT have been regarded as absent in marsupials (12, 18, 27, 30, 31, 38, 46); however, our study represents the first unequivocal demonstration of *UCP1* gene expression in adipose tissue of South American and Australian marsupials. In some marsupials like *M. domestica* or *A. flavipes*, UCP1 may be recruited transiently during early stages of development and is lost during adulthood, whereas other marsupials like *S. crassicaudata* retain UCP1 expression during the entire lifespan. These findings provide the molecular basis to investigate adaptive nonshivering thermogenesis and lead to interesting insights into the evolution of UCP1-mediated heat production. Our results suggest the presence of an archetypal BAT before the divergence of marsupials and eutherians more than 150 million yr ago allowing early mammals to pursue life in the cold.

ACKNOWLEDGMENTS

We thank Sigrid Stoehr for excellent technical assistance.

GRANTS

This research was supported by Deutsche Forschungsgemeinschaft DFG KL973/7 (to M. Klingenspor), by the Australian Centre for Systems Biology (CSBi), Department of Biological and Physical Sciences, University of Southern Queensland (to K. W. Withers and M. Jastroch), and the NGFN2 [01GS0483 (TP23)].

REFERENCES

1. **Altschul SF, Gish W, Miller W, Myers EW, Lipman DJ.** Basic local alignment search tool. *J Mol Biol* 215: 403–410, 1990.
2. **Aquila H, Link TA, Klingenberg M.** The uncoupling protein from brown fat mitochondria is related to the mitochondrial ADP/ATP carrier. Analysis of sequence homologies and of folding of the protein in the membrane. *EMBO J* 4: 2369–2376, 1985.
3. **Berg F, Gustafson U, Andersson L.** The uncoupling protein 1 gene (UCP1) is disrupted in the pig lineage: a genetic explanation for poor thermoregulation in piglets. *PLoS Genet* 2: e129, 2006.
4. **Bininda-Emonds OR, Cardillo M, Jones KE, MacPhee RD, Beck RM, Grenyer R, Price SA, Vos RA, Gittleman JL, Purvis A.** The delayed rise of present-day mammals. *Nature* 446: 507–512, 2007.
5. **Bouillaud F, Ricquier D, Thibault J, Weissenbach J.** Molecular approach to thermogenesis in brown adipose tissue: cDNA cloning of the mitochondrial uncoupling protein. *Proc Natl Acad Sci USA* 82: 445–448, 1985.
6. **Cambon B, Reyne Y, Nougues J.** In vitro induction of UCP1 mRNA in preadipocytes from rabbit considered as a model of large mammals brown adipose tissue development: importance of PPARgamma agonists for cells isolated in the postnatal period. *Mol Cell Endocrinol* 146: 49–58, 1998.
7. **Cannon B, Nedergaard J.** Brown adipose tissue: function and physiological significance. *Physiol Rev* 84: 277–359, 2004.
8. **Casteilla L, Champigny O, Bouillaud F, Robelin J, Ricquier D.** Sequential changes in the expression of mitochondrial protein mRNA during the development of brown adipose tissue in bovine and ovine species. Sudden occurrence of uncoupling protein mRNA during embryogenesis and its disappearance after birth. *Biochem J* 257: 665–671, 1989.
9. **Clements F, Hope PJ, Daniels CB, Chapman I, Wittert G.** Thermogenesis in the marsupial *Sminthopsis crassicaudata*: effect of catecholamines and diet. *Aust J Zool* 46: 381–390, 1998.
10. **Dawkins MJR, Hull D.** Brown adipose tissue and the response of new-born rabbits to cold. *J Physiol* 172: 216–238, 1964.
11. **Dawson TJ, Dawson WR.** Metabolic scope and conductance in response to cold of some dasyurid marsupials and Australian rodents. *Comp Biochem Physiol* 71A: 59–64, 1982.
12. **Dawson TJ, Olson JM.** Thermogenic capabilities of the opossum Monodelphis domestica when warm and cold acclimated: similarities between American and Australian marsupials. *Comp Biochem Physiol A* 89: 85–91, 1988.
13. **Galgoczy P, Rosenthal A, Platzer M.** Human-mouse comparative sequence analysis of the NEMO gene reveals an alternative promoter within the neighboring G6PD gene. *Gene* 271: 93–98, 2001.
14. **Geiser F.** Daily torpor and thermoregulation in Antechinus (Marsupialia). Influence of body mass, season, development, reproduction, and sex. *Oecologia (Berl)* 77: 395–399, 1988.
15. **Geiser F, Drury RL, McAllan BM, Wang DH.** Effects of temperature acclimation on maximum heat production, thermal tolerance, and torpor in a marsupial. *J Comp Physiol [B]* 173: 437–442, 2003.
16. **Gesner C.** *Medici Tigurini Historiae Animalium Liber I de Quadrupedibusuiuiparis.* Froschauer 1551, 840–844.
17. **Golozoubova V, Hohtola E, Matthias A, Jacobsson A, Cannon B, Nedergaard J.** Only UCP1 can mediate adaptive nonshivering thermogenesis in the cold. *FASEB J* 15: 2048–2050, 2001.
18. **Hayward JS, Lisson PA.** Evolution of brown fat: its absence in marsupials and monotremes. *Can J Zool* 70: 171–179, 1992.
19. **Heaton GM, Wagenvoord RJ, Kemp A, Nicholls DG.** Brown-adipose-tissue mitochondria: photoaffinity labelling of the regulatory site of energy dissipation. *Eur J Biochem* 82: 515–521, 1978.
20. **Heldmaier G.** Zitterfreie Wärmebildung und Körpergröβe bei Säugetieren. *Z vergl Physiol* 73: 222–248, 1971.
21. **Heldmaier G, Buchberger A.** Sources of heat during nonshivering thermogenesis in Djungarian hamsters: a dominant role of brown adipose tissue during cold adaptation. *J Comp Physiol [B]* 156: 237–245, 1985.
22. **Hope PJ, Pyle D, Daniels CB, Chapman I, Horowitz M, Morley JE, Trayhurn P, Kumaratilake J, Wittert G.** Identification of brown fat and mechanisms for energy balance in the marsupial, Sminthopsis crassicaudata. *Am J Physiol Regul Integr Comp Physiol* 273: R161–R167, 1997.
23. **Huelsenbeck JP.** Testing a covariotide model of DNA substitution. *Molecular Biology Evolution* 19: 698–707, 2002.

24. **Huelsenbeck JP, Ronquist F.** MRBAYES: Bayesian inference of phylogenetic trees. *Bioinformatics* 17: 754–755, 2001.
25. **Ikonomopoulou MP, Rose RW.** The development of endothermy during pouch life in the eastern barred bandicoot (Perameles gunnii), a marsupial. *Physiol Biochem Zool* 79: 468–473, 2006.
26. **Jastroch M, Buckingham JA, Helwig M, Klingenspor M, Brand MD.** Functional characterisation of UCP1 in the common carp: uncoupling activity in liver mitochondria and cold-induced expression in the brain. *J Comp Physiol [B]* 177: 743–752, 2007.
27. **Jastroch M, Withers K, Klingenspor M.** Uncoupling protein 2 and 3 in marsupials: identification, phylogeny, and gene expression in response to cold and fasting in *Antechinus flavipes*. *Physiol Genomics* 17: 130–139, 2004.
28. **Jastroch M, Wuertz S, Kloas W, Klingenspor M.** Uncoupling protein 1 in fish uncovers an ancient evolutionary history of mammalian nonshivering thermogenesis. *Physiol Genomics* 22: 150–156, 2005.
29. **Jimenez-Jimenez J, Zardoya R, Ledesma A, Garcia dL, Zaragoza P, Mar Gonzalez-Barroso M, Rial E.** Evolutionarily distinct residues in the uncoupling protein UCP1 are essential for its characteristic basal proton conductance. *J Mol Biol* 359: 1010–1022, 2006.
30. **Kabat AP, Rose RW, Harris J, West AK.** Molecular identification of uncoupling proteins (UCP2 and UCP3) and absence of UCP1 in the marsupial Tasmanian bettong, Bettongia gaimardi. *Comp Biochem Physiol B Biochem Mol Biol* 134: 71–77, 2003.
31. **Kabat AP, Rose RW, West AK.** Non-shivering thermogenesis in a carnivorous marsupial Sarcophilus harrisii, in the absence of UCP1. *J Therm Biol* 28: 413–420, 2003.
32. **Klaus S, Heldmaier G, Ricquier D.** Seasonal acclimation of bank voles and wood mice: nonshivering thermogenesis and thermogenic properties of brown adipose tissue mitochondria. *J Comp Physiol [B]* 158: 157–164, 1988.
33. **Loncar D, Afzelius BA, Cannon B.** Epididymal white adipose tissue after cold stress in rats. I. Nonmitochondrial changes. *J Ultrastruct Mol Struct Res* 101: 109–122, 1988.
34. **Loncar D, Afzelius BA, Cannon B.** Epididymal white adipose tissue after cold stress in rats. II. Mitochondrial changes. *J Ultrastruct Mol Struct Res* 101: 199–209, 1988.
35. **Loudon ASI, Rothwell NJ, Stock MJ.** Brown fat, thermogenesis and physiological birth in a marsupial. *Comp Biochem Physiol* 81A: 815–819, 1985.
36. **Nicholls DG, Locke RM.** Thermogenic mechanisms in brown fat. *Physiol Rev* 64: 1–64, 1984.
37. **Nicol SC.** Non-shivering thermogenesis in the potoroo, Potorous tridactylus (Kerr). *Comp Biochem Physiol* 59: 33–37, 1978.
38. **Nicol SC, Pavlides D, Andersen NA.** Nonshivering thermogenesis in marsupials: absence of thermogenic response to beta 3-adrenergic agonists. *Comp Biochem Physiol A* 117: 399–405, 1997.
39. **Oliphant LW.** First observations of brown fat in birds. *Condor* 85: 350–354, 1983.
40. **Opazo JC, Nespolo RF, Bozinovic F.** Arousal from torpor in the Chilean mouse-opossum (Thylamys elegans): does non-shivering thermogenesis play a role? *Comp Biochem Physiol A Mol Integr Physiol* 123: 393–397, 1999.
41. **Reynolds W, Hulbert AJ.** Cold acclimation in a small dasyurid marsupial: Antechinus stuartii. In *Carnivorous Marsupials*, edited by Archer M. Mosman, N. S. W. Australia: Royal Zoological Society of NSW, 1982, p. 278–283.
42. **Ricquier D, Kader JC.** Mitochondrial protein alteration in active brown fat: a sodium dodecyl sulfate-polyacrylamide gel electrophoretic study. *Biochem Biophys Res Commun* 73: 577–583, 1976.
43. **Ricquier D, Raimbault S, Champigny O, Miroux B, Bouillaud F.** Comment to Shinohara et al. (1991) *FEBS Letters* 293, 173–174. The uncoupling protein is not expressed in rat liver. *FEBS Lett* 303: 103–106, 1992.
44. **Ronquist F, Huelsenbeck JP.** MrBayes 3: Bayesian phylogenetic inference under mixed models. *Bioinformatics* 19: 1572–1574, 2003.
45. **Rose RW, West AK, Ye JM, McCormick GH, Colquhoun EQ.** Nonshivering thermogenesis in a marsupial (the Tasmanian bettong Bettongia gaimardi) is not attributable to brown adipose tissue. *Physiol Biochem Zool* 72: 699–704, 1999.
46. **Schaeffer PJ, Villarin JJ, Lindstedt SL.** Chronic cold exposure increases skeletal muscle oxidative structure and function in Monodelphis domestica, a marsupial lacking brown adipose tissue. *Physiol Biochem Zool* 76: 877–887, 2003.
47. **Silva JE, Rabelo R.** Regulation of the uncoupling protein gene expression. *Eur J Endocrinol* 136: 251–264, 1997.
48. **Smith RE.** Thermoregulation by brown adipose tissue in cold. *Fed Proc* 21: 221, 1962.
49. **Vaughan TA, Ryan JM, Czaplewski NJ.** *Mammalogy* (4th ed.). Saunders College Publishing, 2000.
50. **Wen G, Ramser J, Taudien S, Gausmann U, Blechschmidt K, Frankish A, Ashurst J, Meindl A, Platzer M.** Validation of mRNA/EST-based gene predictions in human Xp11.4 revealed differences to the organization of the orthologous mouse locus. *Mamm Genome* 16: 934–941, 2005.
51. **Whelan S, Goldman N.** A general empirical model of protein evolution derived from multiple protein families using a maximum-likelihood approach. *Mol Biol Evol* 18: 691–699, 2001.
52. **Ye JM, Edwards SJ, Rose RW, Steen JT, Clark MG, Colquhoun EQ.** Alpha-adrenergic stimulation of thermogenesis in a rat kangaroo (Marsupialia, Bettongia gaimardi). *Am J Physiol Regul Integr Comp Physiol* 271: R586–R592, 1996.

“Hormones Brain and Behaviour - SECOND EDITION”

Imprinted: Elsevier, Academic Press, 2008
Book Editors: Robert T. Rubin[1], Susan Fahrbach, Anne Etgen, Arthur Arnold, Donald Pfaff.
Chapter: "Genetic transmission of behaviour and its neuroendocrine correlates"
Chapter Authors: Boris Hambsch[2], Ludwig Czibere[2], Rainer Landgraf[2] und Chadi Touma[2].

[1)] McGowan Institute for Regenerative Medicine, Psychiatry and Mental Health, UC Pittsburgh, USA
[2)] Max-Planck-Institut für Psychiatrie, Verhaltensneuroendokrinologie, München, Germany

Contribution: Figure and Figure legend showing proteolytic cleavage of pro-opiomelanocortin by pro-hormone convertases and carboxypeptidases as an example of post-translational processing of pro-hormones and neuropeptide precursors.

Synopsis: Profound dysfunctions in diverse neuroendocrine systems have been described in psychiatric patients suffering from affective disorders such as anxiety and major depression. In order to elucidate the mechanisms underlying these functional alterations, animal models including mice genetically modified by either direct gene-targeting or by selective breeding approaches, have been exceedingly used, revealing valuable insights into neuroendocrine pathways conserved between rodents and men. In this chapter we focus on altered function and regulation of the hypothalamic-pituitary-adrenocortical (HPA) axis, including its involvement in emotionality and stress responsiveness. In this context, the corticotropin releasing hormone system and disturbances in glucocorticoid receptor signaling seem to be of central importance. However, changes in the expression and release patterns of vasopressin and oxytocin have also been shown to contribute profoundly to behavioural alterations including emotionality, stress coping, and social behaviours. Furthermore, substantial anxiogenic and nociceptive effects have been described for neurokinin receptors activated by tachykinins. Finally, signaling through opioid receptors was shown to be strongly involved in nociception, reward, anxiety-related and depression-like behaviours, upon binding of endorphin, dynorphin or enkephalin. Thus, research involving animal models and neuropeptide systems significantly contribute to our understanding regarding the transmission of genetic predispositions into clinically relevant neuroendocrine and behavioural endophenotypes.

„Analysis of pro-opiomelanocortin derived neuropeptides by MALDI-TOF mass spectrometry in the brain of the seasonal Siberian hamster (*Phodopus sungorus*).“

Helwig M.[1], Ludewig P.S.[1], Wegener C.[2], Mercer J.G.[3], Klingenspor M.[1]

[1)] *Department of Animal Physiology, Faculty of Biology, Philipps-Universität Marburg, Germany*
[2)] *Emmy Noether Neuropeptide Group, Philipps-Universität Marburg, Germany*
[3)] *The Rowett Research Institute, Division of Obesity and Metabolic Health, Molecular Endocrinology Group, Aberdeen Centre for Energy Regulation and Obesity, Aberdeen, UK*

Contribution: Oral Presentation at the 7th Annual Meeting of the British Society for Neuroendocrinology. 10.09.-11.09.2007, Nottingham, United Kingdom.

Abstract: Endopeptidases such as the prohormone-convertases 1/3 and 2 (PC1/3, PC2) cut the precursors of many neuropeptides at specific sequences (Arg – Arg or Lys – Arg) to generate intermediates with basic amino acid extensions on their C-termini. Related exopeptidases, carboxypeptidase E and D (CPE, CPD), are responsible for removing these amino acids before the peptides achieve biological activity. We investigated the effect of photoperiod on the posttranslational processing of the neuropeptide precursor, pro-opiomelanocortin (POMC), and its derived anorexigenic neuropeptide, alpha-melanocyte stimulating hormone (*α-MSH*), within key energy-balance regulating centres of the hypothalamus. We thus compared hypothalamic protein distribution of CPE, CPD and PC1/3-inhibiting peptide, pro-SAAS (incl. LEN/PEN), using immunhistochemistry (IHC) in short day (SD, 8h/16h light/dark) and long day (LD, 16h/8h light/dark) acclimatised hamsters. We showed up-regulation of PC2-ir (immunoreactivity) and CPE-ir associated with increased total-*α-MSH*-ir in SD hamsters. However, the limitations of IHC prevented us from distinguishing between the fractions of total-*α-MSH* composed of active *α-MSH*-(1-13) and inactive *α-MSH*-(1-16). To evaluate the yield of c-terminally truncated *α-MSH*-(1-13) by CPD/E we utilised for the first time a combination of brain tissue fixation by microwave irradiation and subsequent direct analysis of hypothalamic neuropeptides by *in situ* MALDI-TOF mass-spectrometry. We initially tested this neuropeptidomic approach using brain slices of mice and were able to detect many peptide products resulting from the posttranslational POMC processing pathway including POMC, PC2 and proSAAS. This novel combination of techniques enables us to now elucidate whether increased levels of carboxypeptidases lead to a higher abundance of the bioactive exoproteolytic-cleaved neuropeptide, *α-MSH*-(1-13), in SD acclimatised Siberian hamsters.

„Photoperiodische Regulation post-translationaler POMC Prozessierung im Hypothalamus des Djungarischen Zwerghamsters (*Phodopus sungorus*).“

Helwig M[1, 2], Tups A[1], Barrett P[2], Archer ZA[2], Khorooshi RMH[3], Mercer JG[2] and Klingenspor M[1].

[1)] *Department of Animal Physiology, Faculty of Biology, Philipps-Universität Marburg, Germany*
[2)] *The Rowett Research Institute, Division of Obesity and Metabolic Health, Molecular Endocrinology Group, Aberdeen Centre for Energy Regulation and Obesity, Aberdeen, UK*
[3)] *University of Southern Denmark, Medical Biotechnology Centre, Odense, Dänemark*

Contribution: Oral Presentation at the 22.Jahrestagung der Deutschen Adipositas Gesellschaft, 05.10. – 07.10.2006, Cologne. Akt Ernähr Med 2006; 31; DOI: 10.1055/s-2006-954470.

Das Körpergewicht saisonaler Säugetiere, wie des Djungarischen Zwerghamsters, zeigt einen ausgeprägten photoperiodisch abhängigen Jahresrhythmus welcher über ein komplexes neuronales Netzwerk reguliert wird. Die hauptsächlich im Hypothalamus lokalisierten Regelkreisläufe, welche Informationen über die vorherrschende Photoperiode (Verhältnis von Hell/Dunkel) und die Verfügbarkeit von körpereigenen Energiereserven (z.B. durch das im Fettgewebe synthetisierte Hormon Leptin) integrieren, verrechnen diese Informationen mit Hilfe orektisch und anorektisch wirkender Neuropeptide. Ein Großteil dieser Neuropeptide liegt jedoch zunächst in Form inaktiver Vorläuferpeptide vor und muss eine Reihe post-translationaler Modifizierungen durch endo- und exoproteolytisch schneidende Enzyme durchlaufen, bevor die letztendlich bioaktiven Neuropeptide entstehen. In dieser Studie untersuchten wir den Effekt der Photoperiode auf die Expression der Prohormonkonvertasen 1/3 und 2 (PC1/3, PC2), sowie der Carboxypeptidase E (CPE) und ihren Einfluss auf die Prozessierung Energiemetabolismus regulierender Neuropeptidvorläufer, wie Pro-opiomelanocortin (POMC). mRNA und Immunoreaktivität (-ir) des Enzymes PC1/3 und der durch PC1/3 generierten Neuropeptide ACTH und Orexin-A waren nicht von den photoperiodische Veränderungen beeinflusst. Im Gegensatz dazu resultierte aus einer Verkürzung der Lichtperiode (KT) gesteigerte PC2-ir, welche mit erhöhter ir der POMC Produkte α-MSH and β-Endorphin einherging. Unsere Ergebnisse demonstrieren, dass die Reifung biologisch aktiver Neuropeptide selektiv durch die Aktivität der hormonprozessierenden Enzyme PC1/3, PC2 und CPE auf post-translationaler Ebene reguliert wird. Dieser Prozess ist photoperiodisch gesteuert und stellt, neben der Genexpressionsregulation auf transkriptioneller Ebene des Vorläuferpeptids selbst, eine weitere Kontrollinstanz bei der Proteinbiosynthese von Neuropeptiden dar.

"Photoperiodical Regulation of Post-Translational POMC Processing in the Hypothalamus of the Seasonal Siberian Hamster (*Phodopus sungorus*)."

Helwig M[1, 2], Tups A[1], Barrett P[2], Archer ZA[2], Khorooshi R.M.H.[3], Mercer JG[2] and Klingenspor M[1].

[1)] *Department of Animal Physiology, Faculty of Biology, Philipps-Universität Marburg, Germany*
[2)] *The Rowett Research Institute, Division of Obesity and Metabolic Health, Molecular Endocrinology Group, Aberdeen Centre for Energy Regulation and Obesity, Aberdeen, UK*
[3)] *University of Southern Denmark, Medical Biotechnology Centre, Odense, Denmark*

Contribution: Oral Presentation at the 10th International Congress on Obesity, 03.09.-08.09.2006, Sydney, New South Wales, Australia.

Abstract: Body weight in seasonal animals such as the Siberian hamster (*Phodopus sungorus*) is regulated by a complex interaction of neuropeptides in a hypothalamic network of neurons that integrates environmental photoperiod inputs. Most of these energy balance-regulating neuropeptides derive from larger biologically inactive precursors and have to undergo post-translational processing by endo- and exoproteolytic cleavage. We investigated the effect of photoperiod on the expression of prohormone convertases 1 (PC1/3), 2 (PC2), carboxypeptidase E (CPE) and the proteolytic processing of the neuropeptide precursor pro-opiomelanocortin (POMC) within key energy balance regulating centres of the hypothalamus. We compared mRNA levels and protein distribution of the enzymes PC1/3, PC2, CPE, and the neuropeptide precursor POMC and its derived peptides ACTH, α-MSH and β-endorphin in selected hypothalamic areas of long day (LD, 16h light: 8h dark) and short day (SD, 8h light: 16h dark) acclimated Siberian hamsters. mRNA and immunoreactivity of PC1/3 enzyme and neuropeptides cleaved by PC1/3 such as ACTH in the ARC, and orexin A in the LH, were not affected by photoperiod changes. In contrast increased levels of PC2 mRNA and protein were associated with higher abundance of the mature neuropeptides α-MSH and β-endorphin in SD. CPE immunoreactivity was increased in SD and after leptin injection suggesting increased terminal activation of neuropeptides subsequent to processing by PC2. The photoperiod-driven regulatory mechanism by differential activity of the major neuroendocrine enzymes on a posttranslational level observed in this study could be an additional universal control point for selective maturation of energy balance related neuropeptides.

"Proteolytic Processing of POMC in the Hypothalamus of the Seasonal Siberian Hamster (*Phodopus sungorus*) is regulated by Photoperiod."

Helwig M[1,2], Tups A[1], Barrett P[2], Archer ZA[2], Khorooshi RMH[3], Mercer JG[2] and Klingenspor M[1].

[1)] *Department of Animal Physiology, Faculty of Biology, Philipps-Universität Marburg, Germany*
[2)] *The Rowett Research Institute, Division of Obesity and Metabolic Health, Molecular Endocrinology Group, Aberdeen Centre for Energy Regulation and Obesity, Aberdeen, UK*
[3)] *University of Southern Denmark, Medical Biotechnology Centre, Odense, Denmark*

Contribution: Poster Presentation at the 26th Blankenese Conference, Energy Metabolism: From Feeding Behaviour to Metabolic Diseases. 20.05.-24.05.2006, Hamburg-Blankenese, Germany.

Abstract: Body weight in seasonal animals such as the Siberian hamster (*Phodopus sungorus*) is regulated by a complex interaction of neuropeptides in a hypothalamic network of neurons that integrates environmental photoperiod inputs. Most of these energy balance-regulating neuropeptides derive from larger biologically inactive precursors and have to undergo post-translational processing by endo- and exoproteolytic cleavage. We investigated the effect of photoperiod on the expression of prohormone convertases 1 (PC1/3), 2 (PC2), carboxypeptidase E (CPE) and the proteolytic processing of the neuropeptide precursor pro-opiomelanocortin (POMC) within key energy balance regulating centres of the hypothalamus. We compared mRNA levels and protein distribution of the enzymes PC1/3, PC2, CPE, and the neuropeptide precursor POMC and its derived peptides ACTH, α-MSH and β-endorphin in selected hypothalamic areas of long day (LD, 16h light: 8h dark) and short day (SD, 8h light: 16h dark) acclimated Siberian hamsters. mRNA and immunoreactivity of PC1/3 enzyme and neuropeptides cleaved by PC1/3 such as ACTH in the ARC, and orexin A in the LH, were not affected by photoperiod changes. In contrast increased levels of PC2 mRNA and protein were associated with higher abundance of the mature neuropeptides α-MSH and β-endorphin in SD. CPE immunoreactivity was increased in SD and after leptin injection suggesting increased terminal activation of neuropeptides subsequent to processing by PC2. The photoperiod-driven regulatory mechanism by differential activity of the major neuroendocrine enzymes on a posttranslational level observed in this study could be an additional universal control point for selective maturation of energy balance related neuropeptides.

"Uncoupling protein 1 is expressed in the brain of ectothermic vertebrates."

M. Klingenspor[1], **M. Helwig**[1], T. Fromme[1], M.D. Brand[2], W. Kloas[3], S. Taudien[4], M. Platzer[4], M. Jastroch[1]

[1)] Department of Animal Physiology, Faculty of Biology, Philipps-Universität Marburg, Germany
[2)] Medical Research Council Dunn Human Nutrition Unit, Cambridge, UK
[3)] Dept. of Inland Fisheries, Leibniz-Institute of Freshwater Ecology, Berlin, Germany
[4)] Leibniz Institute for Age Research Fritz-Lipmann-Institute, Genome Analysis, Jena, Germany

Contribution: Co-author to a Poster at the 14th European Bioenergetics Conference, 22.07.-27.07.06 Moscow, Russia. BIOCHIMICA ET BIOPHYSICA ACTABIOENERGETICS: 375-376 Suppl. S 2006.

Abstract: Uncoupling proteins (UCPs) regulate proton conductance of the mitochondrial inner membrane. Until recently the thermogenic uncoupling protein 1 (UCP1) was considered to be unique to brown adipose tissue mitochondria of placental mammals where it dissipates proton motive force as heat (non-shivering thermogenesis, NST). We identified the ortholog of mammalian UCP1, as well as the two paralogs UCP2 and UCP3 in ectothermic bony fishes suggesting that the members of the core UCP family already existed 420 million years ago and are present in all living vertebrates (1). Accordingly, we found all three UCPs in the genomes of the Clawed frog (*Amphibia*) and the Opossum (*Marsupialia*), whereas in the Chicken genome only UCP3 can be found so far. The biological function of thermogenic UCP1 in ectothermic vertebrates is not understood. In the Common Carp (*Cyprinus carpio*) UCP1 is strongly expressed in the liver. In isolated Carp liver mitochondria fatty acids increase proton conductance in a GDP-sensitive manner. Thus, UCP1 orthologs of fish and mammals share key functional characteristics. UCP1 expression is also detected in the brain, albeit at lower expression levels than in liver. We studied the effect of cold acclimation on UCP1 gene expression in the Carp. Whereas UCP1 mRNA levels sharply declined in the liver of cold exposed Carp, Northern blot analysis of whole brain RNA revealed a two-fold increase of UCP1 expression. We therefore performed In Situ Hybridisation (ISH) of coronal and sagittal sections of the Carp brain with a 35S-labelled Carp UCP1 cRNA probe. This analysis revealed distinct localised expression of UCP1 in the forebrain (periventricular grey zone of the optic tectum) and the brain stem (solitary and trigeminal tract). We hypothesise that cold-induced UCP1 expression may increase the capacity for local non-shivering thermogenesis in selected brain regions in order to maintain critical neuronal functions in cold water.

"Differential expression of obesity related genes of the nucleus of the solitary tract in the Siberian hamster (*Phodopus sungorus*)."

Helwig, M.[1, 2], Archer, Z.A.[2], Klingenspor, M.[1], and Mercer, J.G.[2].

[1)] *Department of Animal Physiology, Faculty of Biology, Philipps-Universität Marburg, Germany*
[2)] *The Rowett Research Institute, Division of Obesity and Metabolic Health, Molecular Endocrinology Group, Aberdeen Centre for Energy Regulation and Obesity, Aberdeen, UK*

Contribution: Oral Presentation at the 7th European Congress of Endocrinology, 03.09.-07.09.2005, Gothenburg, Sweden.

Abstract: Information on the status of energy reserves (in terms of fat, leptin), and the quality (sense of taste, glossopharyngeal nerve) and quantity of food (mechanical sensors in the stomach, vagus nerve) converge and are integrated and processed in a specific region of the central nervous system called the nucleus of the solitary tract (NTS) in the hindbrain. Together with the hypothalamus this key neuronal centre is responsible for the generation of feeding behaviour and the storage of fat reserves. Until now the hindbrain has mainly been implicated in regulating only acute responses to food uptake via inducing sense of satiety rather than modulating a chronic response. We suggest that this area could also play a role in the long-term regulation of body weight and energy balance. In order to test this we analysed the expression of different obesity related genes within the hindbrain of the seasonal Siberian hamster. Forty male hamsters were kept in long days (LD; 16h light: 8h dark) at 22-23°C with *ad libitum* access to food (Labsure pelleted diet). After 2 weeks they were divided into two weight matched groups (n=20/group). Twenty animals remained in LD whereas twenty animals were transferred to a short-day (SD; 8 light: 16h dark) photoperiod. After 14 weeks photoperiodic acclimation LD [44.9g (±3.8g)] and SD [30.6g (±2.4g)] hamsters were killed and the brains dissected. Hindbrain gene expression for melanocortin 3-receptor (MC3-R), melanocortin 4-receptor (MC4-R), growth hormone secretagogue–receptor (GHS-R), cocaine- and amphetamine-regulated transcript (CART), pre-proglucagon (PPG) and galanin was measured by *in situ* hybridisation. Messenger-RNA of all candidates was detected within the NTS. MC3-R ($P \leq 0.001$) and PPG ($P \leq 0.001$) gene expression were significantly up-regulated in LD whereas photoperiod did not affect gene expression for MC3-R, GHS-R, CART and galanin. Our data suggest that differential MC4-R and PPG gene expression in NTS are involved in the chronic regulation of energy balance providing evidence of the hindbrain being additionally a neuroanatomical centre in the seasonal regulation of energy balance.

"Differential precursor-protein convertases PC1 and PC2 gene-expression in the hypothalamus of the seasonal Siberian hamster (Phodopus sungorus)."

Helwig, M.[1,2], Tups, A.[1], Barrett, P.[2], Braulke. L.J.[1], Mercer, J.G.[2] and Klingenspor, M.[1].

[1)] *Department of Animal Physiology, Faculty of Biology, Philipps-Universität Marburg, Germany*
[2)] *The Rowett Research Institute, Division of Obesity and Metabolic Health, Molecular Endocrinology Group, Aberdeen Centre for Energy Regulation and Obesity, Aberdeen, UK*

Contribution: Poster Presentation at the ACERO Symposium 10: "Dietary approaches to weight regulation" 14.-15.April 2005, Aberdeen, Scotland, United Kingdom.

Abstract: Endoproteases such as prohormone convertase 1 (PC1) and prohormone convertase 2 (PC2) act in secretory pathways involving tissue-specific processing of prohormones and neuropeptide precursors into mature bioactive products. Consequently they play an essential role in the regulation of neuropeptide maturation [e.g. pro-opiomelanocortin (POMC) into alpha-melanocyte stimulating hormone (α-MSH)] within key energy balance regulating centres like the hypothalamus. In order to investigate the long-term effect of photoperiod on the gene expression of PC1 and PC2 we compared the mRNA levels of natural-day (ND, light phase depending on natural day length), long day (LD, 16h light: 8h dark) and short day (SD, 8h light: 16h dark) acclimated Siberian hamsters in selected hypothalamic areas. To investigate the time depended effect of photoperiod on PC1 and PC2 mRNA in a "switch back" experiment, hamsters were acclimated to SD [n=16, 28g (±3g)] for 16 weeks whereupon they were retransferred to LD. A control group [n=16, 40.5g (±5.5g)] were maintained continuously in LD throughout the experiment. PC2 mRNA, which was mainly expressed in the dorsomedial posterior arcuate nucleus (dmpARC; $P \leq 0.001$) and the arcuate nucleus (ARC, $P \leq 0.01$) of the hypothalamus was significantly higher in ND and reaching its maximum in January. The increase of PC2 gene expression correlated with the decline of day length photoperiod. PC1 gene expression was detected in the ARC and the lateral hypothalamus revealing a trend to higher levels in ND but was not significant.

PC2 gene expression in SD photoperiod within the dmpARC ($P \leq 0.01$) was significantly up-regulated after SD acclimation for 16 weeks. Retransfer to LD decreased gradually PC2 mRNA until after 6 weeks LD levels were attained. Our data reveal a strong photoperiodic regulation of PC2, suggesting a distinct post-translational activity in hypothalamic areas like the dmpARC and the ARC, which may lead to higher concentration of mature neuropeptides in SD photoperiod. In addition we provide further evidence of the dmpARC being a separate area, which exhibits high neuroendocrine activity within the hypothalamus.

"Orexin-B-immunoreactive fibres make close appositions on cell bodies and fibres immunoreactive for Neuropeptide Y within the intergeniculate leaflet of the Djungarian hamster (*Phodopus sungorus*)."

R.M.H. Khorooshi[1], **M. Helwig**[1], M. Klingenspor[1].

[1)] *Department of Animal Physiology, Faculty of Biology, Philipps-Universität Marburg, Germany*

Contribution: Poster Presentation at the 7th Annual Meeting of the Neuroendocrinology Section of the German Society of Endocrinology (DGE), 17.10.-18.10.2003, Lübeck, Germany, Exp. Clin Endocrinol Diabetes 2003; 111;P42.

Abstract: The intergeniculate leaflet (IGL) is part of the neural network involved in the regulation of the circadian timing processes. The IGL receives photic- and non-photic- inputs from retina and midbrain and projects this information to the suprachiasmatic nucleus (SCN) through the geniculohypothalamic tract (GHT) arising mostly from neuropeptide Y (NPY) containing neurons in the IGL. Based on distribution of orexin-B-ir fibers and terminal boutons in the IGL we suggest that one pathway by which orexin-B may influence circadian timing could be through interaction with NPY, the most abundant neuropeptide/neurotransmitter in the IGL of the Djungarian hamster. In order to test this idea we investigated the anatomical basis for such a interaction using dual-label immunofluorescence. Orexin B-ir fibers with terminals had close apposition on NPY-lir perikarya and fibers with terminal boutons in the rostro-caudal extension of the IGL. Furthermore, NPY-lir fibers in the peripheral structures of the SCN had apposition from orexin-B-ir fibers and terminals. These observations provide anatomical basis for orexin-B to interact with NPY and influence the circadian timing system.

ZUSAMMENFASSUNG

Das Körpergewicht saisonaler Säugetiere, wie das des Djungarischen Zwerghamsters (*Phodopus sungorus*), zeichnet sich durch einen ausgeprägten Jahresrhythmus aus. Die jahreszeitliche Anpassung des Körpergewichts erfolgt dabei abhängig von der vorherrschenden Photoperiode und wird zentral im Hypothalamus durch ein komplexes Zusammenspiel unterschiedlicher Neuropeptide und Hormone koordiniert. Viele dieser Hormone und Neuropeptide werden jedoch zunächst als größere, biologisch inaktive Vorläuferpeptide synthetisiert und müssen eine Kaskade unterschiedlicher post-translationaler Modifikationen durchlaufen bevor sie biologisch wirksam werden. Die vorliegende Arbeit befasst sich mit den Enzymen, welche für die proteolytische Prozessierung dieser Vorläufer verantwortlich sind. Es konnte gezeigt werden, dass die Endoprotease Prohormonkonvertase 2 (PC2) und die Exoprotease Carboxypeptidase E (CPE) im Hypothalamus des kurztag-akklimatisierten (KT) Hamsters, vermehrt gebildet werden. Anhand des Vorläuferpeptids Pro-opiomelanocortin (POMC) konnte zudem demonstriert werden, dass mit den erhöhten PC2- und CPE-Spiegeln im KT eine vermehrte Synthese der Neuropeptide alpha-Melanozyten stimulierendes Hormon (α-MSH) und β-Endorphin (β-END) einhergeht. Beide Peptide gehen aus dem Vorläuferprotein POMC hervor und sind dafür bekannt die Nahrungsaufnahme langfristig zu inhibieren. Es konnte somit gezeigt werden, dass die Proteinbioynthese von Neuropeptiden, welche den saisonalen Energiehaushalt des Djungarischen Zwerghamsters steuern, neben der transkriptionellen Steuerung der Genexpression auch durch post-translationale Prozessierung reguliert wird. Des Weiteren konnte in einem weiteren Projekt demonstriert werden, dass peptiderge Komponenten des Hirnstammes, welche für die Steuerung des kurzzeitigen Sättigungs- und Hungergefühls verantwortlich sind, ebenfalls einer photoperiodisch abhängigen Modulation unterliegen. Diese Modulation trägt neben der langfristigern Steuerung des Energiehaushalts durch den Hypothalamus vermutlich ebenfalls zu dem saisonal sehr ausgeprägten Gewichtszyklus des Djungarischen Zwerghamsters bei.

Dipl. Biol. Michael Helwig

- Curriculum vitae -

Philipps-Universität Marburg

Faculty of Biology
Department of Animal Physiology
Karl-von-Frisch-Str. 8
35043 - Marburg - Germany

Email: helwigmi@staff.uni-marburg.de
Tel: +49 (0)6421 28-23395
Fax: +49 (0)6421 28-28937

PERSONAL HISTORY

• Date of birth	03.01.1978
• Place of birth:	Kassel
• Citizenship:	German
• Father:	Günter Rudolf Heinrich Helwig
• Mother:	Maria Helwig
• Sisters:	Sarah Helwig Alexandra Helwig

EDUCATIONAL HISTORY

2005-2008	PhD student at the Philipps-Universität Marburg Faculty of Biology, Department of Animal Physiology	Marburg, Germany
2004-2005	Marie Curie Research Fellow The Rowett Research Institute, Molecular Neuroendocrinology Group	Aberdeen, Scotland, UK
1998-2004	Diploma student at the Philipps-Universität Marburg Main Focus of studies: Animal Physiology, Developmental Biology and Human Neurobiology combined with Pharmacology / Toxicology Leaving certificate: Diploma, Grade: 1.2	Marburg, Germany
1997-1998	Basic military service, 3.PzArtBtl.2	Hess.Lichtenau, Germany
1994-1997	Grammar school „Geschwister-Scholl-Schule“ 1. Foreign language: English (5.-13. class) 2. Foreign language: Latin – Latinum (7.-13. class) 3. Foreign language: Russian (7.-10. class) Leaving certificate: Abitur (A-levels)	Melsungen, Germany
1988-1994	Grammar school „Gesamtschule Melsungen“	Melsungen, Germany
1984-1988	Primary school „Grundschule am Schloth“	Melsungen, Germany

SOCIETY MEMBERSHIPS

Since 2006	Member of the British Society for Neuroendocrinology (BSN)
Since 2006	Member of the Deutsche Adipositas Gesellschafft, DAG (German Obesity Society)
Since 2004	Member of the Deutsche Gesellschaft für Endokrinologie, DGE (German Endocrinology Society)

INTERNATIONAL RESEARCH VISITS

2008	Oral presentation at the Harvard Medical School, Beth Israel Deaconess Medical Centre, Department of Neurology, Group of Prof. Clifford Saper, Boston, USA, July 2008.
2006	Oral presentation at the University of Otago, Department of Anatomy and Structural Biology, Centre for Neuroendocrinology, Group of Prof. Dave Grattan, Dunedin, New Zealand, September 2006.
2005	Recipient of a fellowship funded by the European Commission to attend the ObeS^{e}chool European Union Marie Curie Training Site at the Rowett Research Institute in the group of Prof. Julian G. Mercer.

ORIGINAL PUBLICATIONS

- "Photoperiod-dependent regulation of carboxypeptidases D and E and exoproteolytic processing of pro-opiomelanocortin in the seasonal Siberian hamster (*Phodopus sungorus*)"
  M. Helwig, P.S. Ludewig, G. Heldmaier, J.G. Mercer, and M. Klingenspor. (in preparation)

- "Photoperiodic regulation of satiety mediating neuropeptides in the brainstem of the seasonal Siberian hamster (*Phodopus sungorus*)"
  M. Helwig, Z.A. Archer, G. Heldmaier, A. Tups, J.G. Mercer and M. Klingenspor. (in preparation)

- "Orexin-B interacts with Neuropeptide Y neurons in the Intergeniculate Leaflet and in peripheral parts of the Suprachiasmatic Nucleus of the Djungarian hamster (*Phodopus sungorus*)"
  M.H. Khorooshi, **M. Helwig**, M. Klingenspor. (in preparation)

- "Seasonal leptin resistance is associated with impaired signalling via JAK-STAT3 but not ERK, possibly mediated by reduced hypothalamic GRB2 protein"
  A. Tups, S. Stöhr, **M. Helwig**, P. Barrett, E. Krol, J. Schachtner, J.G. Mercer and M. Klingenspor,. (in preperation)

- "CART neuronal system in the rostral arcuate nucleus mediates seasonal regulation of energy balance in the Djungarian hamster (*Phodopus sungorus*)"
  M.H. Khorooshi, **M. Helwig**, A. Werckenthin. N. Steinberg, M. Klingenspor. (Gen Comp Endocrinol. 2008 Jun;157(2):142-7. Epub 2008 Apr 18.).

- "Marsupial uncoupling protein 1 sheds light on the evolution of mammalian nonshivering thermogenesis"
  M. Jastroch, K.W. Withers, S. Taudien, P. B. Frappell, **M. Helwig**, T. Fromme, V. Hirschberg, G. Heldmaier, B. M. McAlan, B.T. Firth, T. Burmester, M. Platzer, and M. Klingenspor, Physiol Genomics. 2008 Jan 17;32(2):161-9. Epub 2007 Oct 30.

- "Functional characterisation of UCP1 in the common carp: uncoupling activity in liver mitochondria and cold-induced expression in the brain."
  M. Jastroch, J.A. Buckingham, **M. Helwig**, M. Klingenspor and M. Brand. J Comp Physiol [B]. 2007 Oct;177(7):743-52. Epub 2007 Jun 19.

- "Photoperiodic regulation of insulin receptor mRNA and intracellular insulin signalling in the arcuate nucleus of the Siberian hamster, *Phodopus sungorus*"
  A. Tups, **M. Helwig**, S. Stöhr, P. Barrett, JG Mercer and M. Klingenspor, Am J Physiol Regul Integr Comp Physiol. 2006 Sep;291(3):R643-50.

- "PC1/3 and PC2 gene expression and post-translational endoproteolytic POMC processing is regulated by photoperiod in the seasonal Siberian hamster (*Phodopus sungorus*)"
  M. Helwig, M.H. Khorooshi, A. Tups, P. Barrett, C. Exner, J. Rozman, L.J. Braulke, J.G. Mercer and M. Klingenspor. J Neuroendocrinol. 2006 Jun;18(6):413-25.

- "Circulating ghrelin levels and central ghrelin receptor expression is elevated in response to food deprivation in the seasonal hamster (*Phodopus sungorus*)".
  A. Tups, **M. Helwig**, M.H. Khorooshi, Z.A. Archer, M. Klingenspor, J.G. Mercer. J Neuroendocrinol. 2004 Nov;16(11):922-8.

CONFERENCES & PRESENTATIONS

- „Annual regulation of PC1/3 and PC2 in Siberian hamsters; energy balance"
  M. Helwig, Gordon Research Conference on "Proprotein Processing, Trafficking & Secretion" 13-18 July 2008, New London, NH, USA. (***Invited Speaker***)

- „Der Djungarische Zwerghamster als Versuchsmodell für die Erforschung der saisonalen Regulation des Energiehaushalts"
  M.Helwig, 36. Seminar über Versuchstiere und Tierversuche, Federal Institute for Risk Assessment, 12. -13. September 2007, Berlin, Germany. (***Oral presentation***)

- „Analysis of pro-opiomelanocortin derived neuropeptides by MALDI-TOF mass spectrometry in the brain of the seasonal Siberian hamster (*Phodopus sungorus*) "
  M. Helwig, P.S. Ludewig, C. Wegener, J.G. Merer and M. Klingenspor. 7th Annual Meeting of the British Society for Neuroendocrinology, 10. -11. September 2007, Nottingham, United Kingdom. (***Oral presentation***)

- "Photoperiodische Regulation post-translationaler POMC Prozessierung im Hypothalamus des Djungarischen Zwerghamsters (Phodopus sungorus)"
  M. Helwig, A. Tups, P. Barrett, Z.A. Archer, R.M.H. Khorooshi, J.G. Mercer and M. Klingenspor, 22. Jahrestagung der Deutschen Adipositas Gesellschaft, 5. – 7. October 2006, Cologne, Germany. Akt Ernähr Med 2006; 31; DOI: 10.1055/s-2006-954470. (**Oral presentation**)

- "Photoperiodical Regulation of Post-Translational POMC Processing in the Hypothalamus of the Seasonal Siberian Hamster (*Phodopus sungorus*)."
  M. Helwig, A. Tups, P. Barrett, Z.A. Archer, R.M.H. Khorooshi, J.G. Mercer and M. Klingenspor, 10th International Congress on Obesity, 3 - 8 September 2006, Sydney, Australia. (***Oral presentation***)

- "Proteolytic Processing of POMC in the Hypothalamus of the Seasonal Siberian Hamster (Phodopus sungorus) is regulated by Photoperiod."
  M. Helwig, A. Tups, P. Barrett, Z.A. Archer, R.M.H. Khorooshi, J.G. Mercer and M. Klingenspor. 26th Blankenese Conference, Energy Metabolism: From Feeding Behavior to Metabolic Diseases. May 20-24, 2006. Hamburg-Blankenese, Germany. (***Poster***)

- "Uncoupling protein 1 is expressed in the brain of ectothermic vertebrates"
  M. Klingenspor, **M. Helwig**, T. Fromme, M.D. Brand, W. Kloas, S. Taudien, M. Platzer and M. Jastroch. 14th European Bioenergetics Conference, July 22- 27. Moscow, Russia. Biochemica et Biophysica Acta-Bioenergentics 375-376 Suppl. S, 2006. (***Co-author***)

- "Differential precursor-protein convertases PC1 and PC2 gene expression in the hypothalamus of the seasonal hamster (Phodopus sungorus)."
  M. Helwig, A. Tups, P. Barrett, L.J. Braulke, J.G. Mercer and M. Klingenspor. 7th European Congress of Endocrinology, 3-7 September 2005, Gothenburg, Sweden. (***Oral presentation***).

- "Uncoupling protein 1 in fish uncovers an ancient evolutionary history of mammalian nonshivering thermogenesis."
  M. Jastroch, M.D. Brand, W. Kloas, J.A. Buckingham, M. Helwig and M. Klingenspor. 2nd International Meeting on the Physiology and Pharmacology of Temperature Regulation, March 3-6, 2006 Phoenix, Arizona, U.S.A. (Contribution)

- „Molekulare Mechanismen der Leptinresistenz: Was können wir von der saisonalen Gewichtsregulation der Säugetiere lernen? M. Klingenspor, **M. Helwig**, P. Barrett, J. Mercer, A. Tups. 21. Jahrestagung Gesellschaft der Deutschen Adipositas Gesellschaft, 6.– 8. Oktober 2005, Berlin, Germany. (***Co-author***)

- "Differential expression of obesity related genes in the nucleus of the solitary tract in the Siberian hamster (Phodopus sungorus)."
  M Helwig, Z.A. Archer, M. Klingenspor and J.G. Mercer. ACERO Symposium 10: "Dietary approaches to weight regulation" 14-15 April 2005, Aberdeen, Scotland, UK. (***Poster***)

- "Precursor-protein convertases PC1 and PC2 gene expression and colocalisation with obesity related neuropeptide precursors in the hypothalamus of the seasonal hamster (Phodopus sungorus)."
  M. Helwig, A. Tups, P. Barrett, L.J. Braulke, J.G. Mercer and M. Klingenspor. ACERO Symposium 10: "Dietary approaches to weight regulation" 14-15 April 2005, Aberdeen, Scotland, UK. (***Poster***)

- „Effect of acute and chronic reduction in energy intake on circulating ghrelin levels and central ghrelin receptor expression in the seasonal hamster (Phodopus sungorus).
  A. Tups, **M. Helwig**, M.H. Khorooshi, Z.A. Archer, M. Klingenspor, J.G. Mercer. 12th International Congress of Endocrinology, Lisbon, Portugal, 31.08.- 04.09.2004. (***Co-author***)

- "Orexin-B-immunoreactive fibres make close apposition on cell bodies and fibres immunoreactive for Neuropeptide Y within the intergeniculate leaflet of the Djungarian hamster (Phodopus sungorus)"
  M.H. Khorooshi, **M. Helwig**, M. Klingenspor. 17.10.-18.10.03, 7th Annual Meeting of the Neuroendocrinology Section of the German Society of Endocrinology (DGE), Lübeck, Germany, Exp. Clin Endocrinol Diabetes 2003; 111;P42. (***Poster***)

AWARDS & GRANTS

2007 Best Oral Presentation at the 7th Annual Meeting of the British Society for Neuroendocrinology, Nottingham, UK.

2007 Travel Grant, British Society for Neuroendocrinology, 7th Annual Meeting of the BSN, Nottingham, UK.

2006 Travel Grant, Deutsche Forschungsgemeinschaft, 10th International Congress on Obesity, Sydney, Australia.

2006 Travel Grant, Deutsche Gesellschaft für Endokrinologie, 26th Blankenese Conference, Hamburg, Germany.

2006 Best Poster Presentation (runner-up) at the 26th Blankenese Conference, Hamburg, Germany.

2005 Travel Grant, Congress committee, 7th European Congress of Endocrinology (ECE) 2005, Gothenburg, Sweden.

2005 Best Poster Presentation at the ACERO Symposium 10, Aberdeen, Scotland, United Kingdom.

2005 Marie Curie Fellowship Stipend, European Community, Research Training Grant.

ADDITIONAL TRAININGS & POSITIONS

2005-2008 Risk prevention officer at the Group of Prof. Dr. Heldmaier, Animal Physiology, Philipps-Universität Marburg. Advanced training courses: I: 04.10 - 05.10.2005, II: 06.06.2006, III: 31.10. -01.11.2007.

2006-2007 Fire safety engineer at the group of Prof. Dr. Heldmaier, Animal Physiology, Philipps-Universität Marburg. Germany. Advanced training course: 27.06.2007.

2004 Workshop on Bioinformatics, organized by the international PhD program "Transcriptional Control in Developmental Processes". 16.02 - 20.02.2004, Max-Planck-Institute for terrestrial microbiology, Marburg, Germany.

ACKNOWLEDGEMENT

I would like to thank my PhD advisors, Prof. Dr. Martin Klingenspor and Prof. Dr. Julian Mercer, who both contributed a huge amount of intellectual input and personal effort to my PhD project. Thanks for thought provoking questions, for scientific contributions and for kind words when they were necessary. I am also thankful to Prof. Dr. Gerhard Heldmaier, head of the group of Animal Physiology in Marburg, for giving me the chance to do my project in his laboratories. And I would like to extend a special thanks to Dr. Christian Wegener, Prof. Dr. Lloyd Fricker and Prof. Dr. Iris Lindberg who supported me and my project in many respects.

My best appreciations are due to my friends and colleagues in Marburg. Big thanks go to my brainiacs Alexander and Reza who started the fire. Without them, who knows what I would do now? I am very thankful to Flo "The Beau", Tobias, Timo, Isabel, Siggi and Verena for their support, encouragement, sharing vitally important coffee breaks and a lot of fun. They are truly the best friends I can wish for. Thanks go to Carola for her outstanding support concerning the student seminars and courses. I think we were a great team and we have done a good job! Kudos goes to my Diploma students, Christiane and Philip, who made my life even more exciting. And I am deeply indebted to Luzie who saved me in the end.

I also would like to thank my colleagues from Scotland, especially the "Lawson Crew" Zoë, Kim, Lynn, Dana, Dr. Perry Barrett and Dr. Alexander Ross and my flat mates from the "Greenburn House" Vlasta, Joost, Gaston, Marcketa and our "very French" neighbours Sebastièn and Anne-Sophie who gave me an unforgettable time in Aberdeen.

Last, but not least, I am extremely appreciative to my dear family, Günter, Claudia, Alexandra, Sarah, Stefan and Vanessa who supported me all along the way. Zu guter Letzt ein noch ein Kommentar in Deutsch. ☺ Familie…ich danke euch!

ERKLÄRUNG

Ich versichere, dass ich meine Dissertation

Photoperiod-dependent proteolytic processing of neuropeptide precursors

selbständig, ohne unerlaubte Hilfe angefertigt und mich dabei keiner anderen als der von mir ausdrücklich bezeichneten Quellen und Hilfen bedient habe.

Die Dissertation wurde in der jetzigen oder einer ähnlichen Form noch bei keiner anderen Hochschule eingereicht und hat noch keinen sonstigen Prüfungszwecken gedient.

_____ _____

(Ort, Datum) (Unterschrift mit Vor- und Zuname)